221
Fermilab Library
0 1160 0092334 6
CNS-REP-43

ISSN 1343-2230
CNS-REP-43
December, 2001

CNS Report

Proceedings of the International Workshop on developments of Ge detector array and frontiers of gamma-ray spectroscopy

CNS, University of Tokyo
December 11–13, 2001

Center for Nuclear Study (CNS)

Graduate School of Science, the University of Tokyo
Wako Branch at RIKEN, Hirosawa 2-1, Saitama 351-0198, Japan
Correspondence: cnsoffice@cns.s.u-tokyo.ac.jp

FERMILAB
FEB 4 2002
LIBRARY

International Workshop on developments of Ge detector array and frontiers of gamma-ray spectroscopy

CNS, University of Tokyo
December 11 – 13, 2001

International Workshop on developments of Ge detector array and frontiers of gamma-ray spectroscopy

First Circular

Dear colleagues,

We are pleased to inform you that "International Workshop on developments of Ge detector array and frontiers of gamma-ray spectroscopy" will be held from 11 (Tuesday) to 13 (Thursday), December, 2001, in Center for Nuclear Study (CNS), University of Tokyo. It is co-sponsored by CNS, the RIKEN Accelerator Research Facility (RARF), and Research Center for Measurement in Advanced Science, Rikkyo University.

In order to open up a frontier of the gamma-ray spectroscopy of exotic nuclei, Center for Nuclear Study (CNS) has made a decision to construct a segmented germanium detector array (for reference, http://www.cns.s.u-tokyo.ac.jp/ge-ws/pdf/project.pdf, position.pdf). Taking this opportunity, we would like to organize the international workshop, where we can discuss developments of germanium detector array and new perspectives for gamma-ray spectroscopy with germanium detectors. It is hoped that the workshop will offer a unique opportunity to bring physicists together from both high-spin and exotic-nuclei communities for close interactions.

Main topics to be discussed are

- developments of segmented germanium detector array
  - pulse-shape analysis for gamma-ray tracking
  - tracking algorithms
  - digital electronics and data acquisition
  - high counting rate capability
  - hybrid system with germanium and other detectors
- latest frontiers of gamma-ray spectroscopy on high-spin and high-isospin nuclei
- perspectives for nuclear physics with germanium detectors
- other related topics

The workshop will start in the morning of December 11 and end in the afternoon of December 13. It will take place in a seminar room of the new CNS building located in the RIKEN campus. We expect about 50 participants for the workshop. There will be invited talks as well as oral presentations selected from submitted contributions. Those who are interested are recommended to visit the workshop home page; http://www.cns.s.u-tokyo.ac.jp/ge-ws/ .

Organizers of the workshop:
S. Shimoura (CNS, Chair), K. Asahi (TIT/RIKEN), Y. Gono (Kyushu),
H. Iwasaki (CNS, Scientific Secretary), T. Kishida (RIKEN), M. Kurokawa (CNS),
T. Motobayashi (Rikkyo), H. Sakurai (Tokyo)

Correspondence:
Susumu SHIMOURA / Hironori IWASAKI
Center for Nuclear Study (CNS), University of Tokyo
RIKEN campus, 2-1 Hirosawa, Wako, Saitama, 351-0198, Japan
Email: ge-ws@cns.s.u-tokyo.ac.jp, FAX: +81-48-464-4554

List of Participants

Family Name	First Name	Affiliation	E-Mail
Aoi	Nori	the University of Tokyo	aoi@phys.s.u-tokyo.ac.jp
Asahi	Koichiro	RIKEN	asahi@postman.riken.go.jp
Austin	Sam	MSU	austin@nscl.msu.edu
Ando	Shingo	NIKI GLASS Co., LTD.	sando@nikiglass.com
Baba	Hidetada	Rikkyo University	baba@daq.rikkyo.ac.jp
Baktash	Cyrus	Oak Ridge National Laboratory	baktash@mail.phy.ornl.gov
Beck	Francis	IReS - Strasbourg	francis.beck@IReS.in2p3.fr
de France	Gilles	GANIL	defrance@ganil.fr
Demichi	Kimihiko	Rikkyo University	demichi@ne.rikkyo.ac.jp
Gelberg	Adrian	Universität zu Köln/RIKEN	gelberg@rarfaxp.riken.go.jp
Gerl	Juergen	GSI	gerl@axp602.gsi.de
Gomi	Tomoko	Rikkyo University	gomi@ne.rikkyo.ac.jp
Gono	Yasuyuki	Kyushu University	gono@kutl.kyushu-u.ac.jp
Hasegawa	Hirokazu	Rikkyo University	hasegawa@ne.rikkyo.ac.jp
Ideguchi	Eiji	RIKEN	ideguchi@postman.riken.go.jp
Imai	Nobuaki	the University of Tokyo	imai@nucl.phys.s.u-tokyo.ac.jp
Ishihara	Masayasu	RIKEN	ishihara@rarfaxp.riken.go.jp
Ishii	Tetsuro	JAERI	ishii@popsvr.tokai.jaeri.go.jp
Iwasaki	Hironori	CNS	iwasaki@cns.s.u-tokyo.ac.jp
Kanno	Syouko	Rikkyo University	komacha@ne.rikkyo.ac.jp
Kishida	Takashi	RIKEN	kishida@rikaxp.riken.go.jp
Komatsubara	Tetsuro	University of Tsukuba	komatsubara@tac.tsukuba.ac.jp
Kröll	Thorsten	INFN-LNL	Thorsten.Kroell@lnl.infn.it
Kubo	Toshiyuki	RIKEN	kubo@rarfaxp.riken.go.jp
Kubono	Shigeru	CNS	kubono@cns.s.u-tokyo.ac.jp
Kurokawa	Meiko	CNS	meiko@harrods.riken.go.jp
Lampert	Marie-Odile	EURISYS MESURES	lampert_eurisys@compuserve.com
Lee	I-Yang	LBL	iylee@lbl.gov
Matsuyama	Yuuichi	Rikkyo University	kite@ne.rikkyo.ac.jp
Minemura	Toshiyuki	RIKEN	minemura@rarfaxp.riken.go.jp
Mitimasa	Shin'ichiro	CNS	mitimasa@cns.s.u-tokyo.ac.jp
Motobayashi	Tohru	Rikkyo University	motobaya@rikkyo.ne.jp
Murakami	Hiroyuki	Rikkyo University	murakami@se.rikkyo.ac.jp
Murakami	Tetsuya	Kyoto University	murakami@nh.scphys.kyoto-u.ac.jp
Nakamura	Takashi	Tokyo Institute of Technology	nakamura@ap.titech.ac.jp
Notani	Masahiro	CNS	notani@rlus1.riken.go.jp
Ohta	Shinsuke	Kyoto University	ota@nh.scphys.kyoto-u.ac.jp
Saito	Akito	Rikkyo University	akito@ne.rikkyo.ac.jp
Sakai	Hideyuki	CNS/the University of Tokyo	sakai@phys.s.u-tokyo.ac.jp
Sakai	Mitsuo	CNS	msakai@cns.s.u-tokyo.ac.jp
Sakurai	Hiroyoshi	the University of Tokyo	sakurai@phys.s.u-tokyo.ac.jp
Satou	Yoshiteru	CNS	ysatou@rarfaxp.riken.go.jp
Sekimoto	Michiko	KEK-IPNS	sekimoto@post.kek.jp
Shimoura	Susumu	CNS	shimoura@cns.s.u-tokyo.ac.jp
Suda	Toshimi	RIKEN	suda@rarfaxp.riken.go.jp
Suzuki	Toshikazu	Saint-Gobain Crystals & Detectors KK	toshikazu.suzuki@saint-gobain.com
Takeshita	Eri	Rikkyo University	eri@ne.rikkyo.ac.jp
Takeuchi	Satoshi	Rikkyo University	takeuchi@ne.rikkyo.ac.jp
Tamura	Hirokazu	Tohoku University	tamura@lambda.phys.tohoku.ac.jp
Teranishi	Takashi	CNS	taranisi@cns.s.u-tokyo.ac.jp
Ue	Koji	CNS	ue@rlus1.riken.go.jp
Watanabe	Shinichi	CNS	watasin@cns.s.u-tokyo.ac.jp
Yamaguchi	Akinori	NIKI GLASS Co., LTD.	ayama@nikiglass.com
Yanagisawa	Yoshiyuki	RIKEN	yanagisa@rarfaxp.riken.go.jp
Yoneda	Ken-ichiro	RIKEN	yoneda@rarfaxp.riken.go.jp

Program

December 11th

8:30 – REGISTRATION

8:55 – 11:40 (Chairperson: T. Motobayashi)

- H. Sakai (CNS/Tokyo) (15) Opening address
- I.Y. Lee (LBL) (50+10) " Gamma ray energy tracking array : status of the development and physics opportunities "

—— COFFEE BREAK (10:10–10:40) ——

- J. Gerl (GSI) (50+10) " The Advanced Gamma tracking Array AGATA "

—— L U N C H (11:40–14:00) ——

14:00 – 16:30 (Chairperson: K. Asahi)

- S. Shimoura (CNS) (50+10) " CNS Ge array for in-beam γ spectroscopy of fast moving exotic nuclei "

—— COFFEE BREAK (15:00–15:30) ——

- C. Baktash (ORNL) (50+10) " Gamma Spectroscopy with Radioactive Ion Beams at the HRIBF "

December 12th

9:30 – 11:50 (Chairperson: Y. Gono)

- T. Ishii (JAERI) (50+10) " Isomer γ-ray Spectroscopy of Neutron-rich Nuclei Produced by Deep-inelastic Collisions "

—— COFFEE BREAK (10:30–10:50) ——

- G. deFrance (GANIL) (50+10) " Gamma-ray spectroscopy of exotic nuclei at GANIL "

—— L U N C H (11:50–13:30) ——

13:30 – 15:00 RIKEN–CNS Tour

15:00 – 16:40 (Chairperson: H. Sakurai)

- E. Ideguchi (RIKEN) (30+10) " Superdeformation in the doubly magic nucleus $^{40}_{20}Ca_{20}$ "

—— COFFEE BREAK (15:40–16:00) ——

- M. Kurokawa (CNS) (30+10) " Pulse-shape analysis of CNS segmented Ge detector "

December 13th

9:30 – 12:00 (Chairperson: T. Kishida)

- H. Tamura (Tohoku) (50+10) " Hyperball and a new frontier in hypernuclear physics "

—— COFFEE BREAK (10:30–10:50) ——

- Y. Gono (Kyushu) (50+10) " Ge-Telescope and Compton camera "
- T. Motobayashi (Rikkyo) (10) Summary

Gamma ray energy tracking array: status of the development and physics opportunities.

I. Y. Lee[A],

[A] *Lawrence Berkeley National Laboratory, Berkeley, CA 94720*

Email: iylee@lbl.gov

Gamma-ray energy tracking array consisting of highly segmented HPGe detectors is a new concept for the detection of gamma radiation. In this array, each interaction of a gamma ray is identified by its energy and position. The three-dimensional position and the energy of interactions are determined by using a two-dimensionally segmented Ge detector together with pulse-shape analysis of the signals. Using tracking algorithms based on the properties of photo absorption, Compton scattering and pair production, we could reconstruct the scattering sequences, even if many gamma rays hit the array at the same time. Such a detector will have new and much improved capabilities compared to current generation of gamma-ray spectrometer. For example, the efficiency of a 4-pi tracking array would be 0.6 for 1.3 MeV gamma rays (compare with a efficiency of 0.1 for Gammasphere) and 0.12 for 15 MeV gamma rays (0.005 for Gammasphere). The peak-to-total ratio could be 0.8 at 1.3 MeV (0.55 for Gammasphere). More important is the excellent position resolution of about 1-2 mm which is needed for Doppler shift correction at large recoil velocity.

One implementation of this concept, called GRETA (Gamma Ray Energy Tracking Array), is currently under development at LBNL. In this presentation I will show the progress which have been made in a number of key areas; the manufacture of segmented detectors and pre-amplifiers that can provide high quality signals needed to resolve and locate individual interaction points; a data processing system including fast ADCs and processing units to digitize and process the segment signals; signal processing methods for determining energy, time, and position based on digital signal processing; and the development of a tracking algorithm that uses the energy and position information to identify interaction points belonging to a particular gamma ray.

Work supported by US Department of Energy, under contract DE-AC03-76SF00098.

Gamma Ray Energy Tracking Array: Status of the Development and Physics Opportunities

I-Yang Lee

Lawrence Berkeley National Laboratory

Outline

- **Gamma-ray tracking principles**
- **Physics opportunities**
- **Technical challenges and proof of principle**
- **R/D plan and schedule**
- **Organization of the U.S. gamma-ray tracking efforts**
- **Conclusions**

Acknowledgement

I like to thank the following colleagues
who have contributed to this presentation.

T. Glasmacher
A. Kuhn
A. O. Macchiavelli
G. J. Schmid
K. Vetter

Performance measures of a Gamma-ray detector

- Energy resolution
- Efficiency
- Peak-to-total ratio
- Position resolution
- Time resolution
- Direction information
- Gamma-ray polarization
- Counting rate

Gamma ray detector technology

Energy resolution, Efficiency, Peak-to-total

- Compton Suppressed Ge
- Ge Sphere
- Gamma Ray Tracking

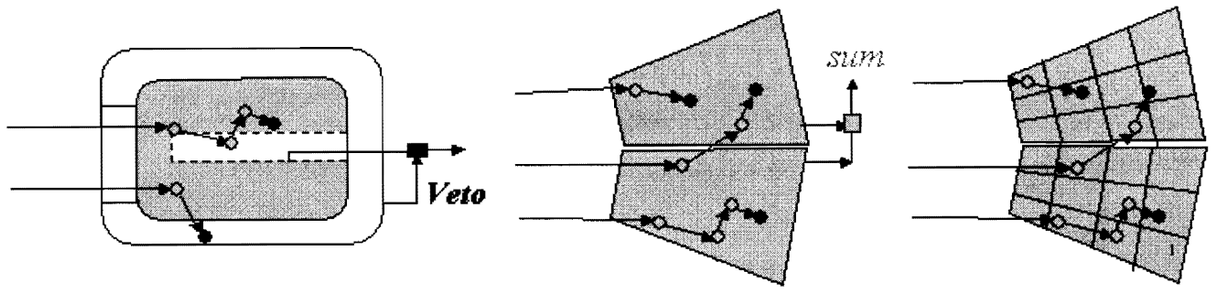

N = 100	N = 1000 (summing)	N = 100
NΩ ε = 0.1	NΩ ε = 0.6	NΩ ε = 0.6
Efficiency limited	**Too many detectors**	**Segmentation**

Doppler Broadening

Position resolution

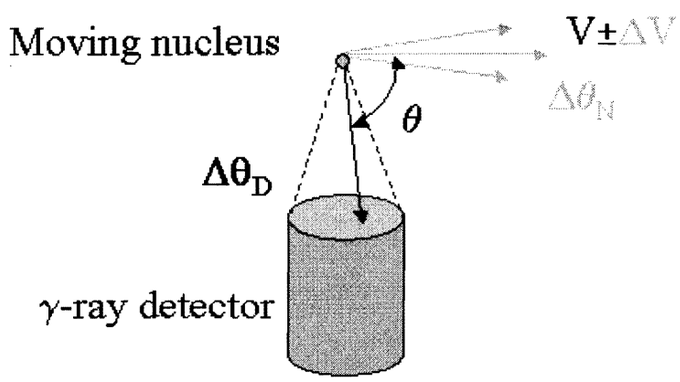

Doppler shift

$$E_\gamma = E_\gamma^0 \frac{\sqrt{1-\frac{V^2}{c^2}}}{1-\frac{V}{c}\cos\theta}$$

Broadening of detected gamma ray energy due to:

- Spread in speed ΔV
- Distribution in the direction of velocity $\Delta\theta_N$
- Detector opening angle $\Delta\theta_D$

➔ **Need accurate determination of V and θ.**

➔ Position sensitive γ-ray detector and particle detector

Gamma-ray tracking principles

1) Highly segmented Germanium detectors

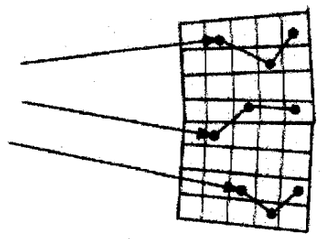

2) Pulse shape analysis in segments ➔ 3D position

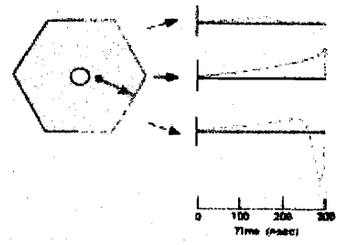

3) Tracking of photon interaction points ➔ energy, position

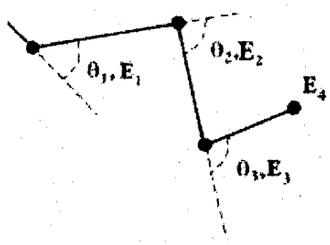

Compare GRETA with Gammasphere

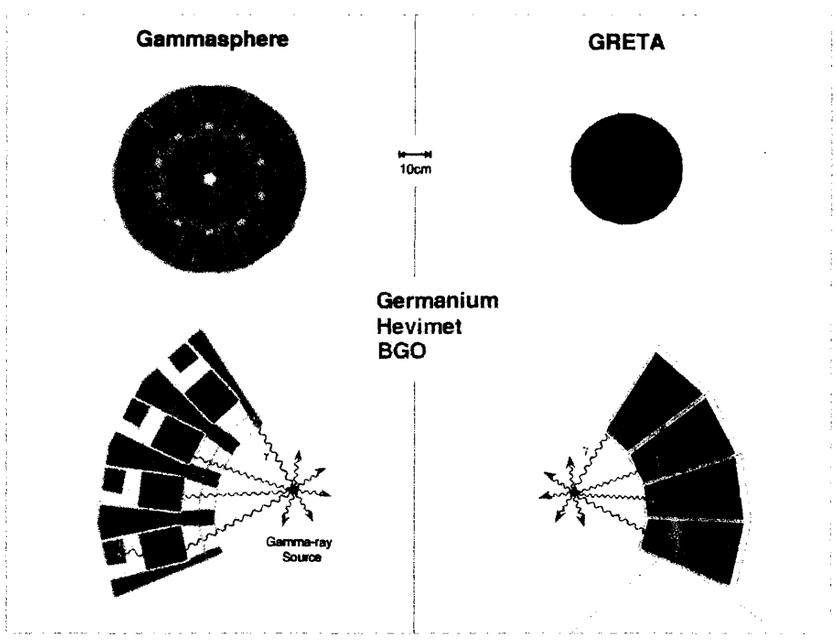

Efficiency (1 MeV)	**8%**	**55%**
Efficiency (15 MeV)	**0.5%**	**12%**
Peak/Total (1 MeV)	**55%**	**85%**
Position resolution	**20mm**	**1 mm**

Resolving Power of gamma-ray detector

Figure of Merit

Resolving power per coincidence fold is

$$r = 0.76 \frac{\Delta E}{\delta E} \frac{P}{T}$$

Where ΔE is the separation of gamma-ray peaks and δE is the energy resolution (FWHM) of the peak. The factor 0.76 takes into account the Gaussian shape of the peak, and P/T is the peak-to-total ratio of the detector response. For f-fold coincidence the resolving power is

$$\frac{1}{\alpha} = r^f \qquad (1)$$

Where α is the fractional intensity of an f-fold cascade that can be resolved. On the other hand, due to the lower efficiency for detecting higher fold coincidences, there is an upper limit of fold, which is determined by the detector efficiency, ε and the intensity of the cascade under study.

$$N = N_0 \, \alpha \, \varepsilon^f \qquad (2)$$

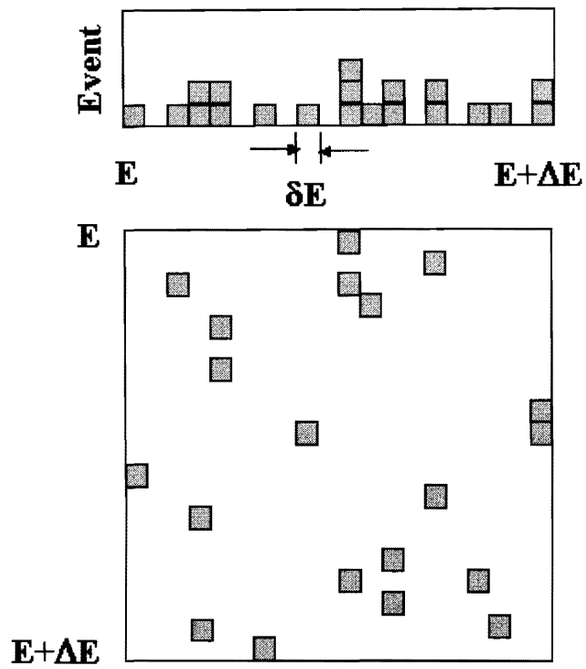

Resolving Power of gamma-ray detector

Where N_0 is the total number of event produced in an experiment, and N is the desired number of events for the cascade with intensity α. Solve (1) and (2) for f, we obtain

$$f = \frac{\ln\left(\frac{N_0}{N}\right)}{\ln\left(\frac{r}{\varepsilon}\right)}$$

and the resolving power.

$$RP = \frac{1}{\alpha} = r^f$$

However, for the cases in which the multiplicity M_γ of the cascade is less than the fold f, than we have.

$$RP = \frac{1}{\alpha} = r^{M_\gamma}$$

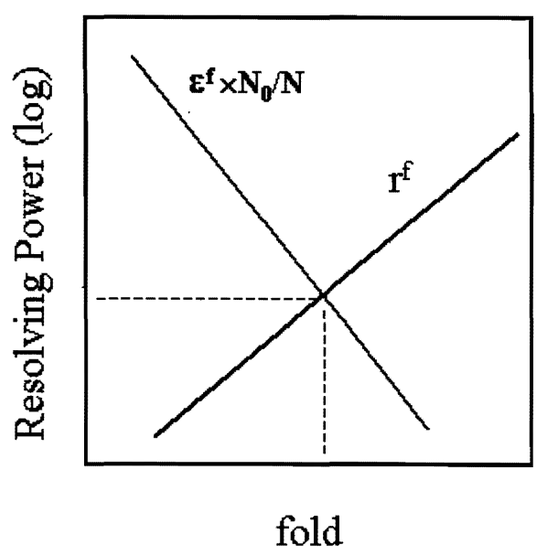

GRETA Resolving Power

Reaction	<Eγ> (MeV)	β	Mγ	Resolving Power	× Gammasphere
Stopped	**5.0**	**0.0**	**4**	**6.0×10^7**	**760**
High spin					
normal kine.	**1.0**	**0.04**	**25**	**1.5×10^7**	**700**
inverse kine.	**1.0**	**0.07**	**25**	**1.5×10^7**	**2000**
Coulex/transfer	**1.5**	**0.1**	**15**	**3.7×10^7**	**8100**
Fragmentation					
in beam	**1.5**	**0.5**	**6**	**6.4×10^7**	**290000**
Coulex	**5.0**	**0.5**	**2**	**7.4×10^3**	**590**

Gamma-ray tracking advances resolving power by three orders of magnitude

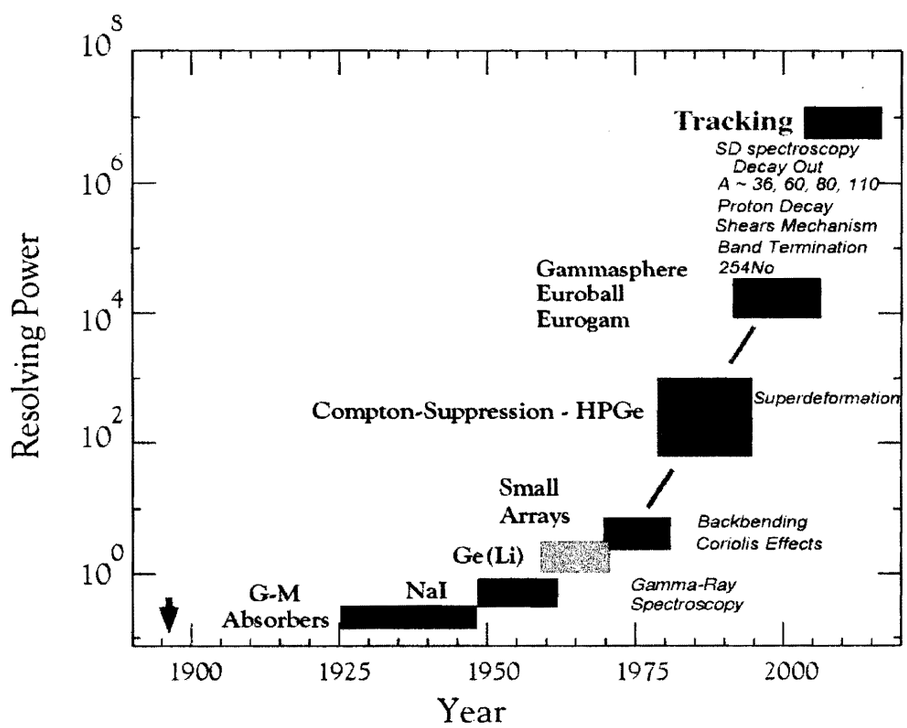

GRETA Capabilities

Broad physics opportunities

- Resolving power: 10^7 vs. 10^4
  - Cross sections down to ~1 nb
    - Most exotic nuclei
    - Heavy elements (e.g. ^{253,254}No)
    - Drip-line physics
    - High level densities (e.g. chaos)
- Efficiency (12% vs. 0.5% at E_γ=15 MeV)
  - Shape of GDR
  - Studies of hypernuclei
- Efficiency (slow beams) (55% vs. 9% at E_γ=1.3 MeV)
  - Fusion evaporation reactions
- Efficiency (fast beams) (55% vs. 0.5% at E_γ=1.3 MeV)
  - Fast-beam spectroscopy with low rates -> RIA
- Angular resolution (0.2° vs. 8°)
  - N-rich exotic beams
    - Coulomb excitation
  - Fragmentation-beam spectroscopy
    - Halos
    - Evolution of shell structure
    - Transfer reactions
- Count rate per crystal (50 kHz vs. 10 kHz)
  - More efficient use of available beam intensity
- Linear polarization
- Background rejection by direction

Gamma-ray tracking array: Discovery potential in many areas of nuclear structure physics

Goal: Gain a quantitative understanding of the atomic nucleus

- What are the properties of the heaviest nuclei?
- How deformed can a nucleus become and how fast can a nucleus rotate before it breaks up?
- Does the atomic nucleus display new symmetries?
- What are the properties of atomic nuclei with extreme neutron-proton ratios?
- How does the structure of nuclei change towards the limits of stability when binding becomes weak?
- What are the wave functions of spatially very extended halo nuclei?

Properties of super-heavy nuclei

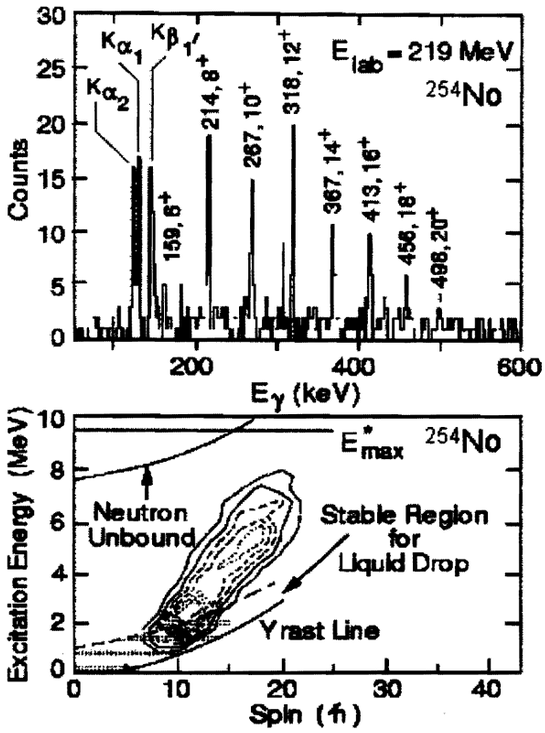

P. Reiter *et al.*, Phys. Rev. Lett. **82** (1999) 509; **84** (2000) 3542.

■ What are the properties of super-heavy nuclei?
■ Why does a super-heavy nucleus not explode from Coulomb repulsion?

Experiment
- Fusion-evaporation with recoil-decay tagging trigger

Challenges
- Small cross section (1 μb – 10 nb)
- Fission background

The gamma-ray tracking advantage
- ⌧ Resolving power
- ⌧ Efficiency
- ⌧ Count rate capability
- ⌧ Linear polarization

Nuclei with extremely deformed shapes

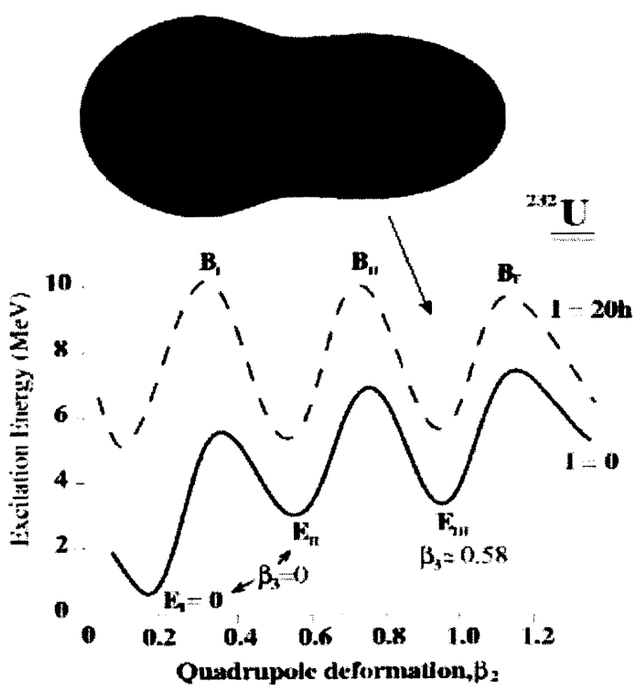

■ How deformed can a nucleus become and what is its structure?

- Exotic shapes with 3:1 axis ratio
- Predicted to exist near fission limit: Very heavy nuclei or at high angular momentum

Challenges
- Small cross section
- Weak channel
- Fission background

The gamma-ray tracking advantage
- ⌧ Resolving power
- ⌧ Efficiency
- ⌧ Count rate capability
- ⌧ Linear polarization

Nuclei with large angular momentum

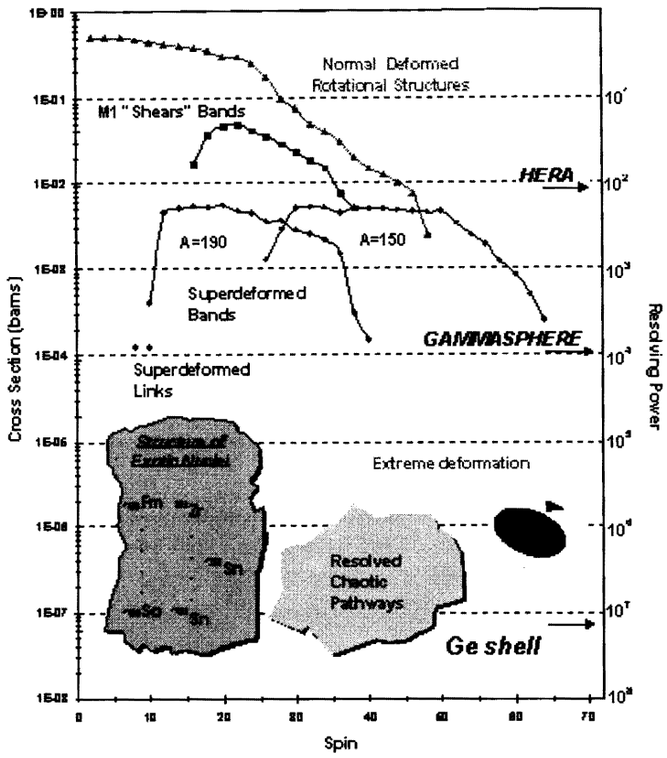

■ How much angular momentum can a nucleus sustain?
■ Are there new symmetry effects?
■ What are the roles of pairing and the proximity to the continuum?

Experiment
- Fusion-evaporation

Challenges
- Small cross section
- Weak channel

The gamma-ray tracking advantage
- ⌧ Resolving power
- ⌧ Efficiency
- ⌧ Count rate capability
- ⌧ Linear polarization

Collective properties of neutron-rich nuclei with fast exotic beams

■ How do the structure and shapes of nuclei evolve when the drip lines are approached?

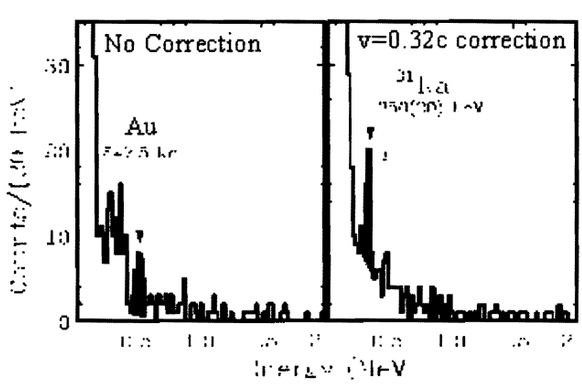

B.V. Pritychenko et al., Phys. Rev. ***C63*** *(2001) 011305(R).*

Experiment
- Intermediate-energy inelastic scattering
- Thick secondary targets require γ-ray detection to indicate inelastic scattering

Challenges
- Need γ-ray emission angle for Doppler-shift reconstruction
- Low beam rate (few/s)

The gamma-ray tracking advantage
- ⌧ Angular resolution
- ⌧ Extends reach of NSCL CCF and RIA two neutrons further
- Efficiency
- ⌧ from stability

Mapping wave functions of exotic nuclei

■ What are the spectroscopic factors in the wave function of exotic nuclei?

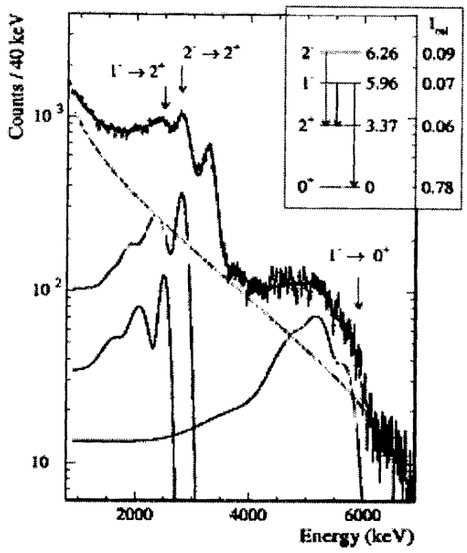

T. Aumann *et al.*, Phys. Rev. Lett. **84** (2000) 35.

Experiment
- Intermediate-energy nucleon knockout
- Thick secondary targets require γ-ray detection to indicate inelastic scattering

Challenges
- Need γ-ray emission angle for Doppler-shift reconstruction
- Low beam rate (0.1/s)

The gamma-ray tracking advantage
- ⌦ Efficiency
- ⌦ Angular resolution
- ⌦ Extends reach of NSCL CCF and RIA two neutrons further from stability

Giant resonances built on excited states and in exotic nuclei

■ What is the angular momentum dependence of the giant resonance width?

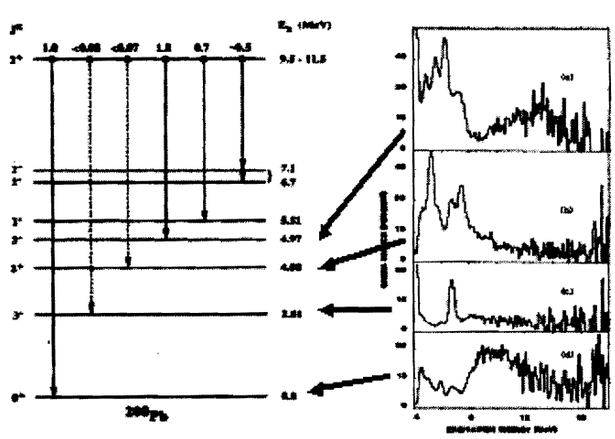

J.R. Beene et al., Phys. Rev. C ***39*** *(1989) 1307.*

Experiment
- Virtual photon scattering
- Tag on low-energy transitions
- Simultaneously detect high-energy γ-rays

Challenges
- Need γ-ray emission angle for Doppler-shift reconstruction

The gamma-ray tracking advantage
- ⌦ Efficiency at low and high photon energies
- ⌦ Angular resolution

Beta-decay properties of the most exotic nuclei

■ What are the properties of the most exotic nuclei?

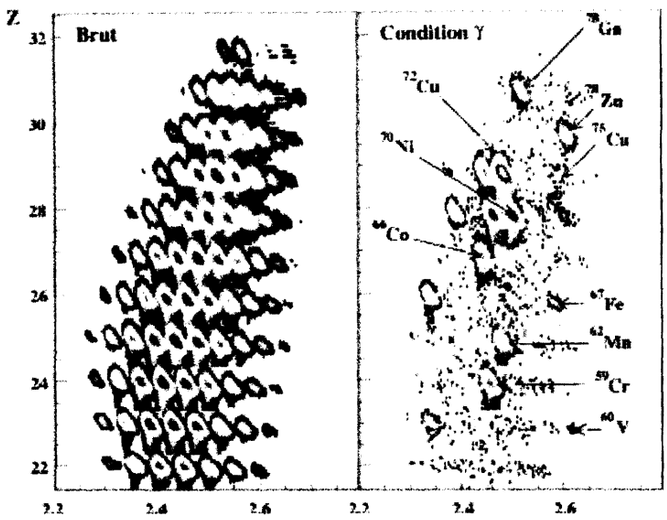

Experiment

- Beta-decay after implantation
- Bound excited states of daughter
- Clean beta trigger, beta detection >98% efficient

Major challenge

- Minute cross section: 1 atom/week (fb)

The gamma-ray tracking advantage

⊠ Efficiency

⊠ Background rejection by photon direction

Technical Challenges

- ***Advances in detector segmentation***
- ***Electronics development***
  - ***Low noise high bandwidth preamplifier***
  - ***Rapid sampling, high resolution pulse digitizer***
- ***Signal analysis algorithm***
- ***Tracking algorithm***
- ***Computing power for on-line processing***

Proof of principle

No show stoppers

- **Segmented prototype detector**
  - Energy resolution: 1.2 keV at 60 keV and 1.9 keV at 1332 keV
  - Total integrated noise: < 5 keV (bandwidth 35 MHz)
  - 3-D position sensitivity: < 1 mm at 374 keV (single interaction)
- **Signal analysis (experiment)**
  - 1-2 mm: Adaptive grid search (very slow, 10 min)
  - 2 mm: Genetic algorithm (slow, few sec)
  - 5-6 mm: wavelet transformation (fast 10 msec)
  - 2-3 mm: wavelet transformation (fast 100 msec)
- **Tracking algorithms (simulation)**
  - Compton tracking (150 keV < E_g < 5 MeV)
    - Tracking efficiency 50% for multiplicity 25
  - Pair tracking (E_g> 5 MeV)
    - Tracking efficiency 50%

Proof of Principle 1: Segmented Germanium detectors

MSU
In use

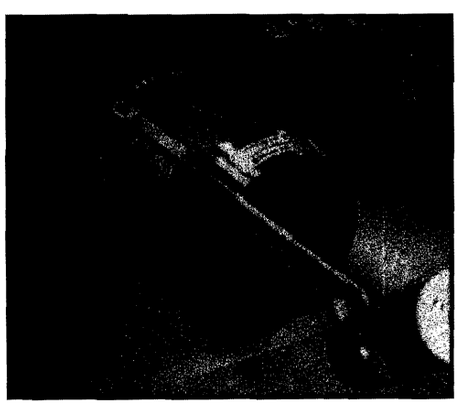

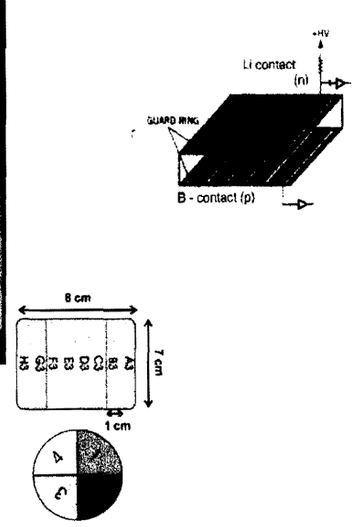

ANL - GARBO
R/D

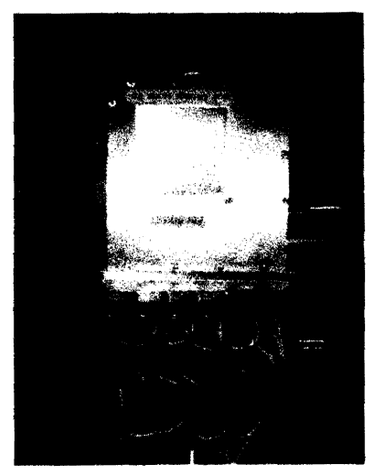

The ANL HpGeDSSD
Planar Detector

Proof of Principle 1: Segmented Germanium detectors

Exogam	***Miniball***	***AGATA***
Under construction	**Under construction**	**Planned**

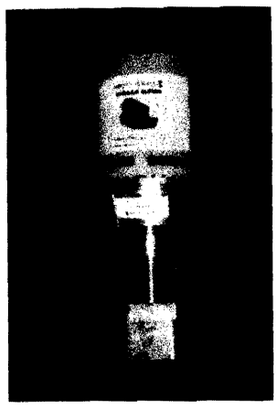

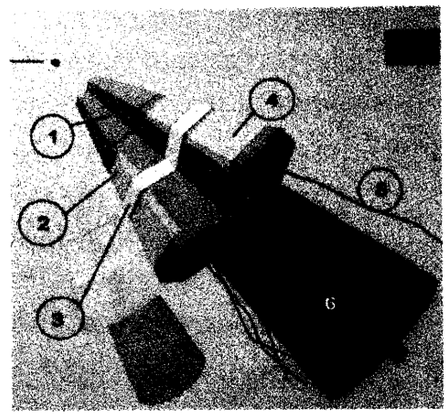

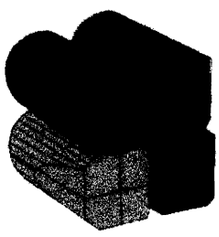

front segments FWHM [keV]	
@122keV	@1.33MeV
1.2	2.3
1.2	2.4
1.3	2.4
1.2	2.2
1.0	2.2
1.2	2.6

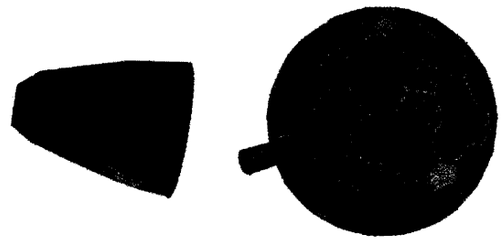

Prototype detector at LBNL

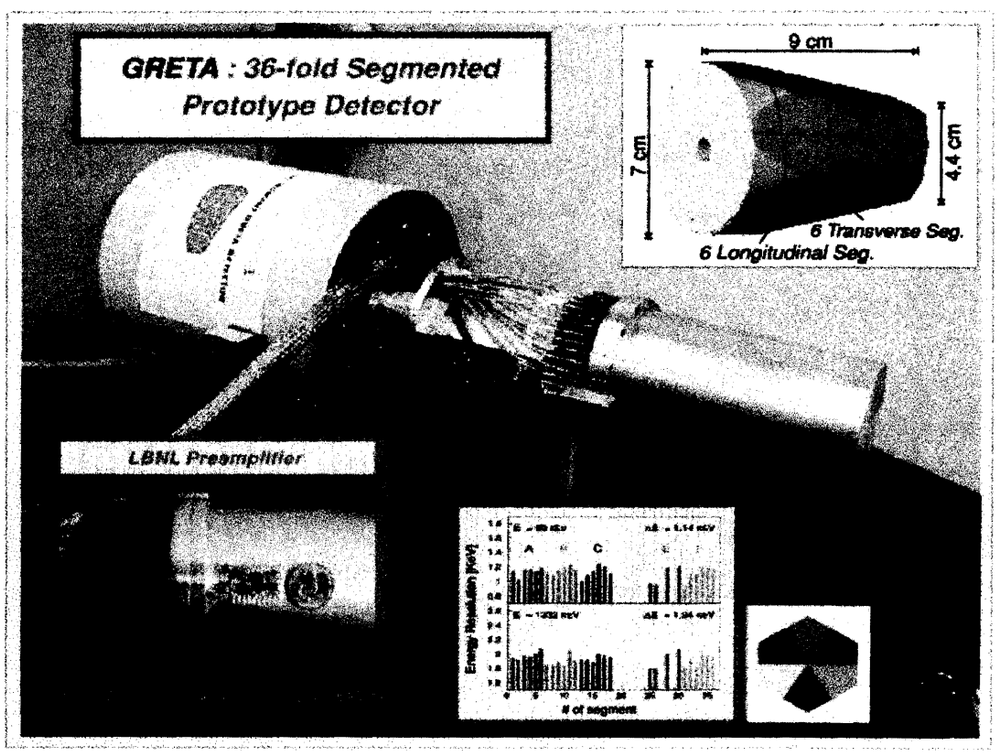

Proof of Principle 2: Pulse shape analysis

Measurement of net and induced signals

Collimation: 2mm in X,Y and 1mm in Z

Decomposition on 0.5mm grid

Interaction takes place in B1 at X=16, Y=3, Z=4 mm

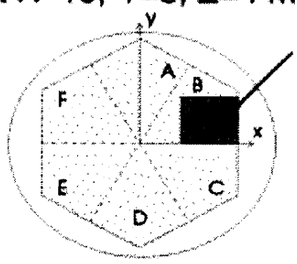

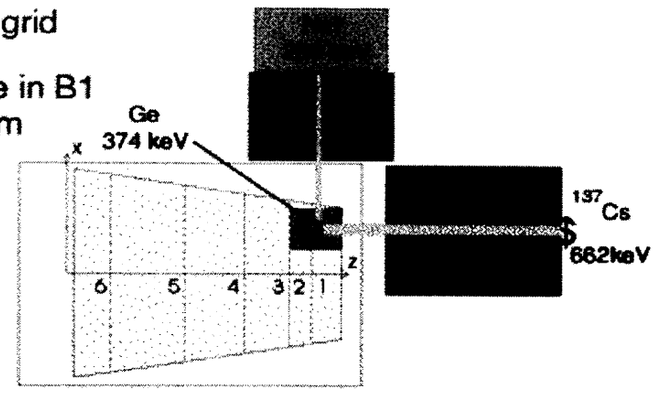

Proof of Principle 2:

Understanding the measured signals

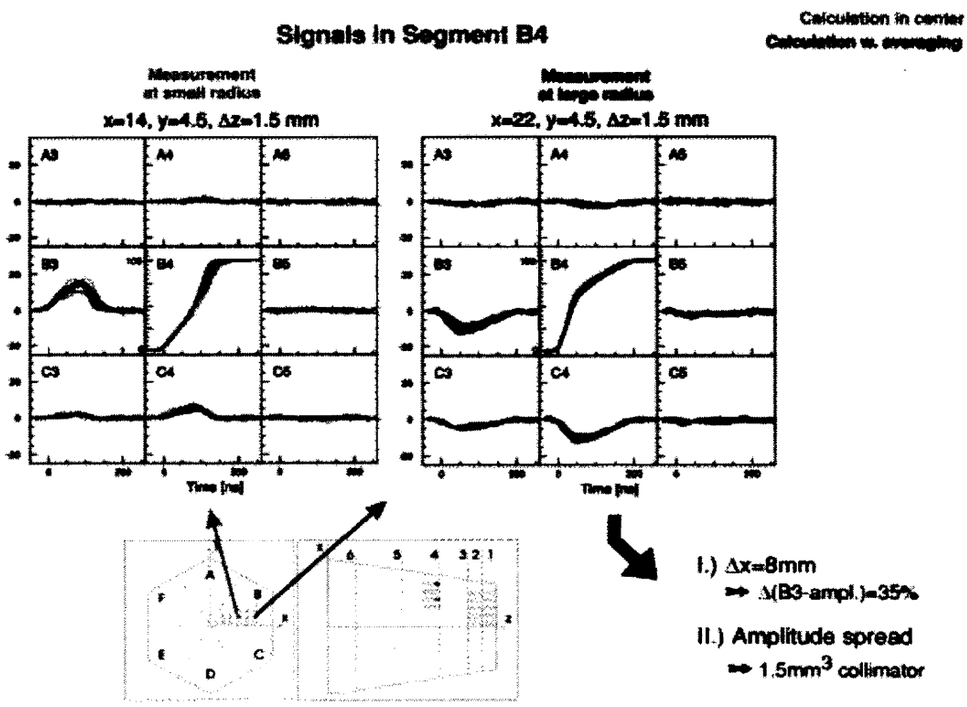

I.) Δx=8mm
➡ Δ(B3-ampl.)=35%

II.) Amplitude spread
➡ 1.5mm^3 collimator

Position determination for a single interaction of a 662 keV photon

K. Vetter *et al*, Nucl. Instr. Meth. A 452 (2000) 223

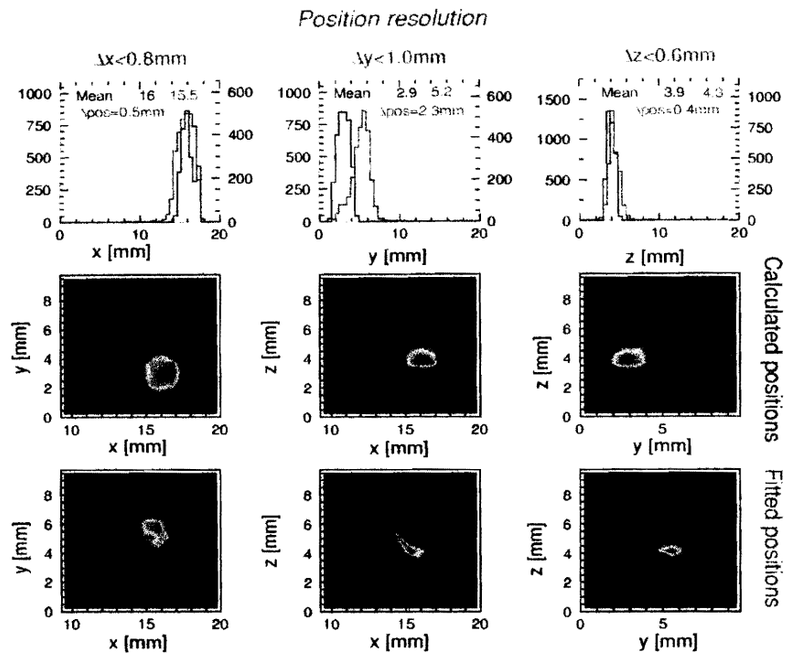

Crystal Orientation Effects on Charge Carrier Collection

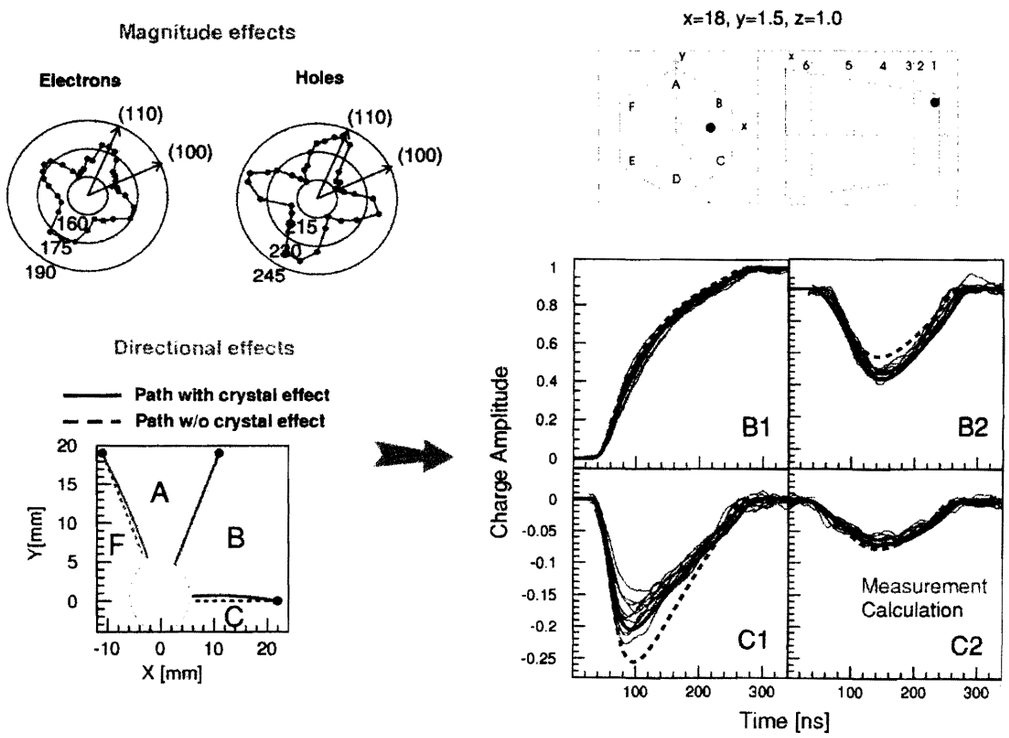

Separation of two interaction points

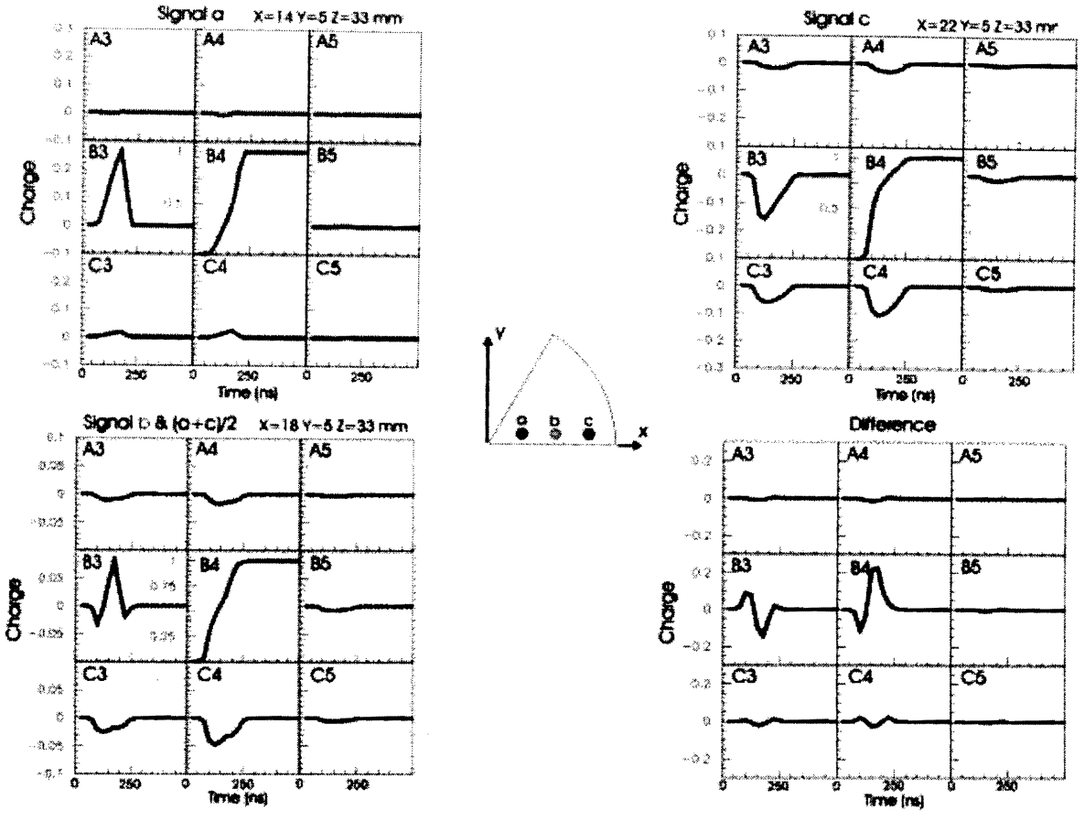

Sensitivity for separating two interaction points

E_γ=1.3 MeV, noise=5keV

$$\chi^2_{ii} = \sum \left(\frac{(q_d(t)-q_a(t))-(q_b(t)-q_c(t))}{\sqrt{2}\,\sigma} \right)^2$$

$$\chi^2_{ij} = \sum \left(\frac{(q_d(t)-q_a(t))-(q_b(t)-q_c(t))}{\sqrt{2}\,\sigma} \right)^2$$

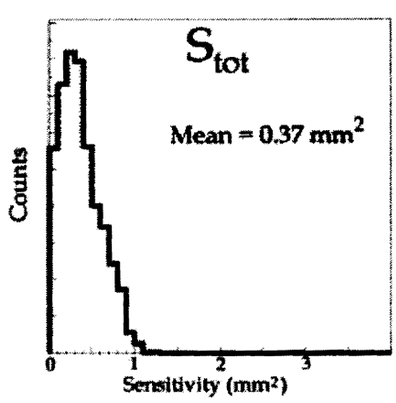

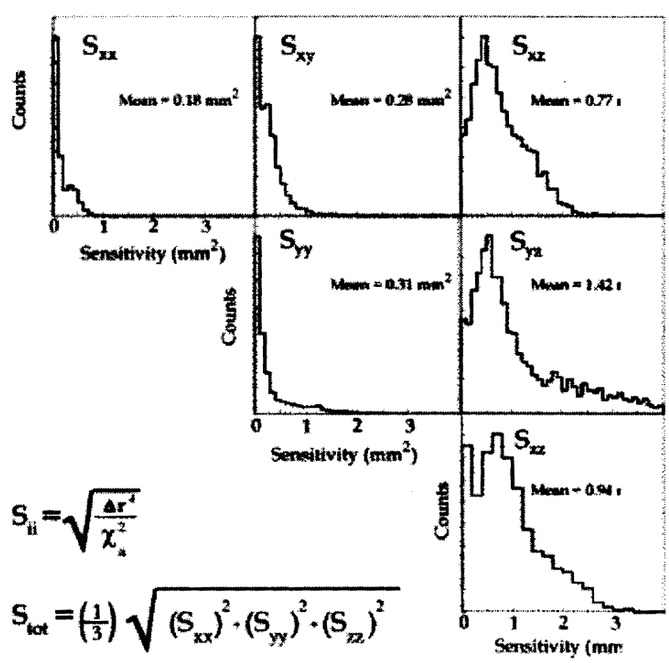

$$S_{ii} = \sqrt{\frac{\Delta r^2}{\chi^2_{ii}}}$$

$$S_{tot} = \left(\frac{1}{3}\right)\sqrt{(S_{xx})^2 + (S_{yy})^2 + (S_{zz})^2}$$

Signal decomposition of multiple interactions in one segment

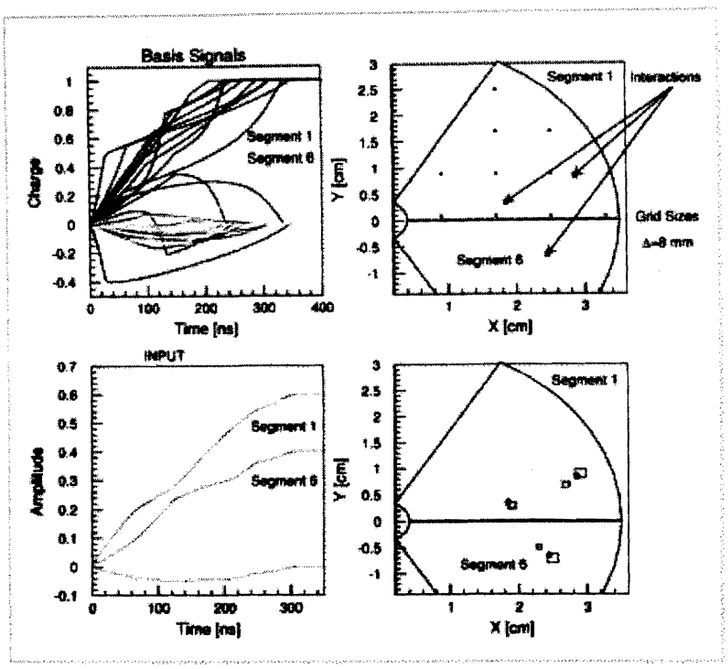

- Calculate signal in each segment for interactions on a grid ➔ base signals
- Decompose the composite signal into a linear combination of base signals
- Interpolate to improve position resolution

Signal decomposition

Singular Value Decomposition Method

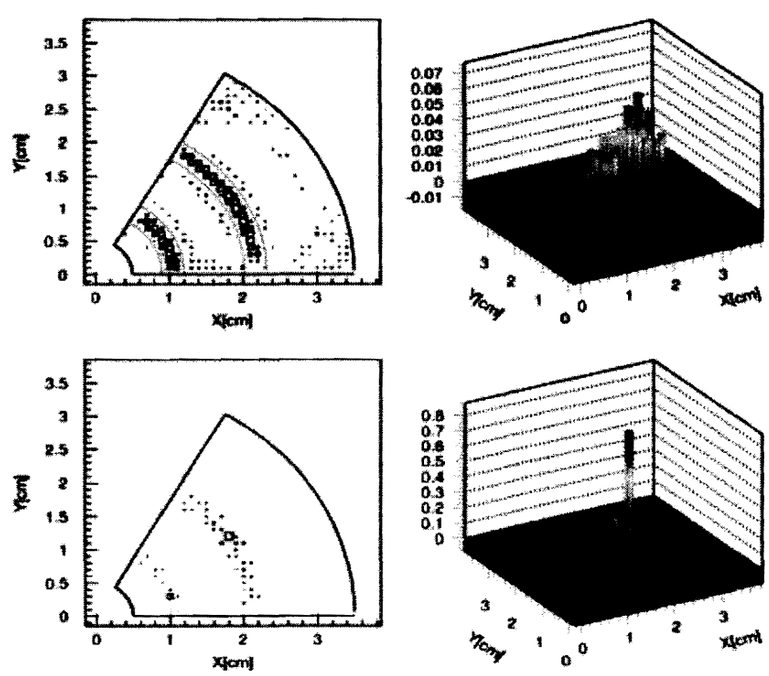

Proof of Principle 3: Tracking of interaction points

first step – cluster finding

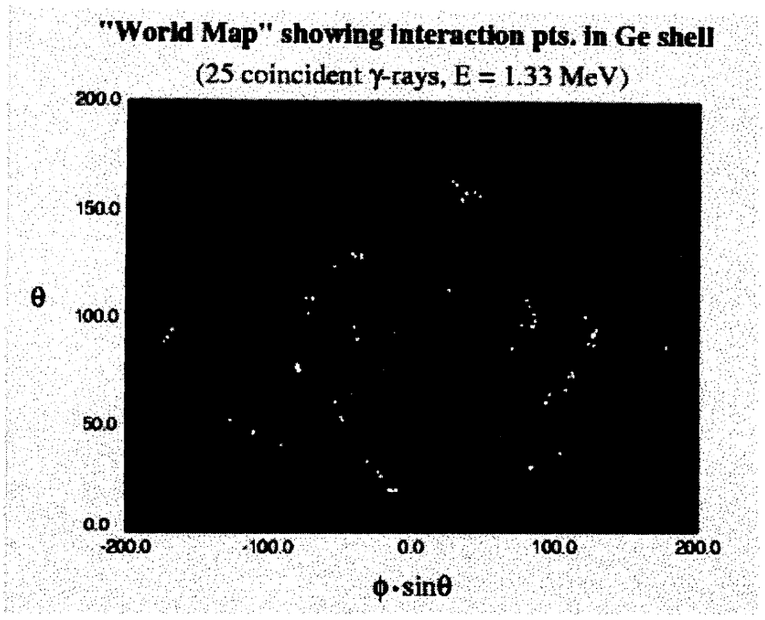

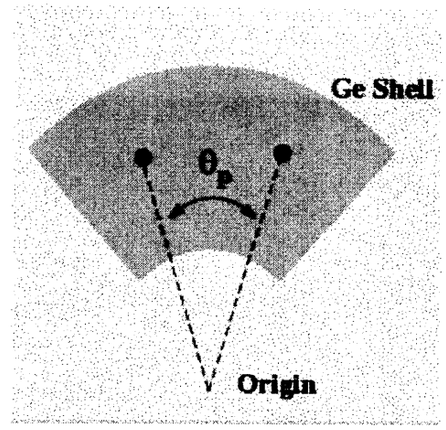

Any two points with $\theta < \theta p$ are grouped into the same cluster

Tracking of Compton scattering interaction points

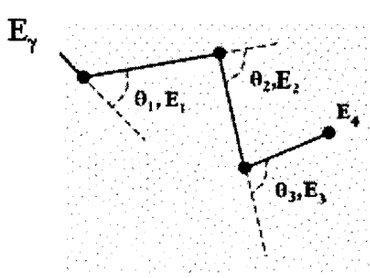

$$E_e = E_\gamma \left(1 - \frac{1}{1 + \frac{E_\gamma}{0.511}(1 - \cos\theta)} \right)$$

Problem: 3!=6 possible sequences

Assume $E_\gamma = E_{e1} + E_{e2} + E_{e3}$

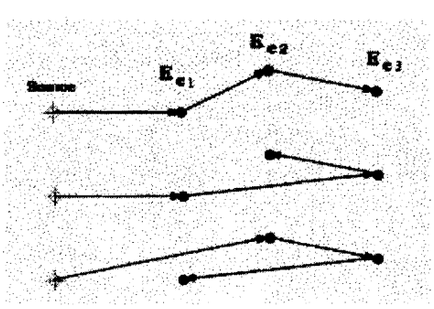

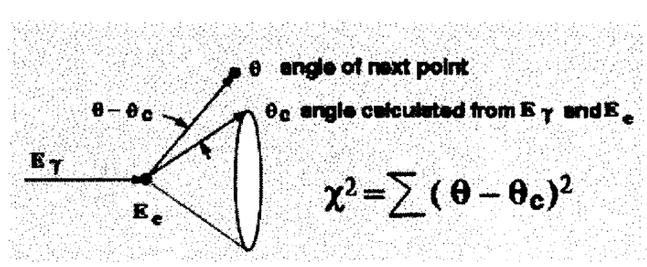

Sequence with the minimum χ^2

Tracking Results

G.J. Schmid *et al*, Nucl. Instr. Meth A 430 (1999) 69

0.1 MeV < E_γ <5 MeV : Compton Effect dominant

"Compton Tracking"

Cluster generation → Tracking →Split/Add/Split-add

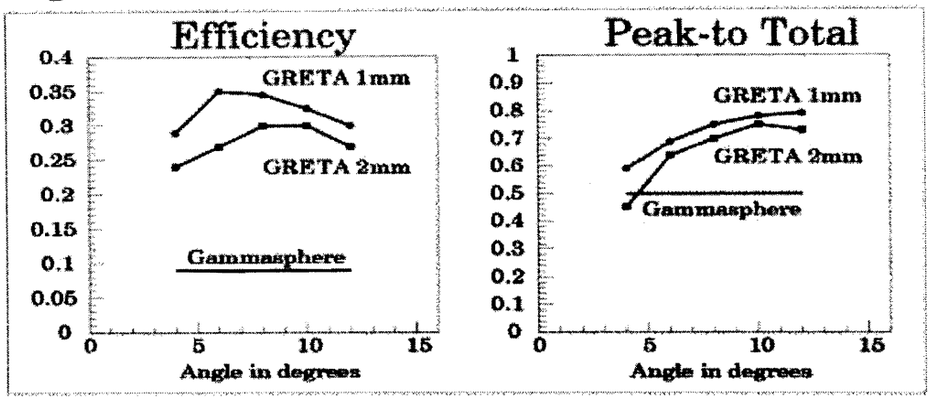

→ *Tracking efficiency about 50%*

Tracking Results

E_γ > 5 MeV : Pair Production dominant

"Pair Tracking"

T. Teranishi and N. Aoi

First hit recognition → Tracking 0.511's

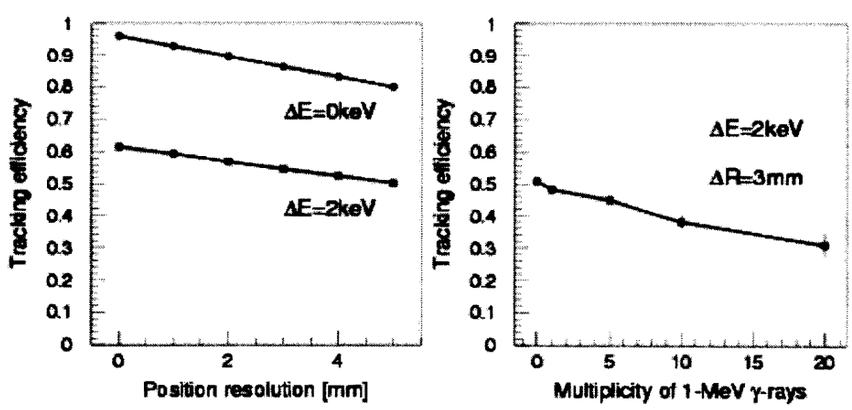

Tracking efficiency about 50%

Time resolution from digital processing

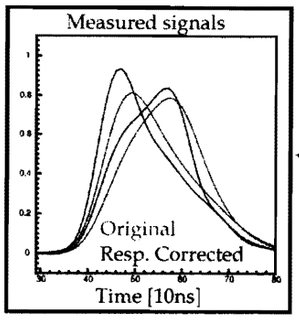

Digitizer: Gagescope 12bit 100MHz
Signals: Fast output of Gammasphere detector vs. BaF detector

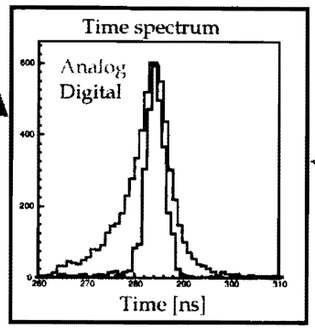

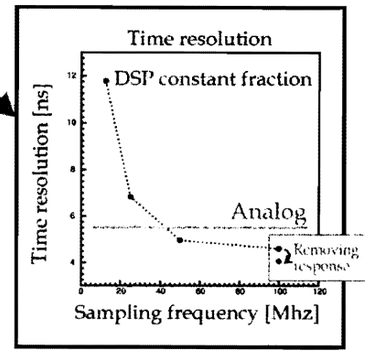

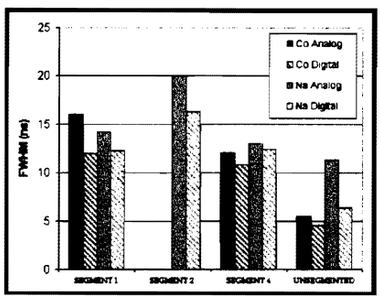

Time resolution of segmented (GRETA) vs. non-segmented (Gammapshere) Ge detector

GRETA in-beam test

^{129}Xe + ^{12}C, 600 MeV

Coulomb excitation ^{129}Xe, fusion evaporation ^{138}Nd

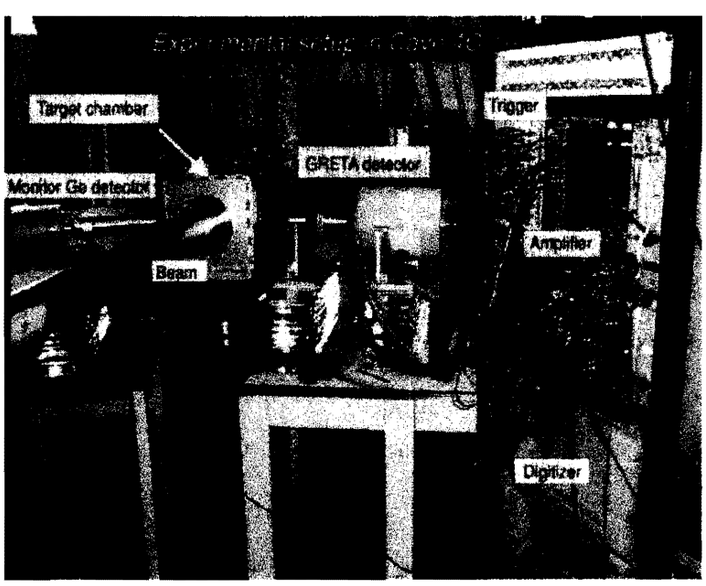

Schematic setup (top view)

Monitor Ge spectrum

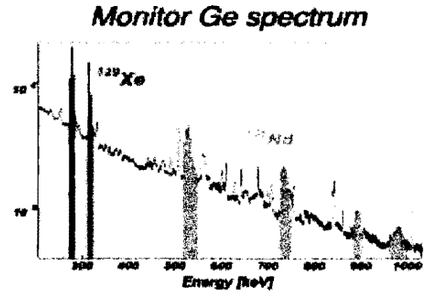

Future R/D plan

- Triple detector cluster module
- Pulse shape digitizer electronics
- Signal processing computer
- Signal processing algorithm

Detector Prototype

Triple Detector Cluster Module

Design completed

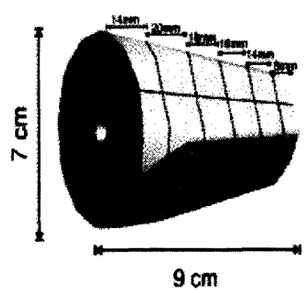

B-C-D Cluster

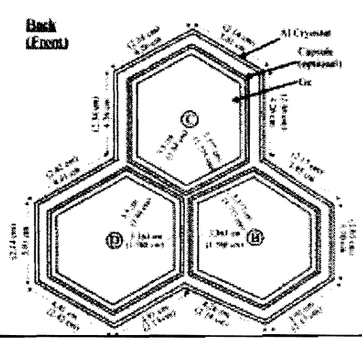

- Close pack of detectors
- Tracking across detectors

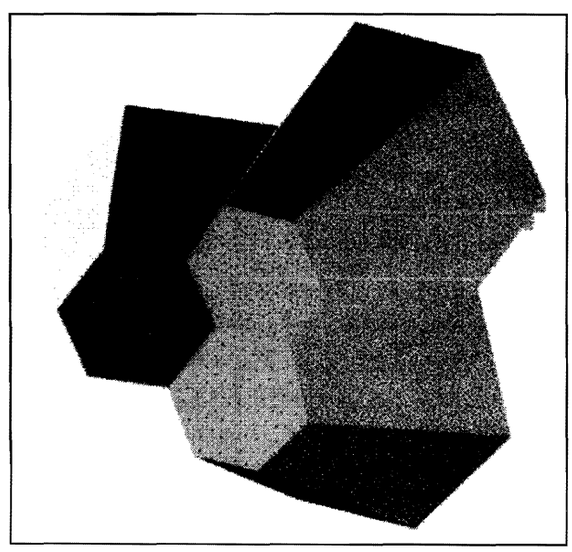

Electronics Developments

Pulse Shape Digitizer

Prototype available for testing in 2 months

- Sampling rate = 100 MHz
- Resolution = 12 bits

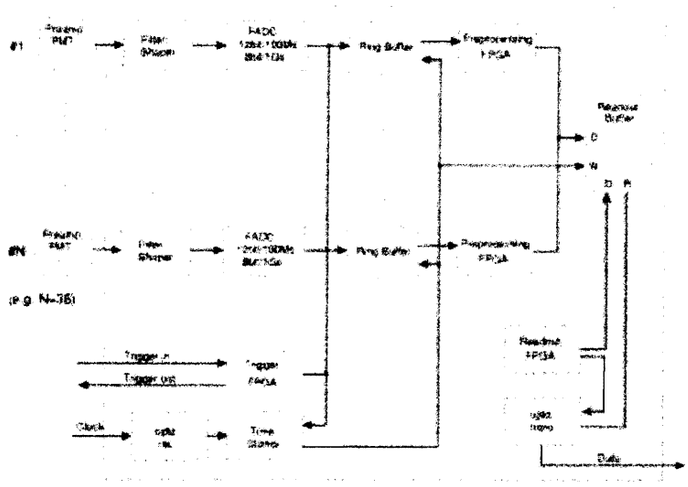

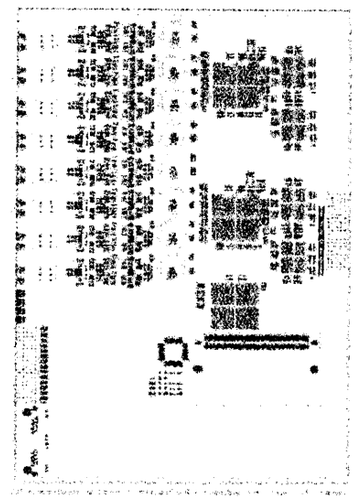

Tracking Detector Schedule

Preliminary 9/01

Calendar year	2001	2002	2003	2004	2005	2006	2007	2008
CD0 (Mission needs)								
CD1 (Baseline Range)								
Req. FY03 PED funds								
PED								
CD2 (Performance baseline)								
Req. FY05 Construction funds								
PED (final)								
CD3 (Approve construction)								
Start construction								
3-detector module		***#1***	***#2, 3***					
Pulse digitizer electronics								
Signal processing computer								
Signal processing algorithm								
Number of modules			1	3	7	17	27	40

U.S. Gamma-Ray Tracking Steering Committee for Nuclear Structure Physics

- Con Beausang, *Yale University*
- Doug Cline, *University of Rochester*
- Thomas Glasmacher, *Michigan State University*
- I-Yang Lee, *Lawrence Berkeley National Lab.*
- C. Kim Lister, *Argonne National Laboratory*
- David Radford, *Oak Ridge National Laboratory*
- Mark Riley, *Florida State University*
- Demetrios Sarantites, *Washington University*

History and organization of the U.S. gamma-ray tracking effort

- 1995 Duke Town meeting first discussion
- 1997 First prototype received and tested
- 1998 Workshop on GRETA physics (LBNL)
- 1998 Workshop on experimental equipment for RIA (LBNL)
- 1999 GRETA advisory committee formed
- 1999 Second prototype received and tested
- 2000 Workshop on GRETA physics (MSU)
- 2000 Proposal for a GRETA module cluster submitted
- 2001 National Steering Committee for Gamma-ray tracking in Nuclear Structure Physics formed
- 2001 Workshop on Digital Electronics in Nuclear Physics (ANL)
- 2001 Workshop on Gamma-ray tracking detectors for nuclear science (Lowell)

Conclusions

- **Gamma-ray tracking is a qualitatively new concept which advances detection sensitivity by three orders of magnitude.**
- **A gamma-ray tracking array yields immediate discovery potential at current stable and exotic heavy-ion beam facilities.**
- **The efficiency of a fully-implemented gamma-ray tracking array is a must for any facility where beam time is at a premium, such as RIA.**
- **The gamma-ray tracking concept has brought together scientists from different areas into one well organized community.**
- **There are no show stoppers in gamma-ray tracking detector technology.**

Gamma Ray Energy Tracking Array

END

The Advanced Gamma tracking Array AGATA

J. Gerl (GSI Darmstadt, Germany) for the AGATA collaboration

Any array designed for γ spectroscopy of very exotic nuclei must combine the highest possible efficiency, selectivity and energy resolution with a simultaneous capability to handle total γ-ray multiplicities of up to M_γ=30. The instrument must also accept a wide range of beam velocities (from stopped to $\beta \approx 50\%$) and must function in high γ and particle background levels. These features can only be achieved with a closely packed arrangement of Ge detectors, which allows the "tracking" [Lie01] of the detected γ quanta, i.e. the possibility to detect the energy, time and position of the interactions of individual γ quanta throughout the detector volume. This requires a large solid angle (4π) shell of highly segmented Ge crystals, with properties such as those detailed in table 1.

The on-going research on γ-ray detection arrays [Ger00] has led to the proposal of **AGATA,** the **A**dvanced **GA**mma **T**racking **A**rray [AGA01]. The geometrical structure of AGATA is based on the geodesic tiling of a sphere (inner diameter 17 cm) with 12 regular pentagons and 180 slightly irregular hexagons. The total number of segments in the array is 6780, which provides the optimum position sensitivity. The total solid angle covered by germanium material is close to 80% of 4π.

An AGATA detector module contains three 36-fold segmented Ge detectors of hexagonal, tapered shape. To improve reliability, each individual Ge detector is encapsulated in an aluminum can – a new technology developed in the framework of the Euroball [Sim97] and Miniball [Ebe97] projects. The preamplifiers consist of a cold part including the FETs mounted inside the cryostat and a warm part behind the Ge detectors. Highly integrated digital pulse processing electronics is mounted in a second layer behind the preamplifiers. The data are transferred via a fiber-optic channel for further analysis.

The AGATA electronics will be based on digital signal processing, by which the preamplifier output is sampled and digitized with fast ADCs to record the time evolution (shape) of the signals. From the signal detected in a segment and the mirror charges observed in its neighbours the interaction position of a γ ray can be determined with an accuracy of 1-2 mm. Digital processing electronics, placed directly adjacent to the detectors, will extract energy, timing and interaction positions from the sampled signals. Each data item will be time stamped, allowing later event reconstruction as well as the construction of delayed coincidences without dead-time problems. In addition, software triggering will be implemented, providing an easily configurable and flexible event filter, especially important for rare events.

With the help of sophisticated computer tracking algorithms to disentangle the event information, the resultant increase in effective detector granularity allows a precise reconstruction of the γ event including emission angle. Apart from the superior ability for geometric characterization of the events (e.g. Doppler corrections) leading to improvements in resolution, the maximum counting rates of the detector system is also greatly increased.

Table 1: *Basic properties of AGATA*

Photopeak efficiency	(E_γ=1 MeV, M_γ=1, β<50%)	50%
	(E_γ=1 MeV, M_γ=30, β<50%)	25%
	(E_γ=10 MeV, M_γ=1)	10%
Peak/Total ratio	(M_γ=1)	> 60%
Angular resolution $\Delta\theta_\gamma$	($\Delta E_\gamma / E_\gamma$<1%)	< 1°
max. event rate	(M_γ=1)	3 MHz
	(M_γ=30)	0.3 MHz

[AGA01] AGATA - Technical Proposal, ed. J. Gerl and W. Korten, GSI Darmstadt 2001.

[Ebe97] J. Eberth et al., Prog.Part. Nucl.Phys. Vol. 38(1997) 29.

[Ger00] J. Gerl, Nucl. Instr. Meth. A442 (2000) 238.

[Lie01] R.M. Lieder et al. Nucl. Phys. A682 (2001), 279c.

[Sim97] J. Simpson, Z.Phys. A358 (1997) 139.

Future of Nuclear Spectroscopy?

The Nucleus at its Limits!

- **Structure far off Stability**
- **Shape and Spin Response**
- **Nucleosynthesis**
- **Fundamental Interactions**
- **Hypernuclear Structure**

AGATA

Advanced GAmma Tracking Array

J. Gerl

for the
AGATA Collaboration

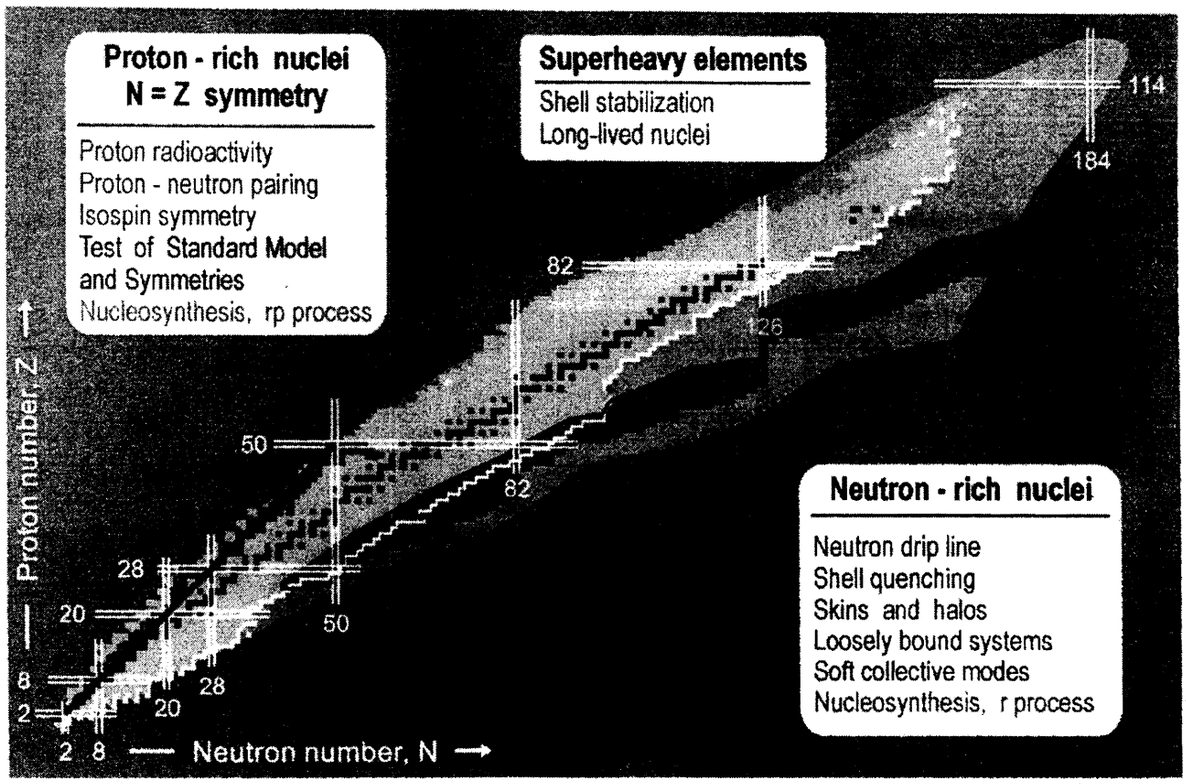
Proton - rich nuclei
N = Z symmetry
Proton radioactivity
Proton - neutron pairing
Isospin symmetry
Test of Standard Model
and Symmetries
Nucleosynthesis, rp process
Superheavy elements
Shell stabilization
Long-lived nuclei
Neutron - rich nuclei
Neutron drip line
Shell quenching
Skins and halos
Loosely bound systems
Soft collective modes
Nucleosynthesis, r process
Proton number, Z
Neutron number, N
2
8
20
28
50
82
126
114
184

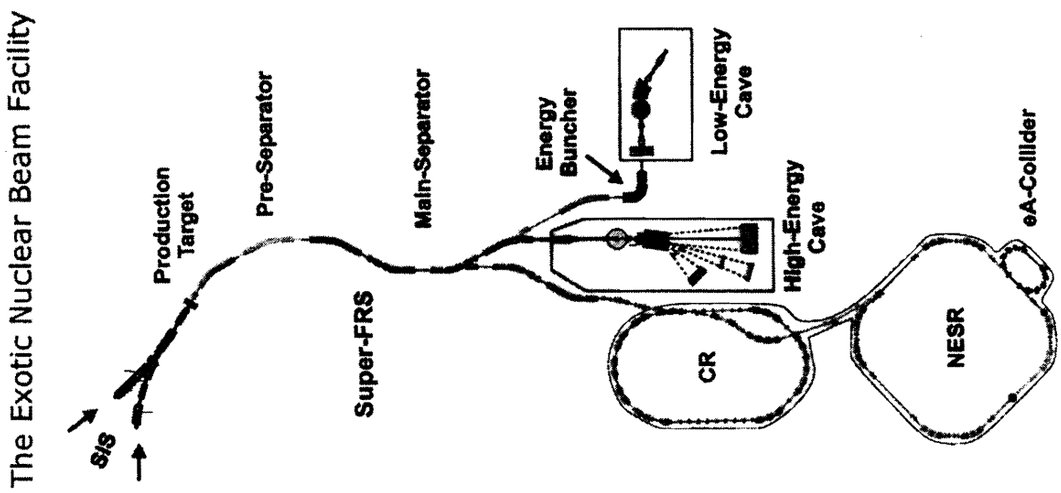
The Exotic Nuclear Beam Facility
SIS
Production Target
Pre-Separator
Super-FRS
Main-Separator
Energy Buncher
Low-Energy Cave
High-Energy Cave
CR
NESR
eA-Collider

RISING Experiments

<u>Fast beams at ≥ 50 A MeV</u>

- Coulex
- Secondary fragmentation
- g-factors

<u>Slow beams at 4-10 A MeV</u>

- Multiple Coulex
- Transfer
- Compound reactions

<u>Stopped, low-intensity beams with ≤ 1/s</u>

- β-decay
- Isomer spectroscopy
- Nuclear moments

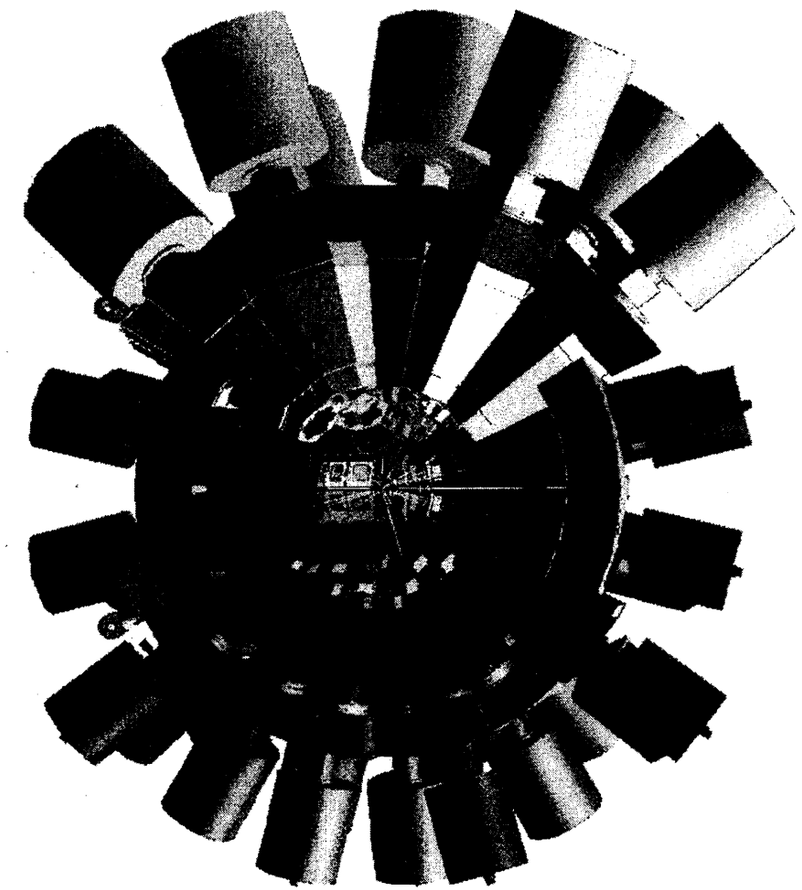

Targets at relativistic energies

Thick targets compensate for low beam intensities.

5 MeV/u: 1 mg/cm^2

100 MeV/u: 500 mg/cm^2

Target thickness: >1g/cm^2 @ 100 MeV/u

→ $\Delta v/c \geq 1$ %

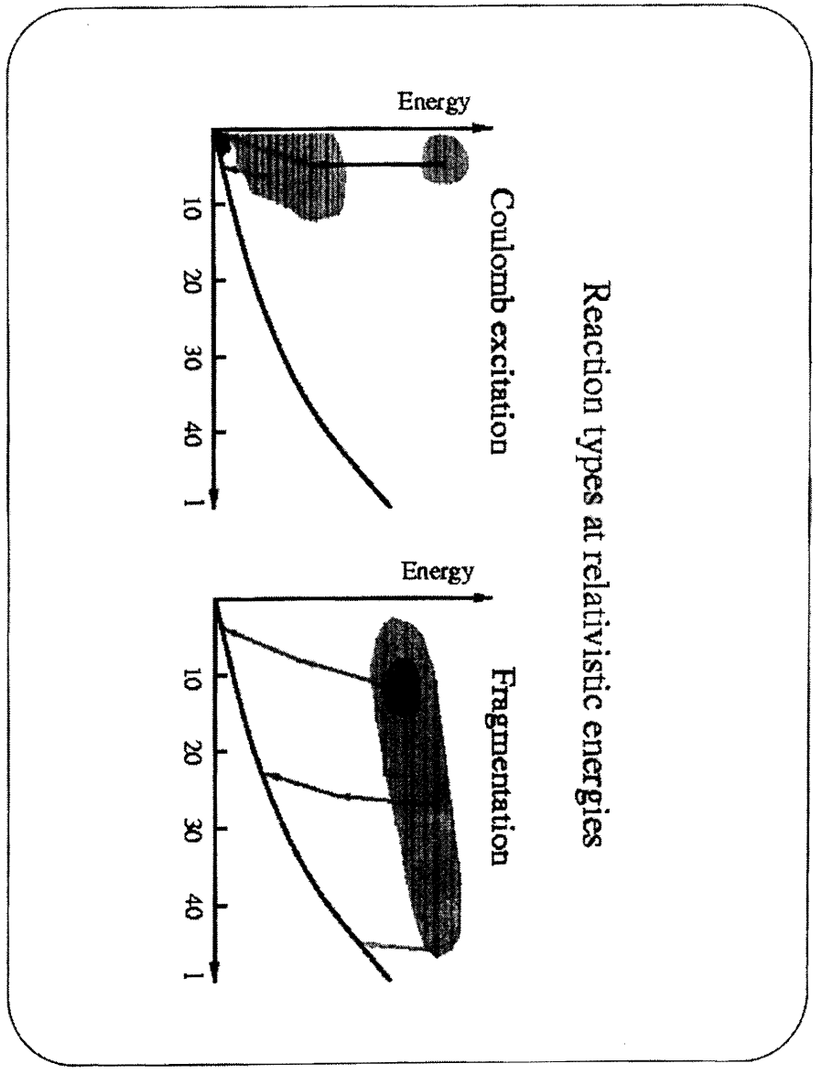

Rising fast set-up

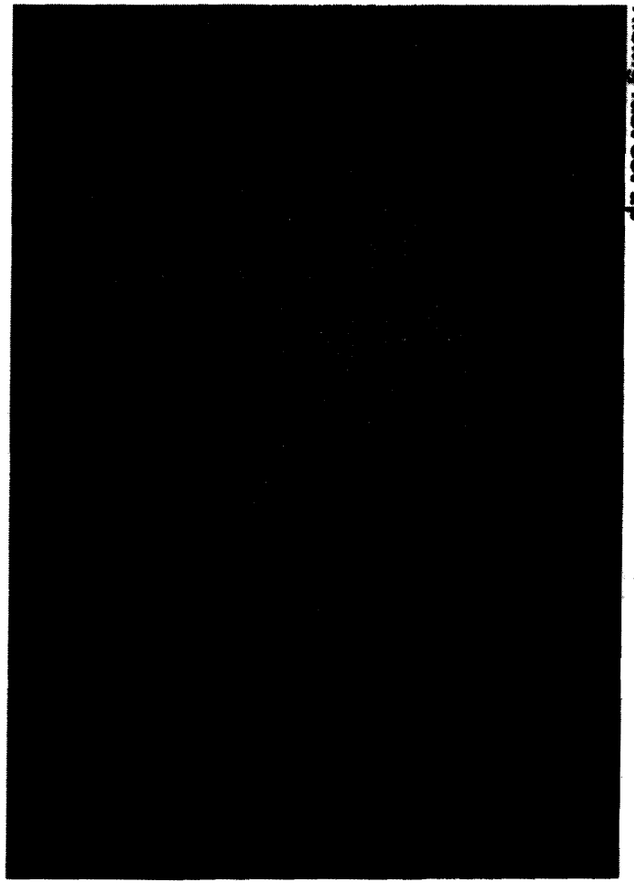

$^{43}Ar + ^{208}Pb$, E_{lab} = 222 AMeV, β = 0.59

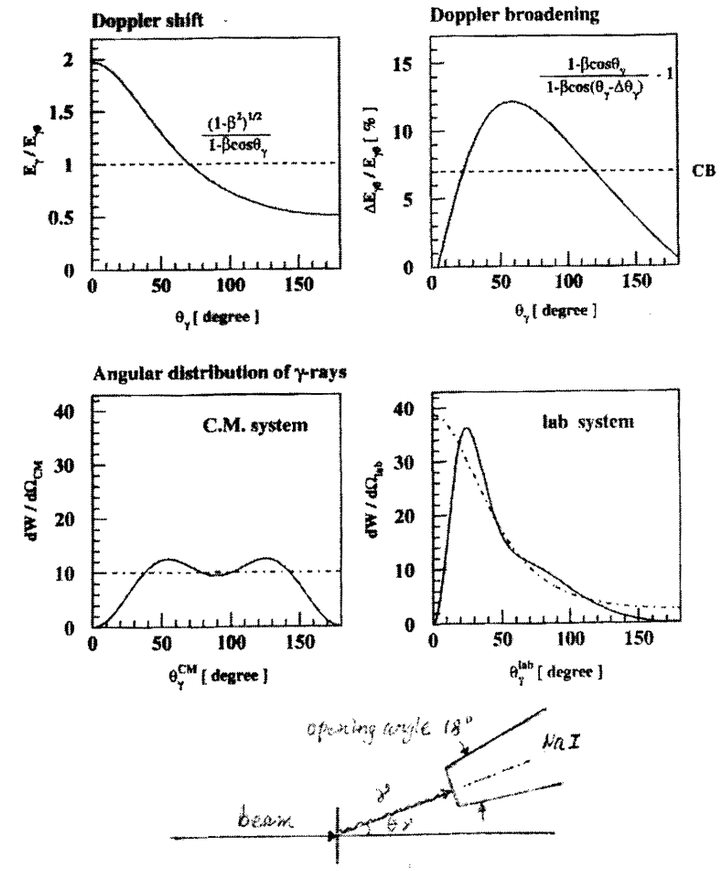

Compound systems accessible with 132Sn

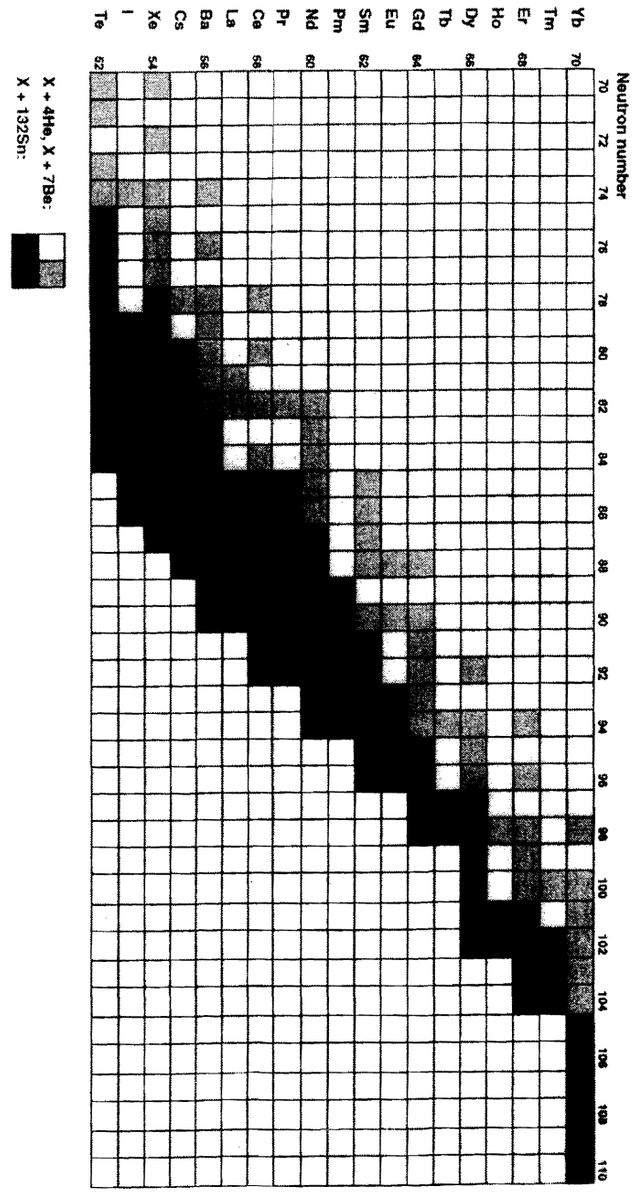

$^{43}Ar \rightarrow Pb \rightarrow {}^{42}Ar$

$E = 200\ MeV/u$

Crystal Ball

$\Delta E_\gamma \approx 12\%$

(S. Wan et al. GSI)

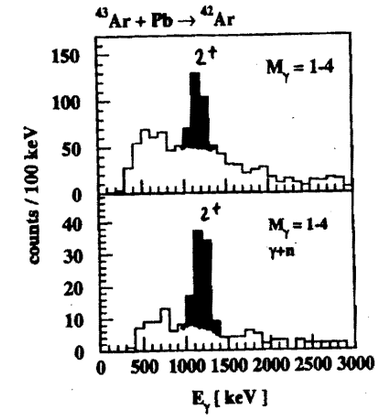

$^{36}S \rightarrow Be \rightarrow {}^{32}Mg$

$E = 77\ MeV/u$

Ge - Clover

$\Delta E_\gamma \approx 2\%$

(M. Belleguic IPNO)

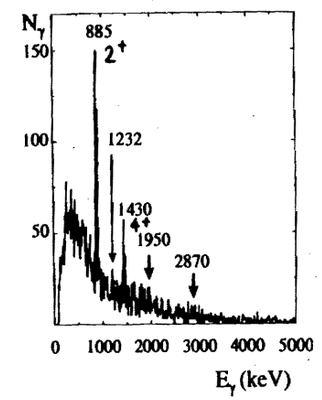

Ge-detector set-ups

Requirements

- Maximal efficiency
- High granularity
- Good peak-to-total ratio

Conditions

- High multiplicity ($M_{det} \leq 30$)
- High emitter velocity ($\beta \leq 50\%$)
- Large beam spot size (< 15 cm)
- Limited space
- Radiation background

A possible Stopped beam configuration?

15 Clusters at 205mm, 10 at ±48° and 5 at 90°
ε_γ ~18% at 1.3 MeV.

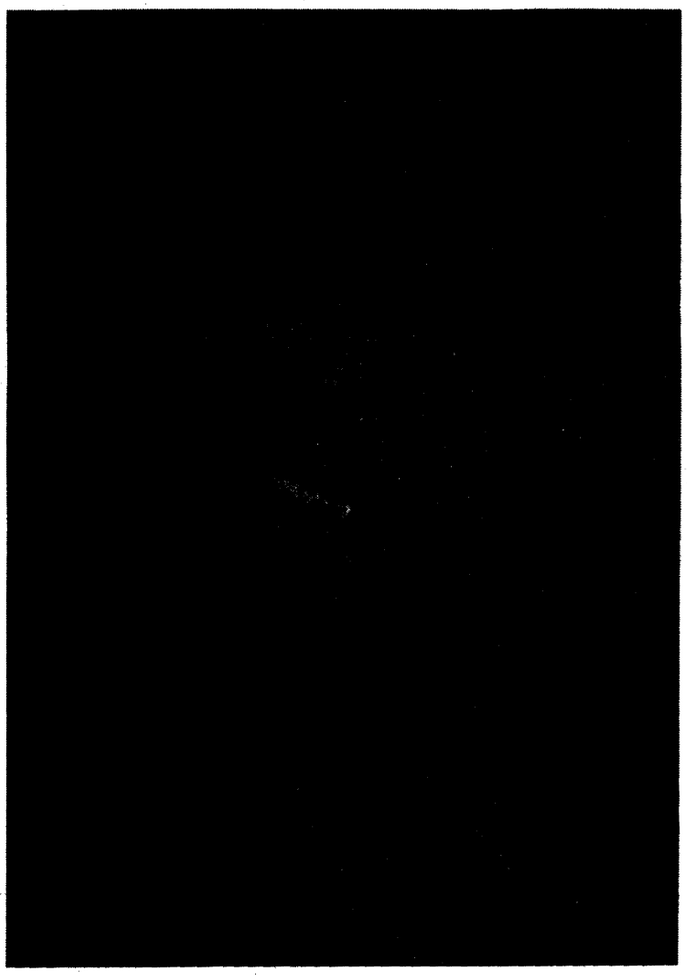

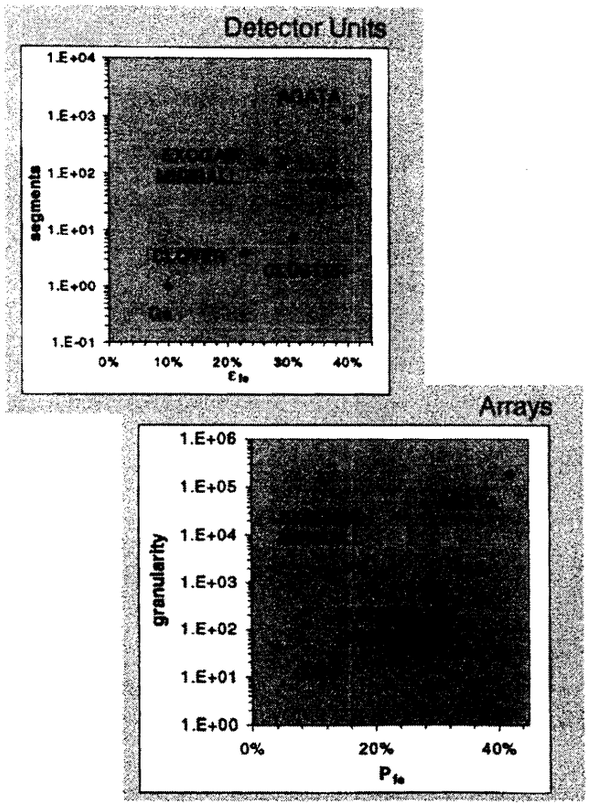

Efficiency and Selectivity

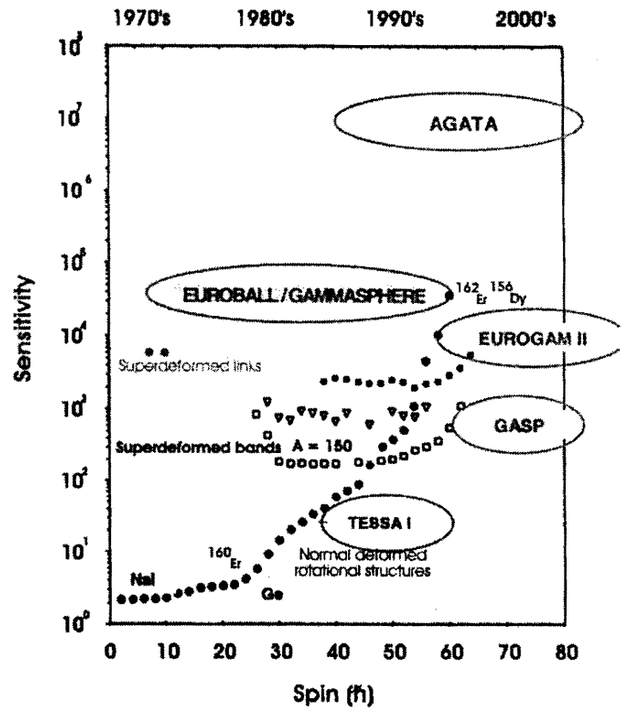

Limit of observation at high angular momentum

Is function of (see the figure) :

- **the photopic efficiency $\varepsilon_p \omega$**
- **the resolving power**
  PR = P/T x δE / ΔE

for M=30 :

	EUROBALL	→	AGATA
fold	**4**	→	**6**
$(\varepsilon_p \omega)^f$	**$1.8\ 10^{-5}$**		**$8.6\ 10^{-5}$**
$(PR)^f$	**$5.7\ 10^4$**		**$6.1\ 10^6$**
limite d'obs.	**10^{-4}**	→	**a few 10^{-7}**

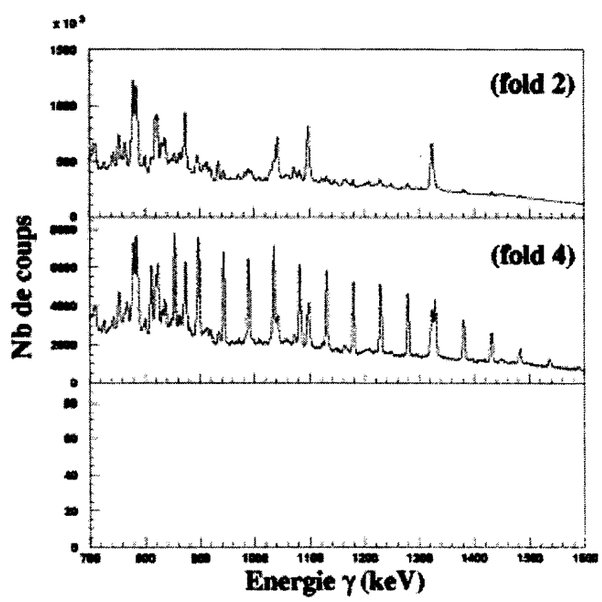

Intensity and peak to background ratio for the gamma spectrum of the ^{151}Tb yrast yrast superdeformed band as a function of the coincidence fold

Scattering volume

R = 8 cm , d = 8 cm

$N_\gamma > 1$, $N_p > 1$ } Multiple hits

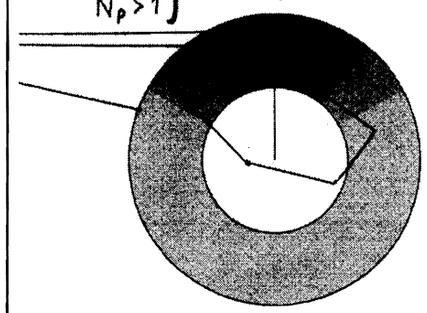

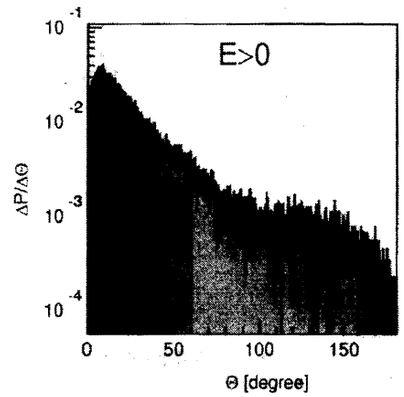

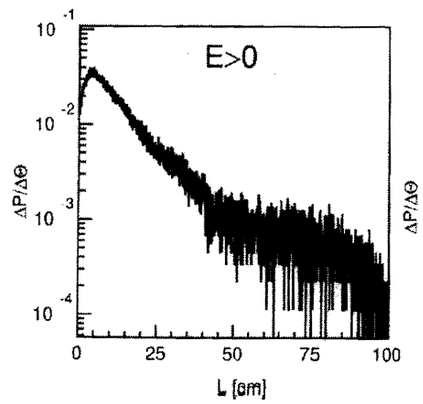

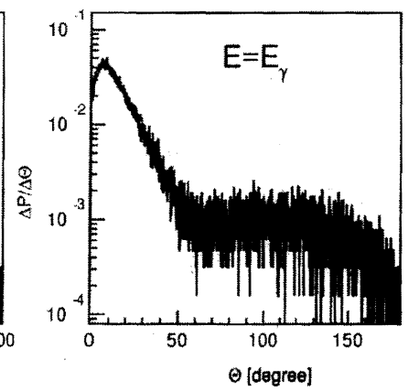

- high granularity
- interaction positions

} Tracking

Shell Thickness

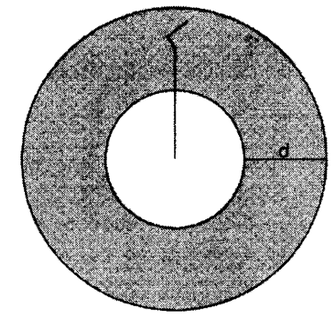

E_γ = 1.33 MeV

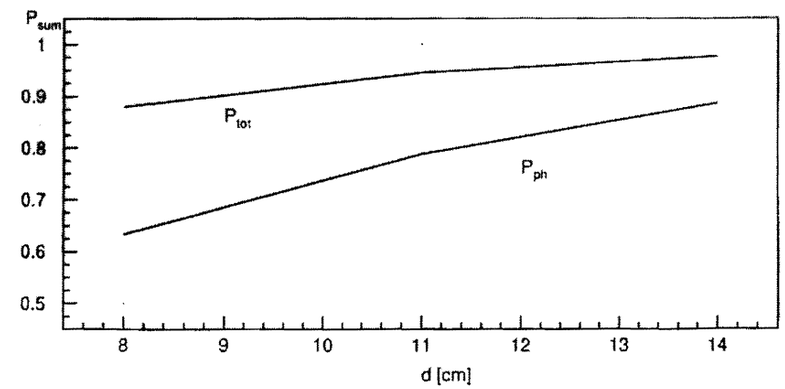

Gamma « tracking » basic elements (1)

➢ **EUROBALL / GAMMASPHERE**

Ge crystals surrounded with BGO anti-Comptonshields

(P/T increased to ≈ 0,5)

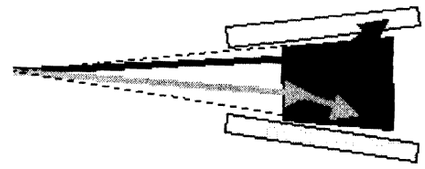

➢ **Multidetectors of the future :**

- increase of the photopic efficiency by :
  - increase of the angular coverage by a factor 2
  - add-back of the energies deposit in several detectors by the same gamma-ray
- P/T ratio equal or better than the present ~ 0.5 value

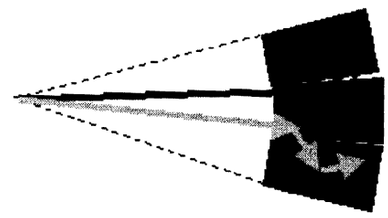

→ **will need a high segmentation of the Ge crystals to be able to measure with accuracy the main characteristics of the interaction points (energy relaxed and scatering angle)**

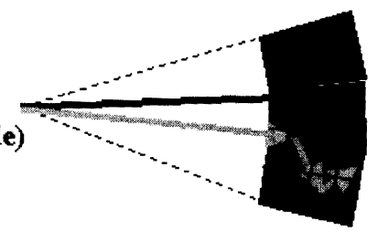

Gamma « tracking » basic elements (2)

➢ **Compton scattering equation**

$$E_{\gamma_{i+1}} = \frac{E_{\gamma_i}}{1 + \frac{E_{\gamma_i}}{m_0c^2}(1 - \cos\theta))}$$

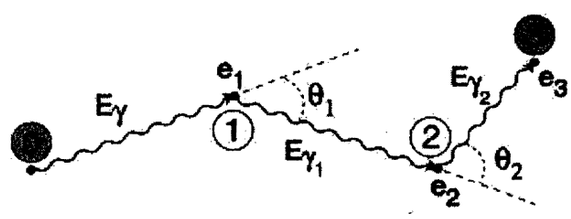

gamma path reconstruction with the help of the scattering équation

➢ **Clusterisation**

$$E_\gamma = E_\Sigma = \Sigma_i e_i$$

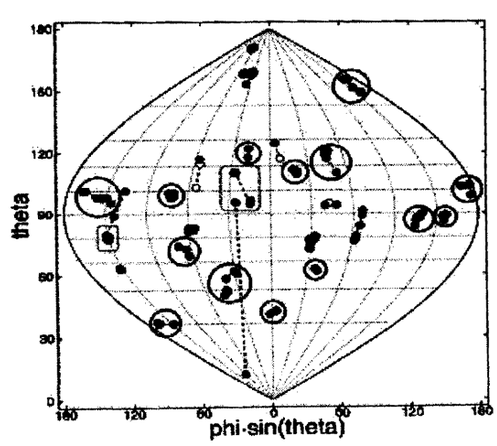

Good event selection

- Logical relations
- Correlations: E – t, t – t, E – E, t – pos.,
  E – pos., pos. –pos., ...
- Multiplicity: Gamma(t), Anc. det.(t)
- Total energy
- "Higher order" criteria

On-Line capabilities

- Pos. determination
- Multiple hit determination
- Arithmetic operations (calib., Doppler, etc.)
- Total event storage: >90% or > 50 kHz
- Good event storage: >90%
- Good event analysis: >90% or > 1 kHz
- Data visualisation
- Remote detector and electronics control
- Easy-to-use experiment control

AGATA Electronics requirements:

Gamma detectors

6840 channels; E, t, pos.
Dynamic range: >15 bit
E-noise: < 500 eV
Dynamic range: >12 bit
Time jitter: <1 ns
xyz-pos.: pulse shape of real and mirror charges (on-line)

Heavy Ion detectors

≤ 30 channels E,t
≤ 60 channels t
Dynamic E range: >12 bit
Dynamic t range: >12 bit
Time jitter: < 0.2 ns ....< 1 ns

Ancillary detectors

≤ 500 channels E, t, (pos. ?)
≤ 500 channels t, (pos. ?)
Dynamic E range: >13 bit
Dynamic t-range: >12 bit
Time jitter: < 0.2 ns ....< 1 ns

MINIBALL Position Resolution

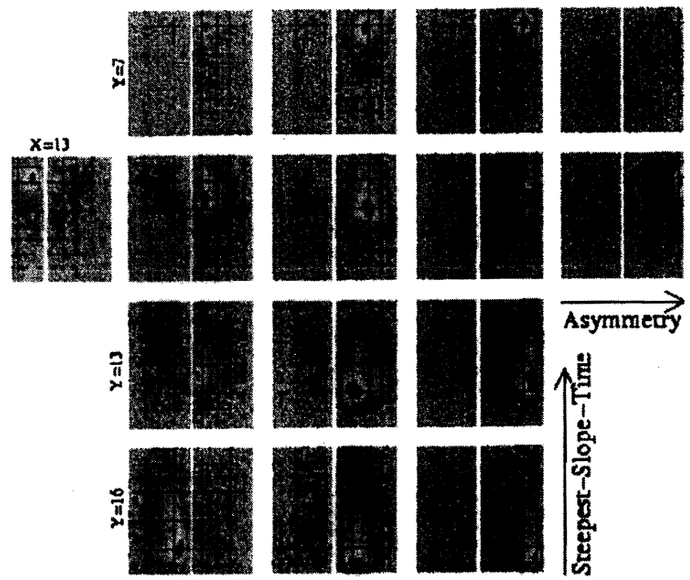

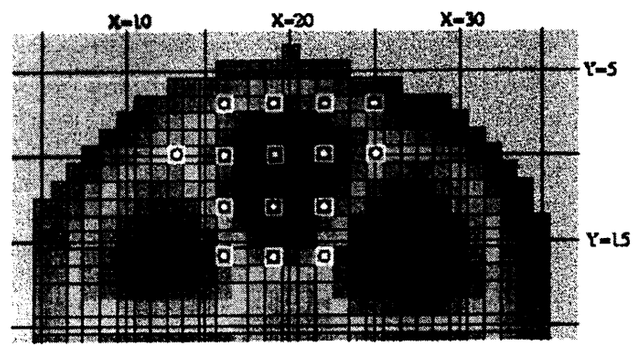

Ge-detector signals

Miniball detector element

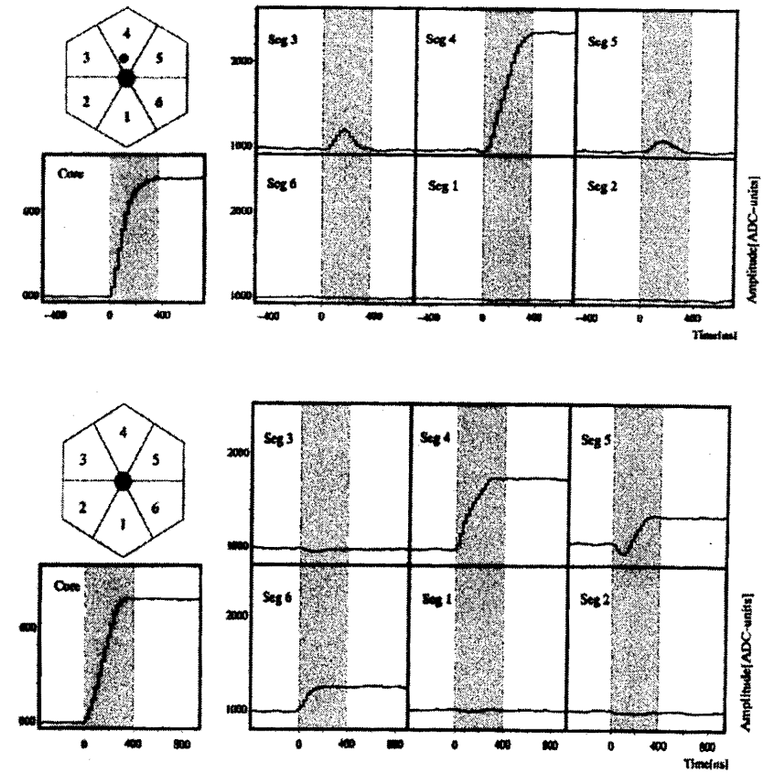

Efficiency of an ideal Ge shell

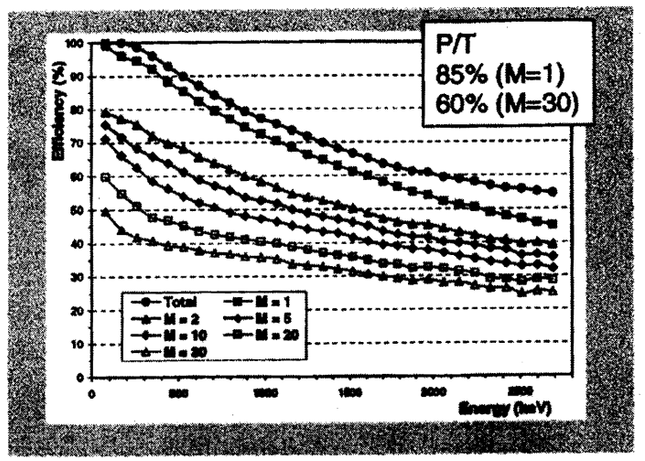

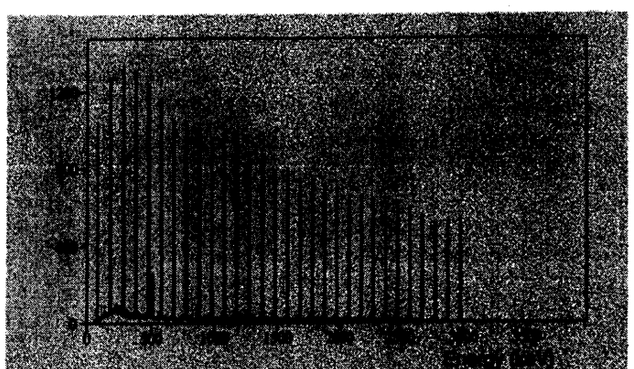

Reconstructed spectrum of a cascade of 30 equally spaced transitions detected in the standard shell.

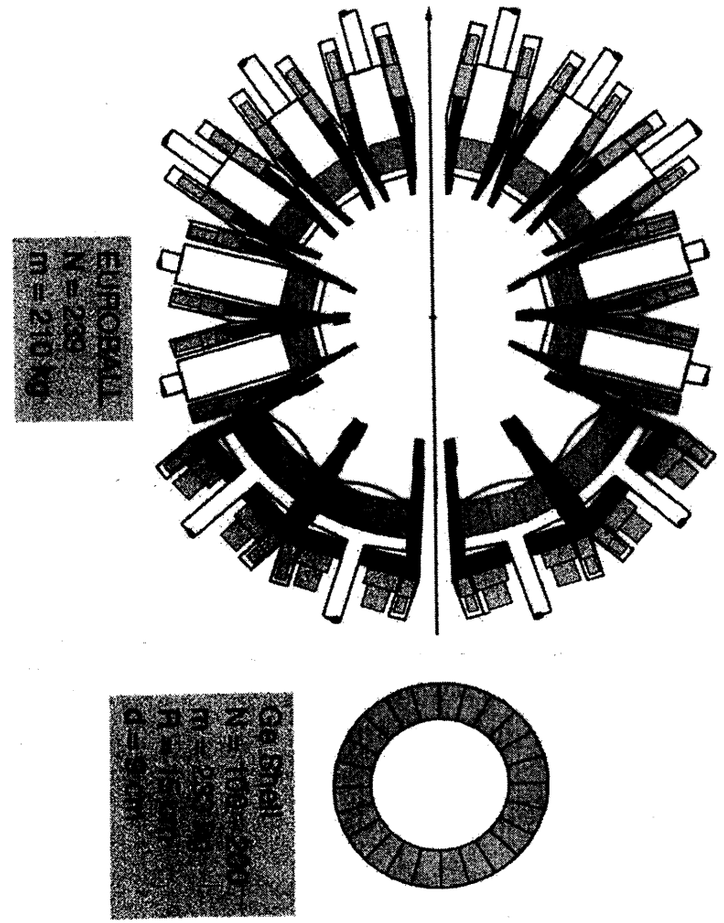

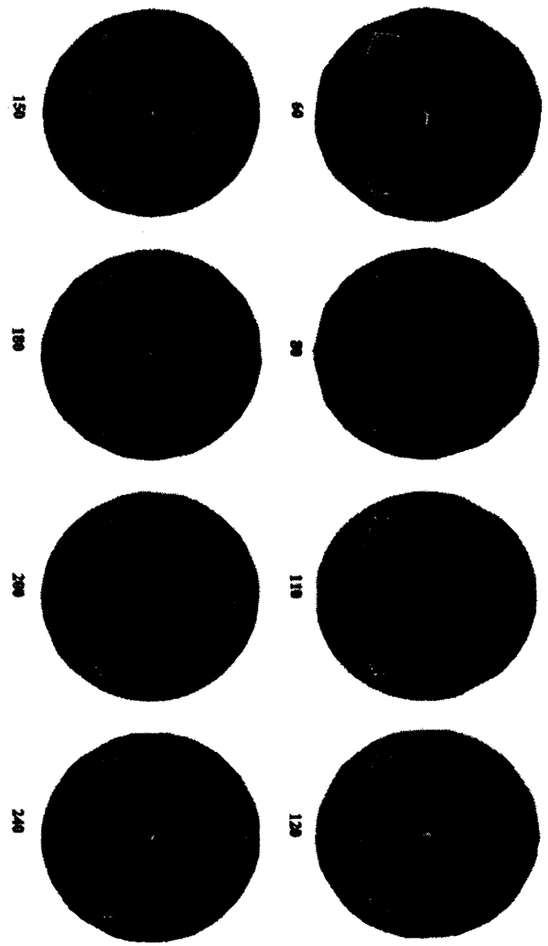

Performance at E_γ = 1.33 MeV for various 4π arrays built out of all-equal regular crystals

	Number of Detectors	Ge Mass (kg)	ε_{ph} [P/T] % M_γ=1	ε_{ph} [P/T]% M_γ=30
Standard shell		233	65 [85]	36 [60]
Ball	120	140	30 [56]	18 [50]
Barrel hexagons	36	90	25 [52]	12 [44]
cylinders		112	26 [56]	14 [50]
Barrel hexagons	54	135	30 [55]	15 [46]
cylinders		169	29 [58]	16 [48]
EUROBALL	239	210	9 [56]	6 [37]

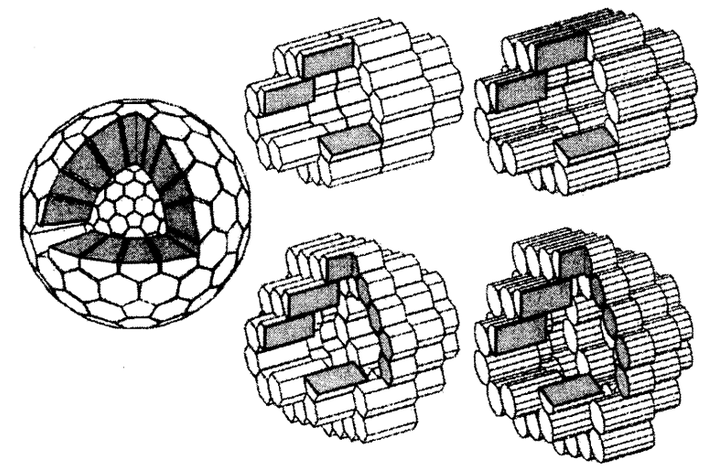

4π arrays built out of all equal, individually canned, regular Ge crystals

AGATA

Suggested design:

- Spherical Ge shell
- Velocity displaced target
- 192 detector units
- Hexagonal Det.: - 180 units
  - 36 fold segmented
  - encapsulated/coated
- Pentagonal Det.: - 12 units
  - 30 fold segmented
  - encapsulated/coated
- Ge coverage: ≈ 80%

Number of hexagons	Number of hexagonal shapes	Shell inner radius (cm)	Solid angle (%)	Amount of Ge (kg)	Cluster types
60	1 (60)	7.2	78.8	66	3
80	2 (20,60)	8.7	78.2	81	
110	3 (20,30,60)	11.4	78.5	116	
120	2 (60, 60)	12.8	78.1	139	2, 4, 6
150	3 (30,60,60)	15.1	78.6	171	
180	3 (60,60,60)	17.1	78.1	215	3, 9
200	4 (20,60,60,60)	18.0	78.3	232	10
240	4 (60,60,60,60)	20.9	78.7	295	

AGATA Detector Module

(1) three 36-fold segmented Ge detectors
(2) preamplifier
(3) frame support
(4) digital pulse processing electronics
(5) fiber-optics read-out
(6) LN_2 – dewar
(7) target position

Ge-crystals:
10 cm long, 8 cm diameter
tapered, hexagonal/pentagonal shape
encapsulated

AGATA configuration

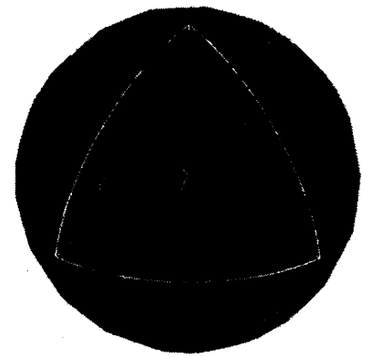

Crystal type	Ge diameter front (cm)	Ge diameter back (cm)	Crystal volume (cm^3)	Corresponding solid angle (%)
12 pent.	2.84	5.09	86.4	2.1
60 hex.	4.24	7.06	180.7	21.9
60 hex.	4.70	7.65	211.2	25.0
60 hex.	4.95	8.00	236.3	28.2

AGATA detector element

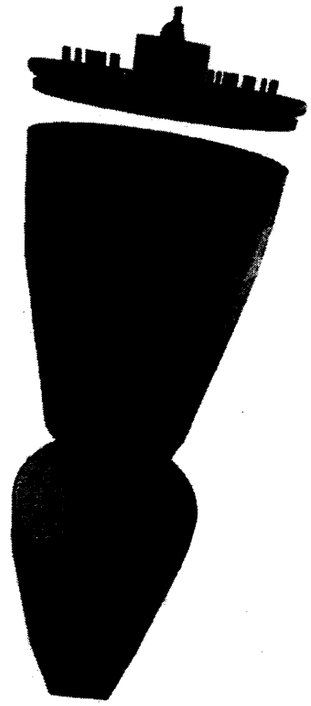

n-type Ge crystal
6x6 fold segmented
encapsulated

Segmented planar detector and difference in collecting time

Segmented planar detector

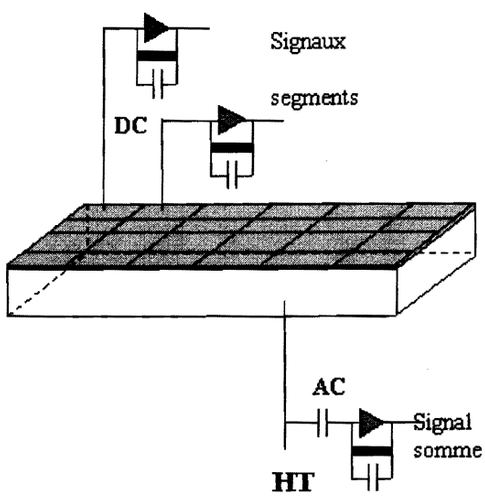

Difference in collection time

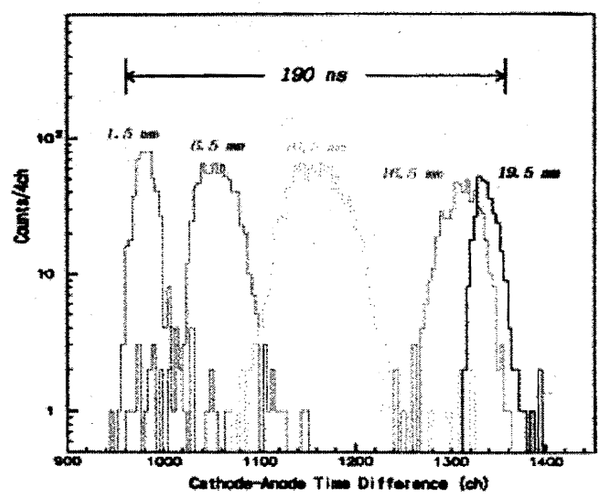

→ much easier to do an on-line collection time-interaction point correlation with planar detectors than with coaxial detectors

Planar Stack

IRES development

Position sensitive Ge planar stack detectors

1 prototype: 2 planar crystals, 3x3 + 4x4 segments
$\Delta E = 0.84\ (1.98)$ keV at 121 (1332) keV

Crystal Size: 120 x 75 x 20 mm^3
Segmentation: 4 x 4 strips
Unit: 4 crystals
Pulse shape analysis: depth information
Segment interpolation

⇒ 4π array

⇒ γ camera

Geometry for a 4π spectrometer with planar stacks

Basic planar stack : four planar detectors segmented 4 x 4 with a common anode by pair of crystals

64 + 2 = 66 electronic channels

4 π array : Château of 72 planar stacks

288 single planars 4 x 4 = 4608 segments

4608 + 144 = 4752 electronic channels

Good event selection

- Logical relations
- Correlations: E – t, t – t, E – E, t – pos.,
  E – pos., pos. –pos., ...
- Multiplicity: Gamma(t), Anc. det.(t)
- Total energy
- "Higher order" criteria

On-Line capabilities

- Pos. determination
- Multiple hit determination
- Arithmetic operations (calib., Doppler, etc.)
- Total event storage: >90% or > 50 kHz
- Good event storage: >90%
- Good event analysis: >90% or > 1 kHz
- Data visualisation
- Remote detector and electronics control
- Easy-to-use experiment control

AGATA Electronics requirements:

Gamma detectors

6840 channels; E, t, pos.
Dynamic range: >15 bit
E-noise: < 500 eV
Dynamic range: >12 bit
Time jitter: <1 ns
xyz-pos.: pulse shape of real and mirror charges (on-line)

Heavy Ion detectors

≤ 30 channels E,t
≤ 60 channels t
Dynamic E range: >12 bit
Dynamic t range: >12 bit
Time jitter: < 0.2 ns ....< 1 ns

Ancillary detectors

≤ 500 channels E, t, (pos. ?)
≤ 500 channels t, (pos. ?)
Dynamic E range: >13 bit
Dynamic t-range: >12 bit
Time jitter: < 0.2 ns ....< 1 ns

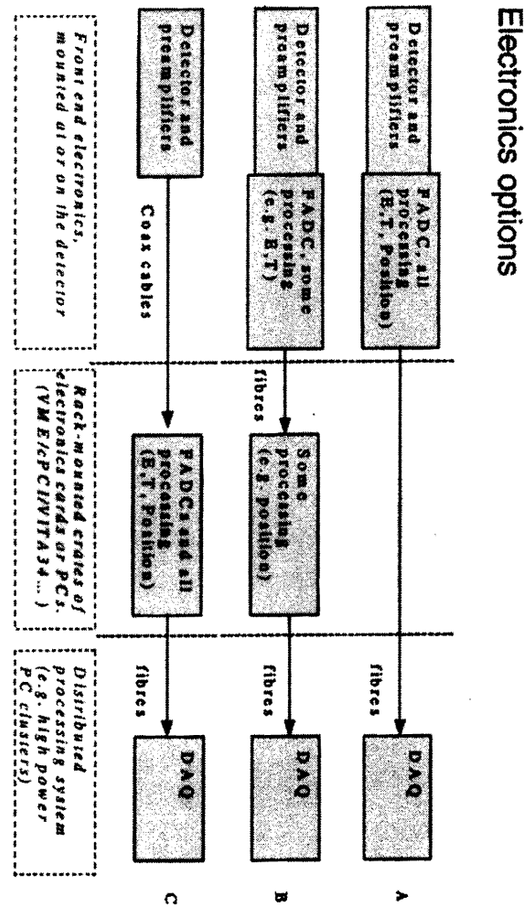

AGATA DACQ requirements:

Types of experiments

A) HI + Gamma + Anc. part.
N(HI): 10^5 ....10^7 /s
N(γ-evt.): 10^4 ....10^5 /s, M(γ): 1 30
N(Anc. part.-evt.) 10^0 ....10^5 /s, M(A.p.): 0 ..10
(prompt or prompt + delayed Gammas)

B) HI + delayed Gamma + delayed Anc. part.
N(HI): 10^{-2} ....10^4 /s
N(γ-evt.): 10^{-3}....10^4 /s, M(γ): 1 10
N(Anc. part.-evt.) 10^{-3}....10^4 /s, M(A.p.): 0 ..10
(prompt *background* Gammas)

C) Gamma + Anc. part.
N(γ-evt.): 10^4 ....10^6 /s, M(γ): 1 40
N(Anc. part.-evt.) 10^0 ....10^6 /s, M(A.p.): 0 ..10
(prompt or prompt + delayed Gammas)

Good event/Total event: 10^{-2} ....10^{-6} (10^{-9})

Option A electronics

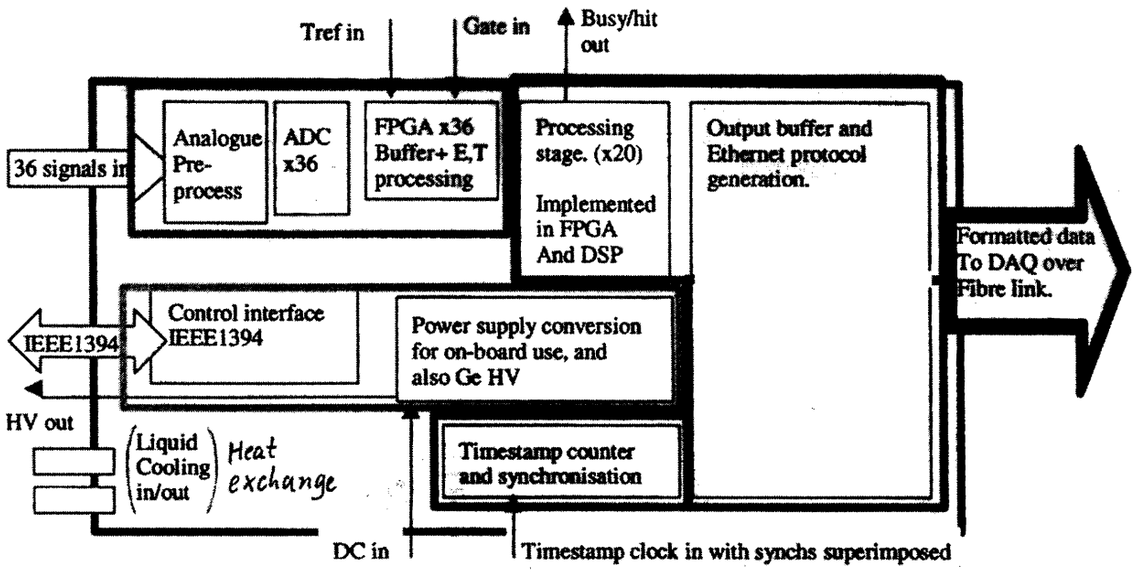

Option B electronics

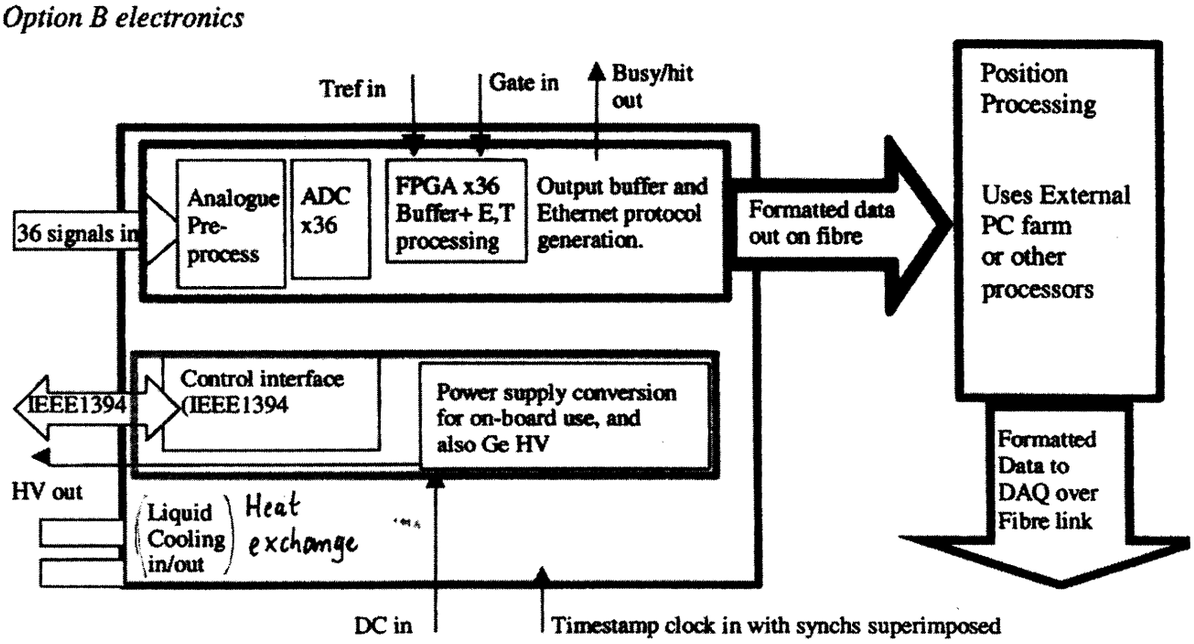

Basic properties as required for AGATA and compared to an ideal Ge shell

(Ideal shell: 9 cm thickness, 150 mm inner free radius)

Detector properties specified for		Ideal Ge-shell	AGATA
Efficiency (P_{fe})	$E_\gamma = 0.1$ MeV, $M_\gamma = 1$, $0 < \beta < 0.5$	100 %	> 70 %
	$E_\gamma = 1$ MeV, $M_\gamma = 1$, $0 < \beta < 0.5$	72 %	~ 50 %
	$E_\gamma = 10$ MeV, $M_\gamma = 1$, $0 < \beta < 0.5$	15 %	~ 10 %
	$E_\gamma = 1$ MeV, $M_\gamma = 30$, $0 < \beta < 0.5$	36 %	~ 25 %
Peak-to-total ratio (P/T)	$E_\gamma = 1$ MeV, $M_\gamma = 1$	85 %	60 – 70 %
	$E_\gamma = 1$ MeV, $M_\gamma = 30$	60 %	40 – 50 %
Angular resolution ($\Delta\theta_\gamma$)	$\Delta E/E < 1\%$	—	better than 1°
Maximum event rates	$M_\gamma = 1$	—	3 MHz
	$M_\gamma = 30$	—	0.3 MHz
Inner free space (R_i)		150 mm	170 mm

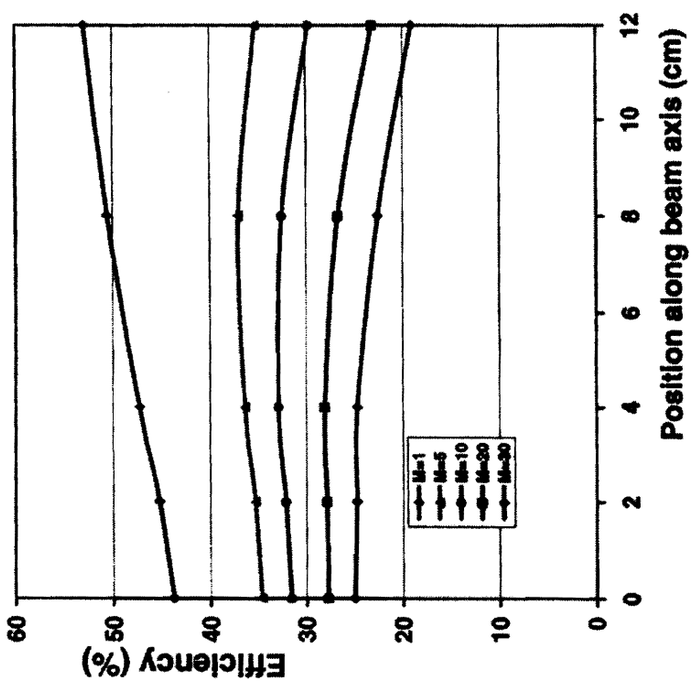

Doppler correction capability

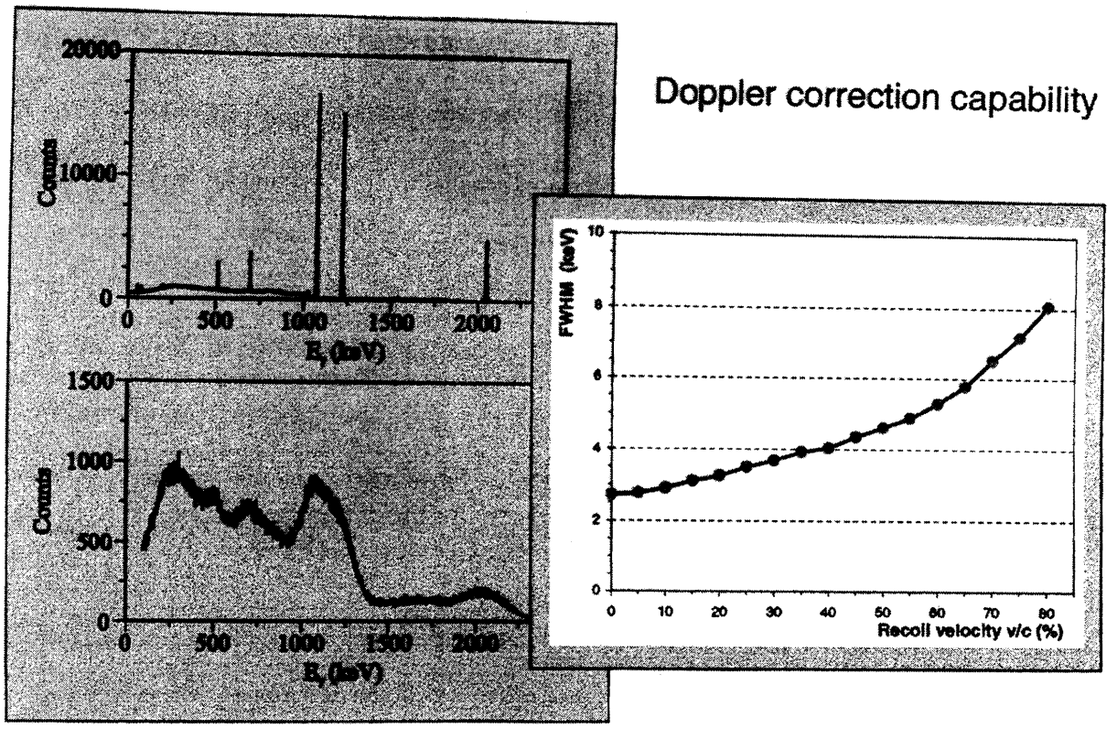

Relativistic 1π set-up

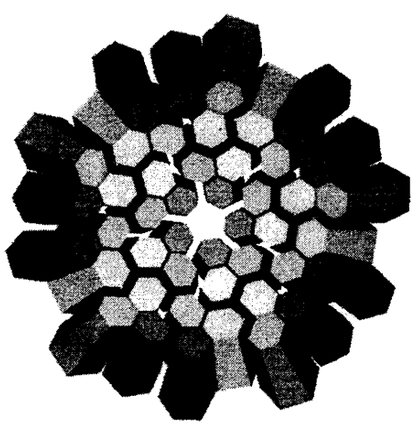

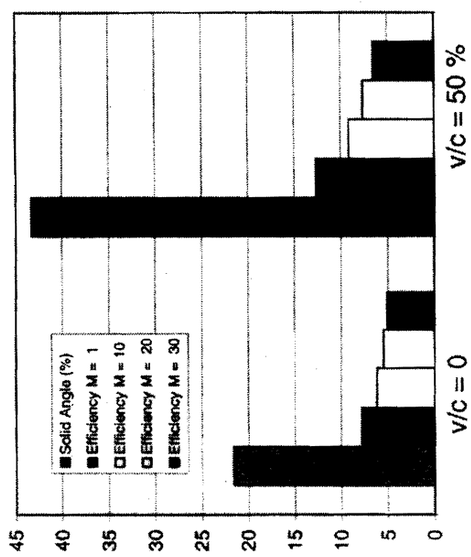

AGATA characteristics for typical reaction types

	Full energy efficiency (P/T ratio)	Maximal event rate	Energy resolution
Relativistic Coulomb excitation: M = 10, v/c ~ 20%	28 % (51 %)	0.9 MHz	~ 3.5 keV (0.6 %)
Secondary fragmentation : M = 15, v/c ~ 50%	24 % (46 %)	0.6 MHz	~ 5 keV (0.7 %)
High-spin spectroscopy : M = 30, v/c ~ 5%	22 % (45 %)	0.3 MHz	~ 2.5 keV (0.3 %)
Isomer spectroscopy : M = 5 + 5, v/c = 0	31 % (53 %)	0.9 MHz	< 2.3 keV (0.2%)

All values are given for a γ-ray energy of 1 MeV.

CNS Ge array for in-beam γ spectroscopy of fast moving exotic nuclei

S. Shimoura

CNS, University of Tokyo, Japan

Email: shimoura@cns.s.u-tokyo.ac.jp

Nuclear spectroscopy of far from the stability line is one of the major interests in the investigation of nuclear structures as functions of proton/neutron numbers. In order to populate various excited states in exotic nuclei, direct reactions between intermediate-energy RI beams and various targets are used and measurements of de-excited γ-rays have been performed for their spectroscopy.

This technique is characterized as an inverse kinematics where the target acts as a probe exciting the beam-like ejectile. Since the velocities of the excited nuclei are similar to that of the beam, i.e. more than 30 % of the light velocity, the energies of the γ-rays suffer from Doppler shift depending on the folding angle between the γ-rays and the direction of the ejectile as well as on its velocity.

Because of the Doppler broadening due to finite angular acceptances of γ-ray detectors, we have used an array of NaI(Tl) scintillators, DALI, for the measurement. Typical energy resolution the array is about 100 keV for 1 MeV γ, which corresponds to angular resolution of 10 – 20 degree for each detector. Although there are expected to be a lot of interesting studies in this kind of experiments, the region of the nuclides have been limited in light and/or even-even nuclei.

If one aims at extending this method to heavier and/or odd exotic nuclei, detector systems with higher energy resolution are needed. Intrinsic resolutions of detectors are improved by using Germanium (Ge) detectors, the resolutions of which are more than 1 order of magnitude better than NaI(Tl) scintillators. In order to balance the Doppler broadening with the intrinsic resolution of Ge, we have to determine the emission angle within a few degree. Recent γ-ray tracking techniques for segmented Ge detectors can be applicable to get good angular resolution without loosing efficiency. Along this considerations, the CNS, University of Tokyo, is now constructing a new segmented Ge array.

In the talk, I discuss the basic idea of inverse kinematics measurements for intermediate-energy direct reactions, introduce the present DALI system and several recent results from the mesurements by using it, and present requirements for the Ge array and its design.

CNS Ge array for In-beam Gamma Spectroscopy of fast moving exotic nuclei

CNS, University of Tokyo
S. Shimoura

International Workshop on developments of Ge detector array and frontiers of gamma-ray spectroscopy, Dec. 11-13, 2001

Menu

- In-beam Spectroscopy of Exotic Nuclei
  - Inverse Kinematics
  - Probes for Direct Reactions
- Spectroscopy of Neutron-Rich nuclei (12Be, 14Be, 32Mg, 34Mg)
- CNS Ge-Array for High Resolution Gamma-ray Spectroscopy

Inverse Kinematics

- Formation of Excited States and Their Decays

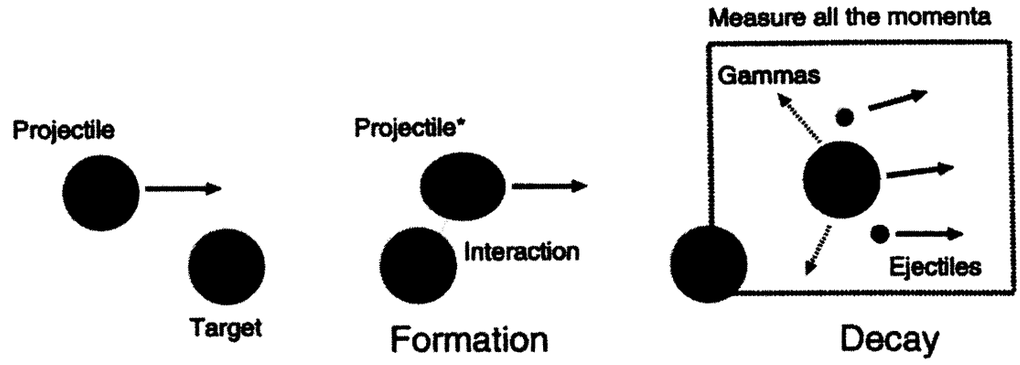

- Direct reactions are important for incident energies above several tens of MeV: Target as a Probe
- Velocities of Ejectiles are almost same as that of projectile
- Gamma-rays are Doppler-Shifted

Spectroscopy of Beam-Like nuclei with Targets as Probes

- Heavy Nuclei: Strong Coulomb Field
  - Coulomb Excitation, Coulomb Dissociation
    - Isovector, E1/E2
- Hydrogen, Deuterium
  - Inelastic Scattering
  - Charge Exchange Reaction
    - Isoscaler/Isovector, Spin Flip/Non-flip
  - Knockout
- Herium-4
  - Inelastic Scattering
    - Isoscaler, Spin Non-flip
- Any target
  - Inelastic Scattering
  - Knockout
  - Fragmentation

Decays of Excited States

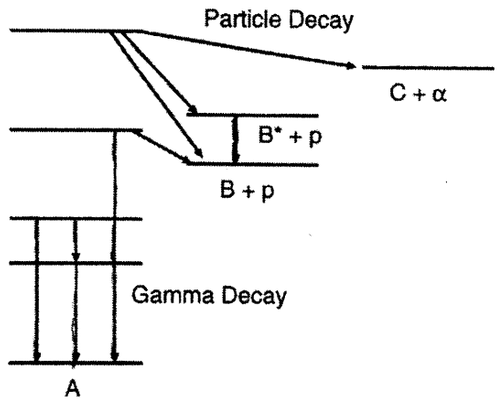

- Momenta of all the decay particles including gamma rays -> Excitation energy (from invariant mass)
- Particle-particle, particle-gamma correlation -> Spins and Parities
- Selectivities of Decay Process

"High resolution Gamma detectors"

Transition Probabilities

- Cross section of Coulomb Excitation -> B(EL)...
- Cross section of Nuclear Excitation -> Deformation Length -> B(EL)...
  - Adequate reaction model required (DWBA ...)
- Lifetime and Branching Ratio -> B(EL)...

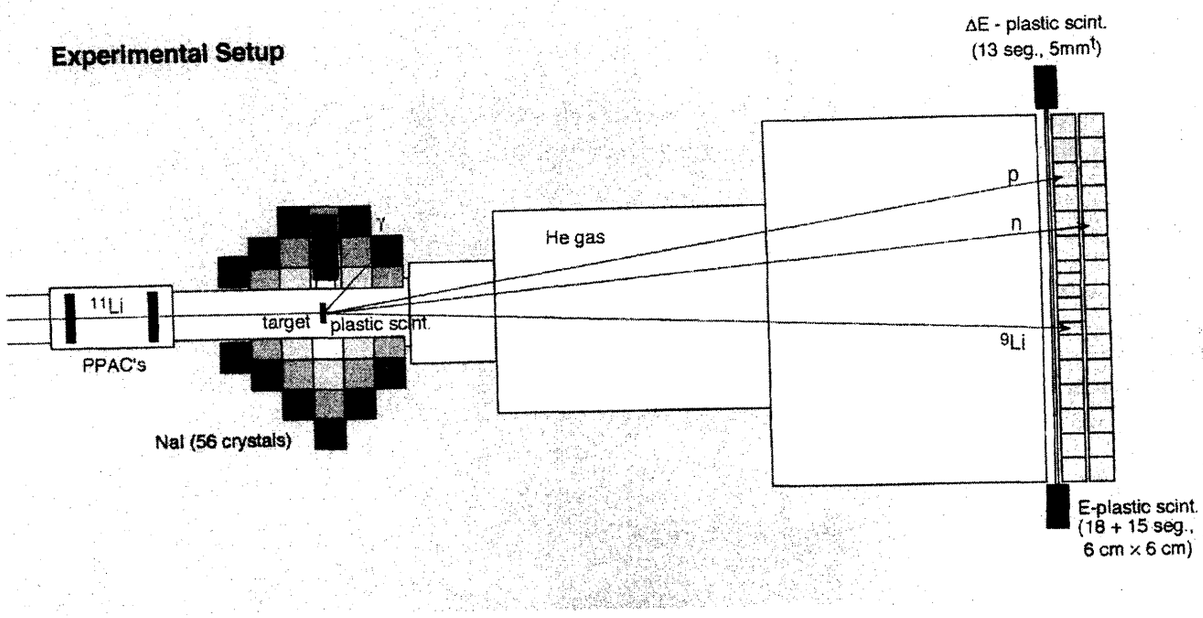
Experimental Setup
ΔE - plastic scint.
(13 seg., 5mm^t)
p
n
γ
He gas
^{11}Li
target
plastic scint.
^{9}Li
PPAC's
NaI (56 crystals)
E-plastic scint.
(18 + 15 seg.,
6 cm × 6 cm)

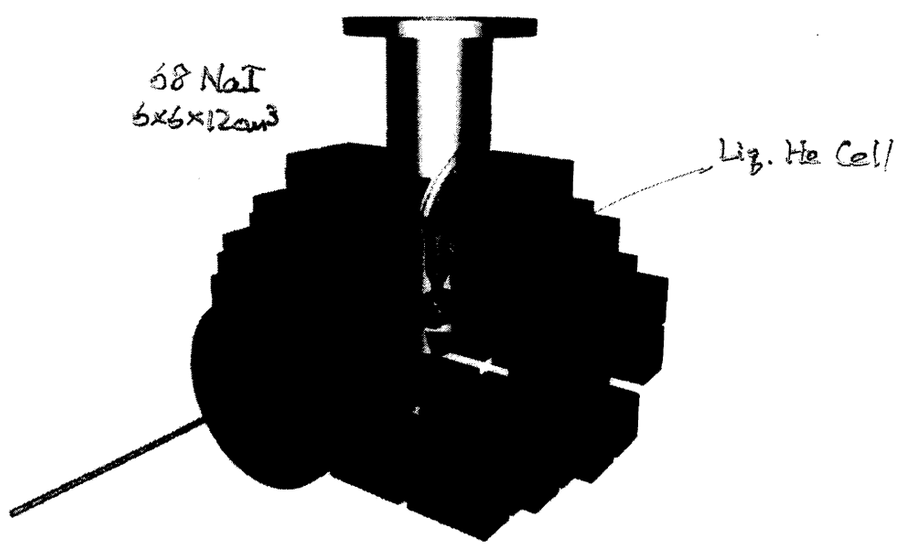
68 NaI
6×6×12cm^3
Liq. He Cell

■Example : NaI(Tl) array

- Scattering angle vs. Energy deposited in detectors (data)
  - 2.1 MeV gamma-rays from in-flight 12Be* are shifted
  - about 0.2 MeV (FWHM) resolution after D.S. corrected
  - 0.5 MeV gamma-rays from positron annihilation are not shifted

$^{12}Be + {}^{4}He \rightarrow {}^{8}Be + \gamma + X$

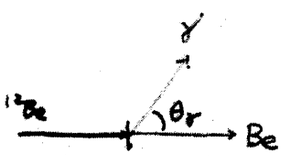

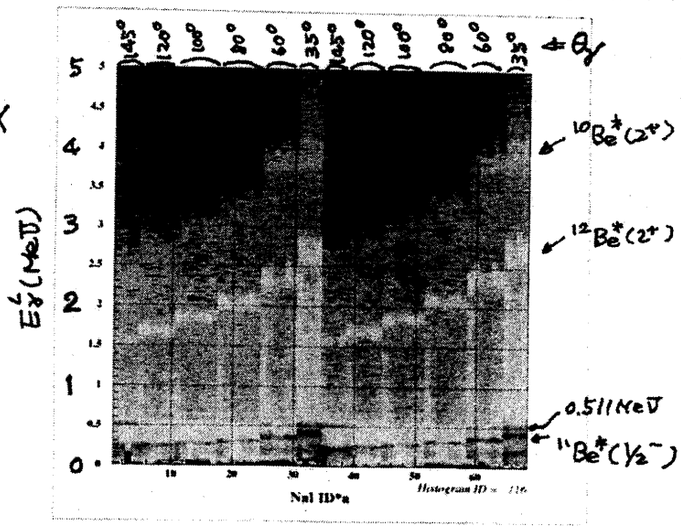

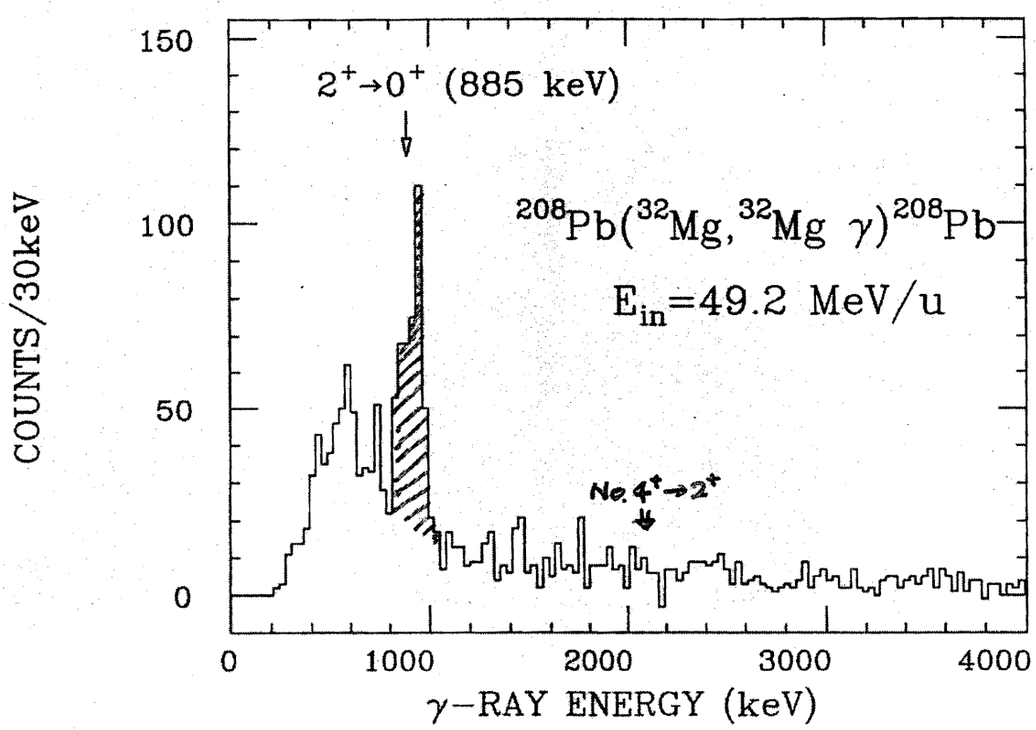

Yoneda et al.

$^{36}S_i$ (38A MeV) + ^{9}Be → ^{A}Mg

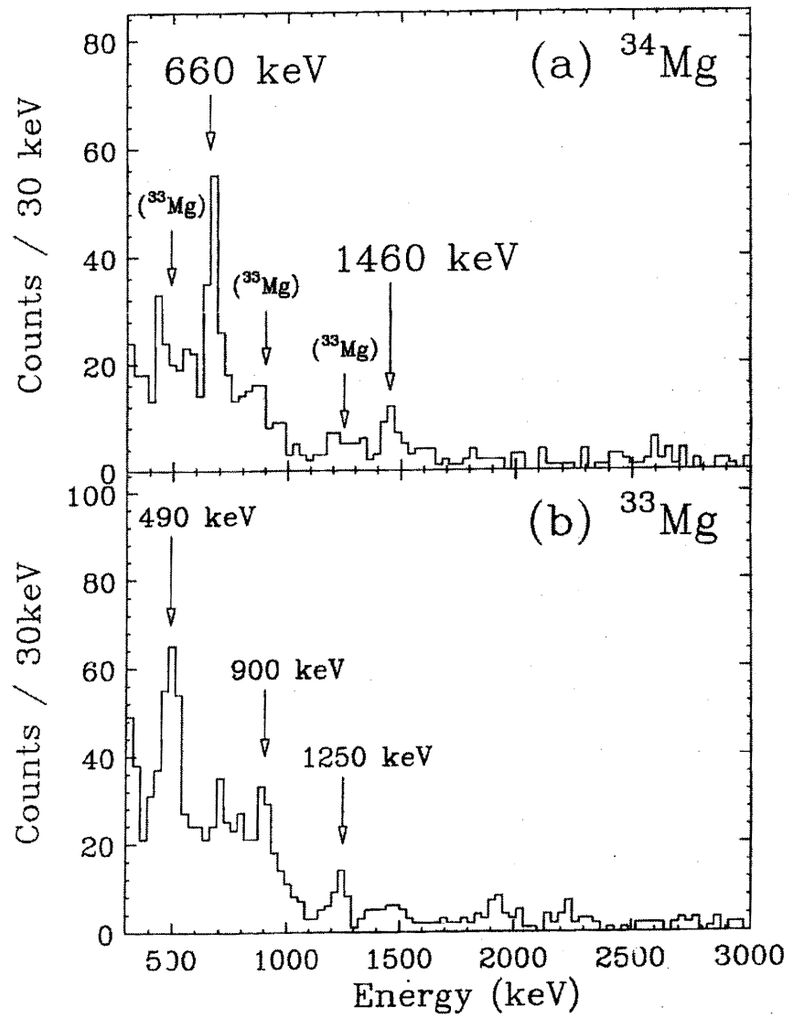

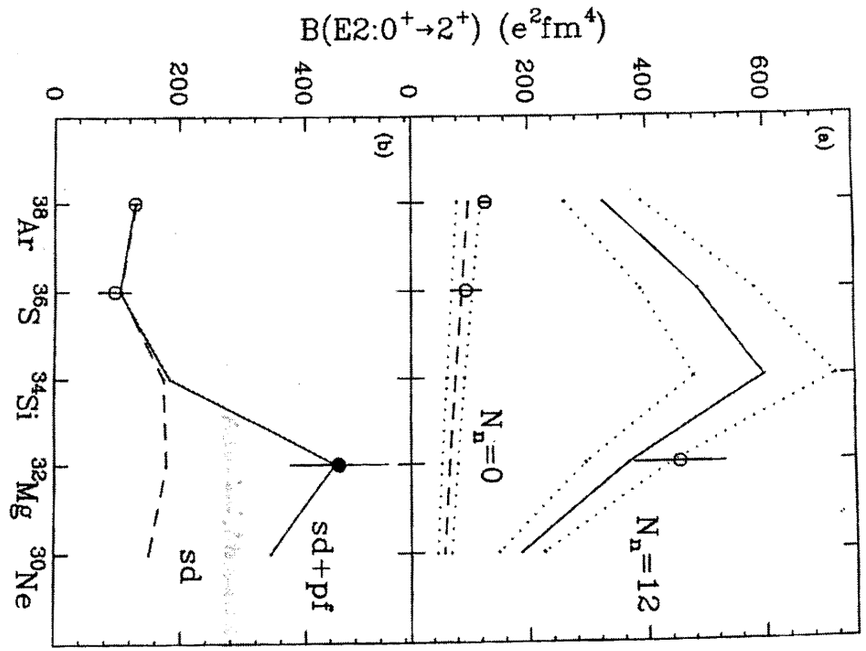

B(E2) = 454 ± 78 (e^2fm^4)

Coulomb excitation of ^{34}Mg

Physics Letters B522(2001)227

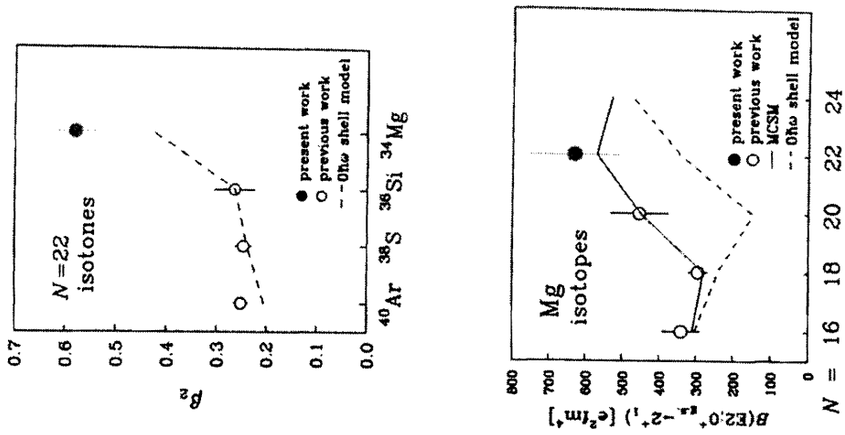

Spectroscopy of Neutron-Rich Be isotopes

- Low-lying 12Be states
  - 1- intruder state (Coulex)
  - collectivity of 2+ state (p,p')
  - isomeric 0+ state (isomeric "beam")
  - proton/neutron matrix elements using different probes
    - (p,p'), (alpha,alpha'), Coulex
- Cluster states in 12Be and 14Be
  - Inelastic excitation
  - Fragmentation
- Halo structure of 14Be using spectroscopy of its IAS by (p,n) reaction

Low-lying intruder 1^- state in ^{12}Be

Iwasaki et al., Phys. Lett. 491B (2000)8

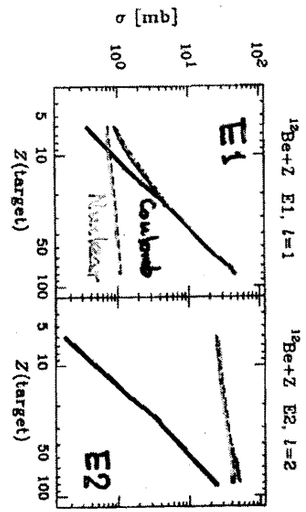

1^- state at Ex = 2.7 MeV

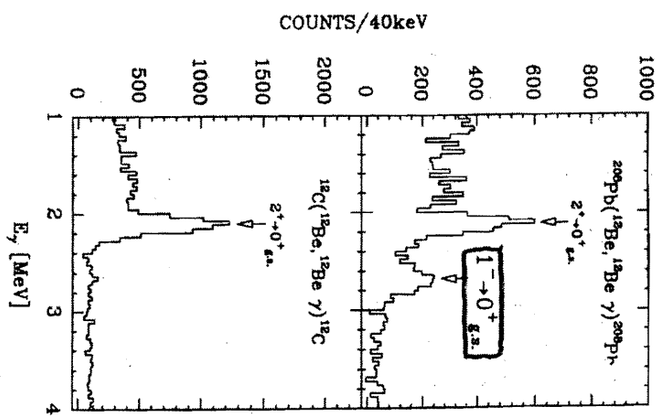

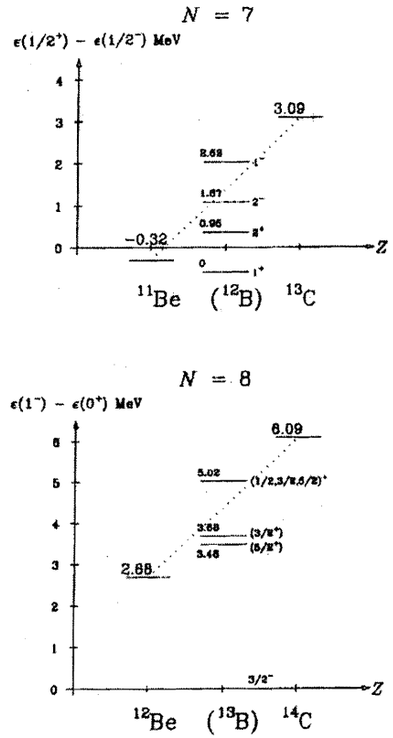

Figure 5.4: Energy levels in the Be and C isotopes with the neutron number N=7 and N=8. In the top panel, the energy differences between the $1/2^+$ state and the $1/2^-$ state are plotted as a function of Z. The bottom panel shows the plots of the excitation energies of the lowest 1^- states. The relevant levels in the B isotopes are also plotted.

Large deformation length of 2^+ state in ^{12}Be

Iwasaki et al., Phys. Lett. 481B (2000)7

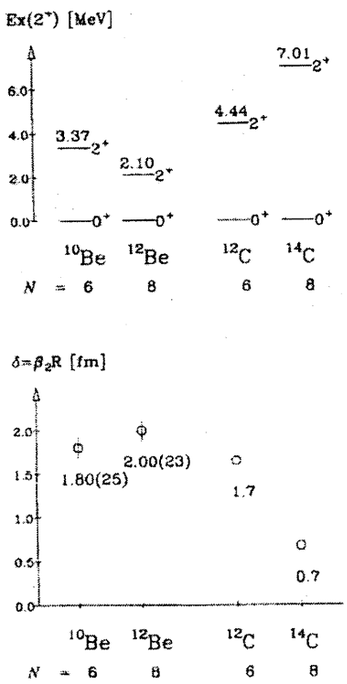

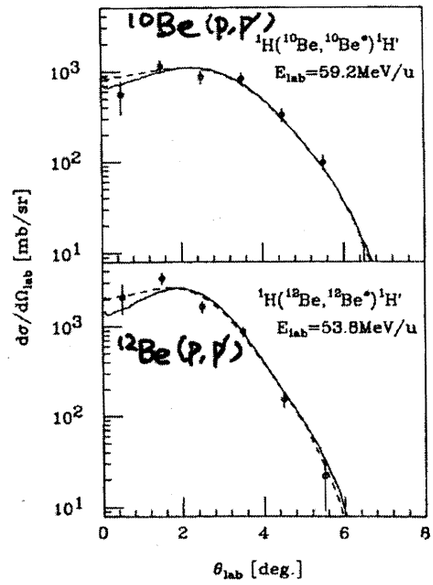

Isomeric 0^+ state in ^{12}Be

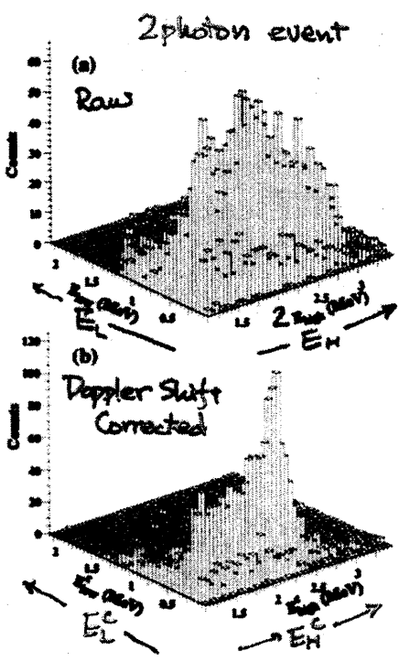

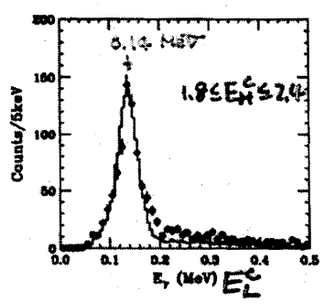

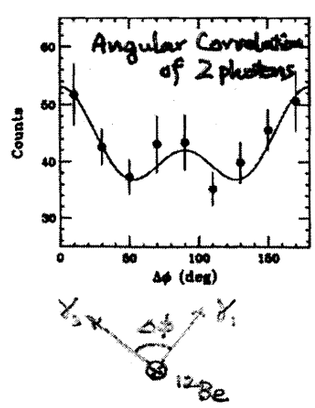

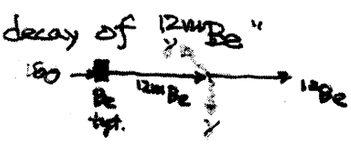

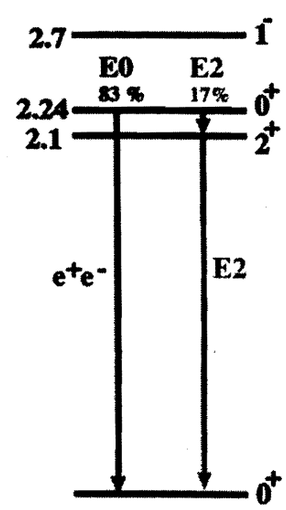

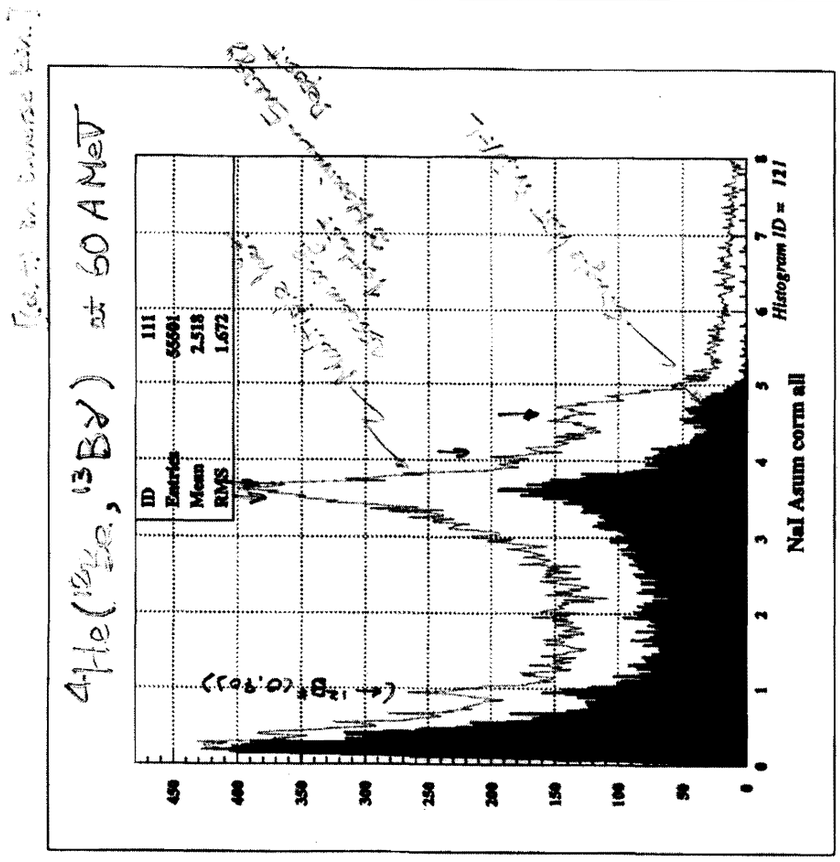

CNS Ge-array project

- Requirement:
  - Detectors should be located as close to the target as possible
    - Detectors around 90 degree with respect to beam axis
      - Largest Doppler-shift-broadening
  - Good angular resolution (1-2 degree) for 1-dim. correspond to intrinsic resolution of Ge detectors (a few keV)
    - Planer-type detector
    - Pulse-shape analysis to determine vertex points in the direction parallel to that of the Electric Field
  - Multiplicity of gammas is not so large
    - No anti-Compton shield is considered at this time
  - Minimize Costs and Time

    "Simple Structure"

Detector specification

- Active volume : 6cm-dia x 2cm-thick
- 2 Ge-crystals
- Each crystal is segmented to 3 x 3

FET in Room Temp.

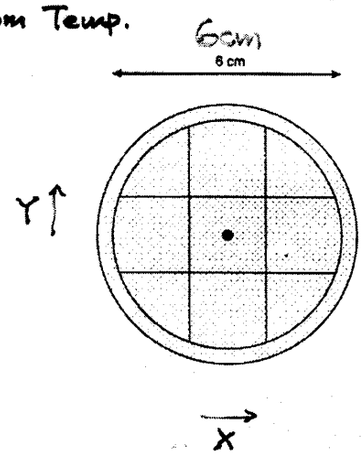

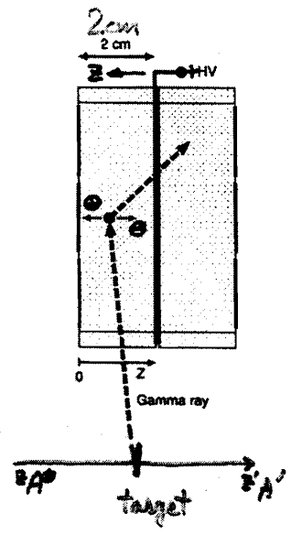

Array Configuration

- Locates 18 detectors around 90 degree with respect to beam

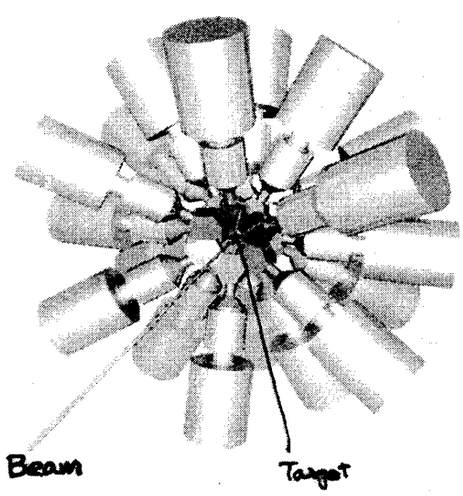

Pulse-shape analysis of segmented Ge

- Good resolution for ONE direction

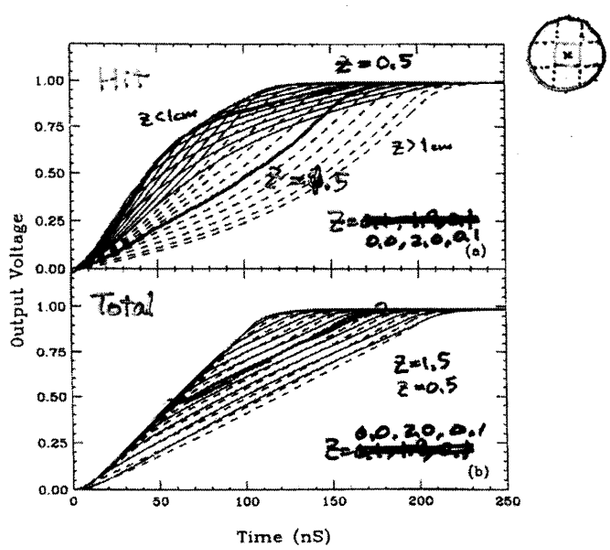

Pulse shapes as a function of depth for Planer Detector (a) hit segment (b) total

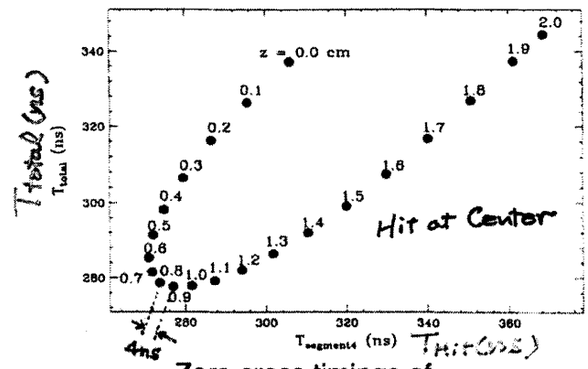

Zero cross timings of 2nd derivative signals for "hit segment" and "total"

$(CR)^2-(RC)^4$

$\tau = 50ns$

Performance (Simulation)

- Energy Resolution after Doppler-Shift Corrected (v/c = 0.3)
  - 8 keV (FWHM) 17 keV (FWTM) for 1-MeV gamma
- Total Detection Efficiency (epsilon x Omega)
  - 5 % (All) 3.4 % (more than single hit)
- Peak-to-Total Ratio
  - 23 % (All) 42 % (more than single hit)

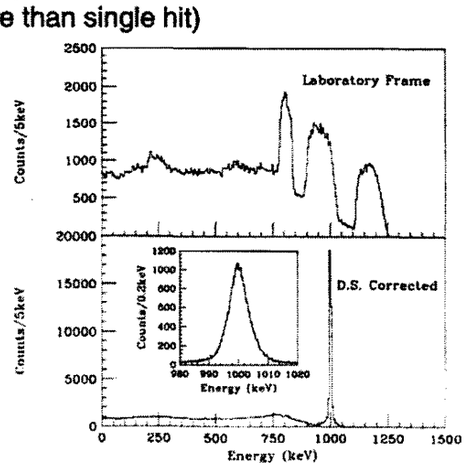

Assuming

1st Hit = Hit w/ Maximum Pulse Height

$\Delta X = \Delta Y = 2$ cm

$\Delta Z = 1$ mm

Gamma Spectroscopy with Radioactive Ion Beams at the HRIBF

Cyrus Baktash

Oak Ridge National Laboratory

Gamma Spectroscopy with Radioactive Ion Beams at the HRIBF

Cyrus Baktash

Outline

- **Introduction:**
  - » **Holifield Radioactive Ion Beam facility**
  - » **experimental challenges**
  - » **Nuclear structure endstation**
- **Coulomb excitation with RIBs**
- **Transfer reactions with RIBs**
- **Fusion reaction with n-rich and p-rich RIBs**
- **Decay spectroscopy**
- **Outlook**

Existing and Planned ISOL Facilities
with Beam Energies up to Coulomb Barrier

Facilities	**Now: HRIBF (p-rich & fission fragments, A< 140)** **Now: Louvain la Nouve (p-rich noble gases, A< 40)** **2001: SPIRAL-I @ GANIL (initially noble gases, A< 90)** **>2005: MAFF @ Munich (fission fragments)** **2006: ISAC-II @ TRIUMF (A< 60)** **2006: SPIRAL-II @ GANIL (fission fragments)**
Physics	***Nuclear Structure & Reaction Studies Around Coulomb Barrier*** **- Coulomb Excitation (multi step)** **- Transfer reactions** **- Fusion (sub-barrier, evaporation, high-spin, fission, heavy elements)** **- Break up reactions** **- Semi- & doubly-magic nuclei** **- Detailed spectroscopy of N~Z nuclei** **- Proton drip line nuclei** **- rp- and r-process nuclei**

The Holifield Radioactive Ion Beam Facility at ORNL

- **Operational ISOL facility with RIBs above the Coulomb barrier**
- **Excellent energy resolution and beam quality: Ideally suited for nuclear structure and astrophysics**
- **Proton-rich beams:As, Ga, F. Long-lived p-rich beams soon.**
- **Neutron–rich RIBs: more than 100 beams with intensities > 10^3 pps.**
- **Many specialized nuclear structure & astrophysics detection equipment are at hand.**

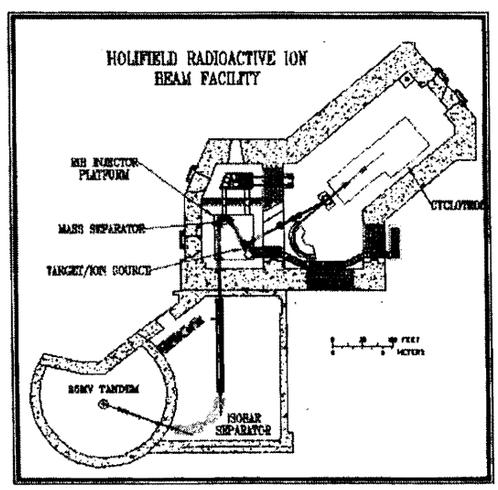

ornl

Target for Neutron-rich RIB Production

- 8-12 μm layers of uranium carbide
- Deposited on R-V Carbon fiber matrix
- Density ~1.4 g/cm^3

Intensities of the neutron-rich beams from HV platform (pps)

Typical required intensities:

Mass measurements: a few pps

Coulomb excitation: 10^3 pps

Transfer reactions: 10^4 pps

Fusion reactions: 10^6 pps

Experimental Challenges With RIBs

- **Experiments with radioactive ion beams are very challenging**
  - » **Low intensities of RIBs (typically 4 to 7 orders of magnitude smaller than SIBs)**
  - » **High β & γ background due to the decay of RIBs**
  - » **Isobaric beam contamination**

- **How to cope with these problems?**
  - » **Low intensity: Maximize detection efficiencies of all subsystems**
  - » **High Background: Require coincidences between two or more detectors**
    - – **Gamma rays, charged particles, beam particles, recoils, recoil decays**
  - » **Isobaric contamination: Identify Z**
    - – **Charged particles, x-ray, Bragg detector, ionization chamber, dE/dx**

- **What is required?**
  - » **Develop detection systems that are specialized, efficient, selective, and flexible.**

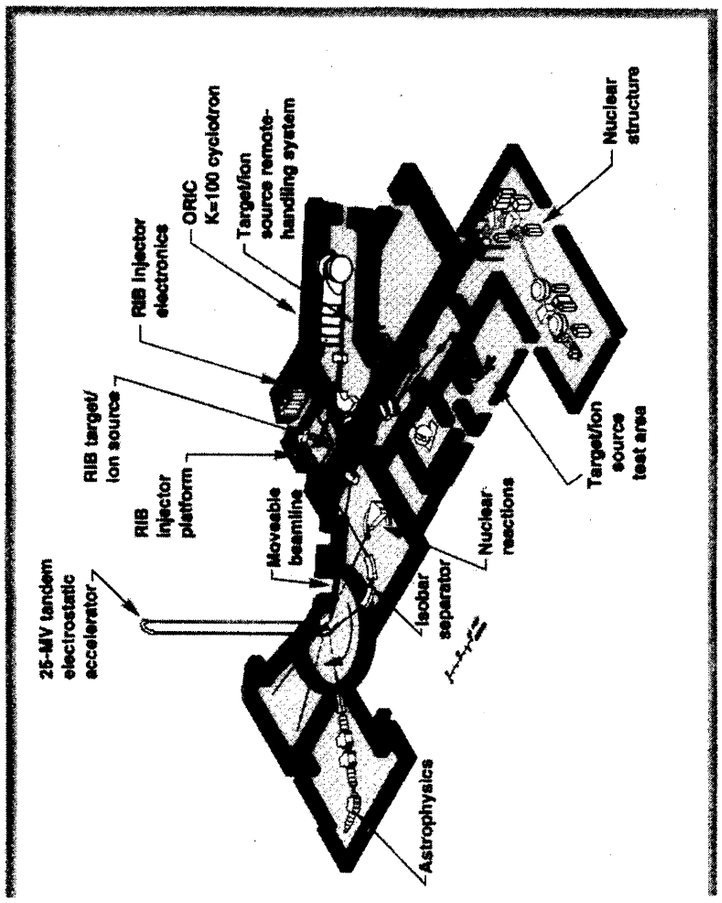

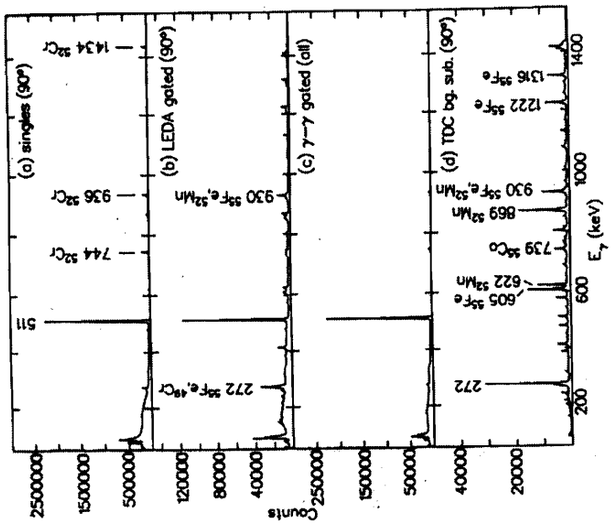

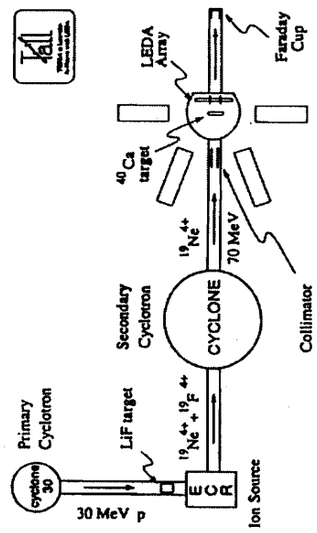

Fig. 1. Schematic diagram of the experimental layout. The secondary cyclotron could be tuned to provide either a $^{19}Ne^{4+}$ beam (as shown) or a $^{19}F^{4+}$ beam.

Recoil Mass Spectrometer Endstation

A poweful & flexible system for nuclear structure studies

CHARMS (CLARION + HyBall Array + RMS): Specifically designed for γ spectroscopy with RIBs

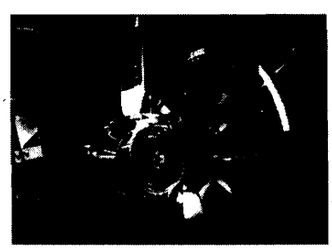

CLARION: Clover Ge
HyBall: CsI + Silicon
Micro Channel Plates

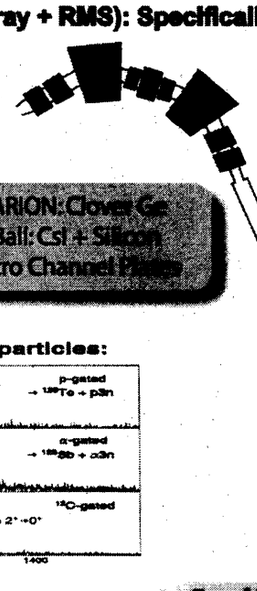

Upgrades in progress:
- Si part of HyBall
- Neutron detectors

Future plans:
- RMS operation in gas-filled mode
- CLARION: Addition of 5 Clovers to double γ-γ efficiency

Gammas gated by charged particles:

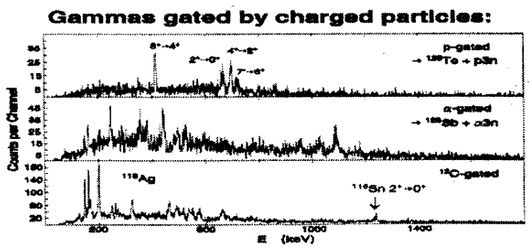

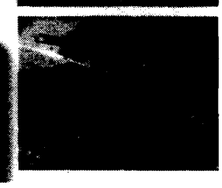

Focal Plane Area:
- Gas Counters
- Silicon Strip & DGF
- Moving Tape Collector
- Clover Ge, x and β detectors

CLARION

Clover Array for Radioactive Ions

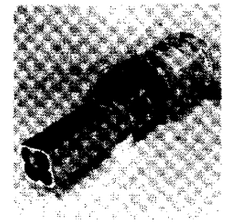

High Efficiency

- 11 clovers. Each clover: ε_γ = 150% @1.3 MeV
- Total photo-peak ε_p= 2.25% @1.3 MeV
  (ε_p= 2.8% with 11 CSS det. added)

High Resolution

- Electronically segmented clovers
- Reduced Doppler broadening
- FWHM = 2.2 keV @1.3 MeV

High P/T ratio

- Add back capability
- BGO shields
- P/T=0.57 @1.3 MeV

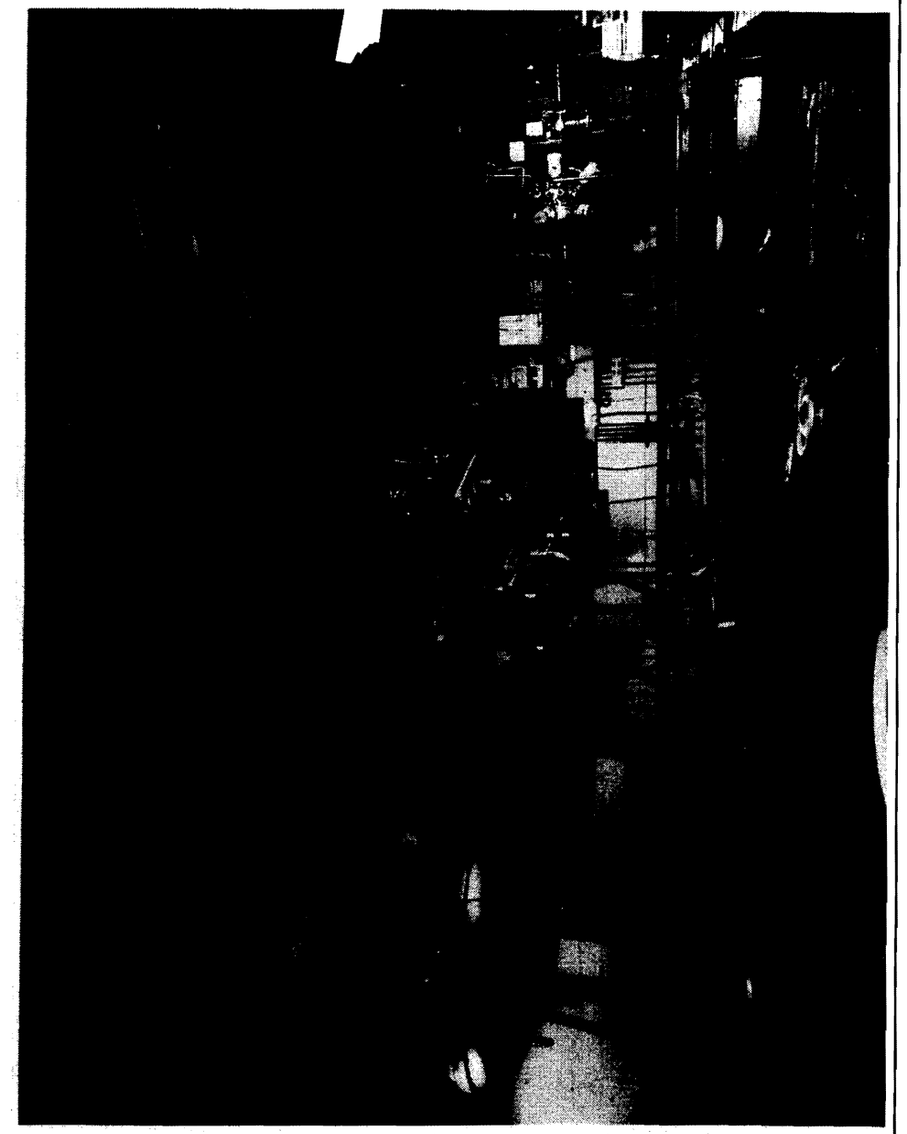

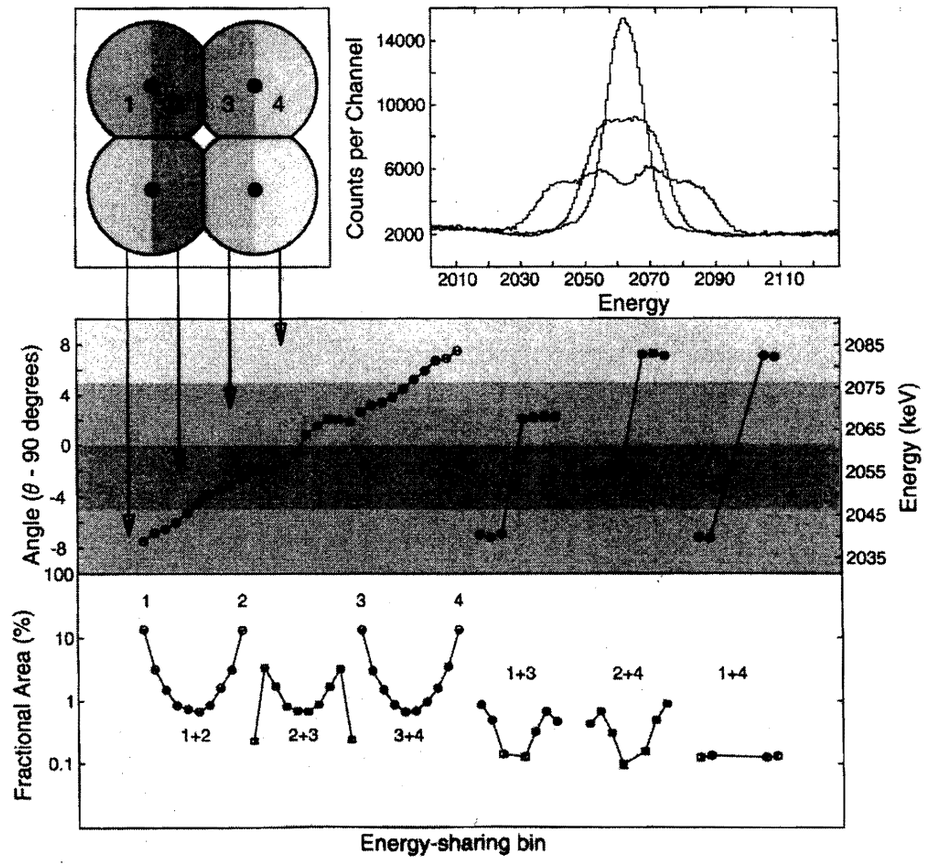

HyBall: A Hybrid Ball of CsI & DSSD Detectors for RIBs

Various components of the HyBall may be used *individually* or *together* for a large variety of RIB experiments.

CsI Array

Characteristics:

- 95 CsI with photodiode readout
- Excellent Particle ID
- 95% geometric efficiency.

Applications:

- **Channel selection in fusion-Evaporation reactions**
- **Coulomb excitation**
- **Transfer reactions.**

DSSD Array

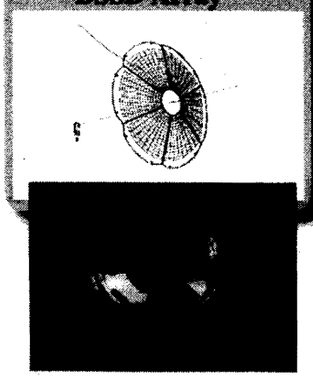

Characteristics:

- Two-layered (ΔE-E) array of DSSDs based on 6-in wafer technology
- Each layer consists of 6 sectors, with a total of 768 pixels
- Flexible geometry: May be mounted at forward, backward, or 90-deg
- Large solid angle coverage.

Applications:

- Coulomb ex. with heavy targets
- Fusion with RIBs, e.g., ^{56}Ni
- Transfer, e.g., (d, p)
- Elastic & inelastic reactions.

Spectroscopy near ^{132}Sn

- ^{132}Sn is arguably the best doubly-magic nucleus: It has the highest first excited state, even after correcting for mass.
- Some open problems:
  - » ^{134}Sn has a very low first 2^+.
  - » Standard parametrization of Nilsson model puts p3/2, p1/2 and f5/2 neutron orbitals at too high an energy. Other mean field potentials too reproduce poorly the ordering and spacing of single particle/hole energies around ^{132}Sn. This has serious implications for modeling of the r-process using these potential. Reducing spin-orbit interaction helps this problem.
  - » Proton s1/2 in ^{133}Sb and neutron i13/2 in ^{133}Sn have not been experimentally identified. Hence ambiguities exist in interpretations of the medium spin states in neighboring nuclei.
  - » Exact positions of the single particle states are still being debated (particle-vibration coupling, monopole term in the Hamiltonian)
- Some good news
  - » Large scale shell model calculations using realistic effective interaction are in remarkable agreement with the available experimental data (Naples group).
  - » Experiments with radioactive ion beams will soon provide more stringent tests of such microscopic models.
  - » At HRIBF, we have begun a program in this direction.

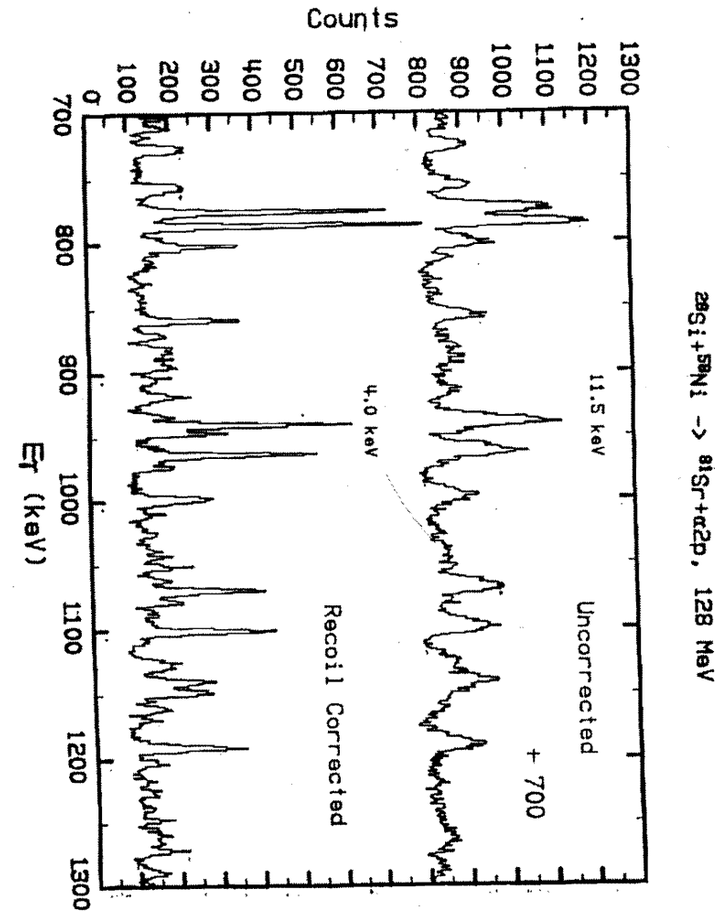

Zhang et. al

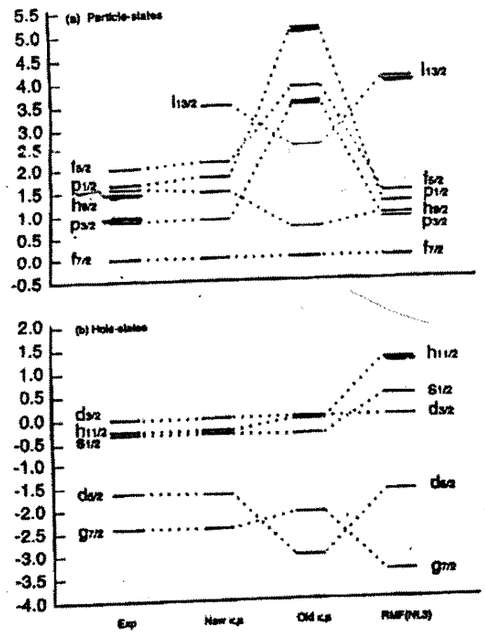

FIG. 1. Single neutron particle (a) and hole (b) states. Experimental (left-most) and calculated results from Nilsson model with new parameter set, from standard set, and from RMF with NL3 parametrization.

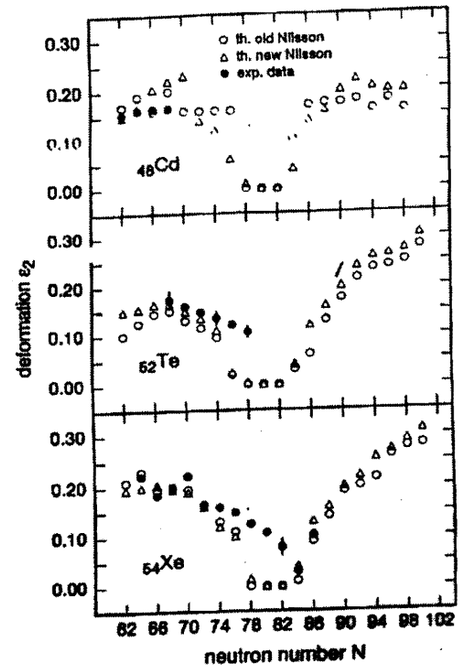

FIG. 2. Ground state deformations: experimental values [15] (dots), absolute values from calculations with new set of parameters (open triangles), and with standard parameter set (open circles) for Cd, Te, and Xe isotopes.

M. Sanchez-Vega et al
PRL 80, 5504 (1998)
missing $h_{11/2}$ proton?
^{134}Te (^{11}B, ^{12}C)
large +ve Q

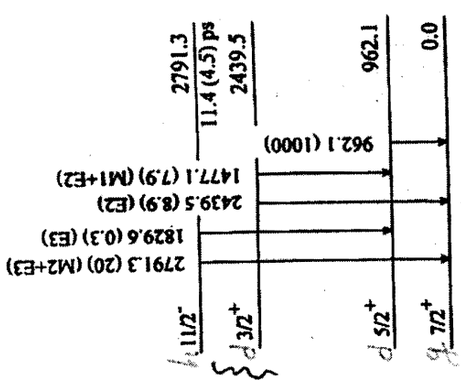

Oros et al

P.J. Daly et al
^{3}Sn($\nu f_{7/2}$) + $\pi h_{11/2}$
(^{3}He, d)

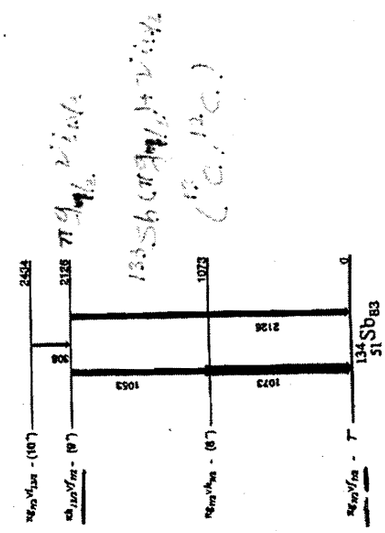

Figure 3: Yrast level scheme for ^{134}Sb. Dominant configurations are indicated.

Some HRIBF beam currents

Singly stripped - suitable for Coulex
For doubly stripped, divide by five

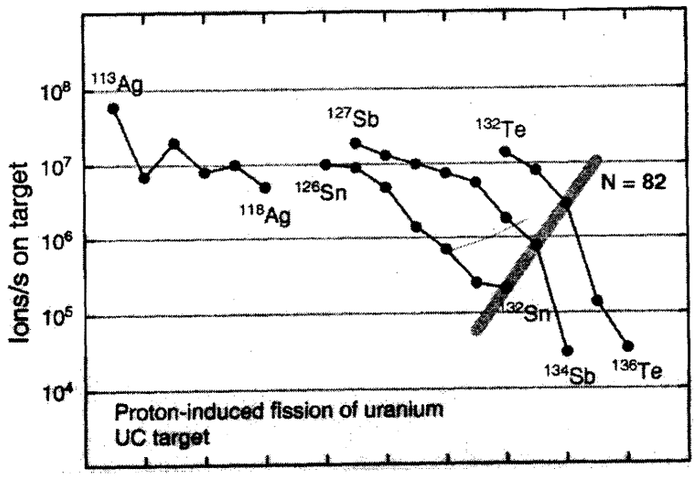

HRIBF will be the only facility that can accelerate these beams above the Coulomb barrier for at least 4 - 5 years.

Total of over 100 beams with at least 10^3 ions/s.

^{118}Ag Test Experiment: Prompt [illegible] Coincidences

HyBall particle ID spectra:

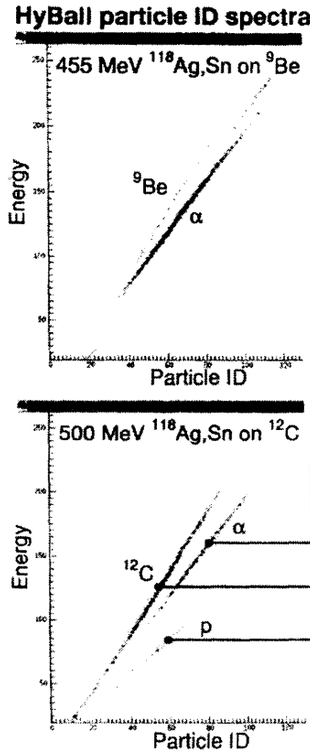

^{118}Ag on Be and C targets
Small ^{118}Sn component of beam (~10%)

Gammas gated by charged particles:

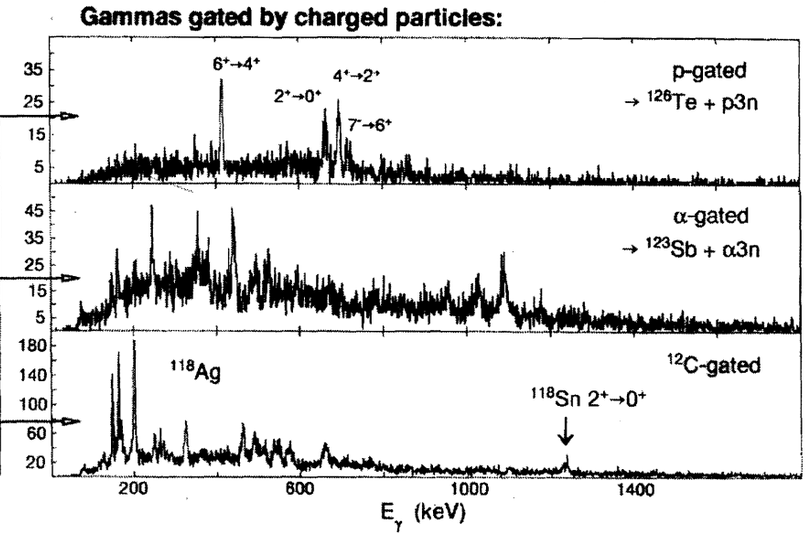

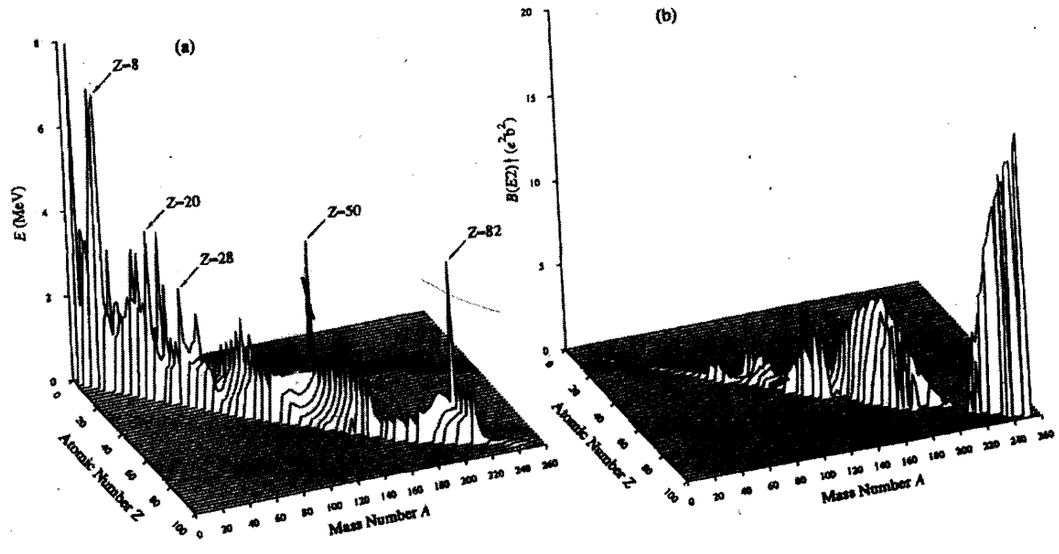

ADNDT 994 Figure A

Setup for experiments with multichannel RIBS

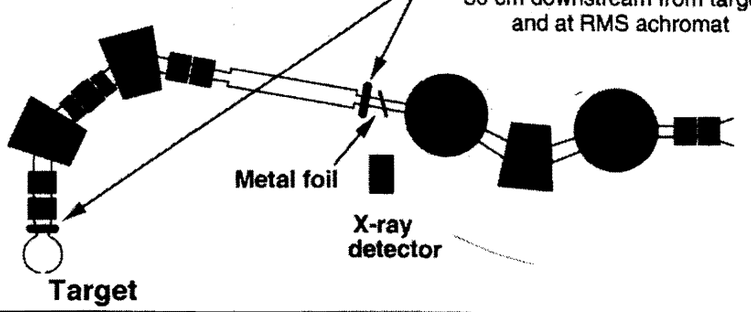

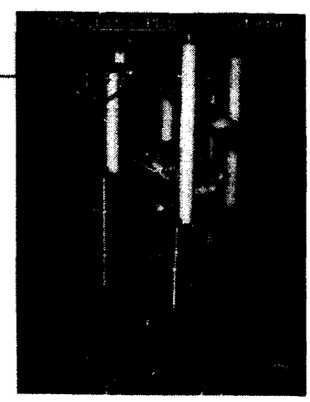

Foil plus multichannel plate

CLARION

11 segmented clover Ge detectors
10 smaller Ge detectors

HyBall

95 CsI detectors with photodiodes

Beam Composition from X-rays

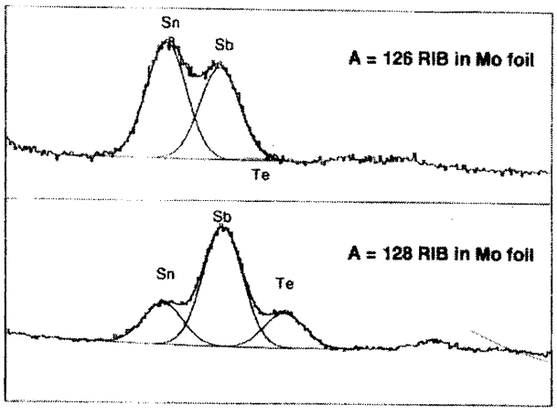

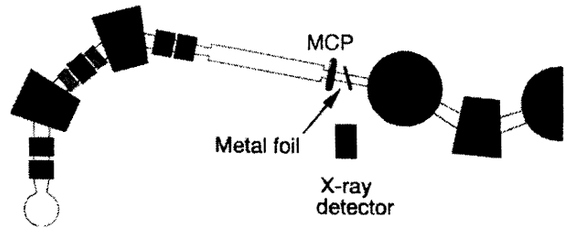

SIB calibrations

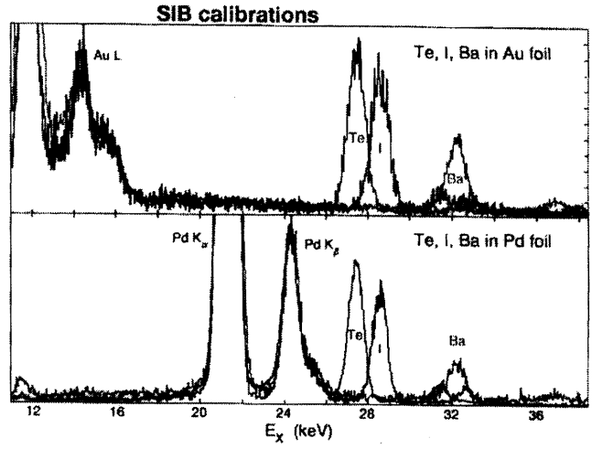

Example: A = 136 Coulex

Particle ID Spectra:

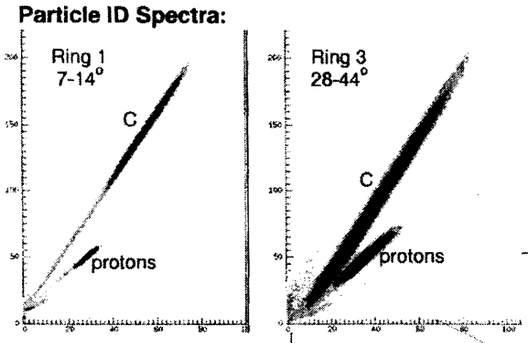

396 MeV ^{136}Te + ^{136}Ba
on 0.83 mg/cm^2 C target

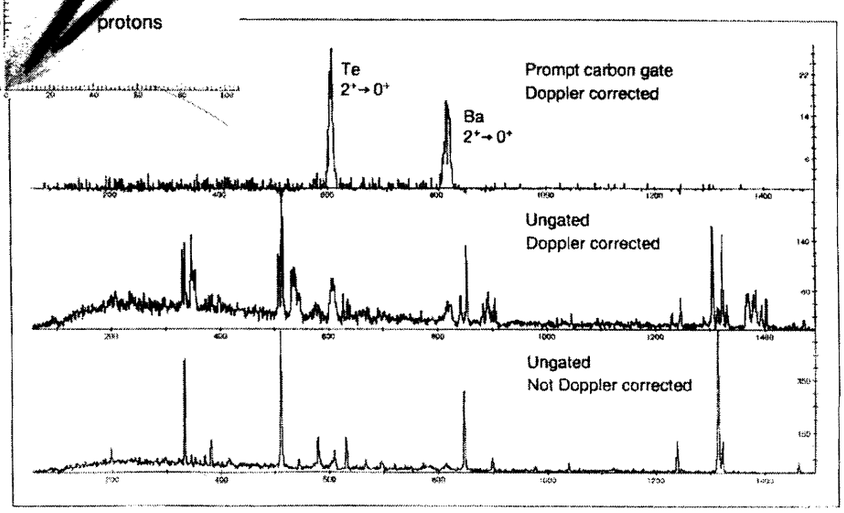

Coulex Results: Sn & Te Spectra

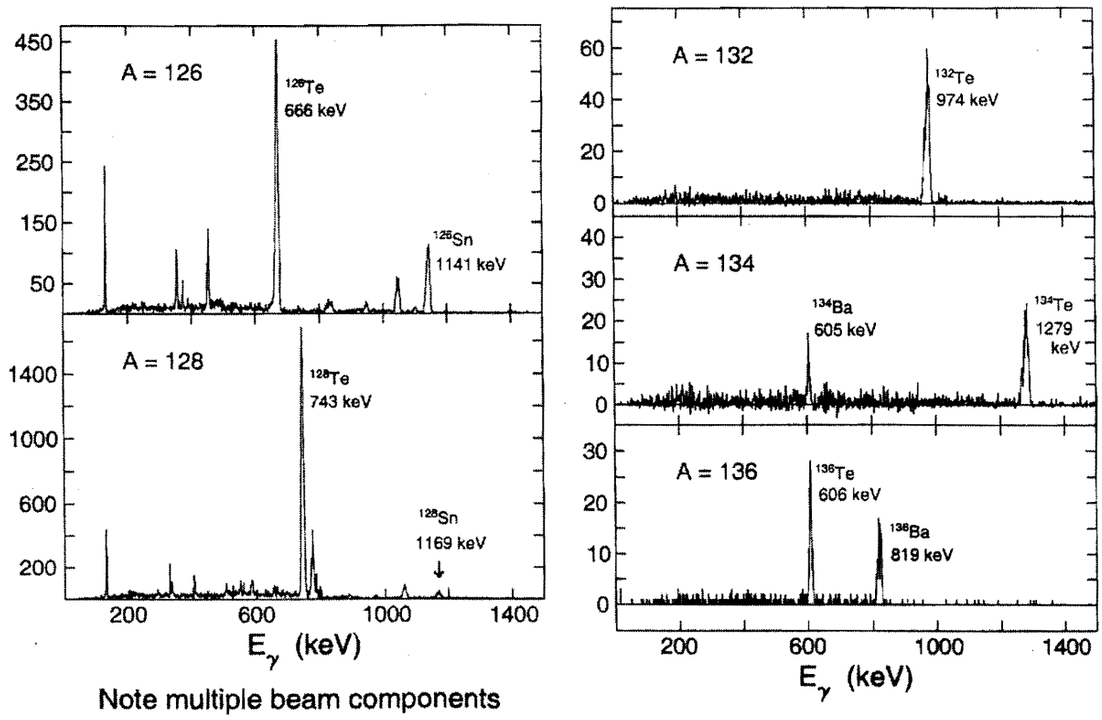

Note multiple beam components

Preliminary B(E2) Results and Systematics

Analysis is not yet complete.

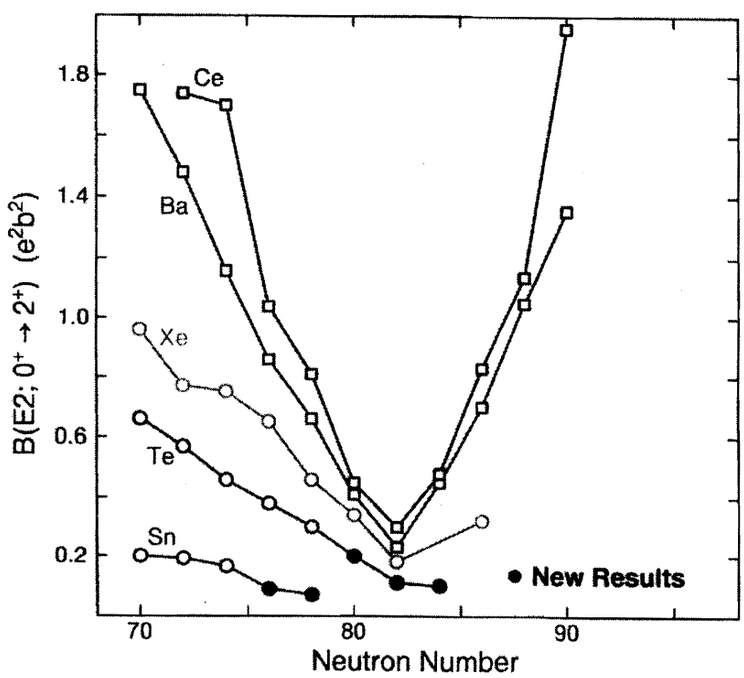

^{136}Te: Low B(E2) Value

The low value for the B(E2) in ^{136}Te is very surprising

- Could it be due to low neutron pairing in N=84?
- Energy of 2^+levels is low

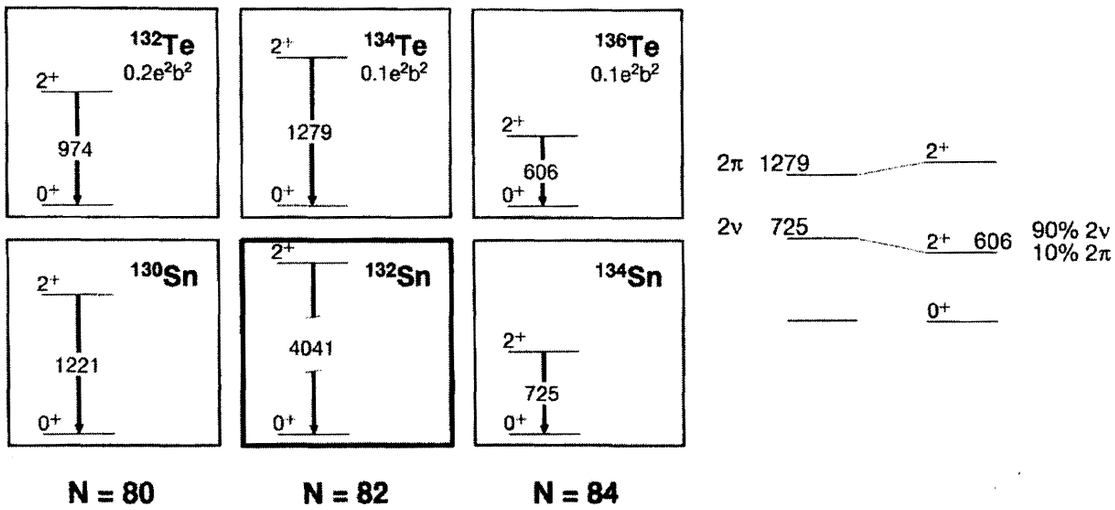

Future Plans: Coulex

- **B(E2) in ^{130}Sn** using pure Sn beam
- **Q_0 in ^{126}Sn by reorientation**
- **Odd-even and odd-odd nuclei**
  - Could populate many levels not observed in beta decay
- **B(E2) of 2^+ in ^{132}Sn** using pure Sn beam
  - $E_x > 4$ MeV
  - Analog to ^{208}Pb?
  - Use BaF array for high γ efficiency (~60%)
  - Use ^{28}Si or ^{48}Ti target and "slightly unsafe" energy

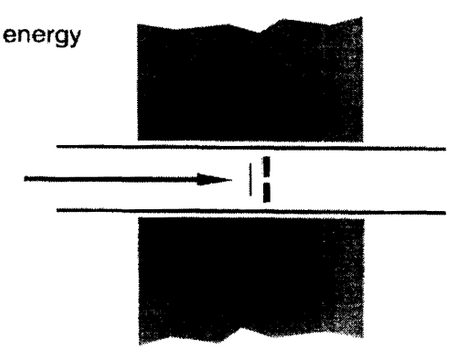

VOLUME 46, NUMBER 24 PHYSICAL REVIEW LETTERS 15 JUNE 1981

Selective Population of High-j Orbitals in Er Nuclei by Heavy-Ion-Induced Transfer

P. D. Bond, J. Barrette, C. Baktash, C. E. Thorn, and A. J. Kreiner
Brookhaven National Laboratory, Upton, New York 11973
(Received 12 February 1981)

Selective population of high-j and high-K states in ^{167,169,171}Er nuclei has been observed in heavy-ion-induced single-neutron-transfer reactions. γ rays in coincidence with outgoing particles have been used to aid in level assignments and several previously unobserved high-j states have been identified.

$P_{13/2}$: enhanced $\Delta J = \ell + 1/2$ $P_{3/2}$: enhanced $\Delta J = \ell - 1/2$

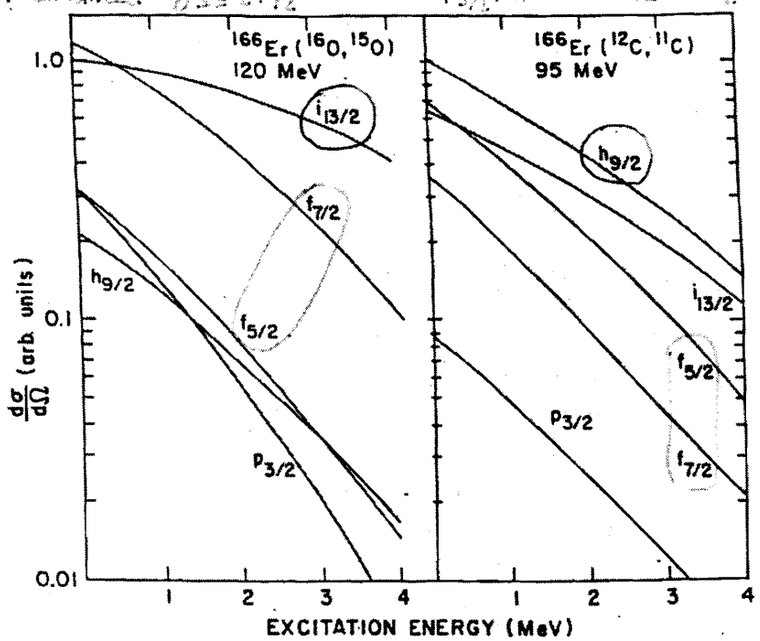

FIG. 1. Expected relative cross sections for active single-particle levels as a function of excitation energy for the reactions ^{166}Er(^{16}O, ^{15}O) and ^{166}Er(^{12}C, ^{11}C) calculated with the distorted-wave Born-approximation code PTOLEMY (Ref. 4). Unit spectroscopic factors were assumed for all states.

Coulex Results: Ge Spectra

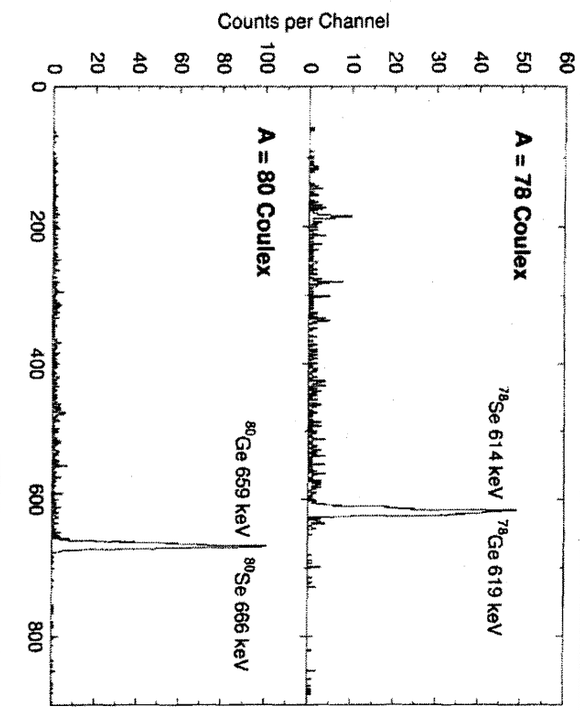

A systematic study of shape coexistence in
Se (A = 74-82) and
Ge (A = 70-80) isotopes
- PhD thesis work of E. Padilla

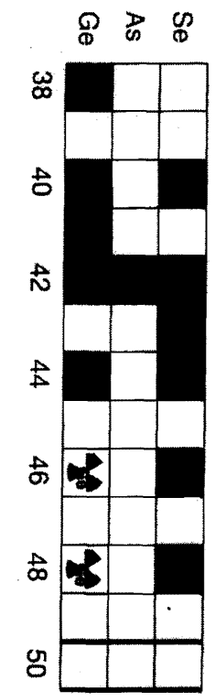

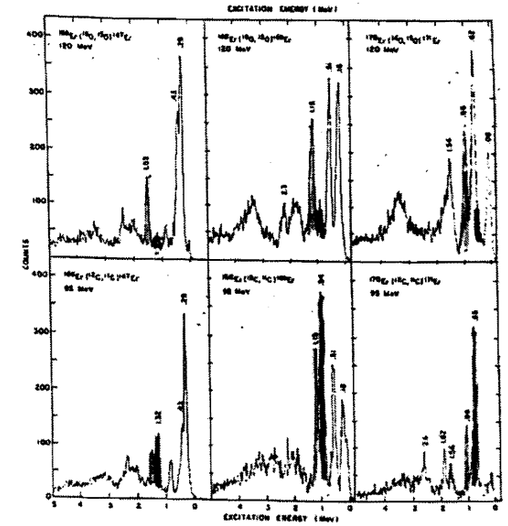

FIG. 2. Outgoing-particle spectra at 42° from the reactions ^{166,168,170}Er(^{18}O, ^{15}O) (top) and ^{166,168,170}Er(^{12}C, ^{11}C) (bottom). Excitation energies are listed above the peaks and have an uncertainty of about 0.02 MeV.

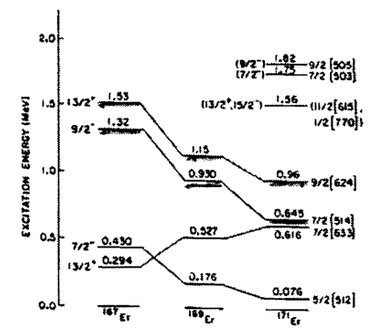

FIG. 3. Deduced single-particle high-spin levels for the erbium isotopes studied here. Spins of the levels appear to the left-hand side, energies on top, and Nilsson band assignments to the right-hand side. Levels whose energies are given in keV have been established in previous work.

Neutron Transfer: different angular momentum

Are $j = l - 1/2 \longleftrightarrow j = l + 1/2$ transitions preferred?

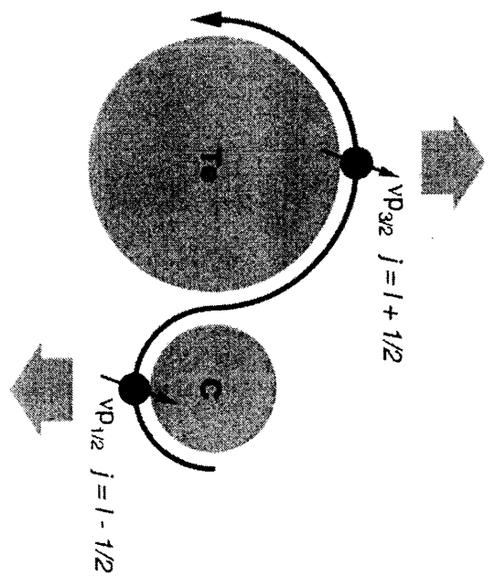

Transfer Reactions with Neutron-Rich RIBS

$^{9}Be(^{134}Te,^{8}Be)^{135}Te$

$\hookrightarrow 2\alpha$

~4 MeV per nucleon

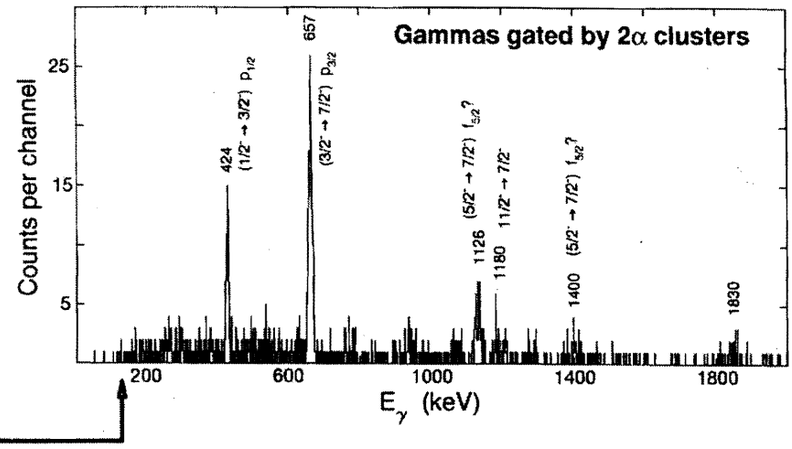

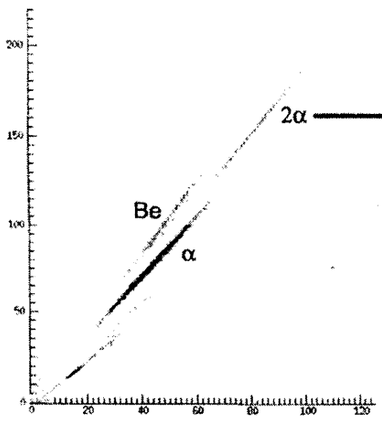

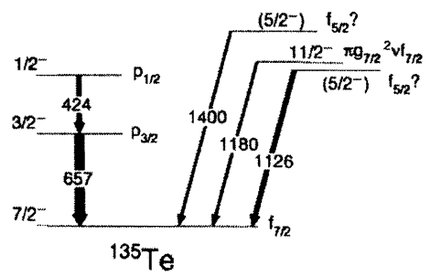

Neutron Transfer: different targets

We were able to collect some n-transfer data with a ^{13}C target

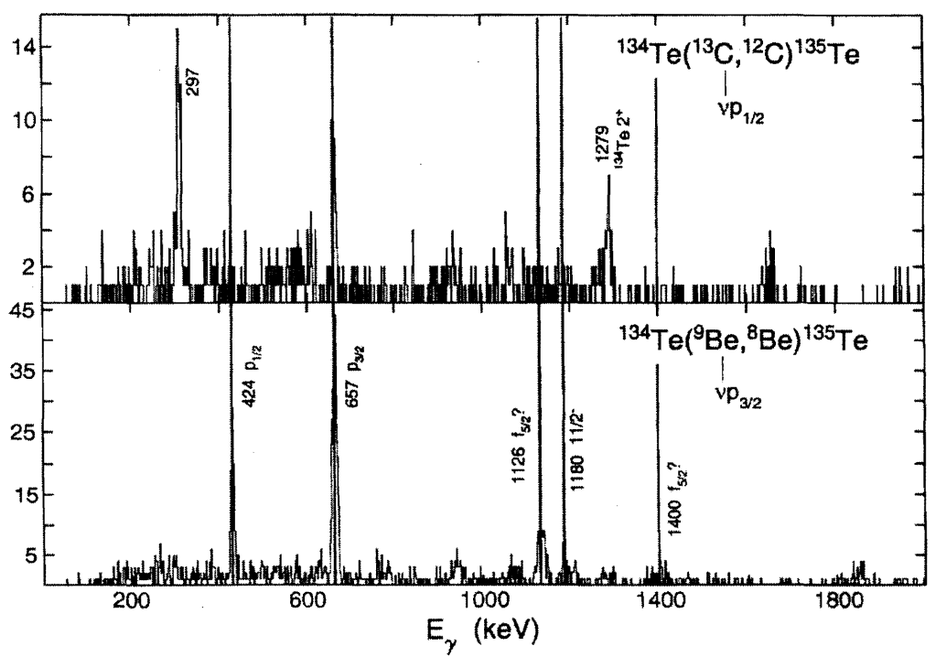

N = 83 Neutron Single-Particle Levels: Energy [illegible]

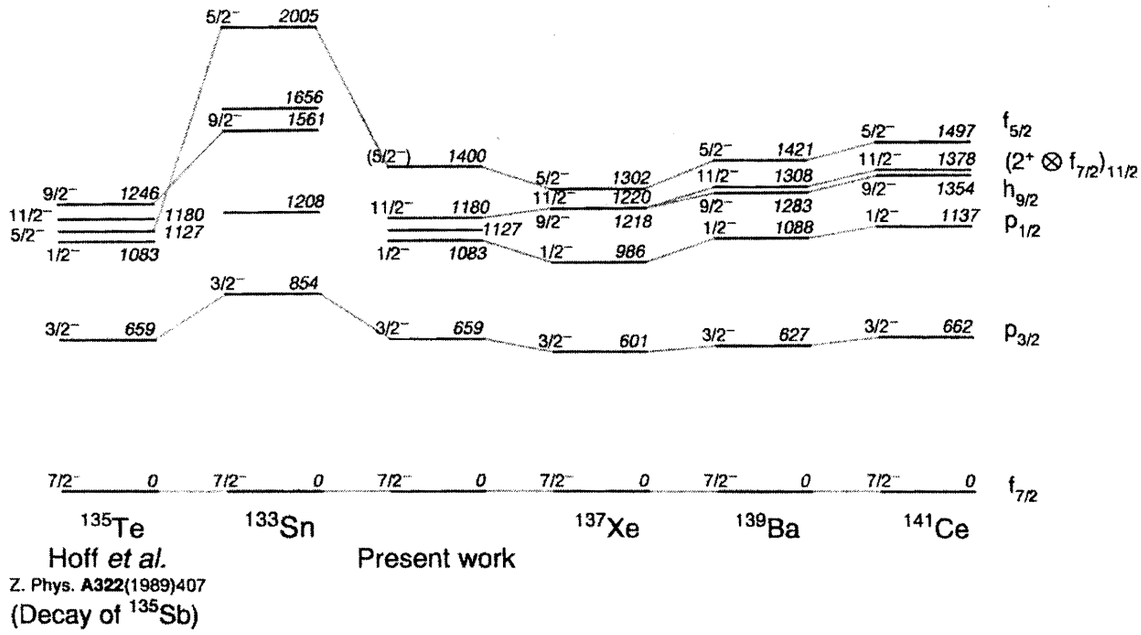

Future Plans: Transfer

- **Understand reaction mechanism**
  - ^{9}Be(^{138}Ba,^{8}Be)^{139}Ba with SIB
  - Particle-γ angular correlations
  - Sensitivity to $j = l \pm 1/2$ by comparing different targets
    e.g. (^{13}C,^{12}C) *vs.* (^{9}Be,^{8}Be)
  - Sensitivity to multistep processes
- **Investigate (^{7}Li,^{8}Be) proton pickup**
- **Search for $\pi s_{1/2}$ state in ^{133}Sb**
- **Search for proton-hole states in ^{131}In**
- **Long-term goal: (d,p), (^{3}He,d)** *etc.* **- spectroscopic factors**
- **Pure Sn beams are very promising, but ^{132}Sn intensity is marginal**
  - 10 - 100 times more beam intensity would allow transfer reactions to all neighbors
  - 2-neutron transfer to ^{134}Sn?

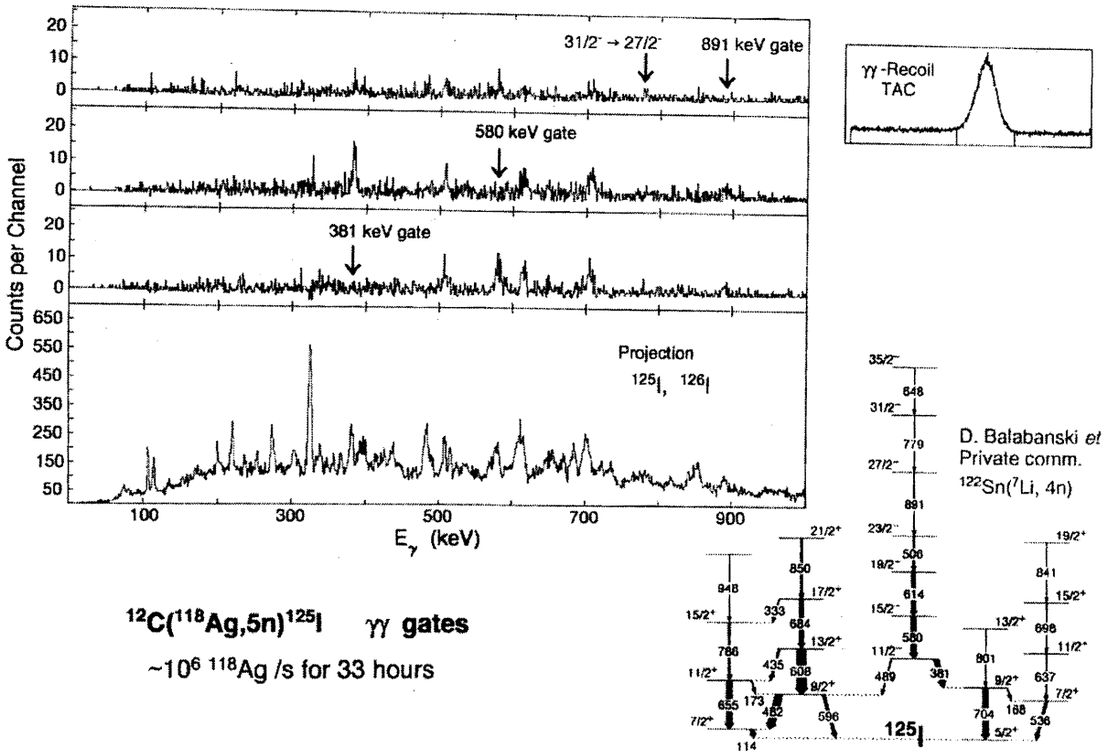

$^{12}C(^{118}Ag,5n)^{125}I$ γγ gates

~10^6 ^{118}Ag /s for 33 hours

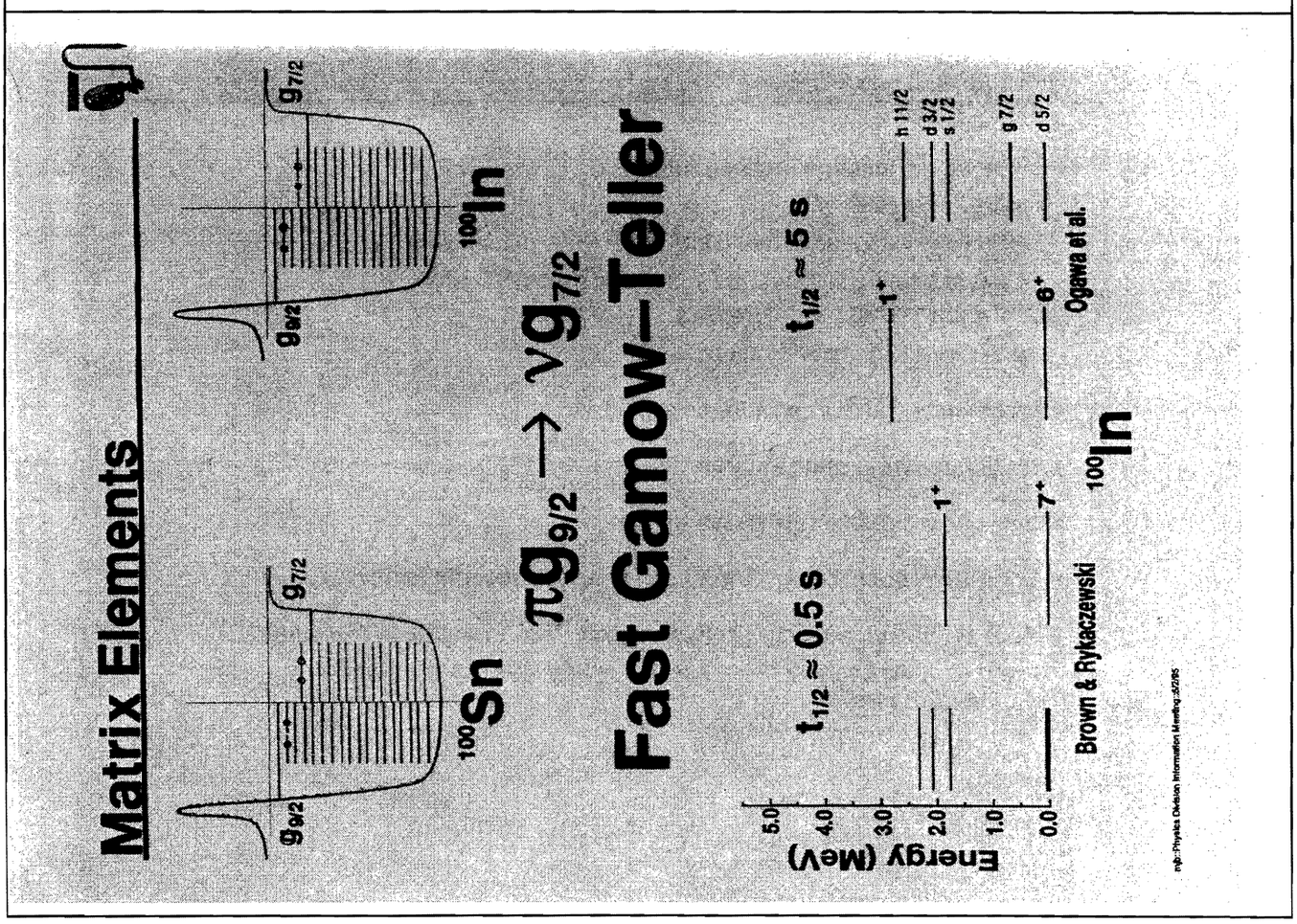

^{101}Sn

beam	^{58}Ni	^{56}Ni
(pps)	I=10^{11}	I=10^{8}
target (1mg/cm^2)	^{50}Cr	^{50}Cr
I×σ(^{101}Sn)	100	10
^{101}In : ^{101}Sn	640	98
^{101}Cd : ^{101}Sn	12 000	200
^{101}Ag : ^{101}Sn	34 000	280

Approaching ^{100}Sn...

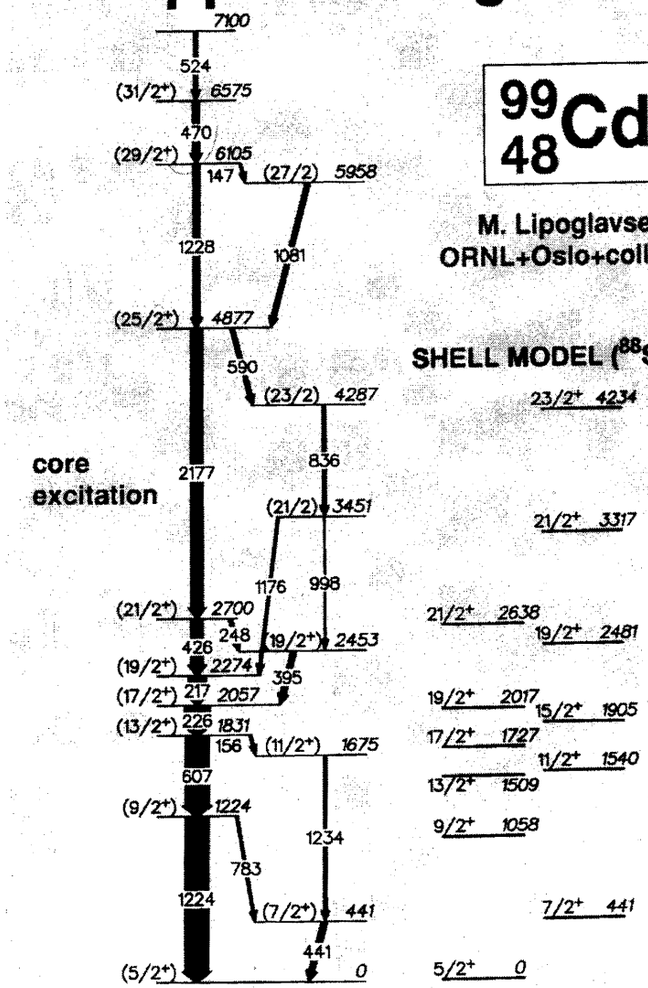

$^{99}_{48}$Cd$_{51}$

M. Lipoglavsek et al.
ORNL+Oslo+collaborators

SHELL MODEL (^{88}Sr core)

23/2+ 4234
21/2+ 3317
21/2+ 2638
19/2+ 2481
19/2+ 2017
15/2+ 1905
17/2+ 1727
11/2+ 1540
13/2+ 1509
9/2+ 1058
7/2+ 441
5/2+ 0

Neutron Detector Array
(RMS Endstation)

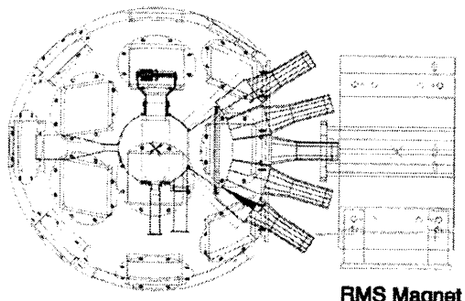

Characteristics:
- Covers +/- 40-deg
- Total detection efficiency of 13-22% (depending on reaction).

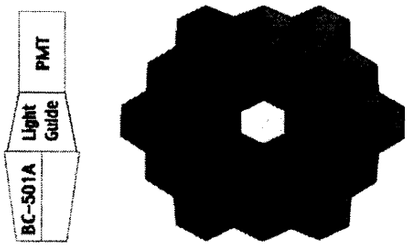

18 detectors, V=0.87 liter each

Application:
- (Z, A) identification of residues by detecting evaporated neutrons & charged particles
- Provides channel selection for weakly produced neutron-deficient nuclei
- Example: Spectroscopy near ^{100}Sn with ^{96}Ru,

Sn Fission Yields from ^{238}U target (UC/RVCF)

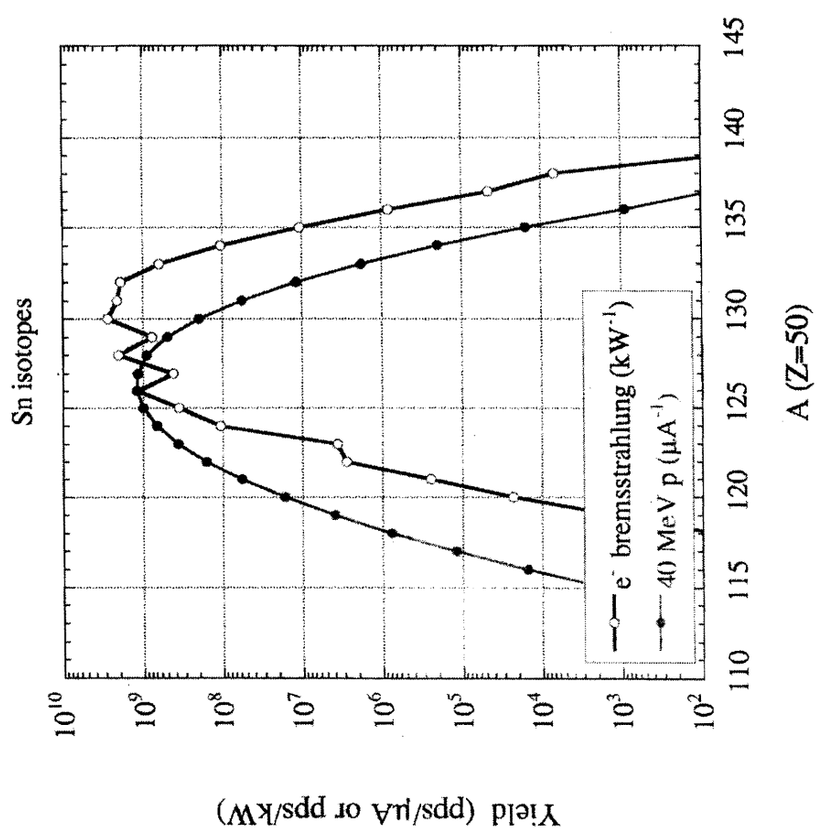

Summary

- **Feasibility of gamma spectroscopy with ISOL beams has been demonstrated. We have successfully performed:**
  - » **Coulomb excitation**
  - » **Transfer reaction**
  - » **Fusion reactions**
- **Some surprising results have been observed just beyond Sn-132**
- **Future directions:**
  - » **Quadrupole measurements**
  - » **Single-particle states around doubly magic Ni-56, Sn-100 & Sn-132 nuclei**
  - » **g-factors**
  - » **Decay studies**
  - » **Spectroscopic factors**
  - » **Measurements of interest to astrophysics**
- **We are exploring production of n-rich RIBs using electron beams @ ORELA, which will enhance beam intensities by ~100.**
- **We welcome users from all over the world.**

Isomer γ-ray Spectroscopy of Neutron-rich Nuclei Produced by Deep-inelastic Collisions

Tetsuro Ishii

Advanced Science Research Center, Japan Atomic Energy Research Institute

Email: ishii@popsvr.tokai.jaeri.go.jp

Heavy-ion deep-inelastic collisions (DICs) open a new way to study nuclear structure of high-spin states in neutron-rich nuclei. However, it is difficult to measure in-beam γ-rays emitted from nuclei produced in DICs, because DICs yield a large number of nuclides. Therefore, it is important to use an apparatus to select a nuclide for measuring in-beam γ-rays through DICs. On the other hand, one may expect many isomers around closed shells. Thus, it is very useful to measure γ rays from isomers to investigate nuclear structure near magic numbers. We have developed an instrument, isomer-scope [1], which selects nuclides by an atomic number and measures γ rays emitting from isomers of projectile-like fragments (PLFs) produced in DICs.

The isomer-scope consists of Si ΔE-E detectors, a tungsten γ-ray shield, and Ge detectors. PLFs are detected by Si ΔE-E detectors (four ΔE detectors of 20 μm thickness and one annular-shape E detector of 100 mm outer diameter) placed near the grazing angle. Gamma rays emitted from PLFs stopped in the Si-E detector are measured with eight Ge detectors (four of them are 60% efficiency and the others are about 30%) surrounding the Si-E detector. Prompt γ rays emitted at the target position are absorbed by a tungsten block placed between the target and the Ge detectors. Flight time between the target and the Si detector is about 1.5 ns, and thus we can measure isomers with $T_{1/2} > 1$ns. Taking the ΔE-E-γ(-γ) coincidences, we can obtain γ-ray spectra selected by each atomic number. Recently, we made ΔE detectors by ourselves by choosing a Si wafer with good uniformity in thickness. The ΔE resolution of these detectors is about twice as good as commercial ones. Using these ΔE detectors, we can identify mass numbers from the ΔE distribution obtained from γ-ray intensities.

Experiments were carried out at the JAERI tandem booster facility, using ^{70}Zn, ^{76}Ge, ^{82}Se beams of ~8MeV/nucleon and a ^{198}Pt target of 4.3 mg/cm^2. We have observed many isomers in neutron-rich Ni region, and about ten new isomers were found until now [2, 3, 4, 5, 6]. In these isomers, the $(\nu p_{1/2}^{-2} g_{9/2}^{2})8^+$ isomer was found in the semi doubly-magic nucleus $^{68}_{28}$Ni$_{40}$ and the level spectrum of ^{68}Ni is found to be a similar structure to that of $^{90}_{40}$Zr$_{50}$. In its neighboring nuclei $^{69,71}_{29}$Cu$_{40,42}$, we have found $(\pi p_{3/2} \nu g_{9/2}^{2})19/2^-$ isomers. The levels decaying from these isomers were predicted very accurately by a parameter-free shell model calculation using experimental levels as two-body residual interactions. Recently, we can assign several unknow γ-ray cascades to ^{68,70}Cu and ^{67}Ni by analyzing ΔE distributions. We have also measured neutron-rich nuclei produced by ^{37}Cl beams, and verified nanosecond isomers in ^{32,33}Si and ^{34}P.

References

[1] T. Ishii *et al.*, Nucl. Instr. Meth. A **395**, 210 (1997).
[2] I. Hossain *et al.*, Phys. Rev. C **58**, 1318 (1998).
[3] T. Ishii *et al.*, Phys. Rev. Lett. **81**, 4100 (1998).
[4] A. Makisima *et al.*, Phys. Rev. C **59**, R2331 (1999).
[5] T. Ishii *et al.*, Phys. Rev. Lett. **84**, 39 (2000).
[6] M. Asai *et al.*, Phys. Rev C **62**, 054313 (2000).

Isomer γ-ray Spectroscopy of Neutron-rich Nuclei Produced by Deep-inelastic Collisions

Tetsuro Ishii
Japan Atomic Energy Research Institute

日本原子力研究所

M. Asai , M. Matsuda, S. Ichikawa, P. Kleinheinz
Japan Atomic Energy Research Institute

A. Makishima
National Defense Medical College

I. Hossain, M.Ogawa
Tokyo Institute of Technology

1. JAERI's activity of γ-ray spectroscopy

2. γ-ray spectroscopy through DIC
   heavy-ion deep-inelastic collisions
   isomer-scope
      Mass determination from ΔE distributions
      in-plane / out-of-plane anisotropy

3. Nuclear structure of neutron-rich nuclei
   $(\nu p_{1/2}^{-2}\, \nu g_{9/2}^{2})8^{+}$ isomer in *doubly-magic* $^{68}Ni_{40}$
   shell model calculation for $(\pi p_{3/2} \nu g_{9/2}^{2})19/2^{-}$ isomers in ^{69,71}Cu
   $(\nu g_{9/2}^{-2})8^{+}$ isomers in *N=48* nuclei
   nano-second isomers in ^{32,33}S, ^{34}P

4. Future plan

JAERI Tandem(18MV) – Superconducting Linac(30MV)

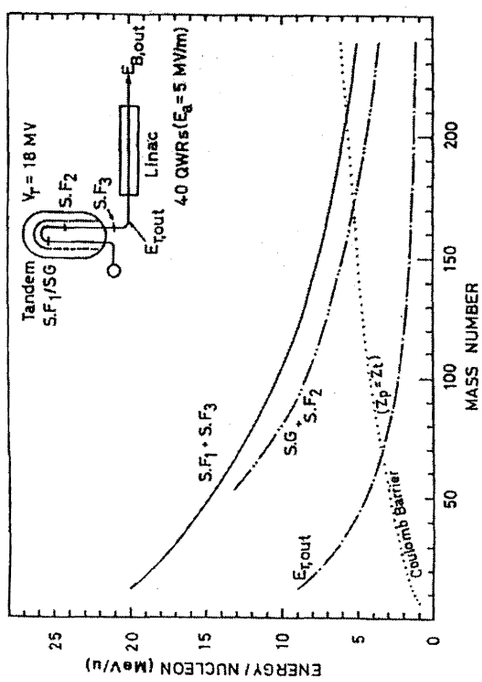

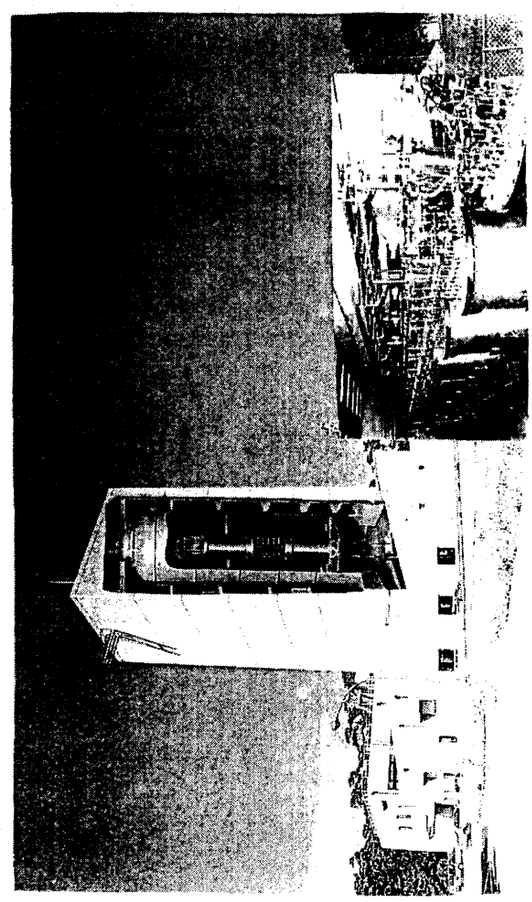

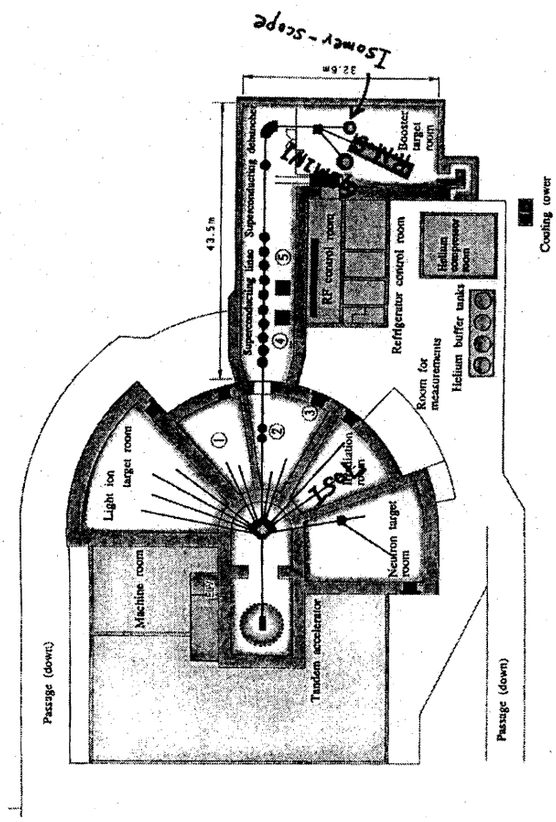

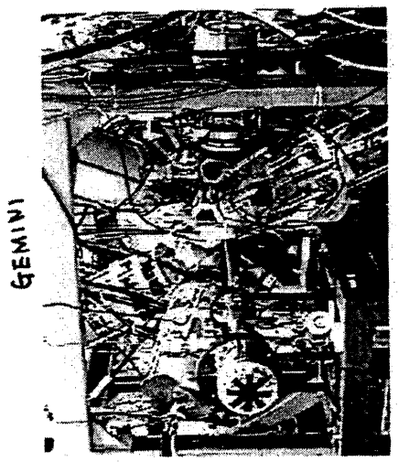

		Neutron number 92	94	96 (Stable isotope)	98	100	102							
66	Dy	158	159 144.4 d	160	161	162	163	164	165 2.334 h 1.257 m	166 81.6 h	167 6.20 m	168 8.7 m	169 39 s	171 53 s / 172 25 s
65	Tb	157 99 y	158 180 y 10.7 s	159	160 72.3 d	161 6.88 d	162 7.60 m	163 19.5 m	164 3.0 m	165 2.11 m		167 19.4 s	168 8.2 s	
64	Gd	156	157	158	159 18.479 h	160	161 3.66 m	162 8.4 m	163 68 s	164 45 s	165 10.3 s			
63	Eu	155 4.961 y	156 15.19 d	157 15.18 h	158 45.9 m	159 18.1 m	160 38 s	161 26 s	162 10.6 s					
62	Sm	154	155 22.3 m	156 9.4 h	157 432 s	158 5.30 m	159 11.37 s	160 9.6 s	161 4.8 s					
61	Pm	153 5.4 m	154 2.68 m 1.73 m	155 41.5 s	156 26.70 s	157 10.56 s	158 4.8 s							
60	Nd	152 11.4 m	153 28.9 s	154 25.9 s	155 8.9 s	156 5.47 s	157							
59	Pr	151 18.90 s	152 3.24 s	153 4.3 s	154 2.3 s	155	156	157						
58	Ce	150 4.0 s	151 1.02 s	152 1.4 s	153	154	155	156						
57	La	149 1.05 s	150 0.7 s	151	152	153	154							

Proton number — Chemical symbol

Synthsized by multi-nucleon transfer reaction at GSI and LBL.

Previous work

Present work

Symbol: 160 (Mass number), 9.6 s (Half-life)

Synthsized by projectile fission of ^{238}U at GSI.

The new limits of the nuclide chart on the neutron-rich lanthanide side.

Isomers

- plentiful physics
- many isomers near the magic numbers

Isomer-scope *T. Ishii et al., NIM A395(1997)210*

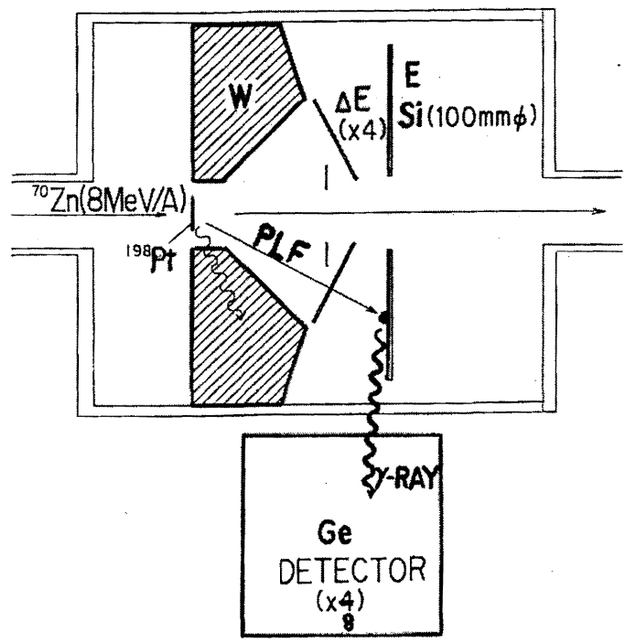

PLF emits near (slightly smaller) grazing angle

Heavy-ion deep-inelastic collisions

- produce neutron-rich nuclei
  - PLF is apt to neutron-rich; $(N/Z)_{Projectile} < (N/Z)_{Target}$
- induce high angular momentum

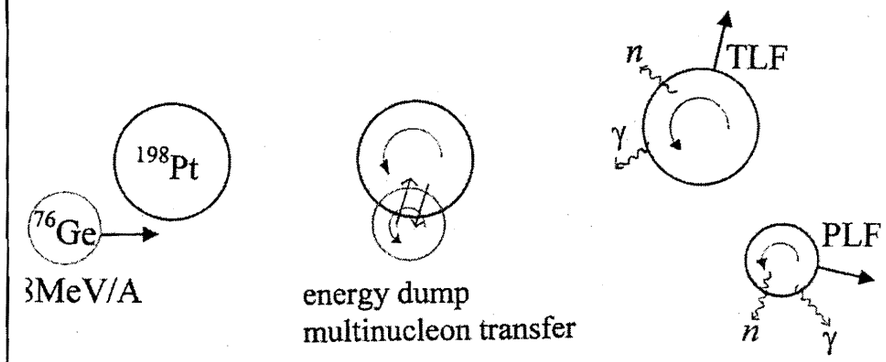

Difficulty in in-beam γ-ray spectrocopy

- many differnt nuclei are produced
- wide scattering angle, high recoil velocity

large crystal ball→ *R. Broda et al. PRL 74(1995)868*
I.Y. Lee et al., PRC 56(1997)753
J.F.C. Cooks et al., PRL 78(1997)2920
.....

Isomer-scope Jan 11-14, 2001

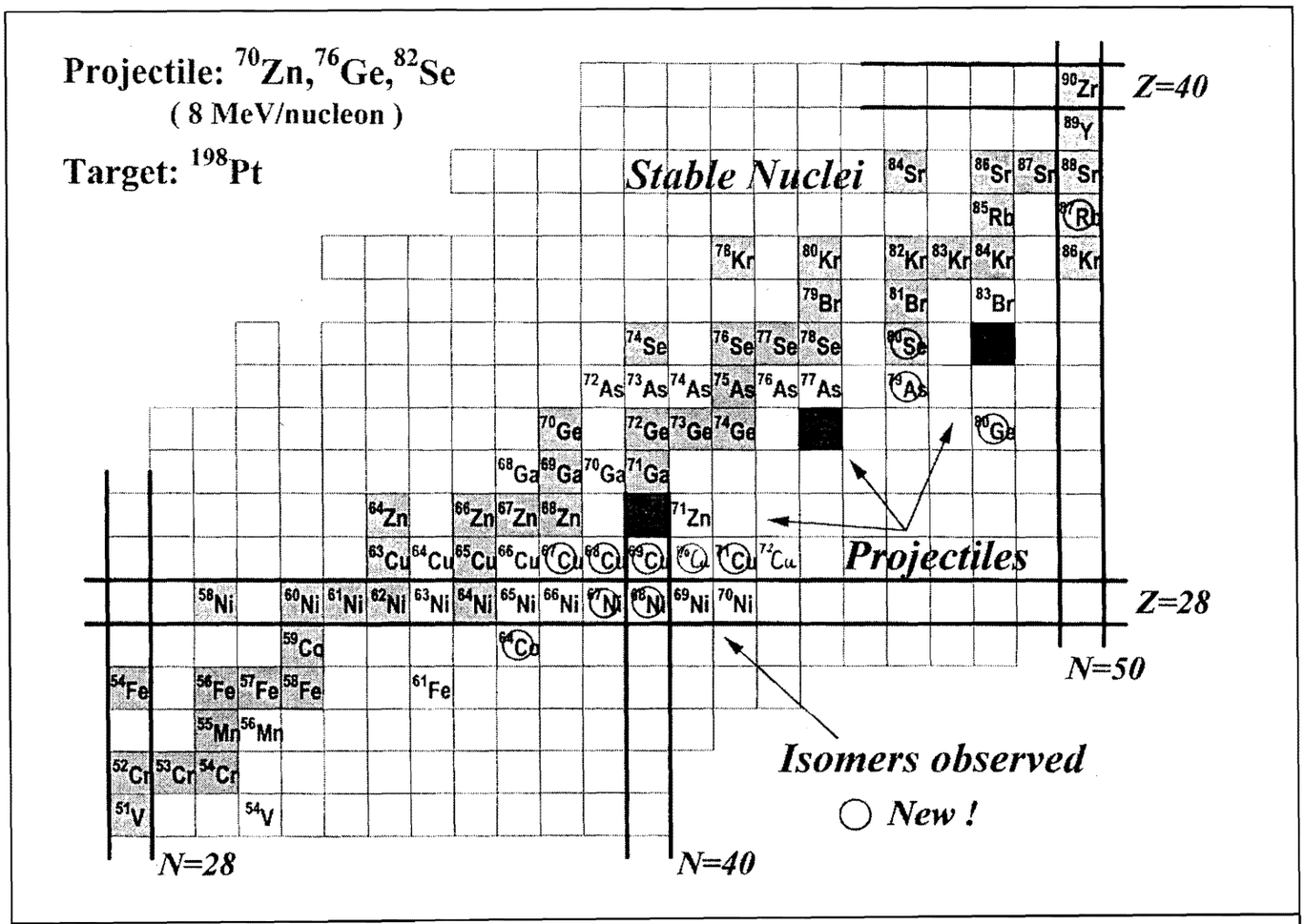
Projectile: 70Zn, 76Ge, 82Se
(8 MeV/nucleon)
Target: 198Pt
Stable Nuclei
Projectiles
Isomers observed
New !
Z=40
Z=28
N=28
N=40
N=50

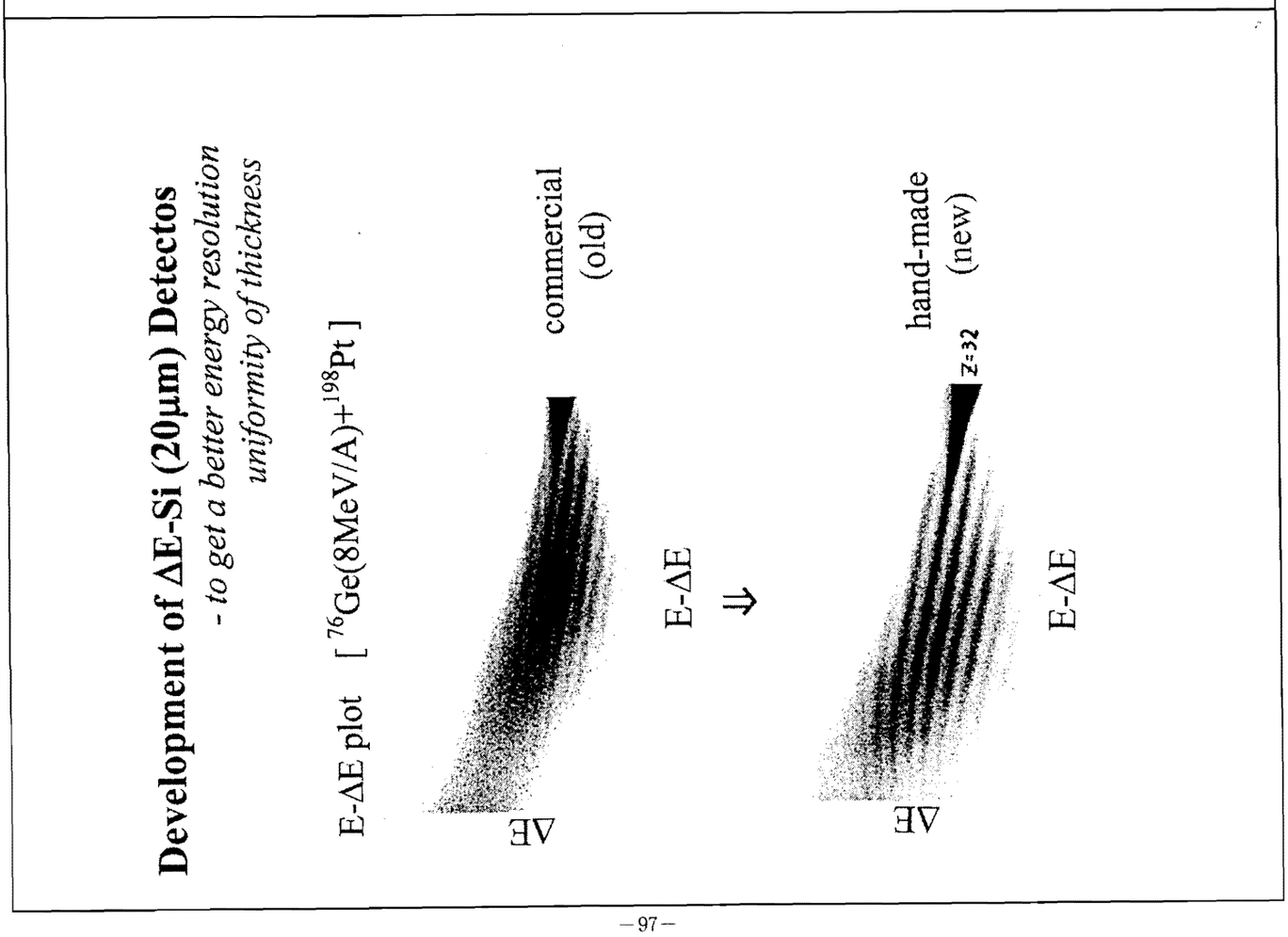
Development of ΔE-Si (20μm) Detectos
- to get a better energy resolution
uniformity of thickness
E-ΔE plot [76Ge(8MeV/A)+198Pt]
commercial
(old)
hand-made
(new)
Z=32
E-ΔE
ΔE
E-ΔE
ΔE

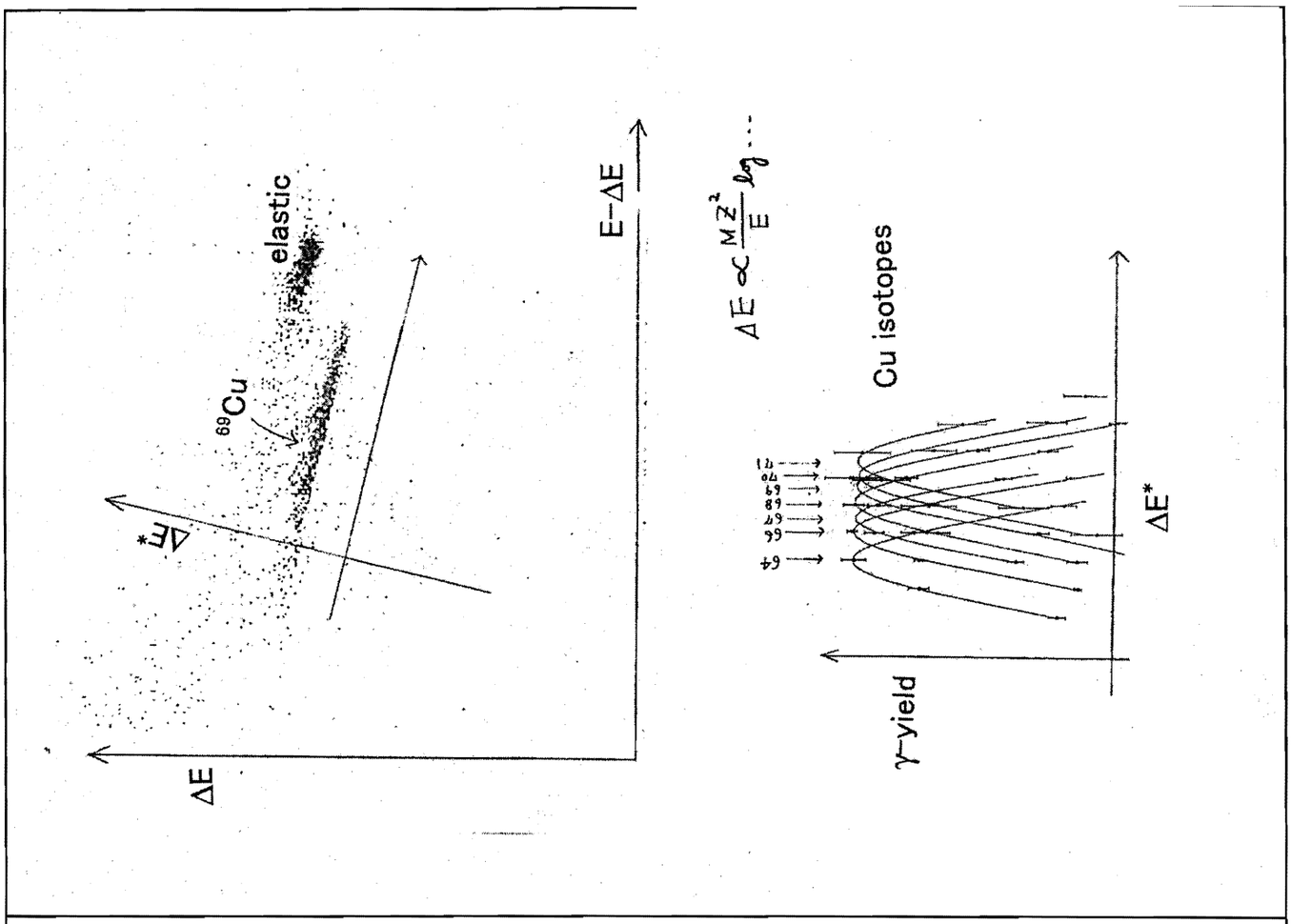
elastic
^{69}Cu
ΔE*
ΔE
E−ΔE
$\Delta E \propto \frac{MZ^2}{E} \log \cdots$
Cu isotopes
γ-yield
ΔE*

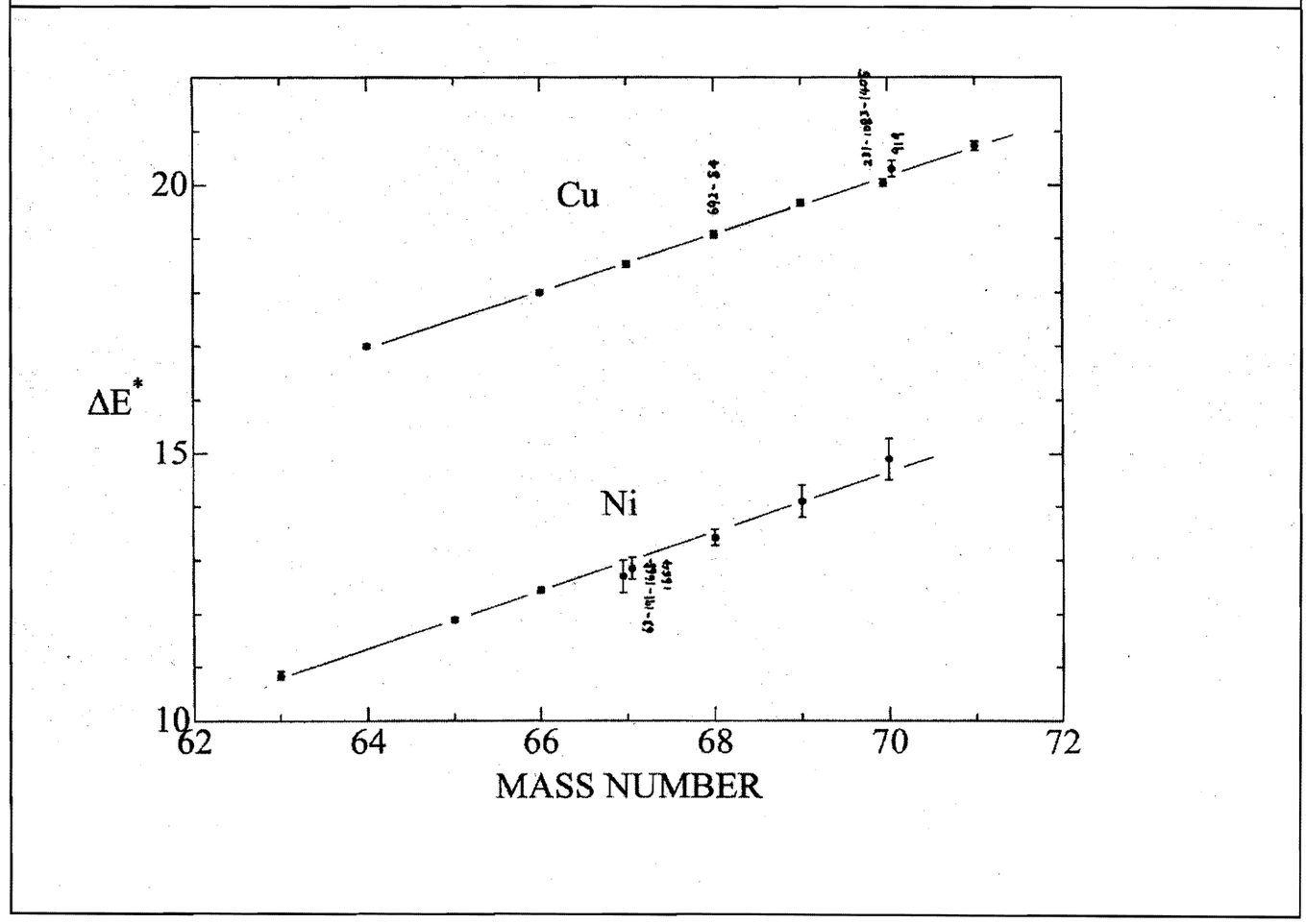
Cu
Ni
ΔE*
MASS NUMBER
10
15
20
62
64
66
68
70
72

γ-ray spectra measured with the isomer-scope

$^{76}Ge(8MeV/A)+^{198}Pt$

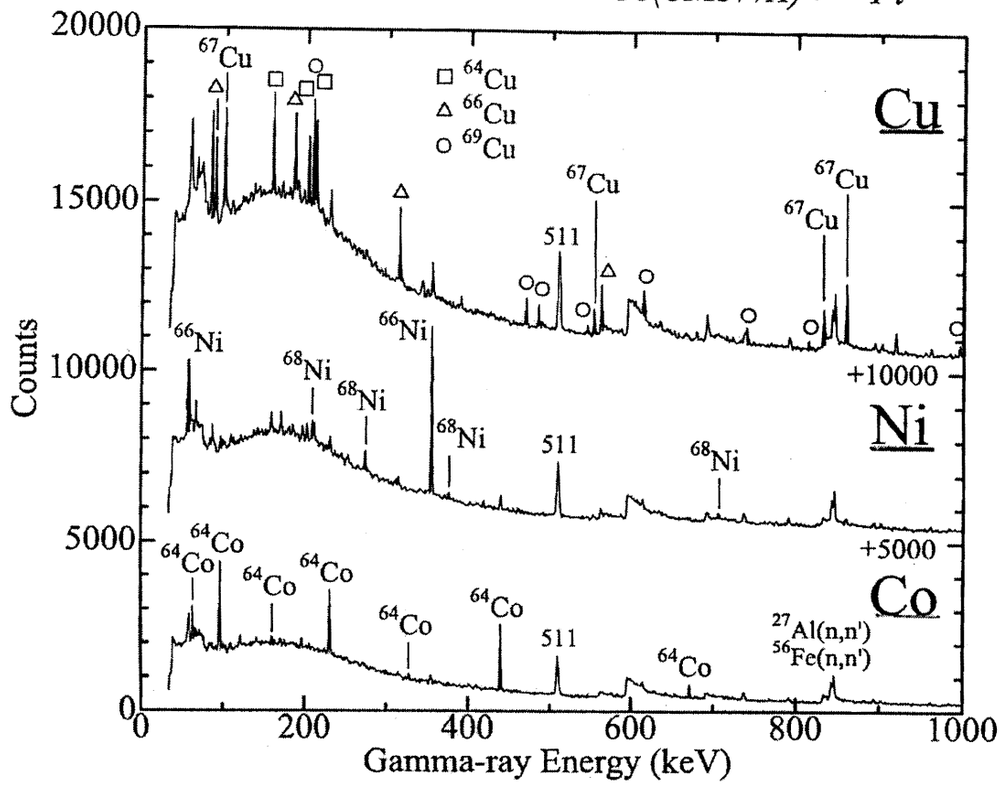

M. Asai et al. , PRC 62 (2000) 054313

γ-ray spectra

ΔE-E-γ-(γ), $t_{PLF-\gamma}$= 20-100 ns

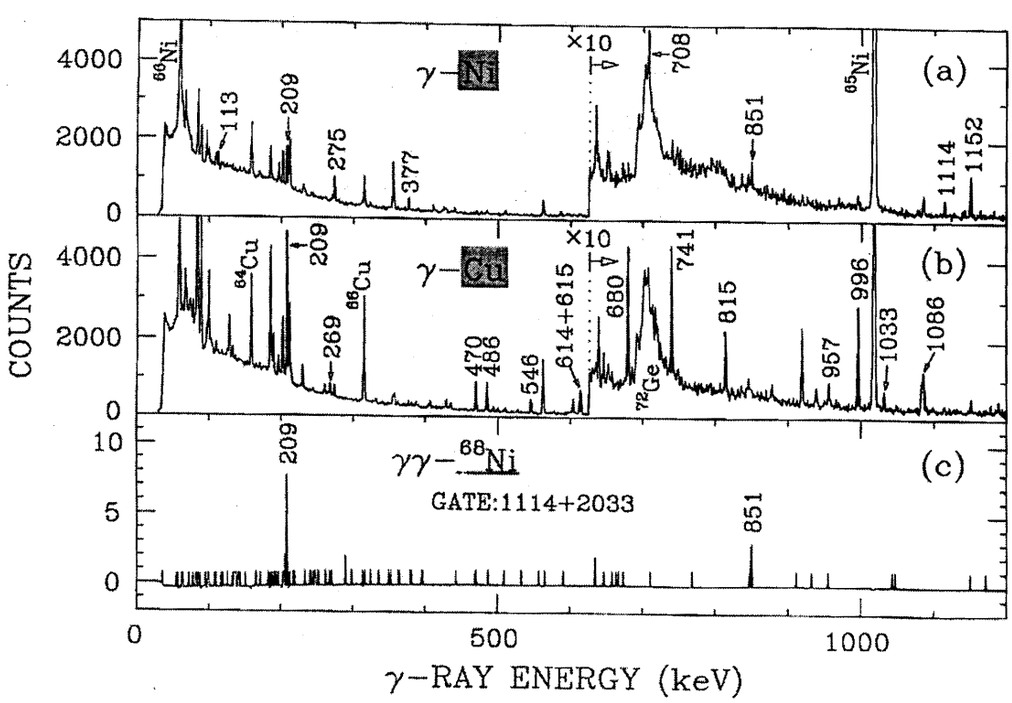

Decay scheme of the 8^+ isomer in ^{68}Ni

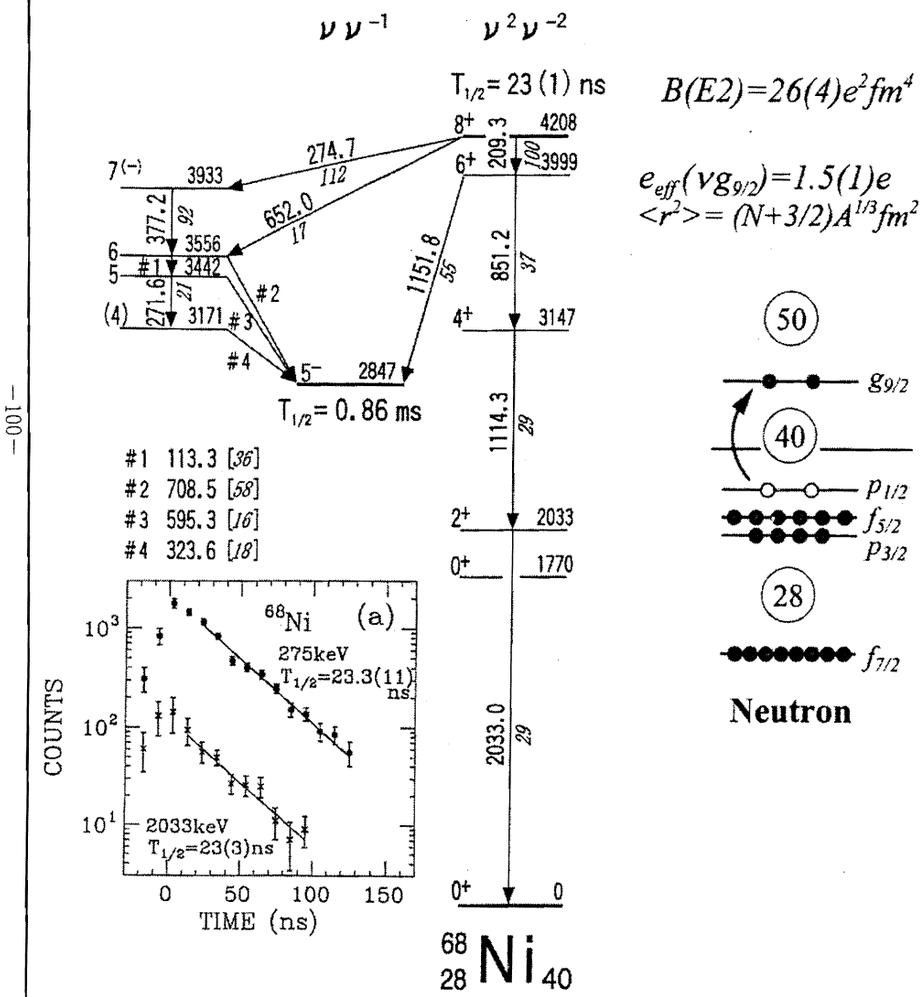

$B(E2)=26(4)e^2fm^4$

$e_{eff}(\nu g_{9/2})=1.5(1)e$

$\langle r^2\rangle = (N+3/2)A^{1/3}fm^2$

Neutron

T. Ishii et al., PRL 84 (2000) 39

In-plane/Out-of-plane anisotropy

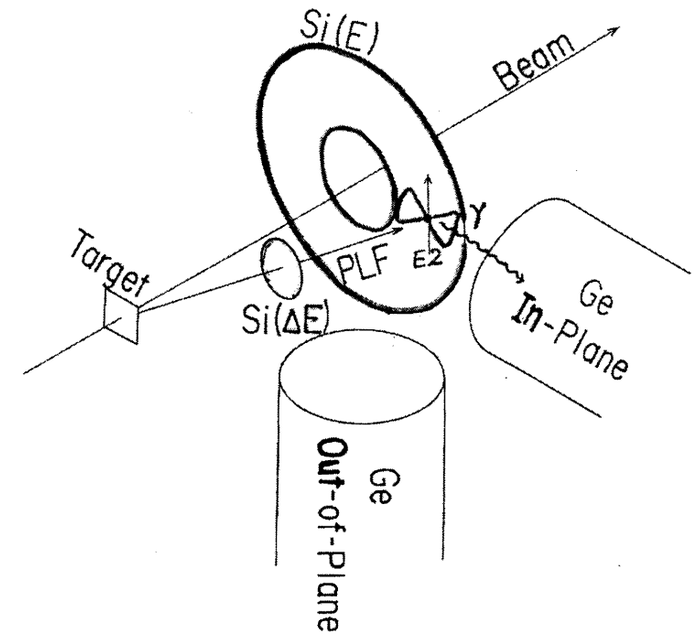

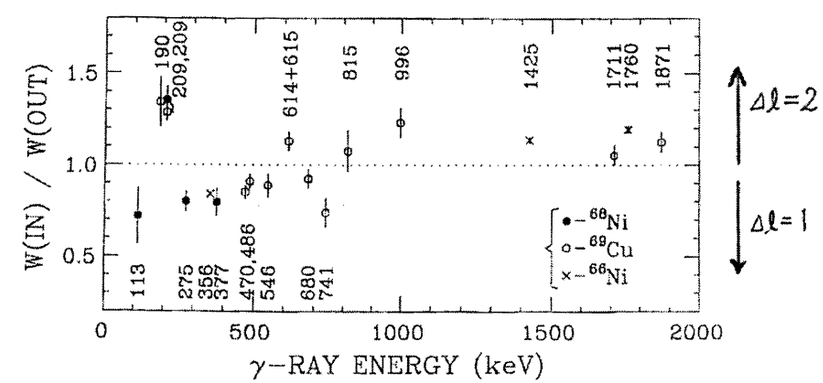

$(\nu g_{9/2}^2\ \pi p_{3/2})19/2^-$ isomer decay in ^{71}Cu and j^2j'-type isomers

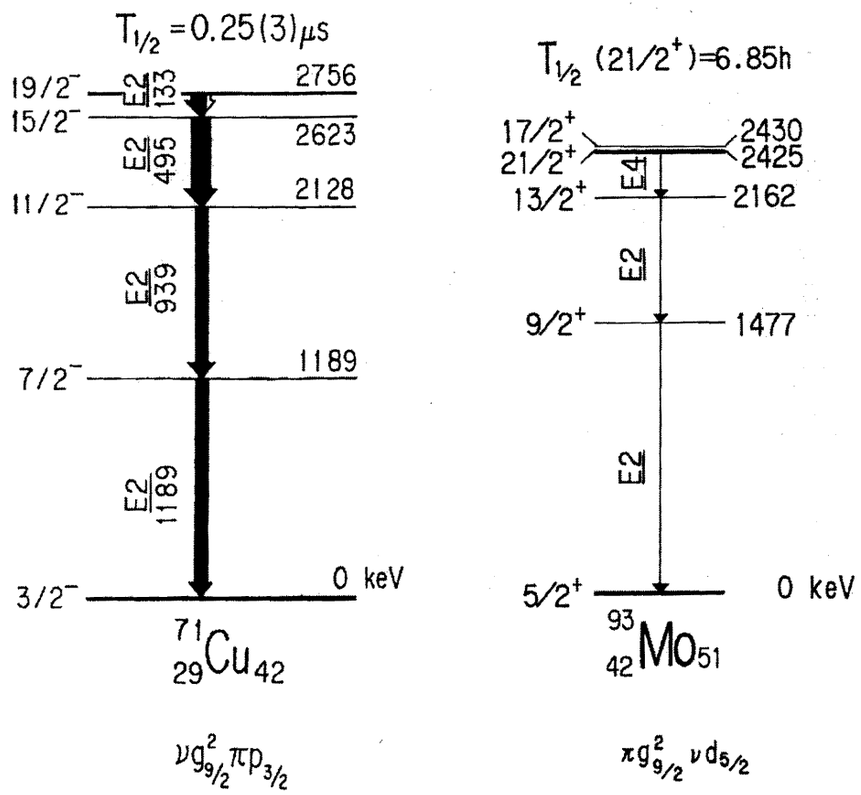

$g_{9/2}^n$ level spectra

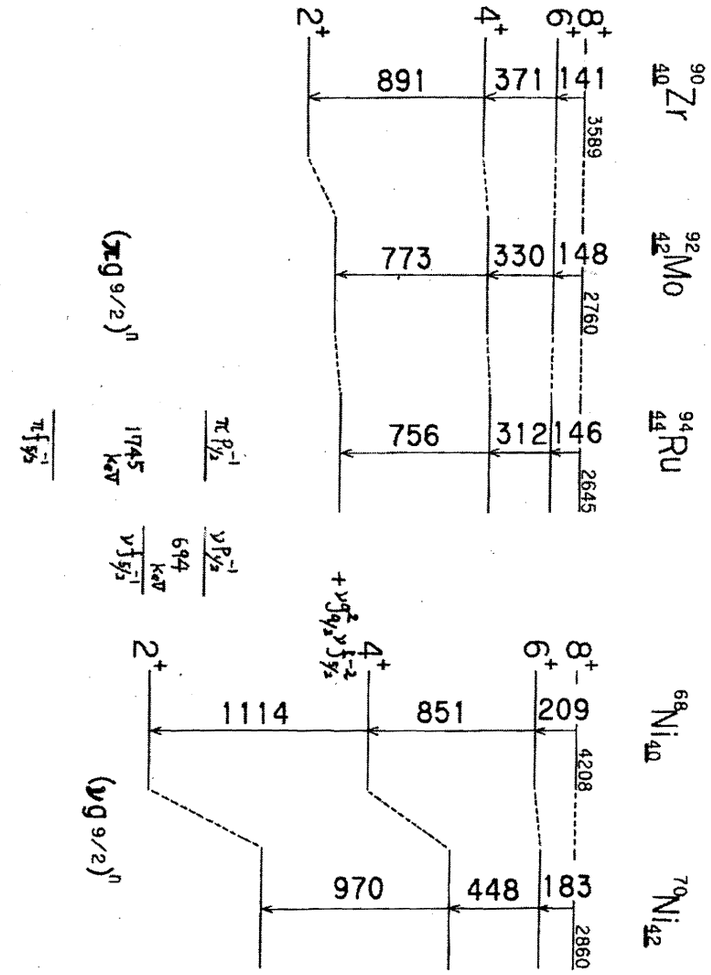

Comparison with a shell model calculation

core: ^{68}Ni
two body residual interactions: energy levels in ^{70}Ni and ^{70}Cu

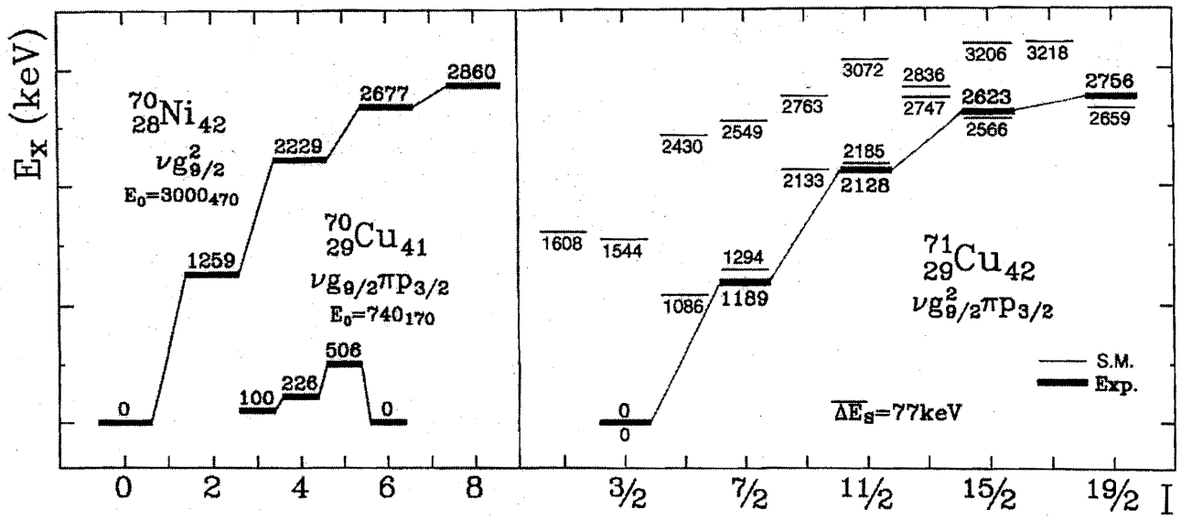

T. Ishii et al., PRL 81 (1998) 4100

$(\nu g_{9/2}^{-2})$ 8^+ isomers in N=48

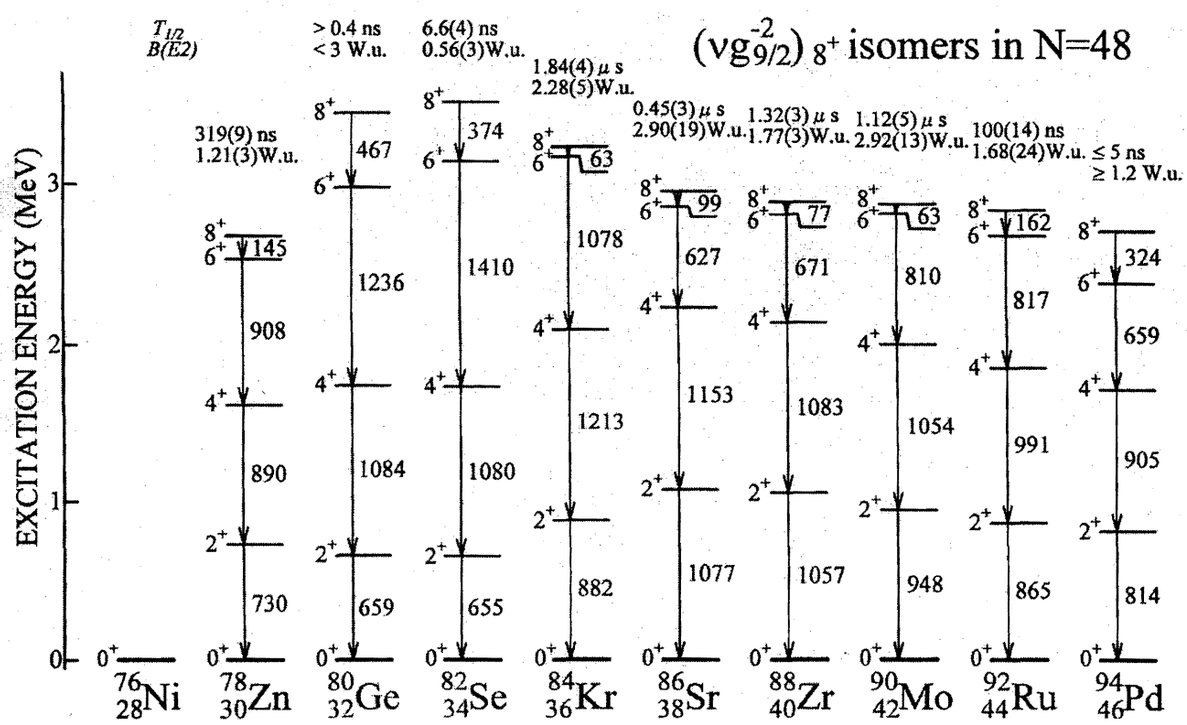

^{80}Ge, ^{82}Se: A. Makishima et al., PRC 59(1999)R2331
^{78}Zn: J.M. Daugas et al., PLB 476(2000)213
^{86}Sr: M. Ishihara et al., PL 35B(1971)398

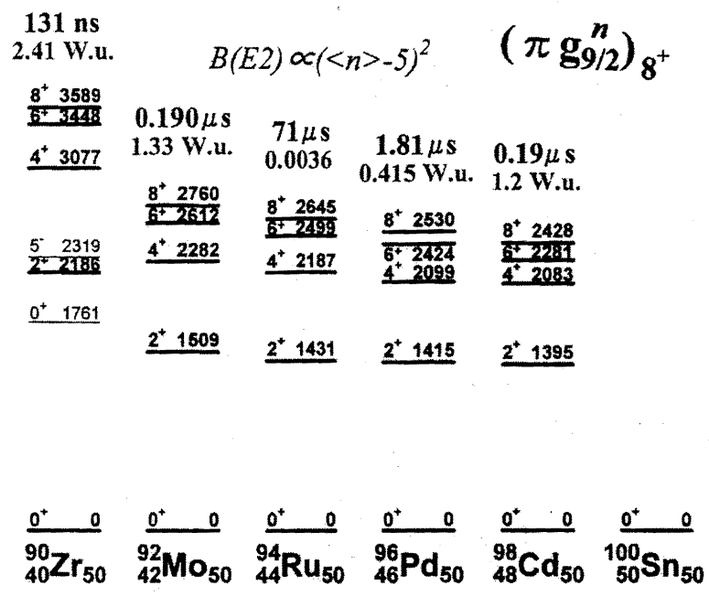
131 ns
2.41 W.u.
B(E2) ∝(<n>-5)²
(π g9/2^n)8+
8+ 3589
6+ 3448
4+ 3077
5- 2319
2+ 2186
0+ 1761
0.190μs
1.33 W.u.
8+ 2760
6+ 2612
4+ 2282
2+ 1509
71μs
0.0036
8+ 2645
6+ 2499
4+ 2187
2+ 1431
1.81μs
0.415 W.u.
8+ 2530
6+ 2424
4+ 2099
2+ 1415
0.19μs
1.2 W.u.
8+ 2428
6+ 2281
4+ 2083
2+ 1395
0+ 0
90 40 Zr 50
92 42 Mo 50
94 44 Ru 50
96 46 Pd 50
98 48 Cd 50
100 50 Sn 50

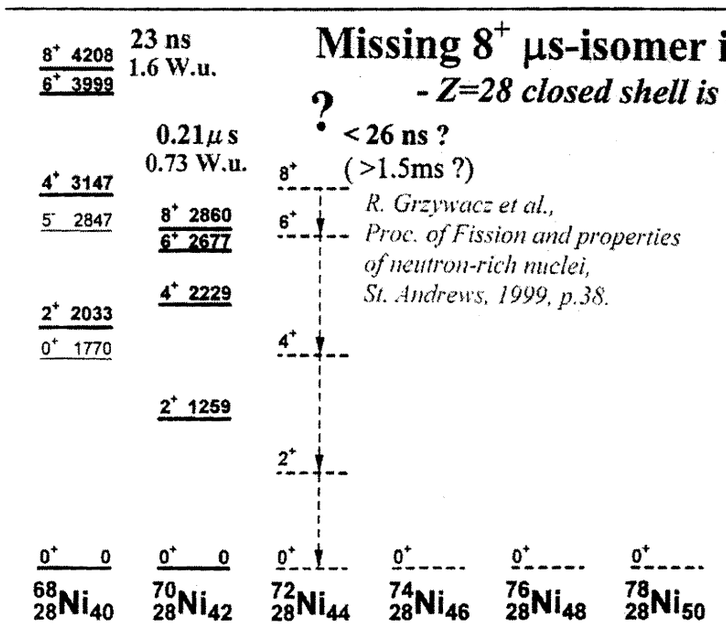
Missing 8+ μs-isomer in 72Ni42
- Z=28 closed shell is broken ?
8+ 4208
6+ 3999
23 ns
1.6 W.u.
4+ 3147
5- 2847
2+ 2033
0+ 1770
0.21μs
0.73 W.u.
8+ 2860
6+ 2677
4+ 2229
2+ 1259
?
< 26 ns ?
(>1.5ms ?)
8+
6+
4+
2+
0+ 0
68 28 Ni 40
70 28 Ni 42
72 28 Ni 44
74 28 Ni 46
76 28 Ni 48
78 28 Ni 50
R. Grzywacz et al.,
Proc. of Fission and properties
of neutron-rich nuclei,
St. Andrews, 1999, p.38.

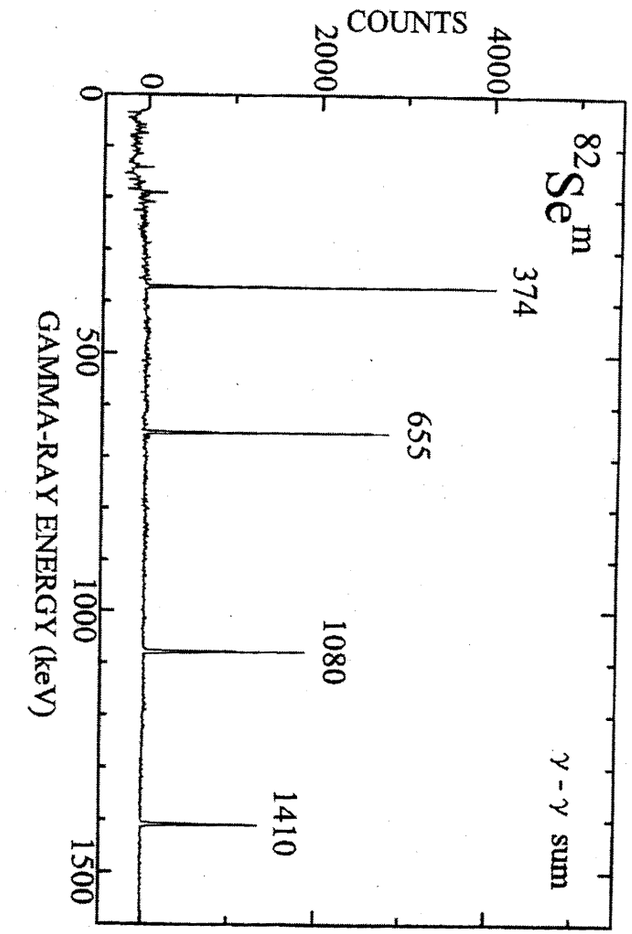
82Sem
γ - γ sum
COUNTS
0
2000
4000
374
655
1080
1410
0
500
1000
1500
GAMMA-RAY ENERGY (keV)

Isomer Spectroscopy

with DIC and Isomer-scope

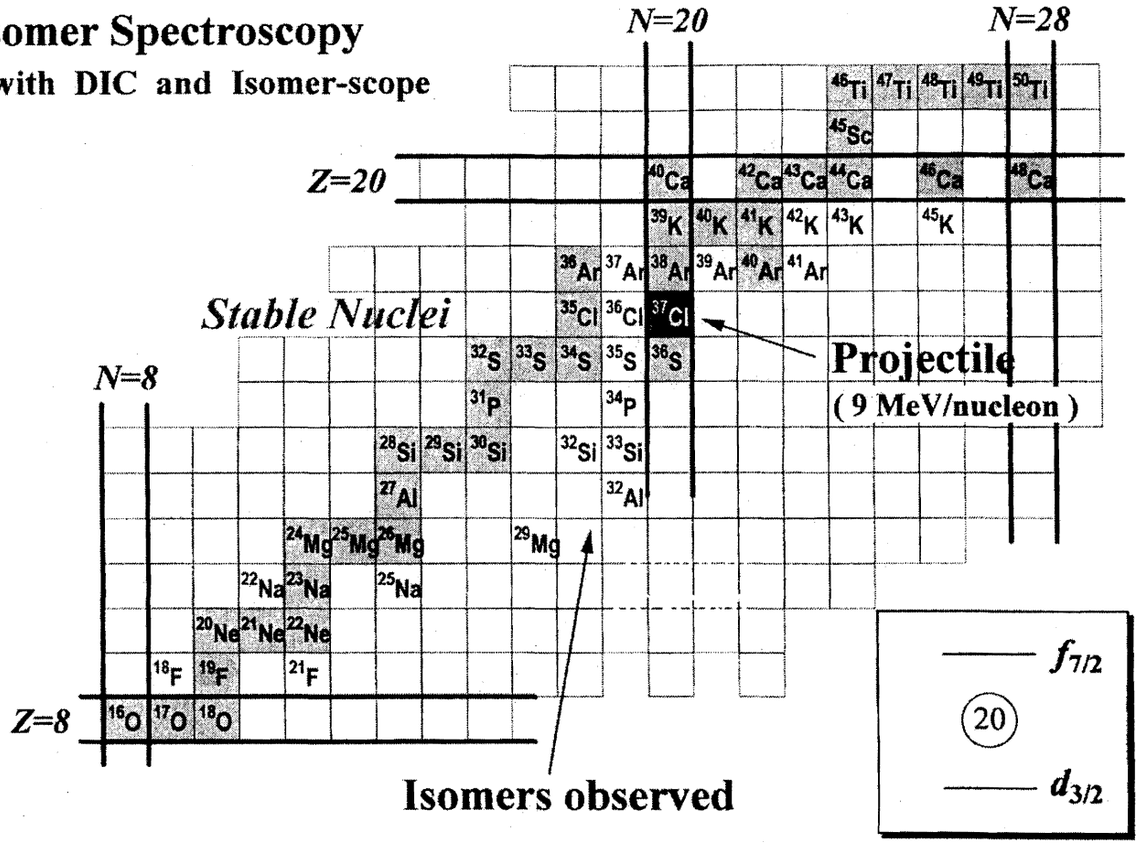

N = 19 isomers

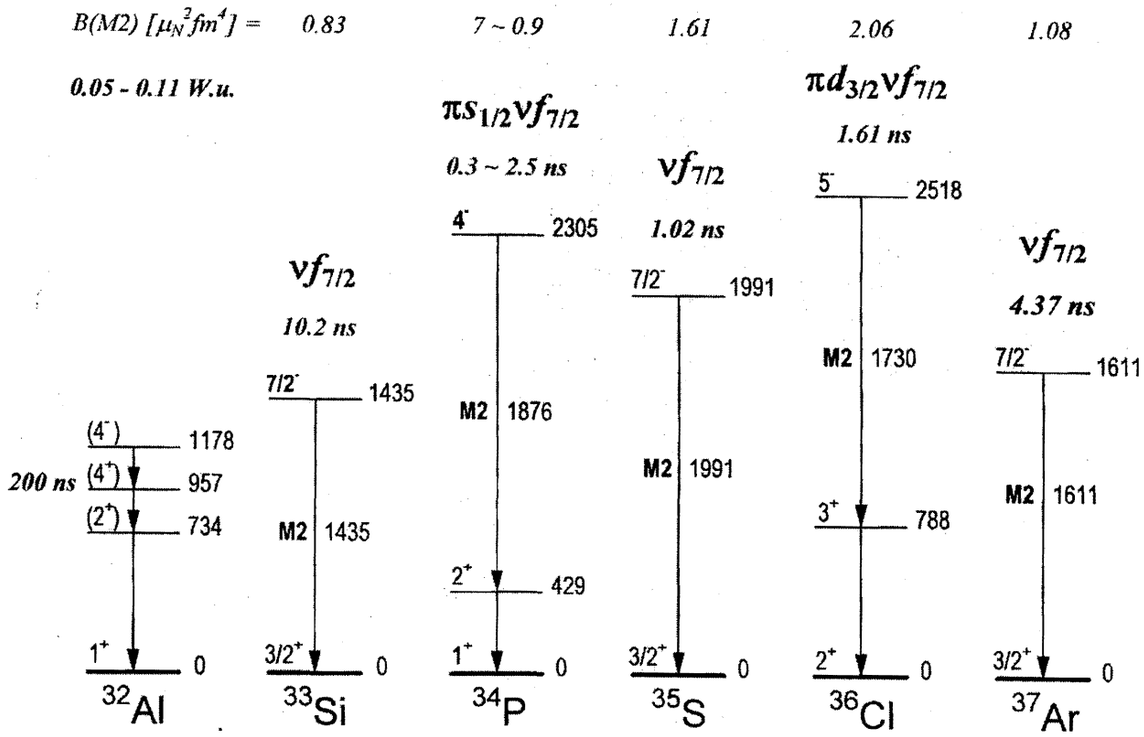

Summary

◎ *Isomer-scope* [γ-shield+ Si(ΔE-E) + Ge],
has great sensitivity for ns-isomers produced in DIC.

- *Mass numbers can be also determined from ΔE.*
- *In-plane to out-of-plane ratios are useful to determine γ-ray multipolarities.*

◎ Several new isomers were found in neutron-rich Ni region.

- $(\nu g_{9/2}^{2} \nu p_{1/2}^{-2})8^{+}$ isomer in the doubly-magic $^{68}Ni_{40}$
  similar structure to $^{90}{}_{40}Zr$; $e_{eff}(\nu g_{9/2})=1.5(1)e$
- $(\pi\, p_{3/2} \nu g_{9/2}^{2})19/2^{-}$ isomers in $^{69,71}Cu_{40,42}$
  Shell model calculation using experimental levels as residual interactions has a predictive power for j^2j'*-type isomer decay.*

- $(\nu g_{9/2}^{-2})\ 8^{+}$ isomers in $^{80}Ge_{48}$ and $^{82}Se_{48}$
  $^{76}Ni_{48}$ *would have* 8^{+} *isomers to be detected by projectile fragmentation techniques.*

◎ Missing 8^{+} μs-isomer in ^{72}Ni may suggests something interesting happens in neutron-rich Ni.

◎ Several isomers were observed in N=20 region using ^{37}Cl beams
M2 isomeric transitions originated from $f_{7/2}$ *to* $d_{3/2}$

Future plan

1. γ-ray measurements above isomers
   ΔE-E- γ(isomer↓) - γ(isomer↑)

2. isomer γ-rays around ^{48}Ca region

3. development of better ΔE Si detectors
   aiming at the resolution of 1.5%
   (at the moment 3.5%)

4. in-beam γ-ray (prompt γ-ray) measurements
   Si-PSD (Δθ=2° , Δφ=10°)
   or another position detectors
   and γ-ray tracking array

Prompt γ-ray measurements above isomers

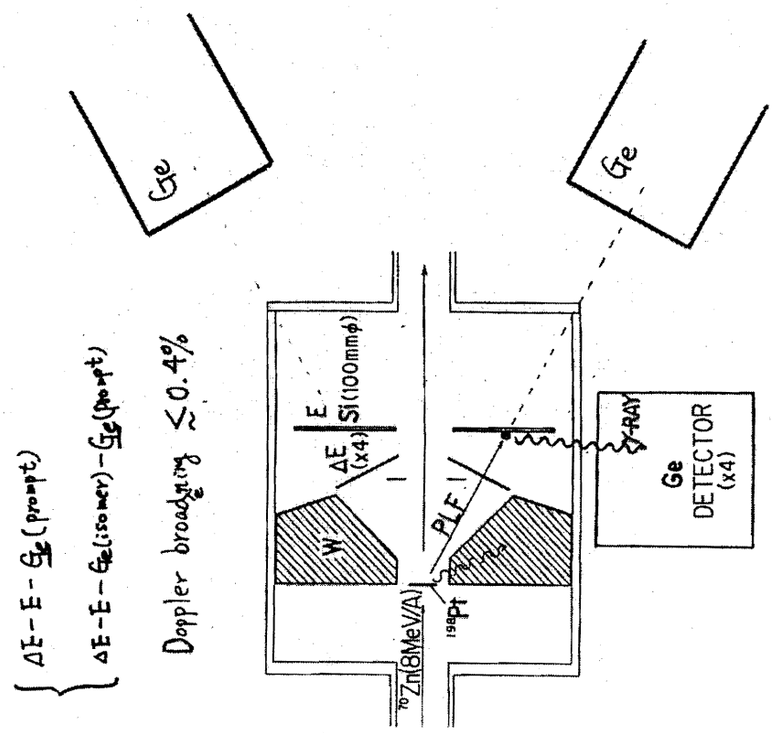

Gamma-ray spectroscopy of exotic nuclei at GANIL

G. de France[1]

[1] *GANIL, BP 55027*
F-14076 CAEN CEDEX 5, FRANCE.

Nuclear structure studies of very exotic nuclei have already started in the several laboratories where radioactive species are produced via fragmentation of the projectile. This is the case at GANIL where many results have been obtained these last years using this production mechanism for both neutron rich and neutron deficient nuclei. Examples will be shown for nuclei around the closed shells and in particular in the $N \sim Z$ Kr isotopes as well as in the case of lighter Ni.

These examples represent an excellent opportunity to go toward radioactive beams and to have a better estimate of their perspectives. New species will be made available as beams but with a reduced intensity as compared to what we are used to with stable beams and other constraints directly related to the radioactive nature of the beams. Possible realistic startup experiments will be discussed in view of these conflicting possibilities. New spectrometers (recoil, gamma and electron) have been or are presently being designed to handle the various constraints. The EXOGAM gamma-ray array is one of these. This setup will be described in more details and future plans related to gamma-ray spectroscopy at GANIL will be discussed.

γ-ray spectroscopy of exotic nuclei at GANIL

G. de France, GANIL

- Exotic nuclei via fragmentation
  - Shell closures
  - Isomers
  - Shape coexistence
  - Island of inversion
- First SPIRAL experiment

- EXOGAM
- EXOGAM+VAMOS

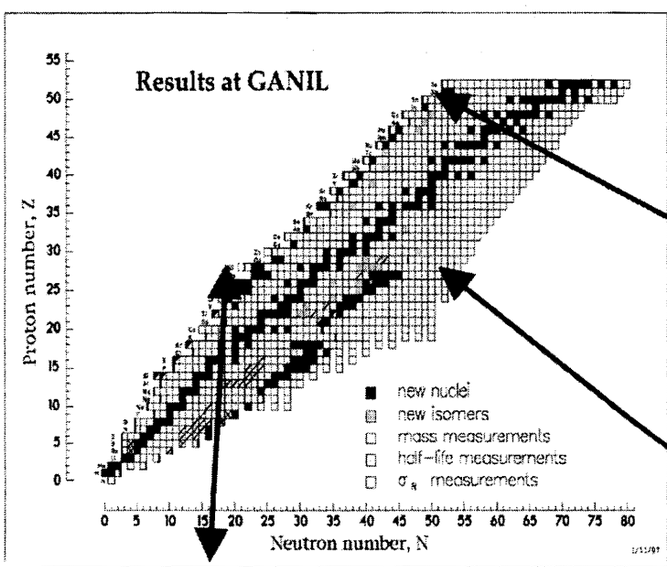

Magic Elements

^{100}Sn

- Heaviest N=Z doubly magic stable vs particle emission
- properties of p-rich elements; mass models
- Mapping the p-drip line; rp-process

^{48}Ni

- Largest Tz value (-4)
- Mirror nuclei stable vs particle emission (symmetry studies)
- 3 doubly magic Ni (48, 56,78)
- Candidate for 2p emission from g.s. (45Fe)

^{78}Ni

- R-process
- Properties of n-rich nuclei; mass models
- A/Z ratio = 2.79

Production Technique

- Production
- SC Solenoids

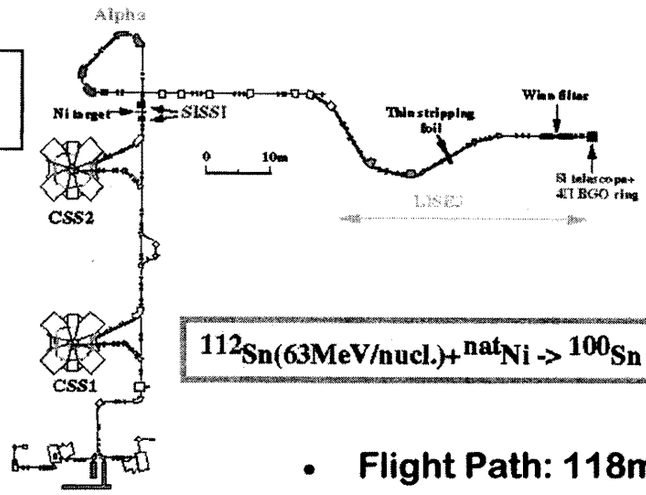

$^{112}Sn(63MeV/nucl.)+^{nat}Ni \rightarrow ^{100}Sn$

- Collection
- Separation
- In-flight identification

- Flight Path: 118m

M. Lewitowicz et al, PLB 332 (1994) 20

The identification

3. Blank et al. PRL 84 (2000) 1116

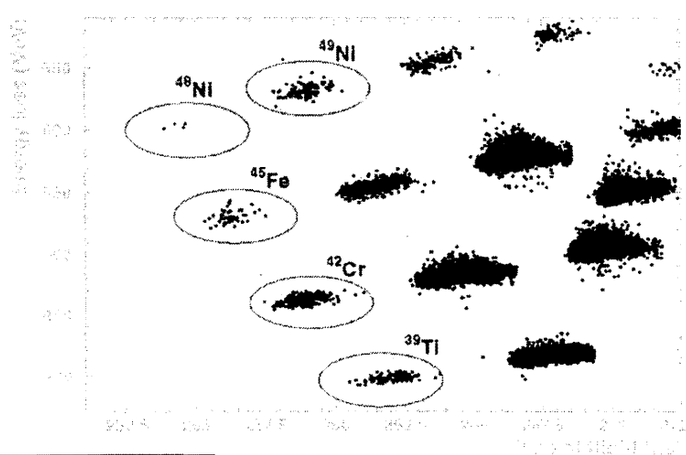

	^{48}Ni	^{49}Ni	^{45}Fe	^{42}Cr
# of counts	4±2	106±22	53±9	287±30
Trans. (%)	9.8±1.2	6.9±1.6	6.7±0.3	0.7±0.6
σ (pb)	0.05±0.02	1.8±0.6	0.9±0.2	$47\pm^{285}_{22}$

^{48}Ni and test of the models

- ^{48}Ni calc. Particle unstable by all common models
- Even Z nucleus: 2p emission favored/1p
- Q_{2p} values: from <1 MeV to > 3 MeV ($T_{1/2}$: 10^{-14} to 1s!)

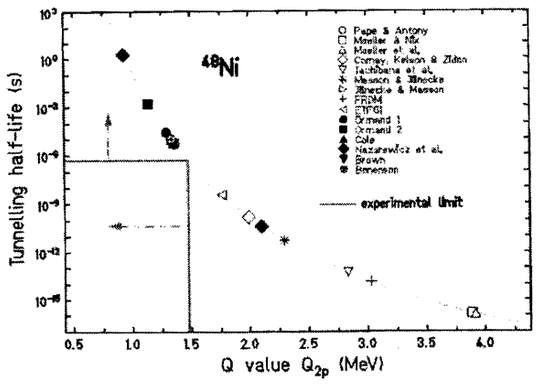

Assuming:
- No in-flight decay of ^{49}Ni
- σ (^{49}Ni)/σ (^{48}Ni) ~ 26
- Spectroscopic factor = 1

Then:
$T_{1/2}$ ~ 2.6 $+\infty$, -2.1 μs

lower limit at 1σ level:
$T_{1/2}$ ~ 0.5 μ s
i.e. Q_{2p} ~ 1.5 MeV

μ-seconds isomers and magicity

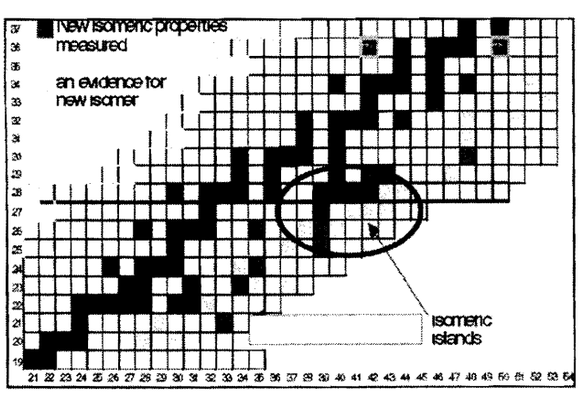

Isomers

- Δ/value
- Spin-orbit term
- Persistance of shell gaps

Residual interactions and nucleon effective charge:

around closed shells: pure transitions

Isomers around the Z=28 gap

$^{86}Kr^{34+}$ @ 60.5 MeV/A+Ni nat

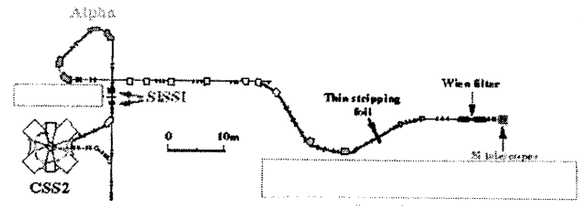

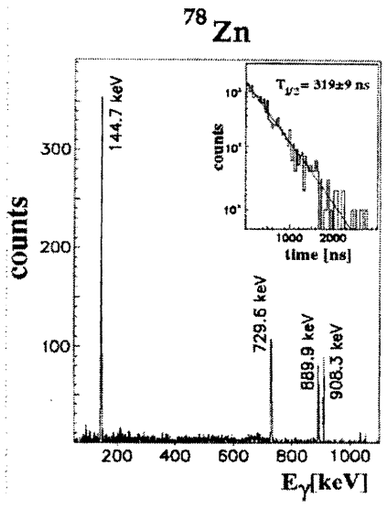

J.M. Daugas et al, PLB 476 (2000) 213

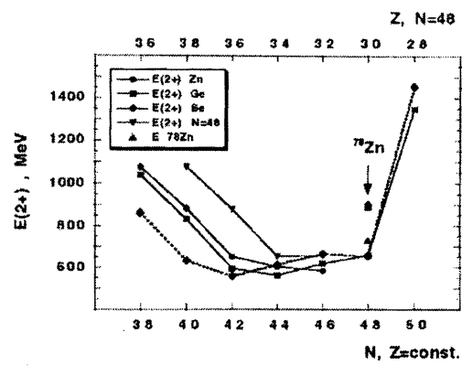

μ-second isomers and SM calculations

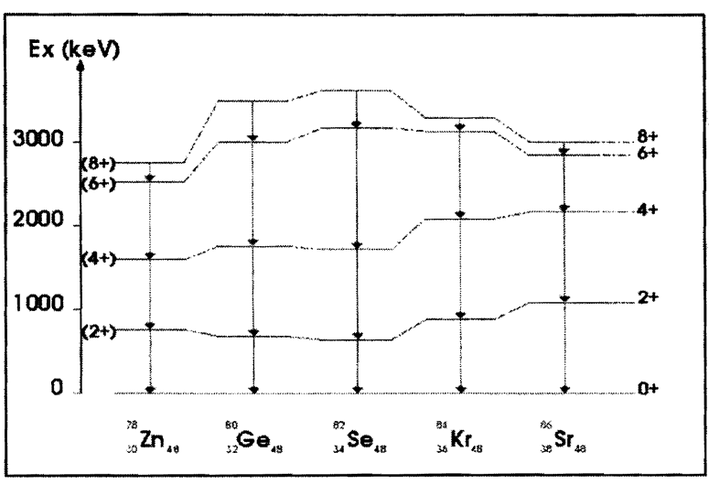

$\nu g_{9/2}^{-2}$

SM calc. + realistic interaction (*Sinatkas et al.*)

Spectrum OK with 0.5e as polarization charge (p and n)

B(E2:8+ → 6+) = 1.21 (5) Wu
= 1.06 (Calc.)

μ-second isomers and symmetries

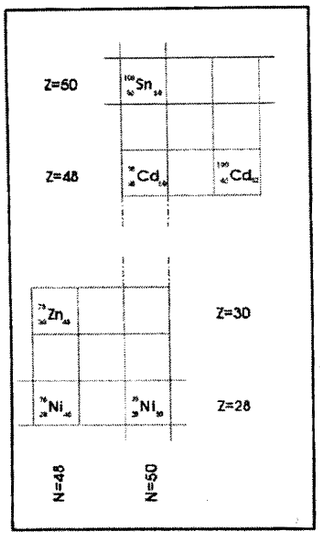

« Valence mirror nuclei »:
p-holes at N=50 \ n at N=28

Except:
→ *A/Z*
→ *No overlap between n and p w.f at Z=28 (no p-n interaction)*

- 8+ isomer in ^{98}Cd associated to N=50 gap
- ^{76}Ni = 2p-holes in ^{78}Zn

8+ isomer in ^{78}Zn ($\nu g_{9/2}^{-2}$)

↓

Persistance of Z=28 gap

R. Grzywacz et al. PRL 81 (1998) 766
M. Górska et al. PRL 79 (1997) 2415

Shape coexistence and magicity

A=70-80 various shell gaps available

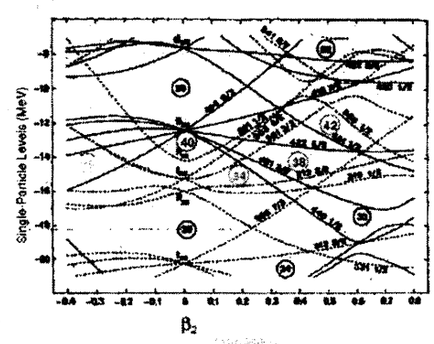

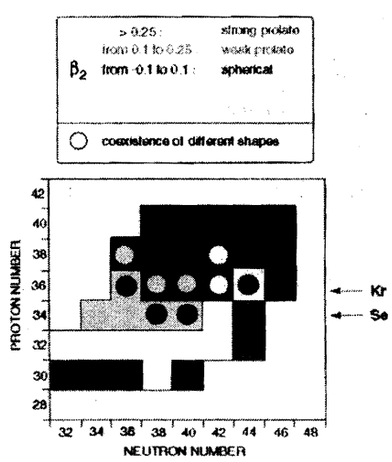

From R. Bengtsson, Nuclear Structure of the Zr Region, Springer (1985) 17

Kr isotopes: best candidates

HF+BCS Nilsson-Strutinsky+BCS HFB	Equ. Def. OK

But: E of shape coex. States depends on pairing*

Shape coexistence

* Energy of low lying states and B(E2)'s : ~ OK
* But level scheme not a rigid rotor: perturbation from shape coexisting states??
* Further evidence for shape coexistence: low-lying 0+ states (related to large change of nuclear radius)

<u>Experimentally: 2 main sources of information:</u>

Conversion e- spectroscopy (E0)
Coulomb excitation (E2)

Isomers and shape coexistence

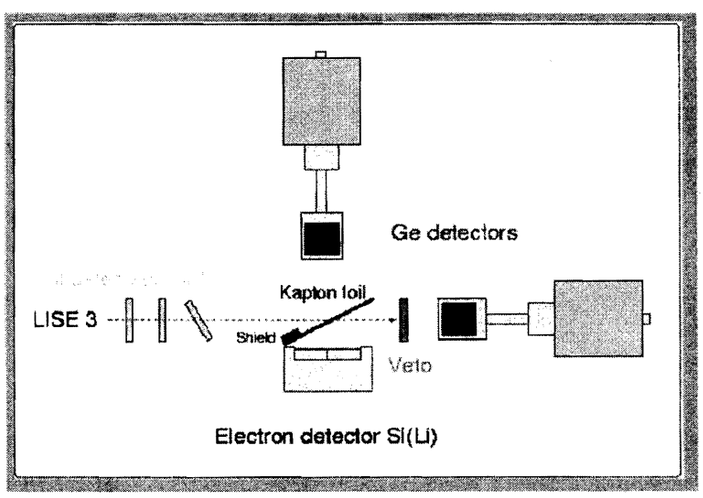

^{78}Kr beam @ 73MeV/A

First: recoil-e$^-$-γ experiment

Identification via ΔE/ToF

Implantation in Kapton foil

Veto detector to reduce background

Isomers and shape coexistence

Confirmation of shape coexistence in ^{74}Kr

C. Chandler et al. PRC 56 (1997) 98
F. Becker et al. EPJ A4 (1999) 103

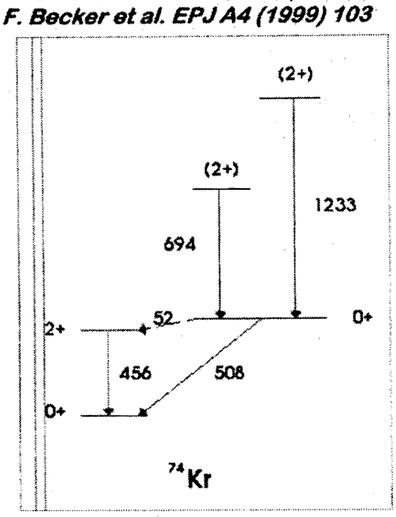

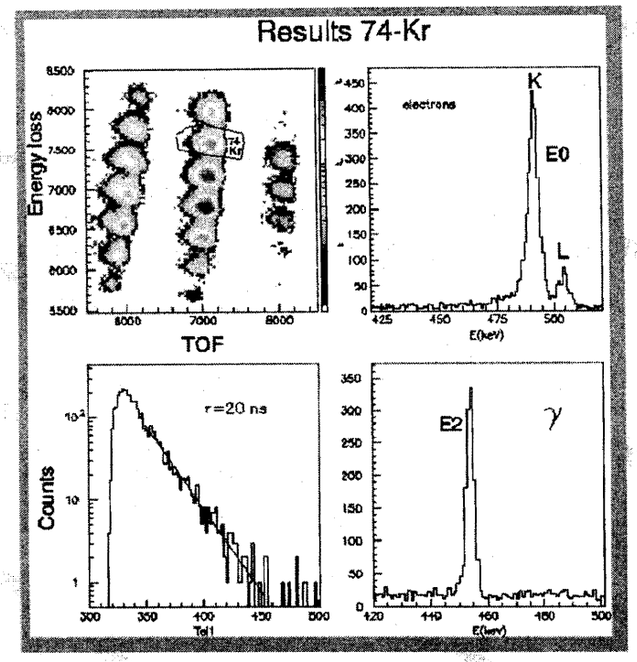

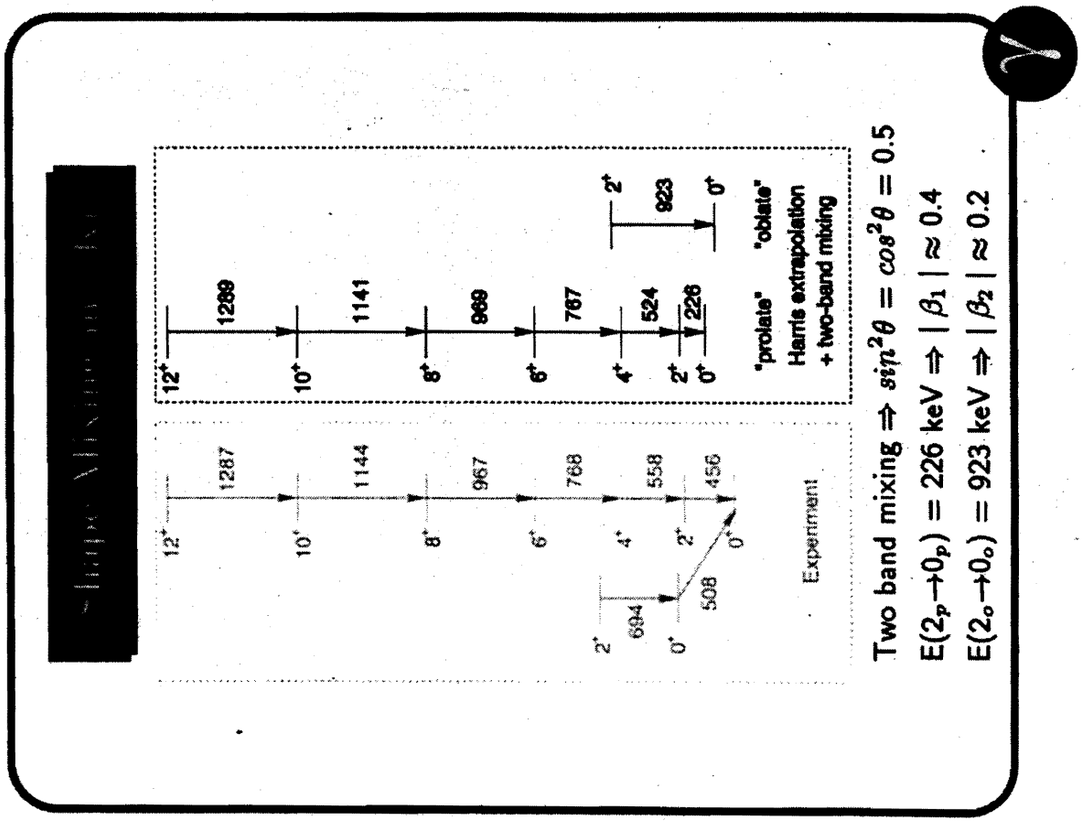

E0 strength in ^{72}Kr

E0 strength between mixed states of different deformation:

$$|\Psi_i> = sin\theta\,|\beta_1> + cos\theta\,|\beta_2>$$

$$|\Psi_f> = sin\theta\,|\beta_2> - cos\theta\,|\beta_1>$$

$$\Rightarrow\ \rho^2(E0) = \left(\frac{3Z}{4\pi}\right)^2 sin^2\theta\, cos^2\theta\,|\beta_1^2 - \beta_2^2|^2$$

$$|\,\rho_{exp}(E0)\,| = \left(\tau\cdot\Omega\left(1 + f(\Omega,\alpha)\frac{I_K(E2)}{I_K(E0)}\right)\right)^{-\frac{1}{2}}$$

$Z = 36$ $\quad \Delta E_{if} = 0.5$ MeV $\Rightarrow \Omega = 0.282$ ns^{-1}

$\tau = 20(9)$ ns $\quad$ Decay branching: $0.5 < \frac{I_K(E2)}{I_K(E0)} < 100$

$\Rightarrow 0.03 < |\,\rho_{exp}(E0)\,| < 0.5$

$\beta_1 \approx 0.35 \cdot \quad sin^2\theta = cos^2\theta = 0.5$

$\Rightarrow 0.14 < \beta_2 < 0.34$

$\Rightarrow$ Coexistence of two well-deformed shapes

γ

Isomer and shape coexistence

No mixing; « pure » shape isomer

N=Z ^{72}Kr pure oblate g.s.

Shape coexistence and test of the models

Avoid nuclear interaction and keep only electromagnetic part

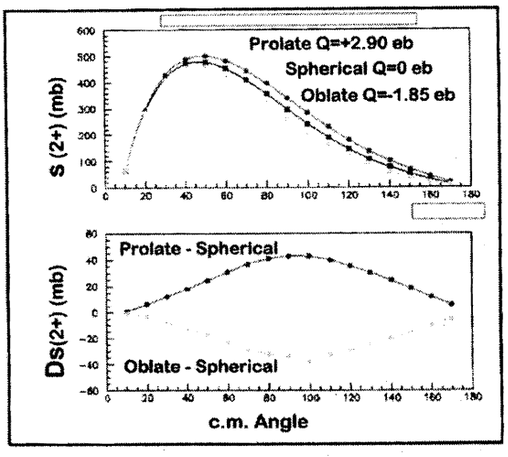

Incident energy << Coulomb barrier

Coulex (large σ) + γ-decay

Matrix elements: σ (Coulex 2+)

σ (2+) = f(Q_0)

Close lying collective states; change in B(E2)'s can have similar effects ➡ several targets and scattering angle dependence of σ (2+)

Island of inversion

1. Mass measurements (S2n) → shell closures
2. E(2+) and B(E2:2+ →0+) → deformation
3. Higher lying excited states → collectivity

1. Fragmentation of the projectile (*F. Sarrazin et al.*)
2. Fragmentation + Coulomb excitation (*M.J. Lopez-Jimenez, M. Belleguic et al.*); Fragmentation + inelastic (p and nuclear) scattering
3. Coulomb excitation; double fragmentation

2 - Time of flight method, Elements of analysis

E290 Experiment: (Nov. 97)
Fragmentation of a ^{48}Ca beam @ 60 A.MeV on a Ta target located in the SISSI device.

The magic formula !

$$B\rho = Mv/Q \quad \text{with } v = L_{flight}/T_{flight}$$

Flight path : 82m
Time of flight : 700ns to 1.2µs

F.Sarazin - Colloque GANIL 99

2 Bρ (2.58 et 2.73 T.m)

Over 100 nuclei transmitted

Known masses = Calibration

The unknown masses are deduced from this calibration

Resolution:

Δt = 200 to 400 ps
$\Delta t/t = x.10^{-4}$

Final Precision:

100keV, $>10^5$ evts ➡ 1MeV, hundred of evts

$\Delta M/M = x.10^{-6}$ to $x.10^{-5}$

F.Sarazin - Colloque GANIL 99

3 - Results & Theoretical considerations

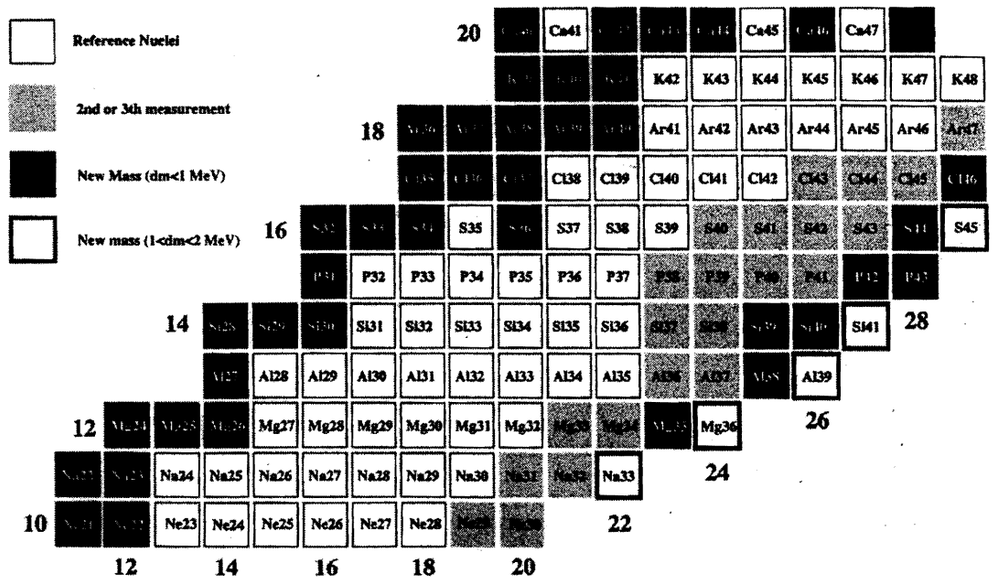

F.Sarazin - Colloque GANIL 99

Magicity far from stability ?

^{32}Mg: deformed semi-magic nucleus

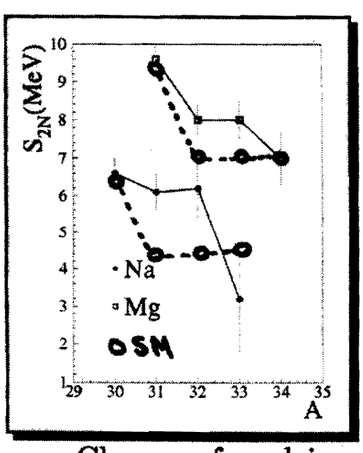

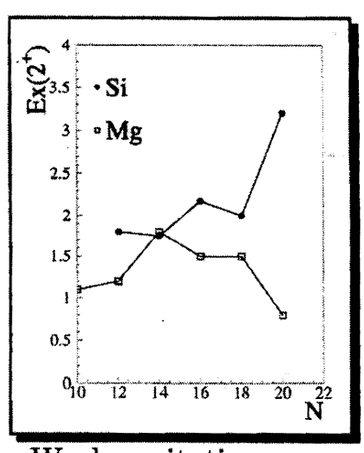

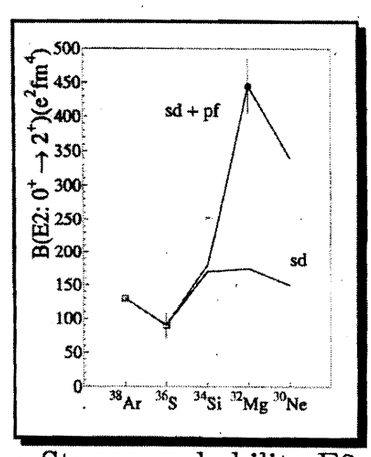

- Change of nuclei mass slope at N=20
- Weak excitation energy of 2^+ level
- Strong probability E2 $2^+ \rightarrow 0^+$ transition

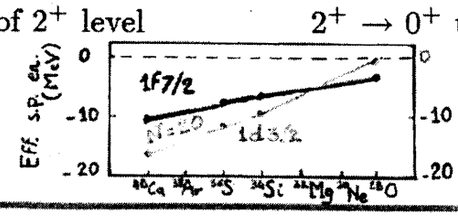

N. Fukunishi et al.
PLB 296 (1992) 279

Island of inversion

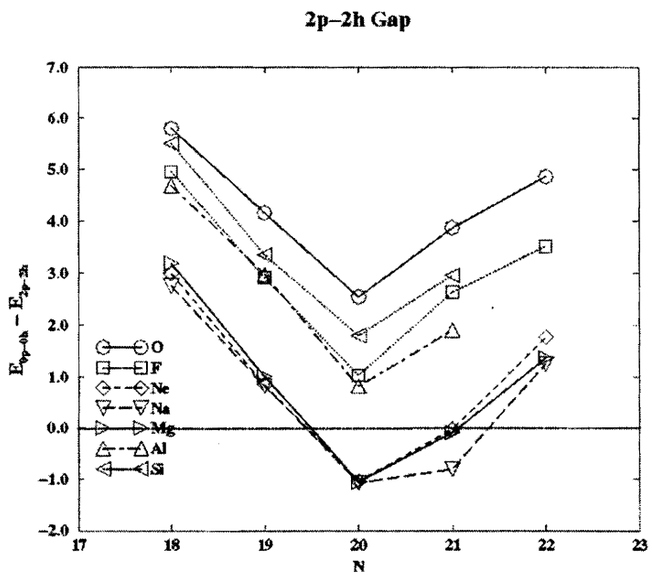

Large Scale Shell Model calculations

Energy difference between intruder/deformed and normal/spherical states

N=20 magic gap disappear for Mg, Al, Si

E. Caurier, priv. Comm.

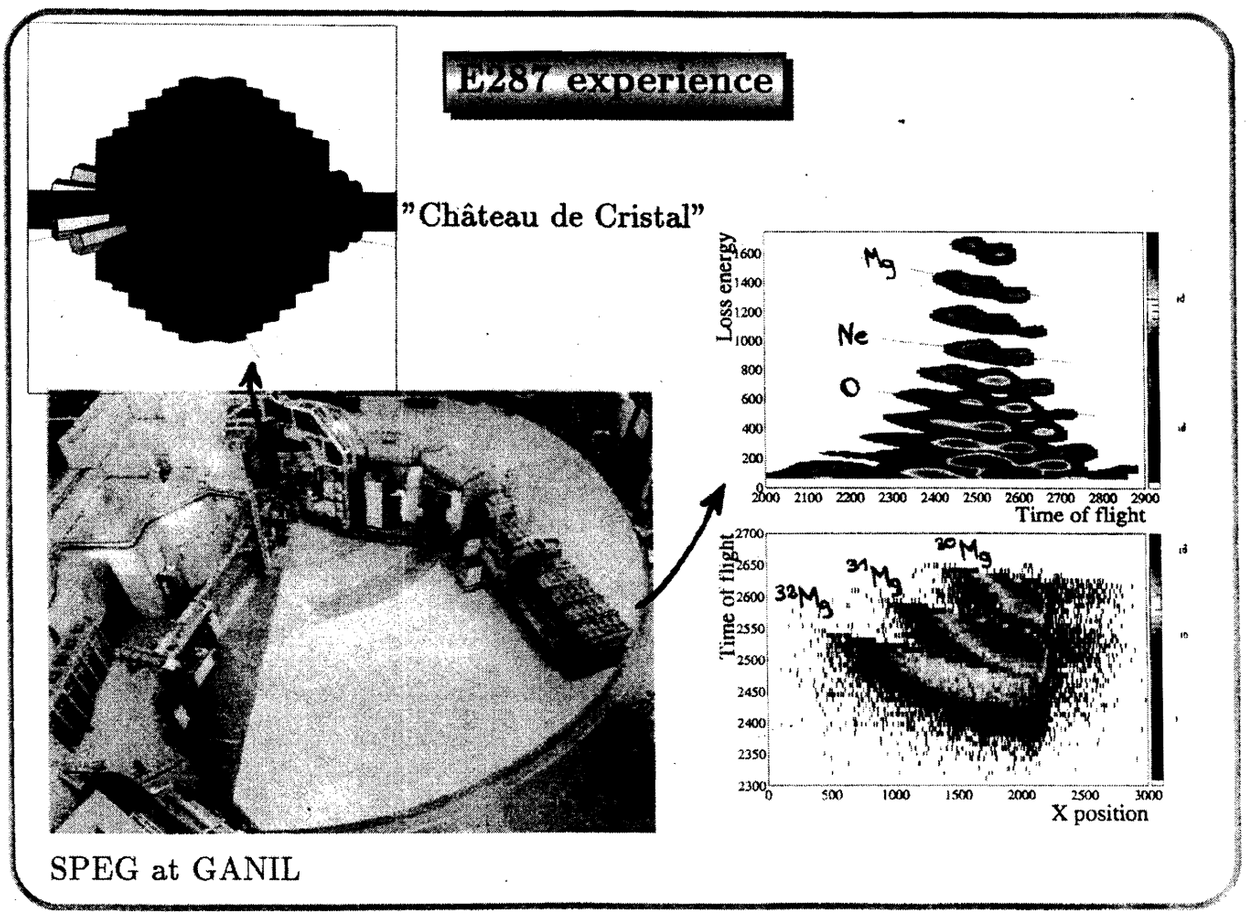

Ne γ spectroscopy

^{26}Ne

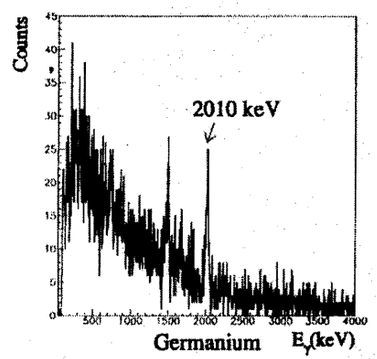

^{28}Ne

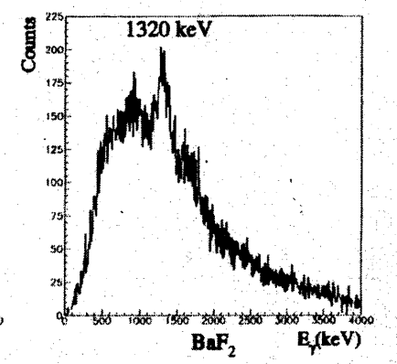

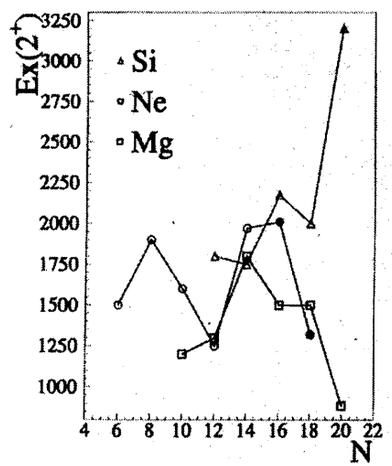

→ [redacted]

^{32}Mg γ spectroscopy

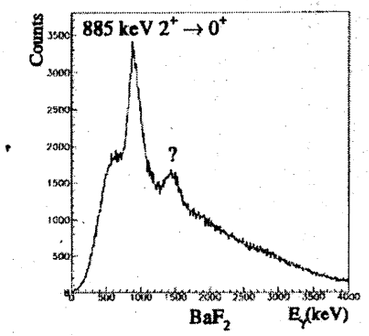

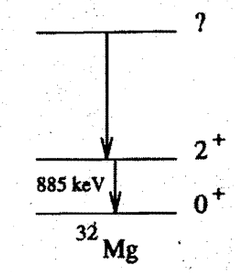

$$Vibrator(2) < \frac{E(4^+?)}{E(2^+)} = 2.6 < Rotator(3)$$

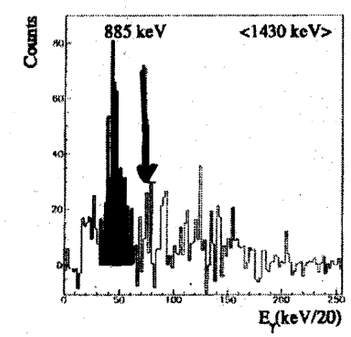

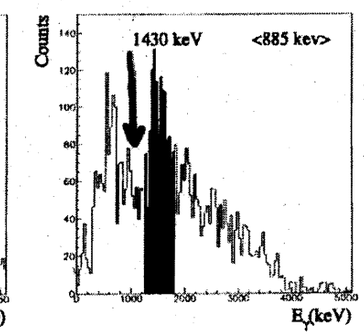

The 1430 keV detected transition is in coincidence with the 885 keV

^{32}Mg puzzle ...

- from β decay *(Klotz et al.)* + shell model: ^{32}Na g.s. is 3- or 4-; decay to positive parity state forbidden *but* feeding is weak (log(*ft*)=5.4): 3+,3-,4+ possible
- Fragmentation reactions seem to favor 4+ (De Jong calcs.)
- Inelastic ^{28}Si scattering and DWBA calcs.: 4+ state would be a double step process ➡ very weak population (much weaker that what is observed): σ(4+)/σ(2+) ~1/20 (rot. or vib.)

EXOGAM

A Gamma Ray Spectrometer for Exotic Beams

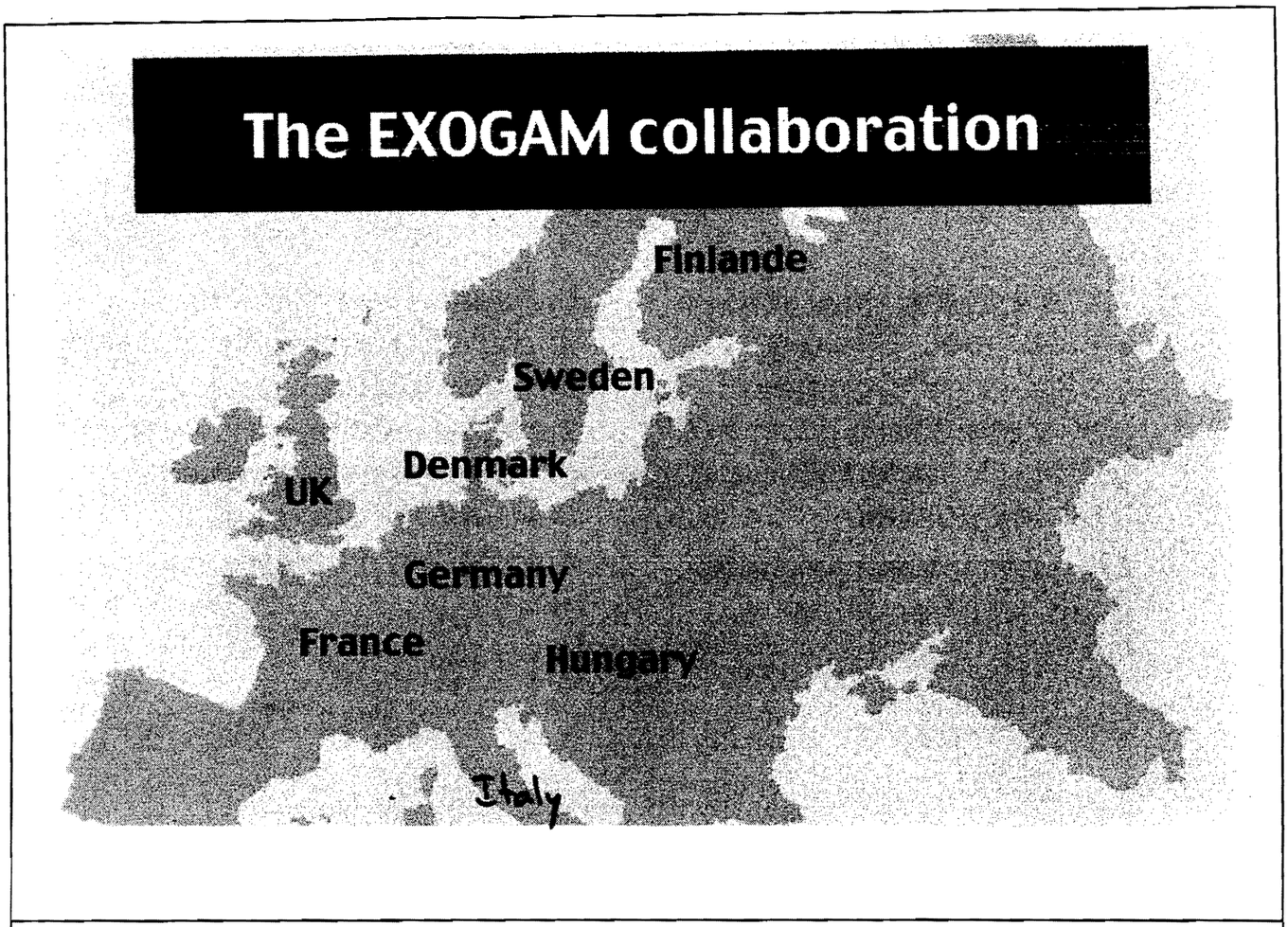
The EXOGAM collaboration
Finlande
Sweden
Denmark
UK
Germany
France
Hungary
Italy

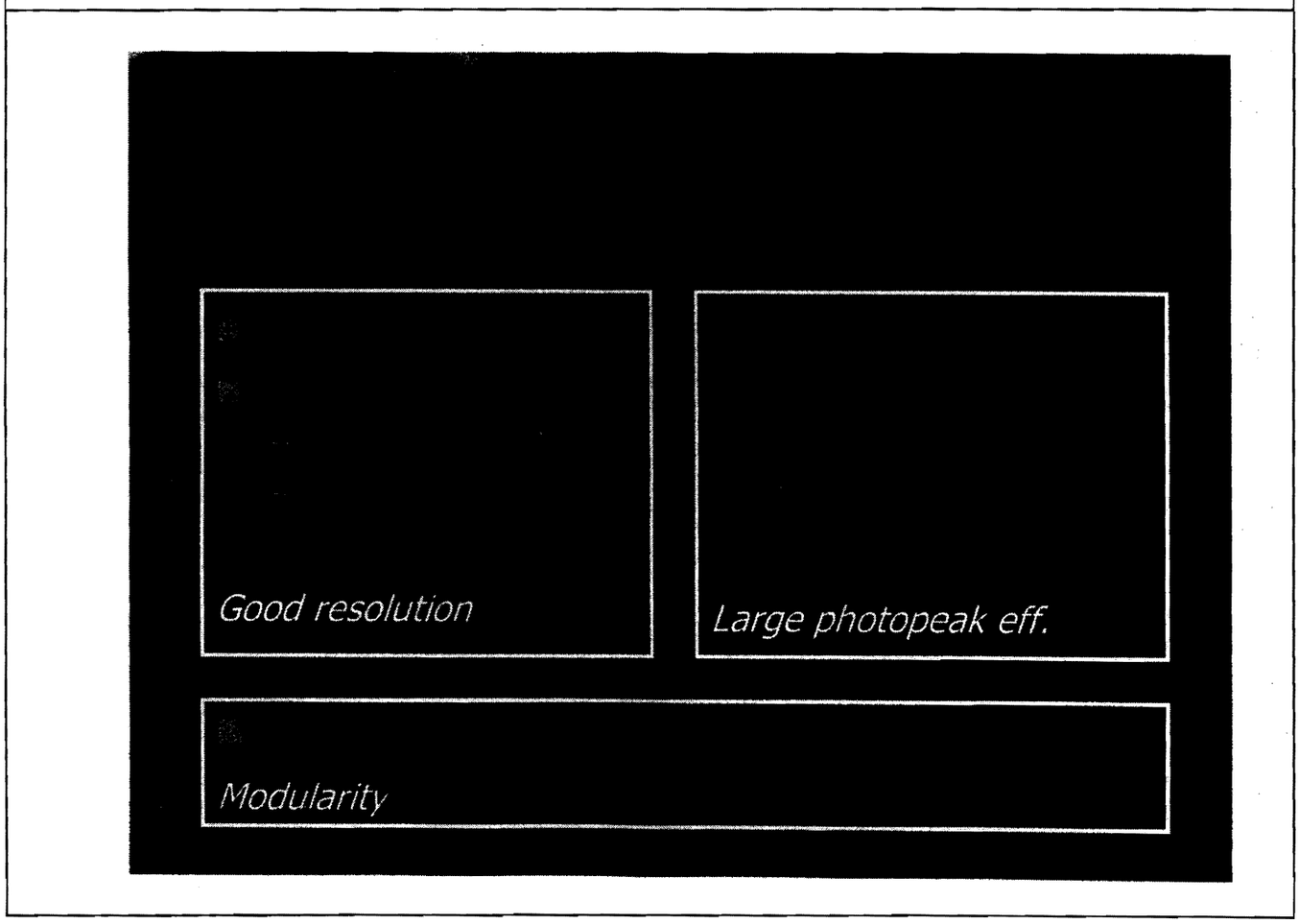
Good resolution
Large photopeak eff.
Modularity

16 HP Ge segmented Clovers

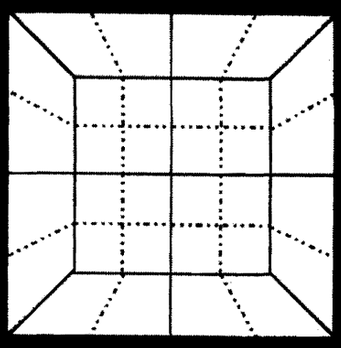

Initial diameter: 60 mm
Length: 90 mm

- 4 crystals in the same cryostat
- Electric segmentation

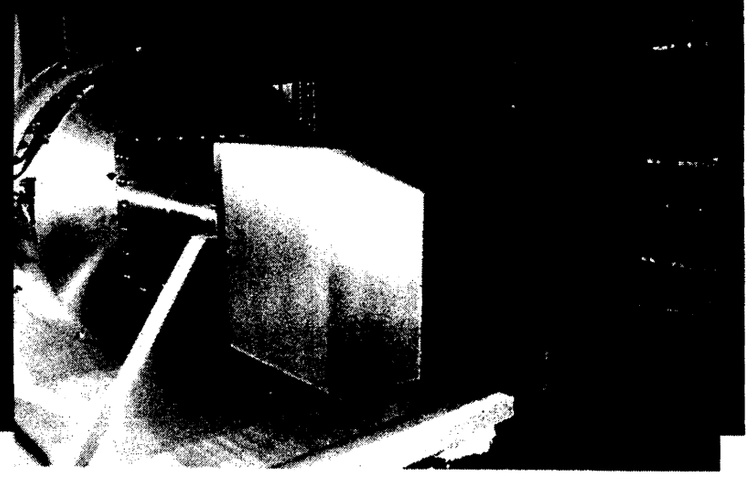

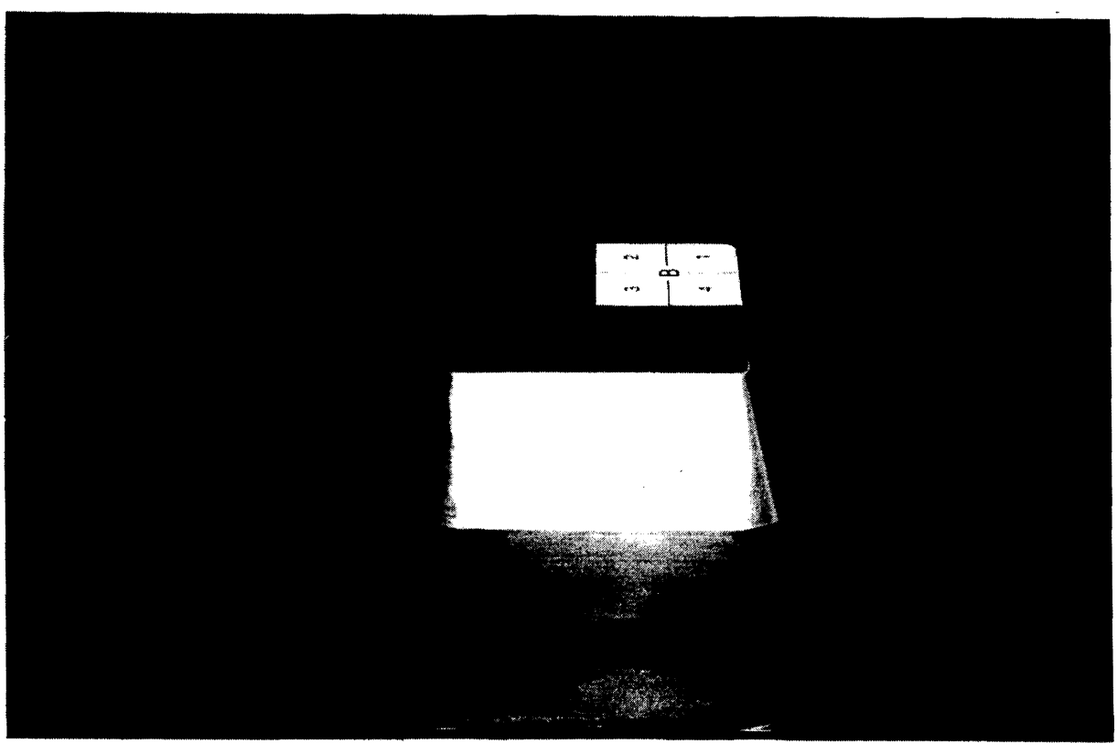

Performances du Clover EXOGAM

$\eta_r = 1$
$d = 11\,cm$

Shield A

$L = 90\ mm$
$\phi_i = 60\ mm$

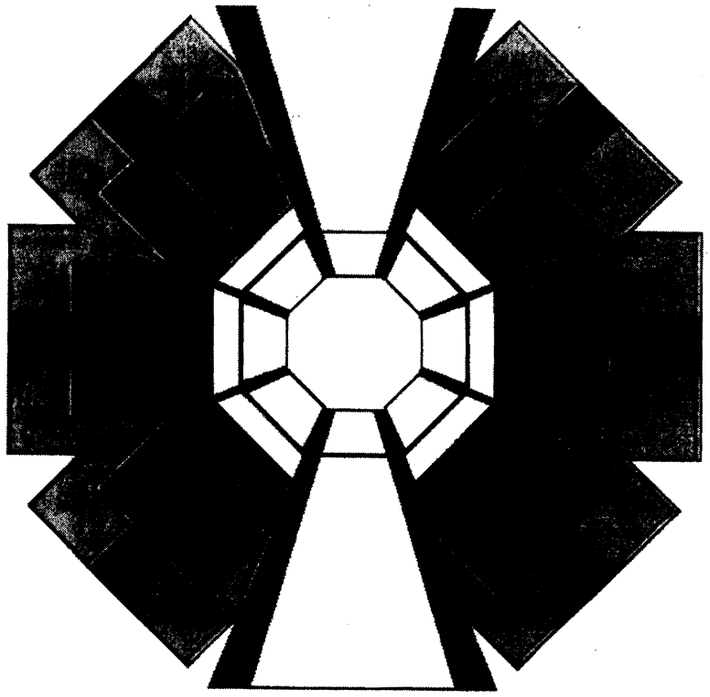

Figure 10: A cross section through the 16 segmented CLOVER EXOGAM array.

+10 % inter clover add back

→ $\varepsilon_{P\gamma} \simeq 20$ % 28%

P/T ≃ 0.47 0.57

1.3 MeV 662 keV

The EXOGAM array

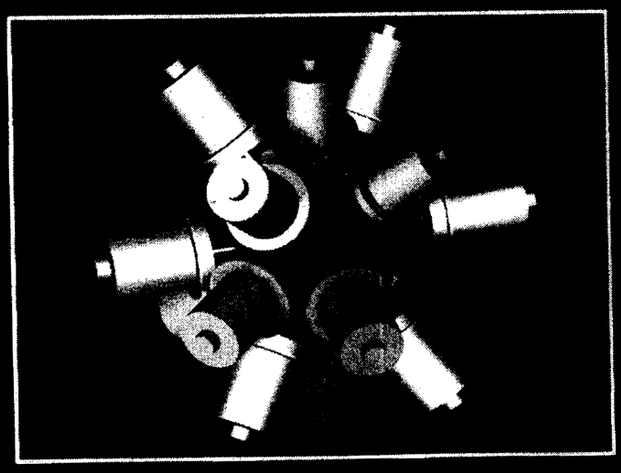

- An array designed for low and medium multiplicity ($M_\gamma < 15$)
- 20 % photopeak efficiency at $M_\gamma = 1$ and $E_\gamma = 1.3$ MeV
- Anti Compton BGO/CsI
- 16 HP Ge Clover detector
- Modularity
- Coupling with auxiliary detectors

G. de France, GANIL

EXOGAM à SPIRAL

Excitation coulombienne de noyaux exotiques

$^{46}Ar + ^{208}Pb$ à 160 MeV (v/c 7.5%) $M_\gamma=2$.

	Efficiency Efficacité photopic (%)	Pic/total (%)	Energy Résolution (keV)
EXOGAM	18.5	45	14.9

Structure nucléaire autour de l'étain 100

$^{72}Kr + ^{32}S$ à 280 MeV (v/c 6.3%) $M_\gamma=15$

	Efficiency Efficacité photopic (%)	Pic/total (%)	Energy Résolution (keV)
EXOGAM	12.6	31	12.6

EXOGAM Clover performances

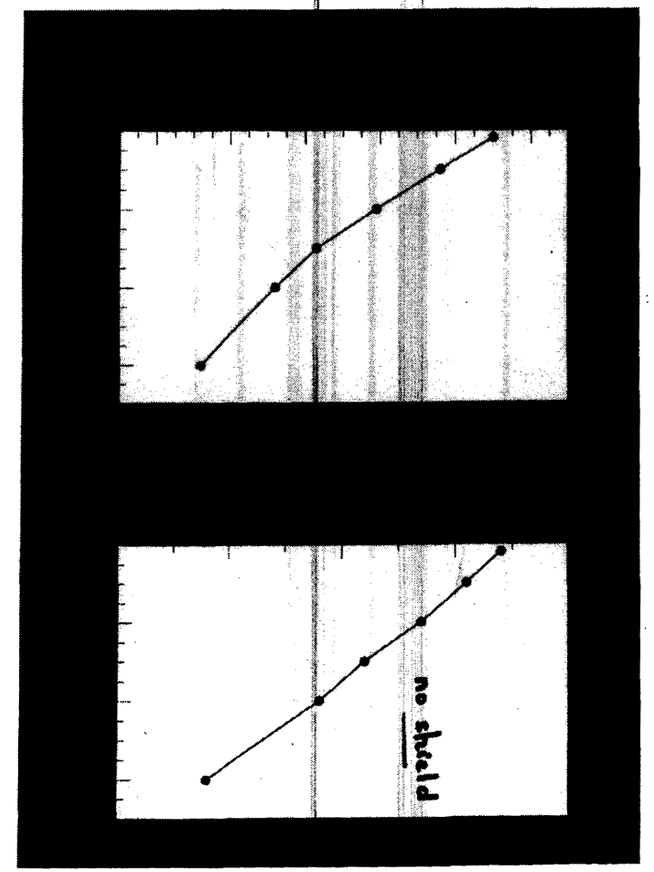

E_γ: 1.3 MeV
d = 11 cm

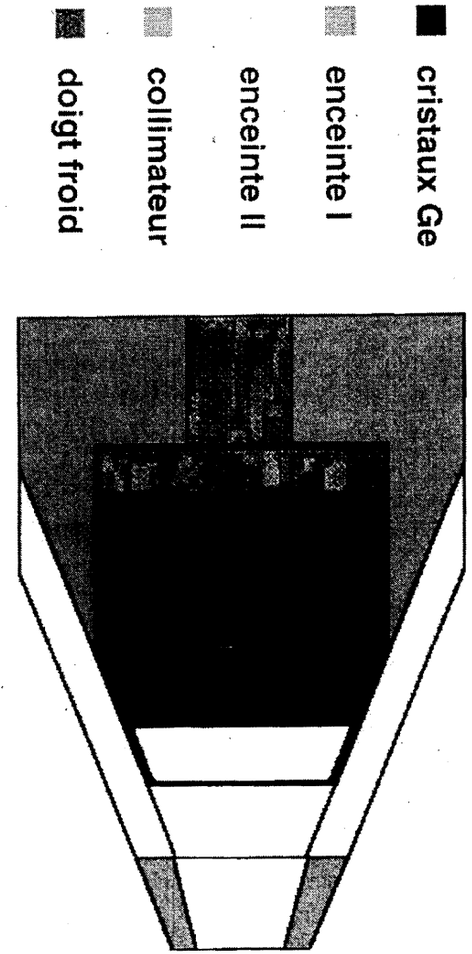

Shield B

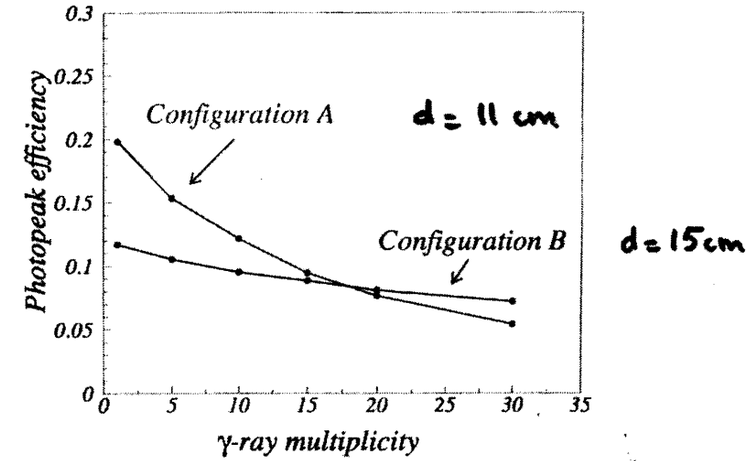

Figure 4: Total photopeak efficiency for the 16 segmented CLOVER array in configurations A and B at 1.3 MeV as a function of γ-ray multiplicity.

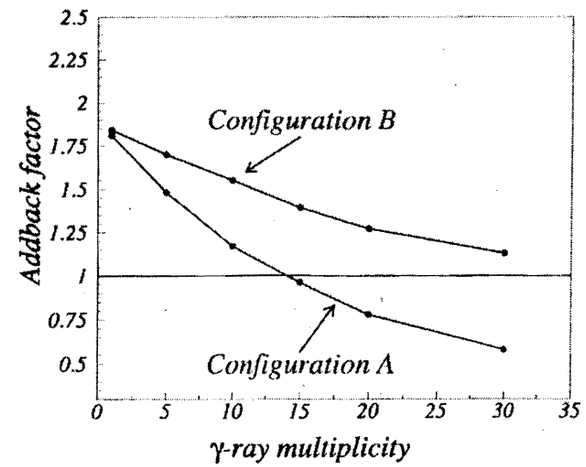

Figure 5: Addback factor for the 16 segmented CLOVER array in configurations A and B at 1.3 MeV as a function of γ-ray multiplicity.

Composite anti-Compton shields

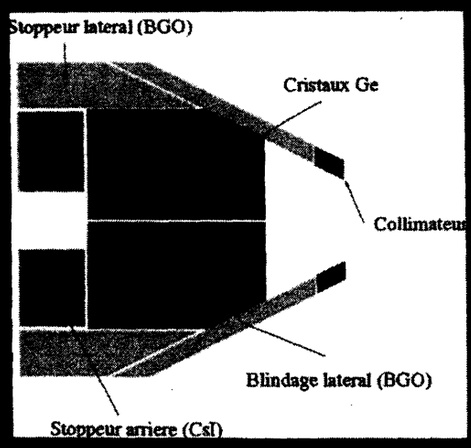

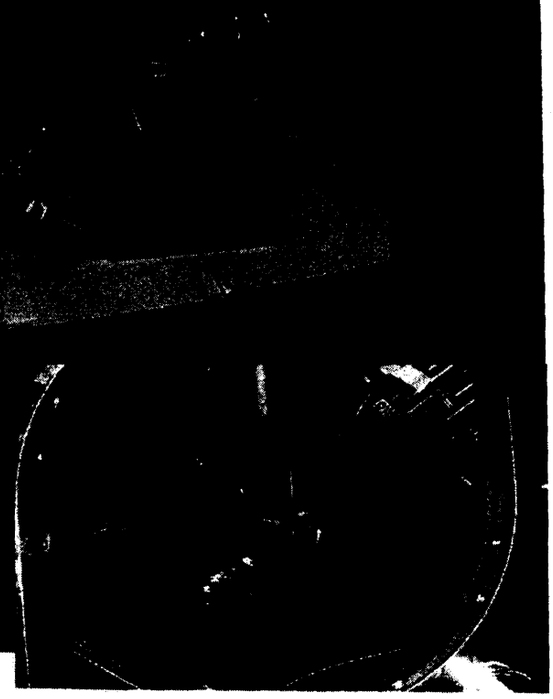

- 3 different elements for a given shield

Segmentation *electrique* du Ge:

Pas de perte d'efficacite
Gain en Signal/Bruit

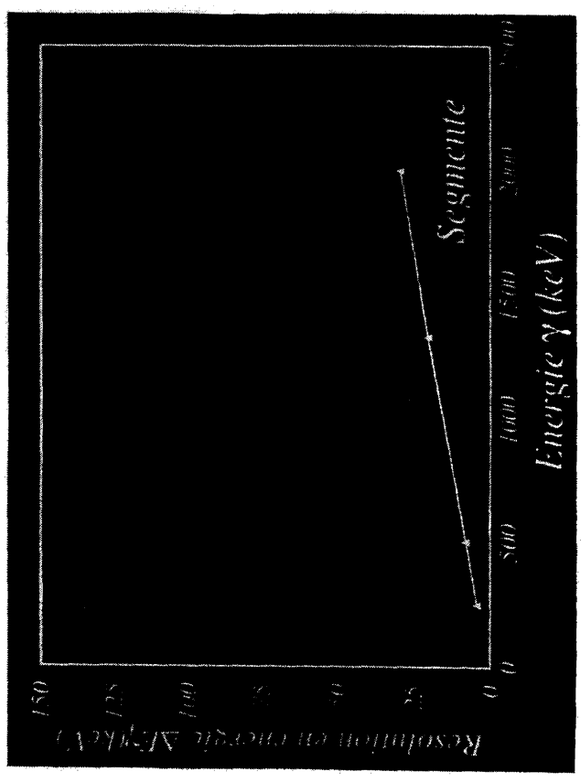

v/c = 7.5 %
90 degres
d = 6 cm

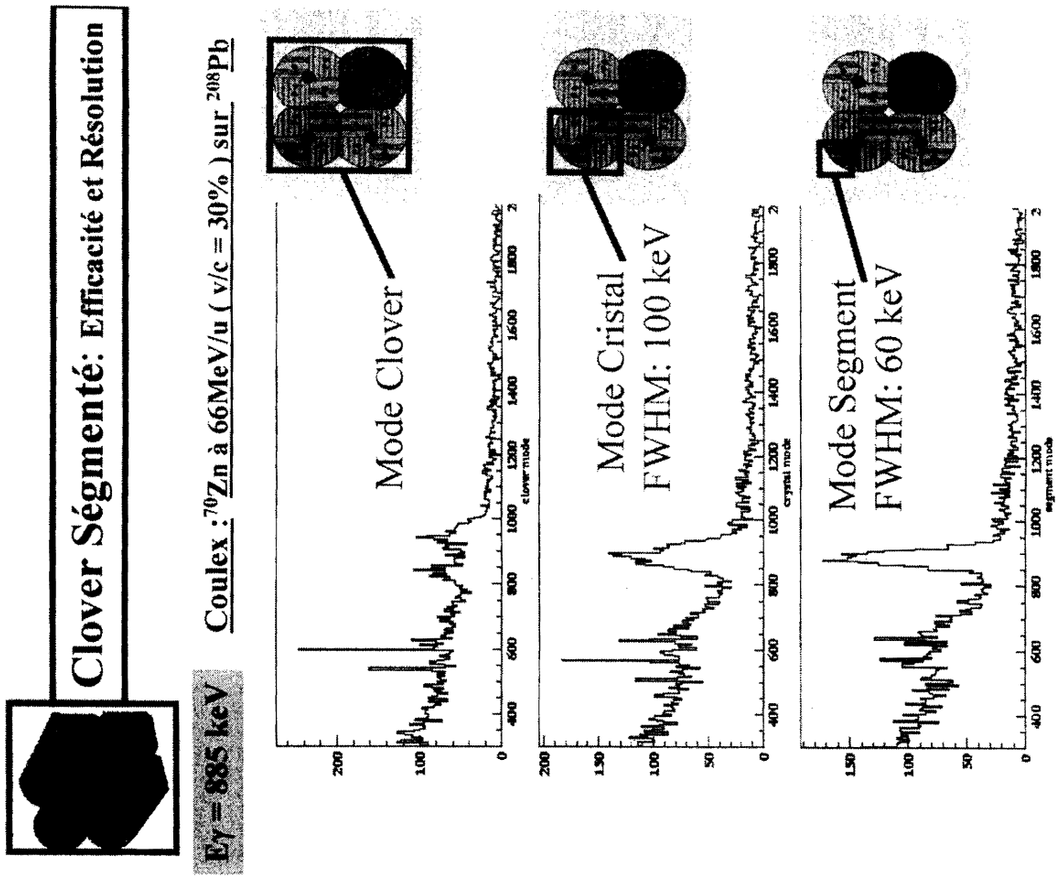

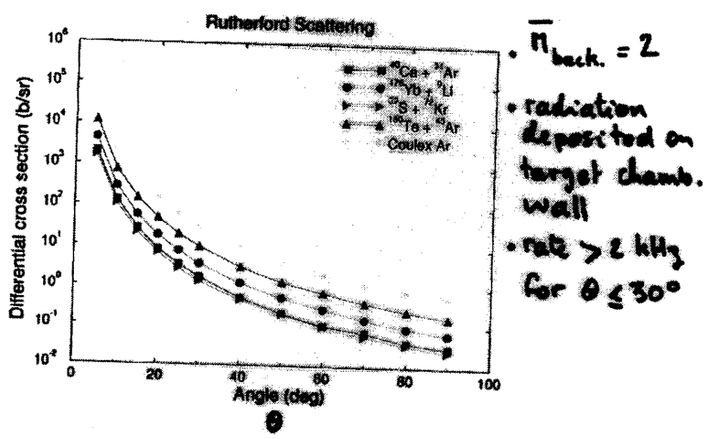

Figure 7: The differential Rutherford scattering cross section as a function of scattering angle for a series of typical reactions, see section 3.7.

VAMOS

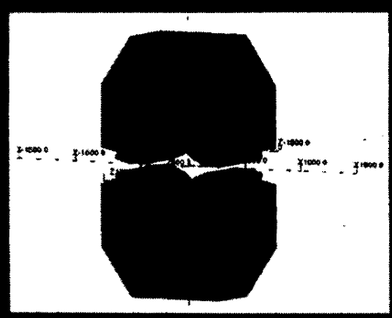

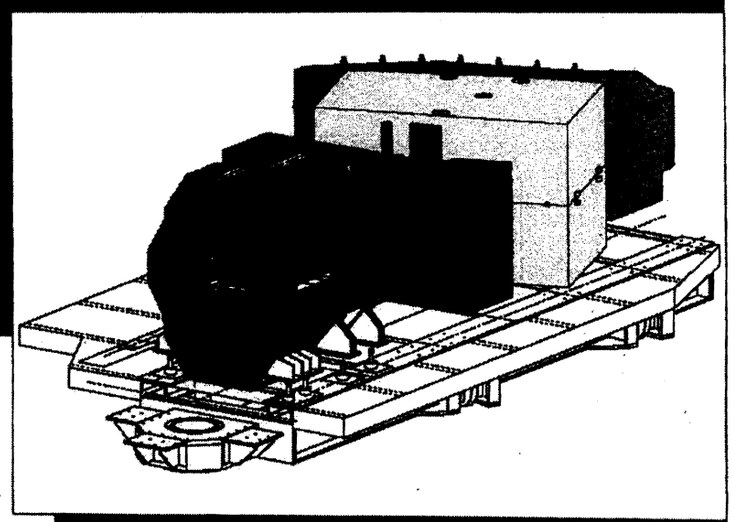

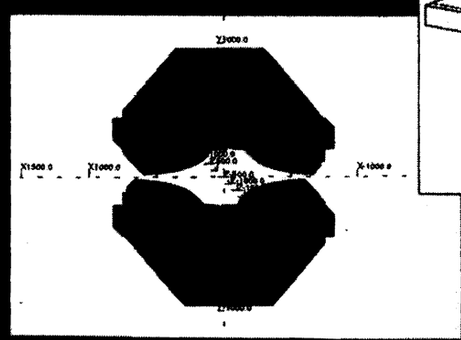

Development in recoil spectrometers (7)

VAMOS=VAriable Mode Spectrometer:

Mode 1: Q-poles only ⇒ SOLENO type, large acceptance facility

Mode 2: Q-poles+D-pole ⇒ SUSAN type, dispersive facility

Mode 3: Q-poles+D-pole+Wien filter ⇒ beam rejection

In all cases: good resolution+large solid angle possible because of trajectory reconstruction up to very high order (8th) and « low » count rates (RIBs) ~10^{n} pps

Development in recoil spectrometers (6)

To obtain the design specifications : « standard » quadripole and dipole association + velocity filter appear to be very good compromise (VAMOS, MAGNEX)

p dispersion	2.8 cm/%	4 cm/%
p acceptance	± 5%	± 10%
acceptance	100 msr	53 msr
max. rigidity	1.6 Tm @ 100msr 2.3 Tm @ 42msr	1.8 Tm
1st ord. res. power	1000	5400

Mode 3 : A/Q Selection

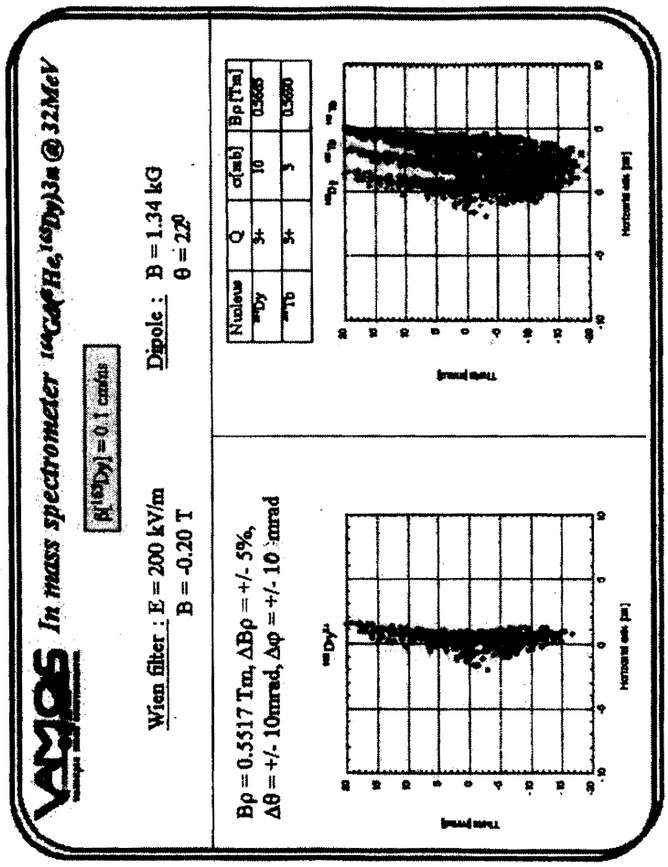

Image aberrations in the dispersive plane :

QQD MODE
$B\rho = 0.334$ Tm $\Delta B\rho = \pm 5\%$
$\Delta\theta = \Delta\Phi = \pm 160$ mrad

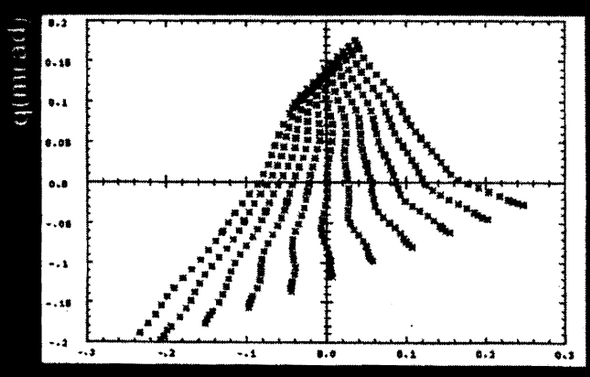

H Savajols et al

X_{foc}(cm)

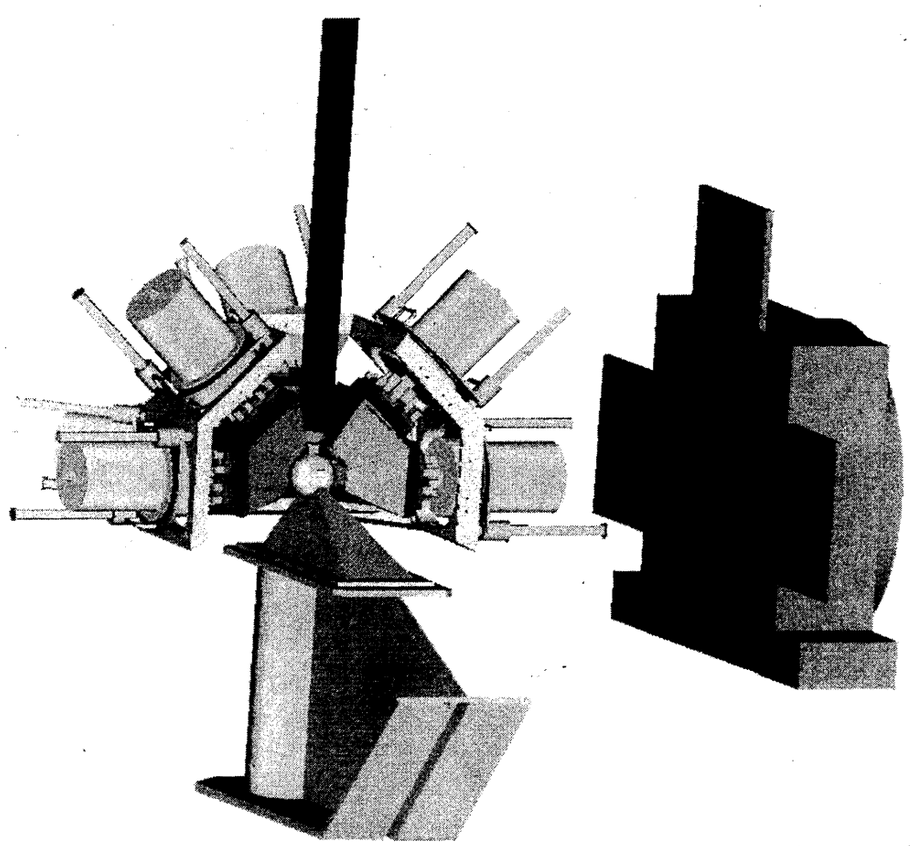

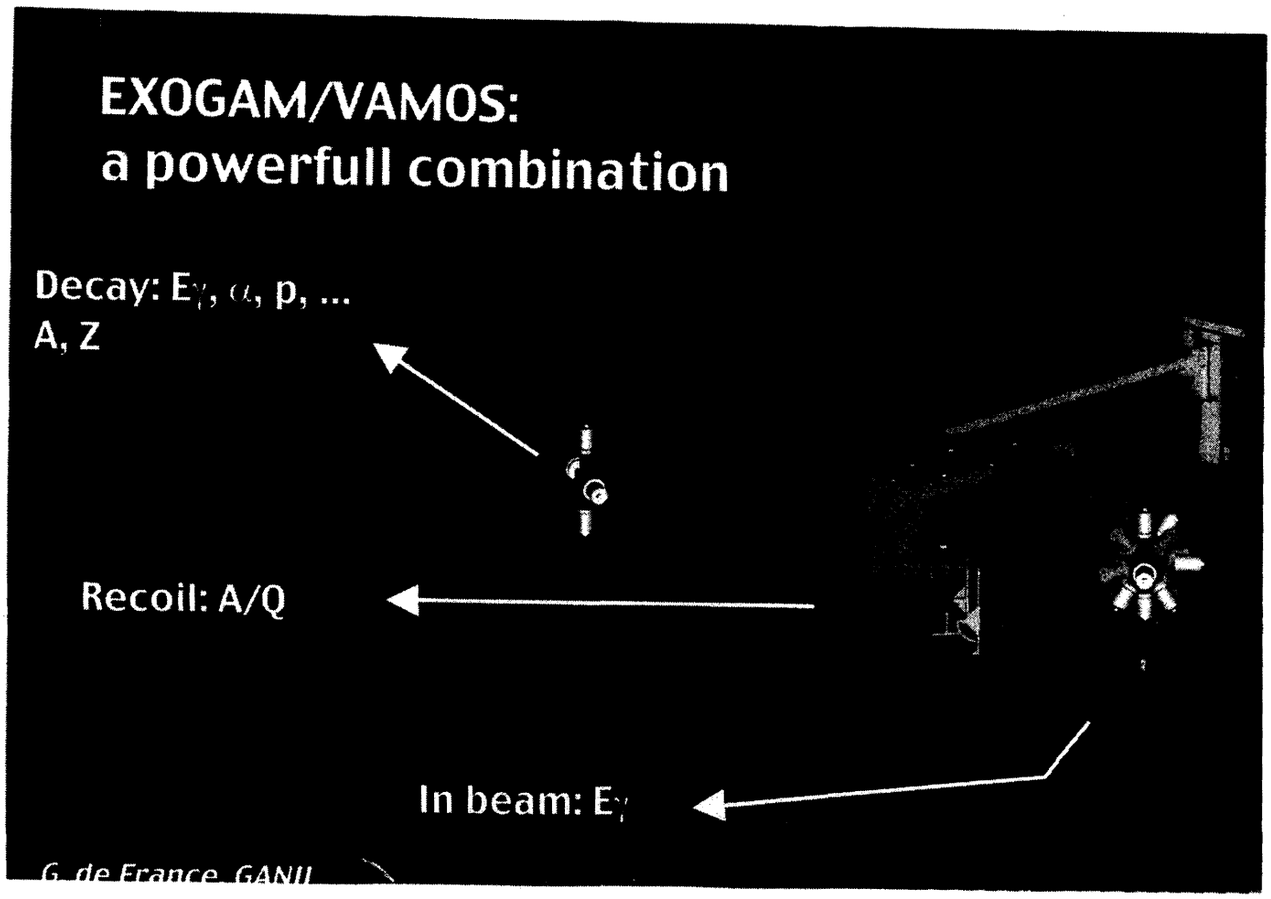
EXOGAM/VAMOS:
a powerfull combination
Decay: Eγ, α, p, ...
A, Z
Recoil: A/Q
In beam: Eγ
G. de France, GANIL

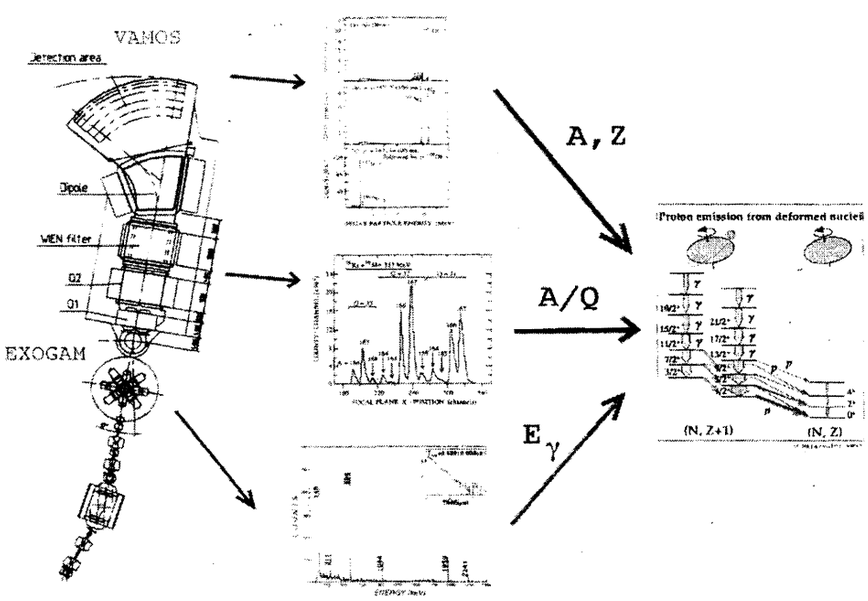
VAMOS
Detection area
Dipole
WIEN filter
Q2
Q1
EXOGAM
A, Z
A/Q
Eγ
Proton emission from deformed nuclei
(N, Z+1)
(N, Z)

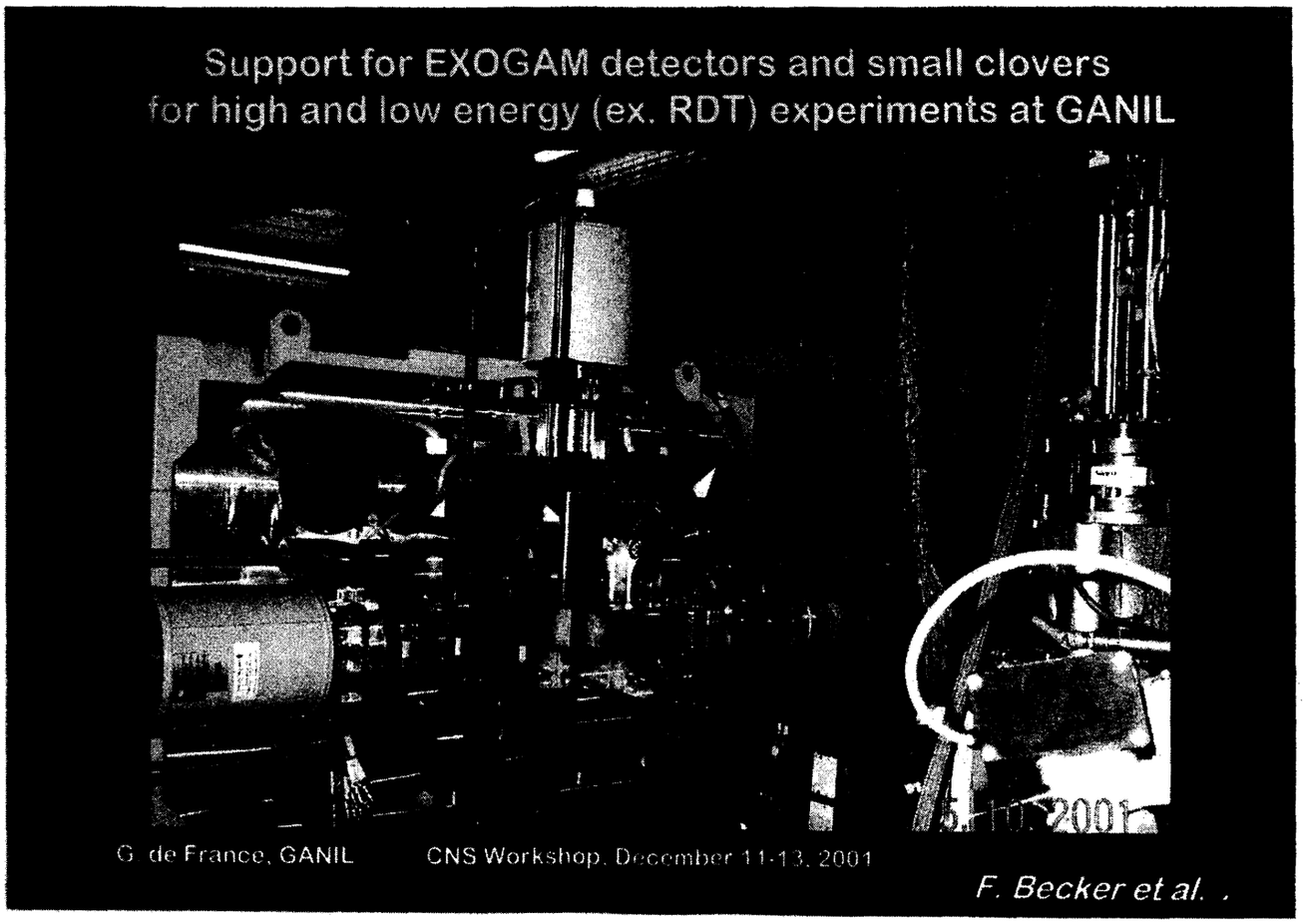
Support for EXOGAM detectors and small clovers
for high and low energy (ex. RDT) experiments at GANIL
G de France, GANIL
CNS Workshop, December 11-13, 2001
F. Becker et al.

Superdeformation in the doubly magic nucleus $^{40}_{20}Ca_{20}$

E. Ideguchi[1,2], D.G. Sarantites[2], W. Reviol[2], M. Devlin[2], C. Baktash[3], A.V. Afanasjev[4,5,6], D. Rudolph[7], A. Axelsson[8], M.P. Carpenter[4], A. Galindo-Uribarri[3], R.V.F Janssens[4], D.R. LaFosse[9], T. Lauritsen[4], F. Lerma[2], C.J. Lister[4], P. Reiter[4], D. Seweryniak[4], M. Weiszflog[8], and J.N. Wilson[2]

[1]RI-Beam Science Laboratory, RIKEN, Hirosawa 2-1, Wako, Saitama 351-0198, Japan
[2]Chemistry Department, Washington University, St. Louis, MO, 63130, USA.
[3]Physics Division, Oak Ridge National Laboratory, Oak Ridge, TN, 37831-6371, USA.
[4]Physics Division, Argonne National Laboratory, Argonne, IL, 60439, USA.
[5]Physics Department, University of Notre Dame, IN, 46556-5670, USA
[6]Laboratory of Radiation Physics, University of Latvia, LV2169, Miera str. 31, Latvia
[7]Department of Physics, Lund University, S-22100 Lund, Sweden.
[8]The Svedberg Laboratory and Department of Radiation Science, Uppsala University, S-75121 Uppsala, Sweden.
[9]Department of Physics and Astronomy, SUNY-Stony Brook, NY 11794, USA.

The study of superdeformed rotational bands in atomic nuclei has been a major experimental and theoretical efforts in the past 15 years. The occurrence of these bands is the manifestation of large shell gaps at a 2:1 axis ratio of the deformed shape for specific particle numbers. With the aid of the the large sensitivity obtained by combining the latest generation of γ-ray spectrometer with charged particle detectors, study of high-spin states in light mass nuclei become available. The attention in this field has been shifted from the "traditional " mass regions of superdeformation, 80, 150 and 190, to the lighter nuclei. This trend was initiated by the recent discovery of superdeformation in mass 60 region [1]. And more recently, an observation of a superdeformed band was reported in ^{36}Ar [2]. In the spectroscopic investigation of Z$\approx$20 nuclei with the GAMMASPHERE spectrometer [3], a rotational band with 7 γ-ray transitions between spin 2 and 16 has been observed in the doubly magic nucleus ^{40}Ca. The measured transition quadrupole moment of the band indicates a superdeformed shape and more elongated than in the neighboring superdeformed nuclei. The features of this band and a second newly observed structure are described by cranked relativistic mean-field calculations [4].

References

[1] D. Rudolph, *et al.* Phys. Rev. Lett. **82**, 3763 (1999).

[2] C.E. Svensson, *et al.* Phys. Rev. Lett. **79**, 1233 (1997).

[3] I.Y. Lee, Nucl. Phys. **A520**, 641c (1990).

[4] A.V. Afanasjev *et al.* Phys. Rev. C **59**, 3166 (1999).

Superdeformation in the doubly magic nucleus $^{40}_{20}Ca_{20}$

Eiji Ideguchi

Washington University

RIKEN

Superdeformation

2:1 axis ratio of the deformed shape

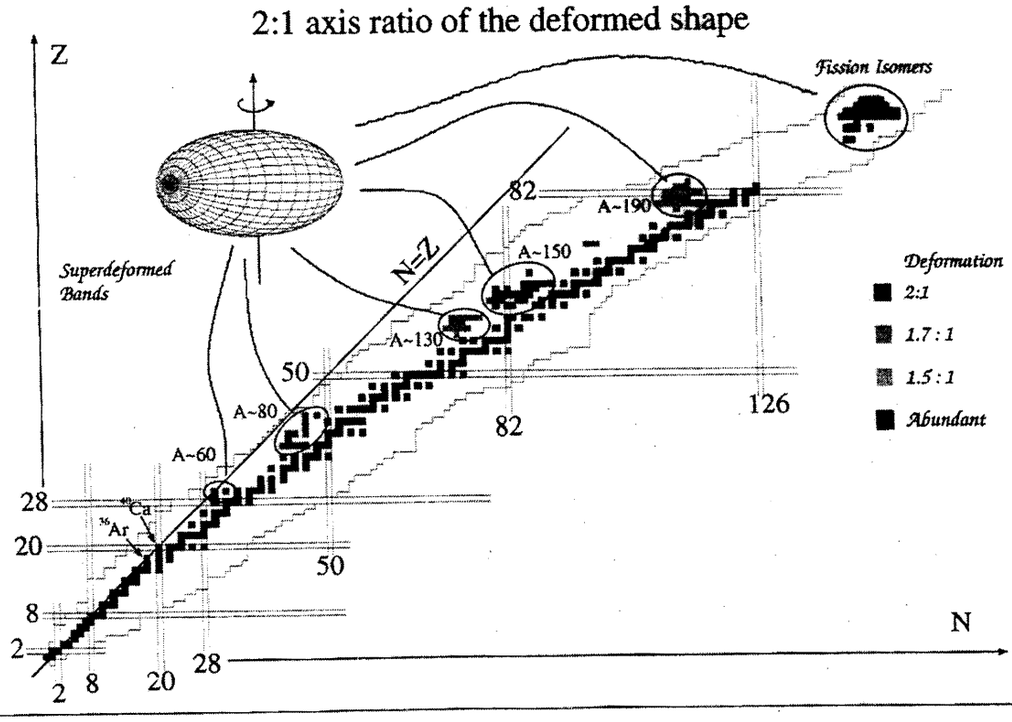

Fixed configuration deformed Hartree-Fock calculation
D.C. Zheng, L. Zamick, D. Berdichevsky : PRC42(1990)1004

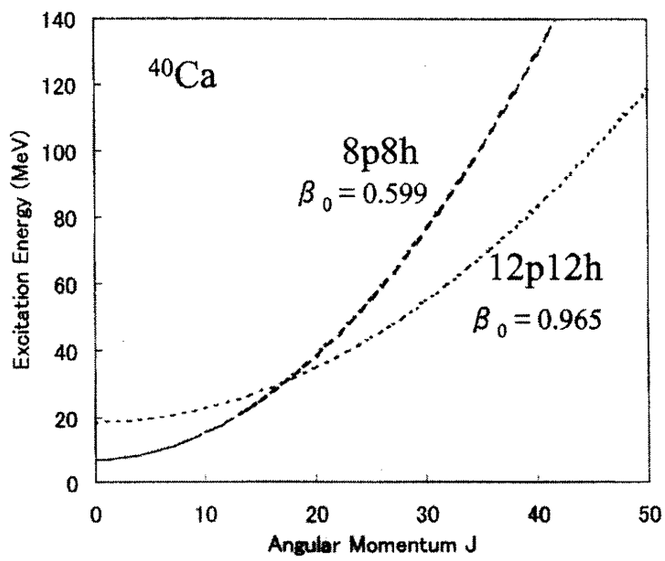

Percentage of wave-functions in ^{40}Ca

W.J.Gerace and A.M.Green, NPA123, 241 (1969).

State	E(exp)	0p-0h	2p-2h	4p-4h	6p-6h	8p-8h
0_1^+	0	82.81	16.81	1.0	0.04	0.0
0_2^+	3.35	2.89	2.25	68.89	20.25	6.76
0_3^+	5.21	1.0	2.25	16.81	12.25	67.24

Shell Model by M.Sakakura, A.Arima, T.Sebe, PL61B, 335(1976).

State	E(exp)	0p-0h	2p-2h	4p-4h	6p-6h	8p-8h
0_1^+	0	46.46	35.04	14.48	3.56	0.46
0_2^+	3.35	25.71	2.24	34.17	29.93	7.95
0_3^+	5.21	15.07	20.49	48.69	12.27	3.49

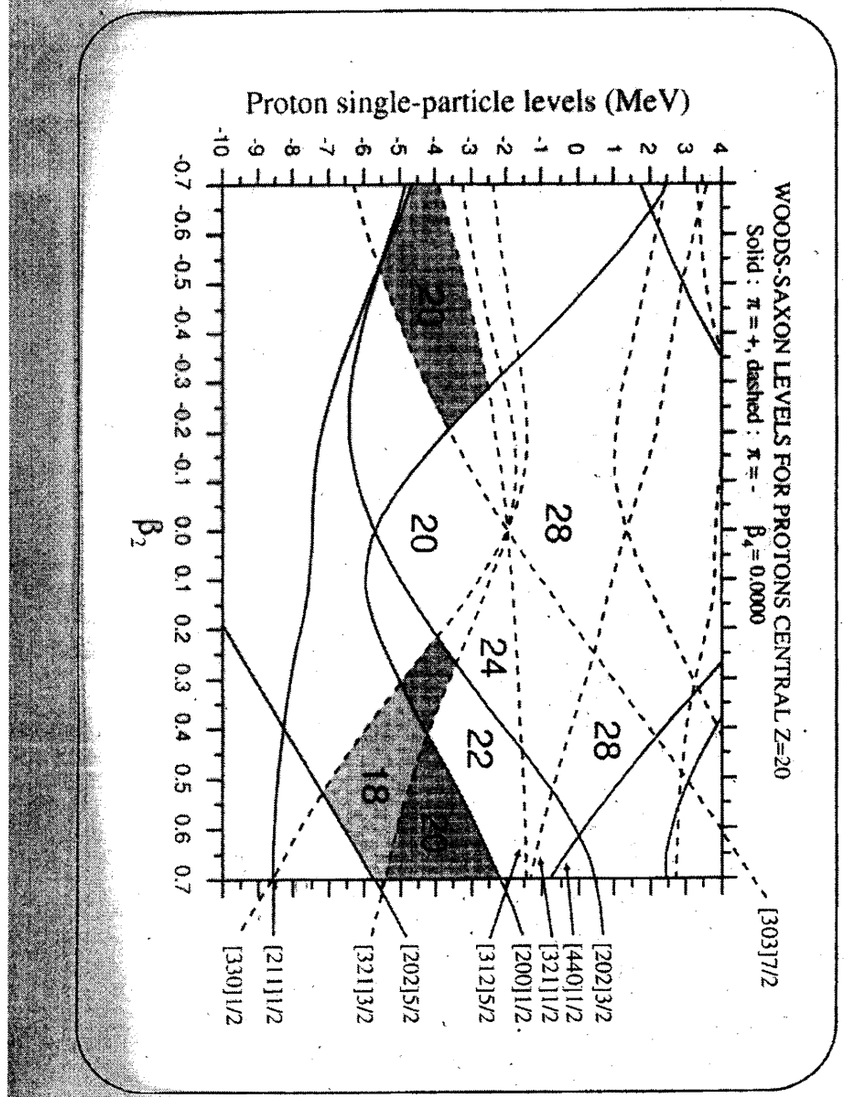

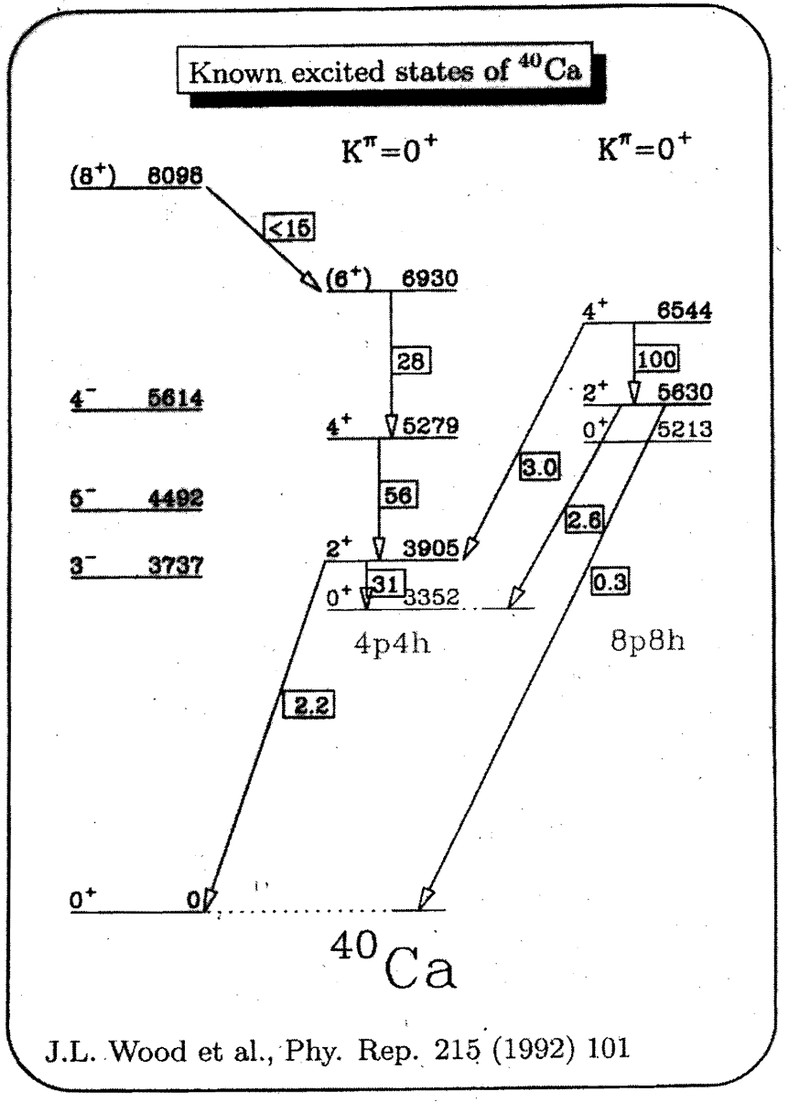

J.L. Wood et al., Phy. Rep. 215 (1992) 101

The experiment

Reaction : $^{20}Ne + {}^{28}Si \rightarrow 2\alpha + {}^{40}Ca$

ATLAS accelerator at the Argonne National Laboratory
Beam : ^{20}Ne 84 MeV (80 MeV after Ta foil)
Target : 0.45 mg/cm^2 ^{28}Si on 1.0 mg/cm^2 Ta supporting foil
Detectors : Gammasphere (101 Ge)
+ Microball (95 CsI(Tl))

$\varepsilon(proton) = 60\%,\ \varepsilon(\alpha) = 47\%$

Level scheme of ^{40}Ca (positive parity)

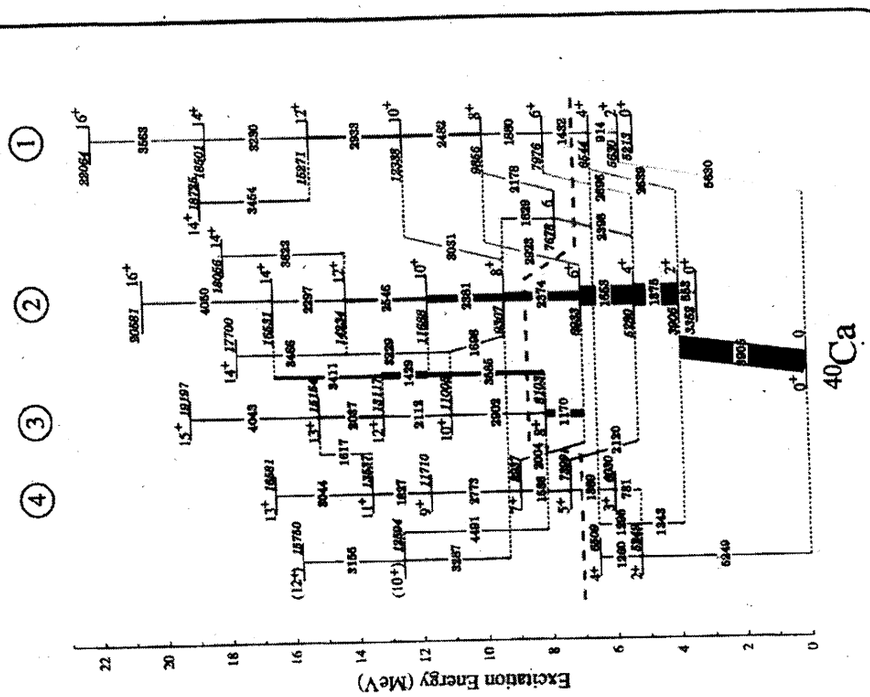

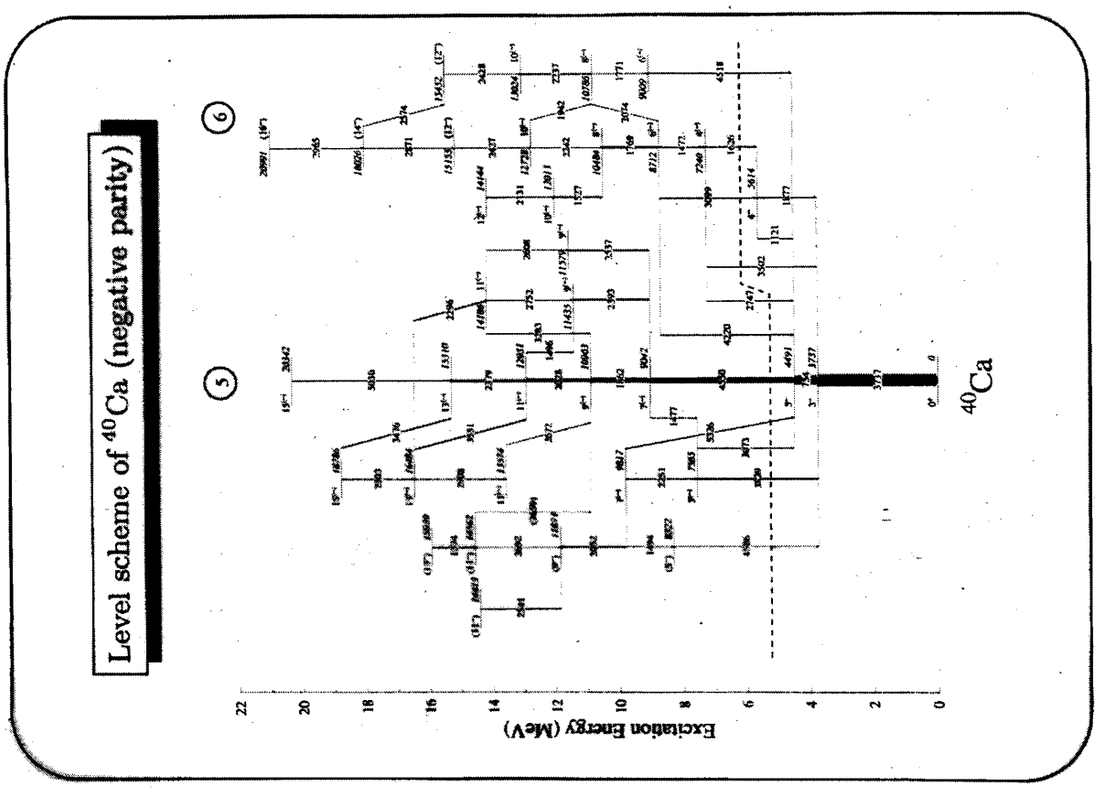
Level scheme of ^{40}Ca (negative parity)
⑤
⑥
Excitation Energy (MeV)
^{40}Ca

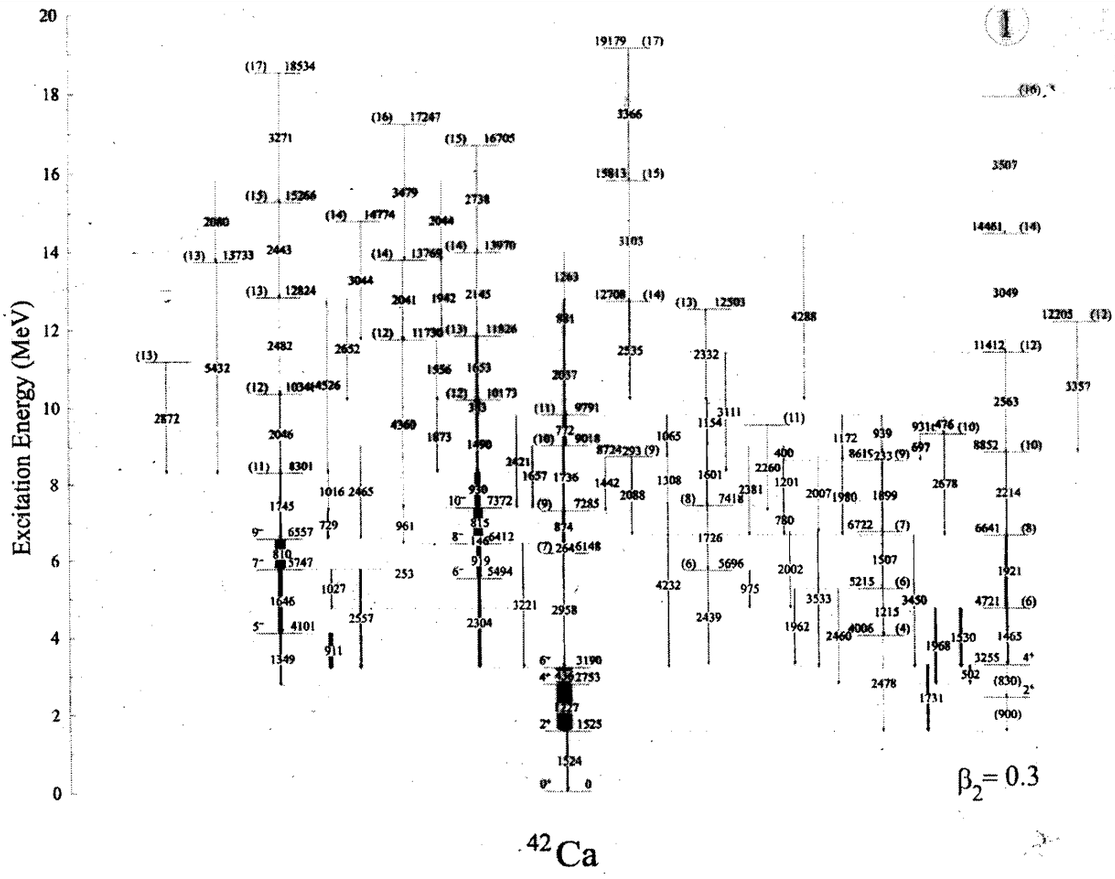
①
Excitation Energy (MeV)
$\beta_2 = 0.3$
^{42}Ca

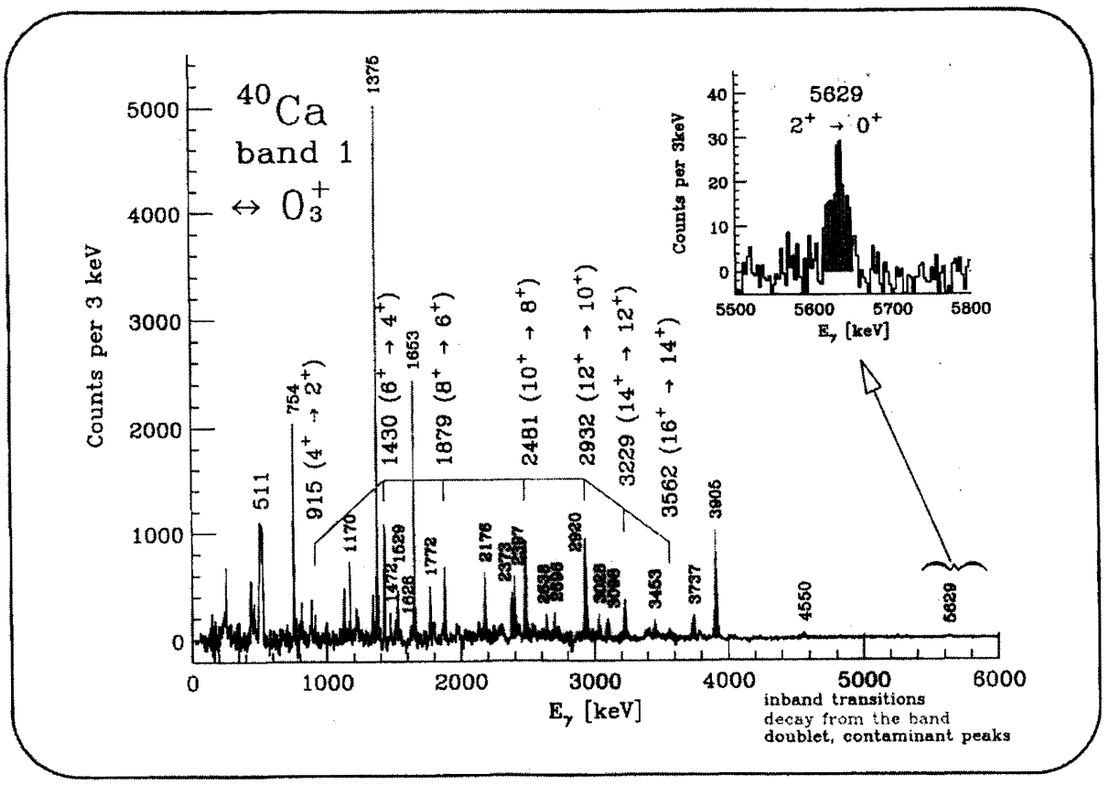
40Ca
band 1
↔ 0+3
Counts per 3 keV
Eγ [keV]
511
754
915 (4+ → 2+)
1170
1375
1430 (6+ → 4+)
1653
1879 (8+ → 6+)
2481 (10+ → 8+)
2932 (12+ → 10+)
3229 (14+ → 12+)
3562 (16+ → 14+)
3905
4550
5629
5629
2+ → 0+
Counts per 3keV
inband transitions
decay from the band
doublet, contaminant peaks

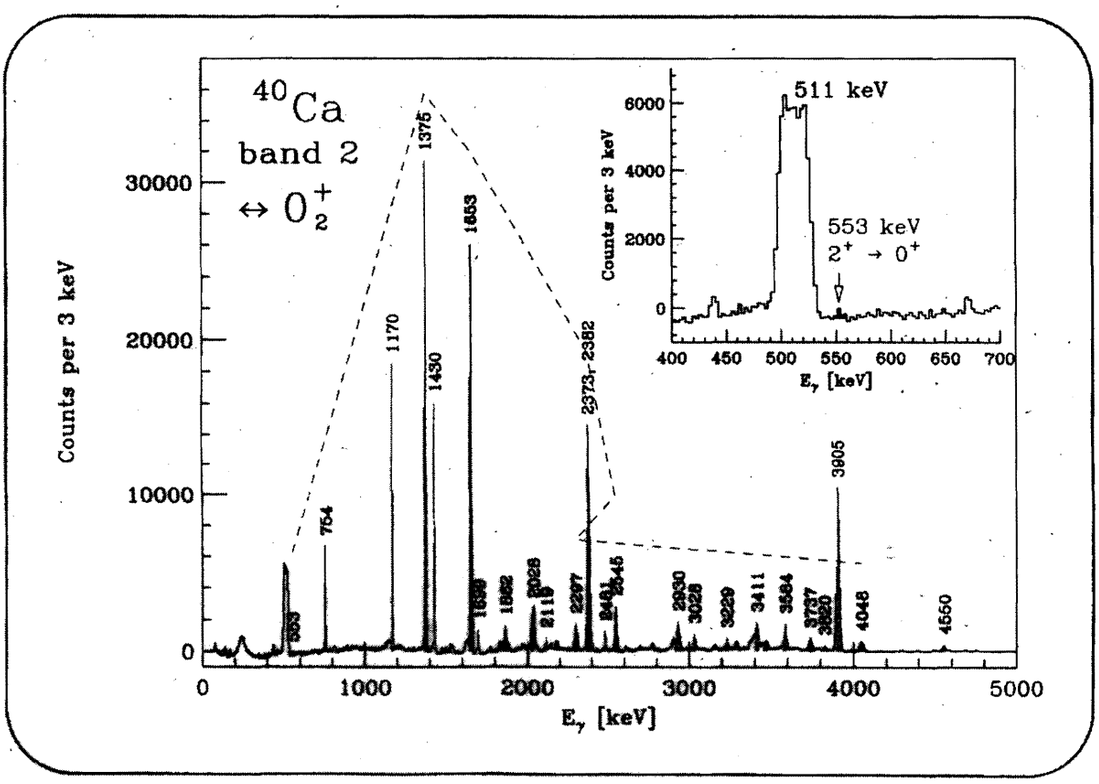
40Ca
band 2
↔ 0+2
Counts per 3 keV
Eγ [keV]
754
1170
1375
1430
1653
2373-2382
3905
4550
511 keV
553 keV
2+ → 0+
Counts per 3 keV
Eγ [keV]

Angular distribution of band 2

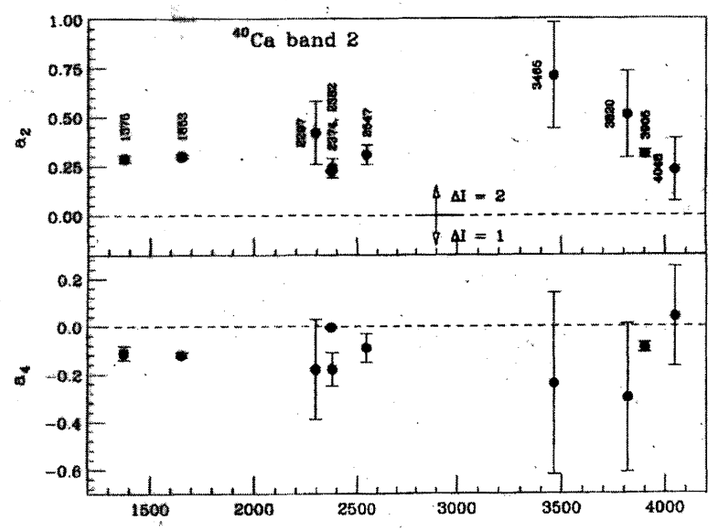

Angular distributions of band 1

$$W(\theta) = a_0(1 + a_2 P_2(cos\theta) + a_4 P_4(cos\theta))$$

$a_2 > 0, a_4 < 0 \rightarrow$ *quadrupole*

$a_2 < 0, a_4 > 0 \rightarrow$ *dipole*

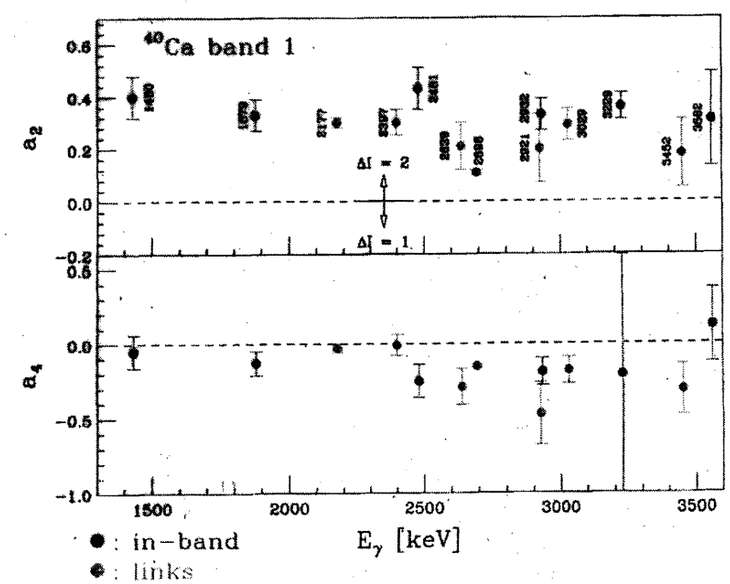

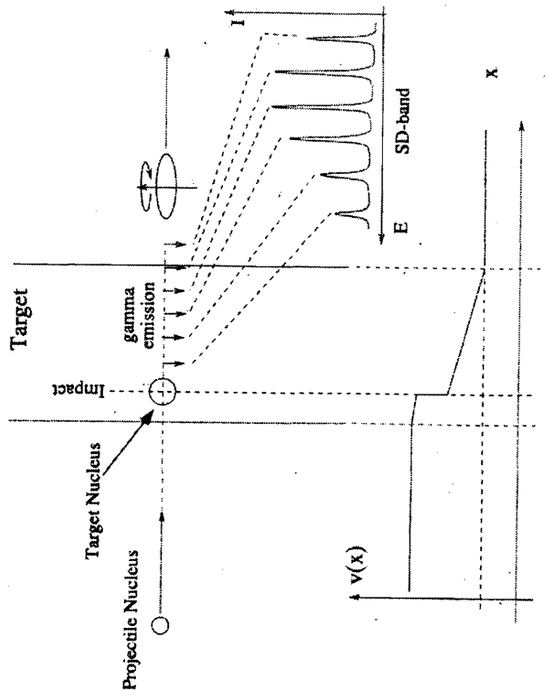

Figure 3.8. The basic idea of the Residual Doppler Shift Method [1]. The incoming projectile has a constant velocity until it reaches the target surface after which it will start slowing down in the target material. After the reaction, the velocity of the recoil is reduced within the target. The extremely fast decay from the SD states will take place from within the target. This means that the gammas will be emitted at different recoil velocities, and therefore with slightly different Doppler shift. This difference in Doppler shift can be measured, and hence the life-times can be deduced.

Residual Doppler shift measurement to extract life time

The fractional Doppler shift F(τ) is defined as

$$F(\tau) = v_{\mathrm{SD}}(E_\gamma)/v_f. \tag{1}$$

v_f : the average velocity at the point of recoil formation in the target
v_{SD} : the velocity of the recoil nucleus at the time of gamma decay
τ : time from recoil formation to decay

The measured F(τ) value $\rightarrow$ compared with calculated values based on the known stopping powers
Side-feeding was modeled in accordance with the experimental intensity profile.
A cascade of two transitions feeding into each SD states was assumed.

Residual Doppler shift measurement

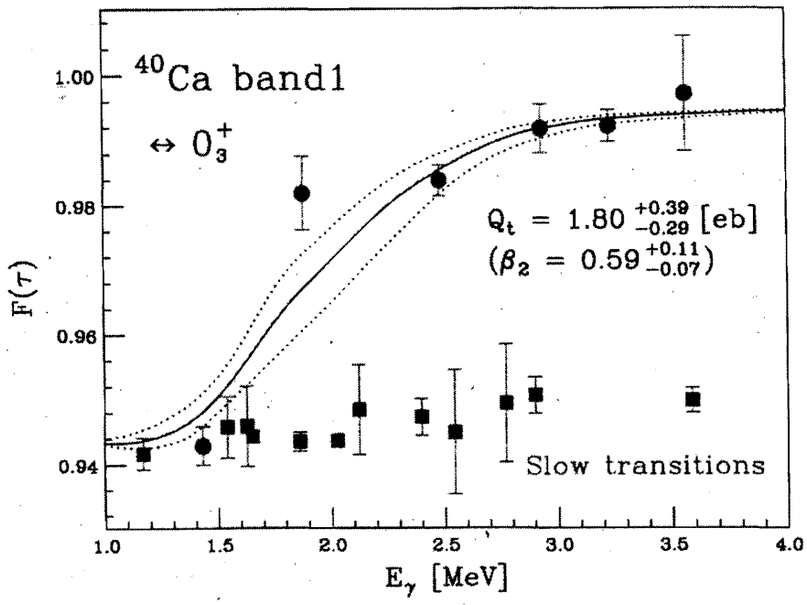

Scaled transition quadrupole moments

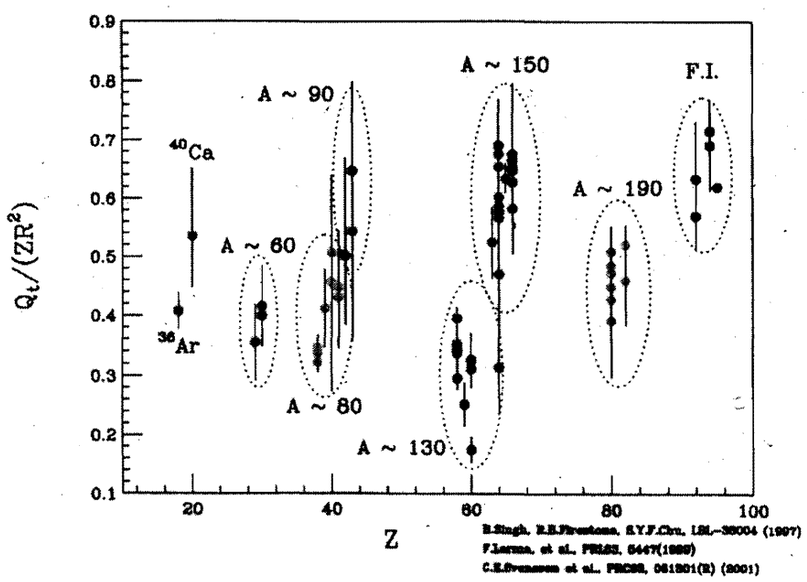

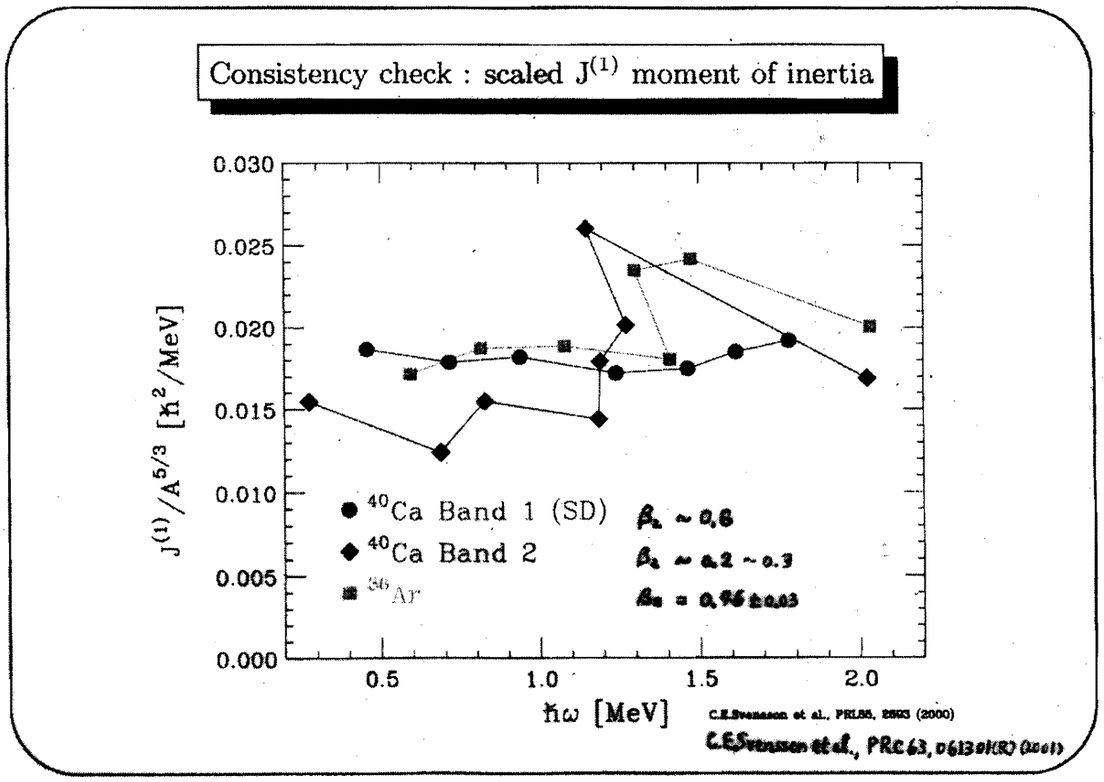
Consistency check : scaled $J^{(1)}$ moment of inertia
$J^{(1)}/A^{5/3}$ [$\hbar^2$/MeV]
0.030
0.025
0.020
0.015
0.010
0.005
0.000
0.5
1.0
1.5
2.0
$\hbar\omega$ [MeV]
^{40}Ca Band 1 (SD)
^{40}Ca Band 2
^{36}Ar
C.E.Svensson et al., PRL85, 2693 (2000)
C.E.Svensson et al., PRC 63, 061301(R) (2001)

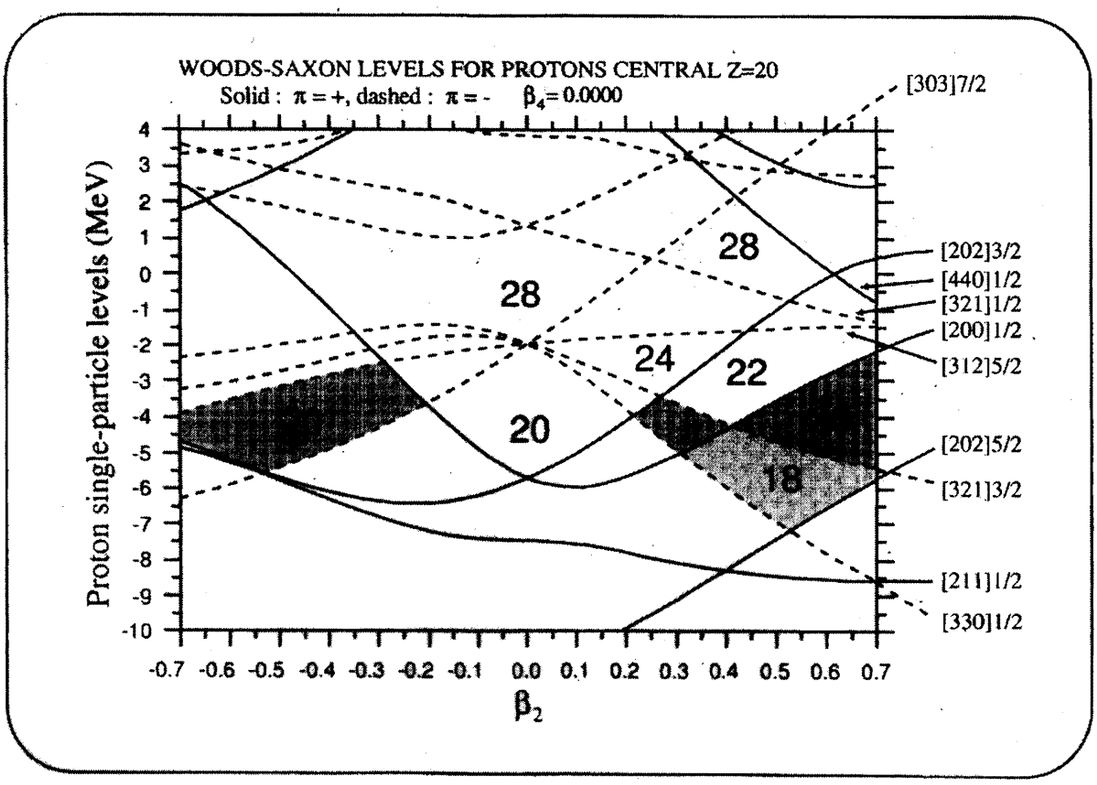
WOODS-SAXON LEVELS FOR PROTONS CENTRAL Z=20
Solid : π = +, dashed : π = - β_4= 0.0000
Proton single-particle levels (MeV)
β_2
28
28
24
22
20
18
[303]7/2
[202]3/2
[440]1/2
[321]1/2
[200]1/2
[312]5/2
[202]5/2
[321]3/2
[211]1/2
[330]1/2

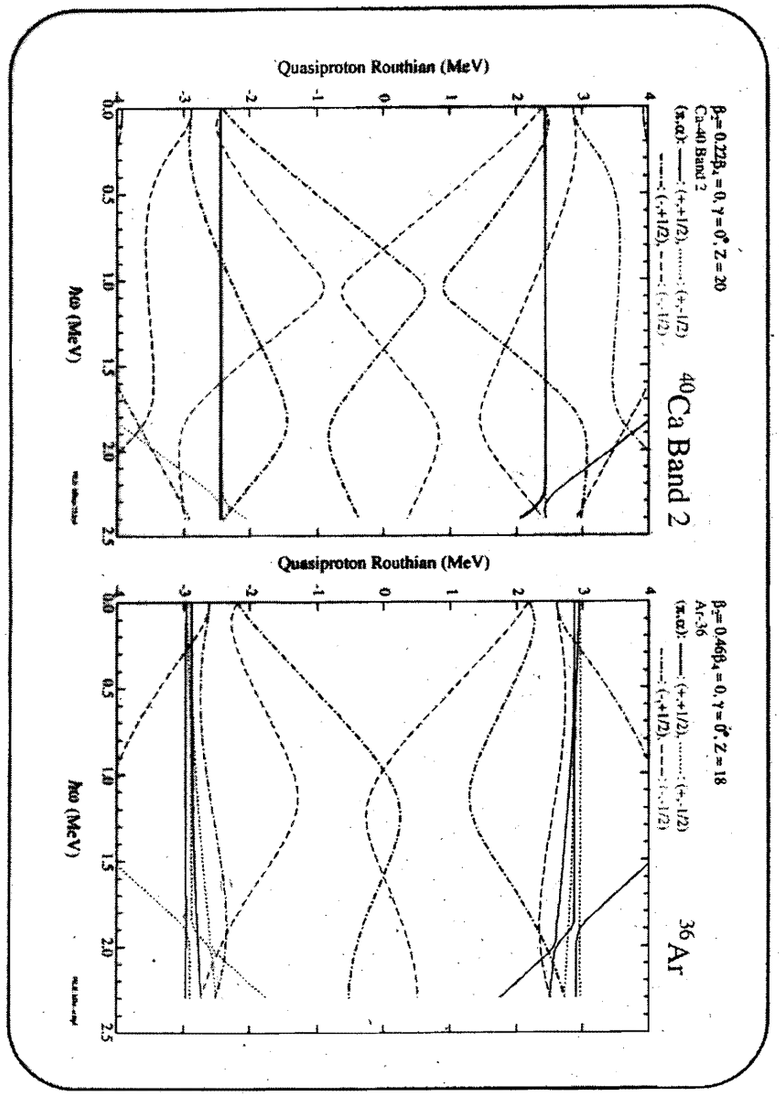

Fixed Deformation CSM Calculations (Preliminary)

- ^{36}Ar and ^{40}Ca (band 2)
  band crossings qualitatively reproduced
- ^{40}Ca (band 1)
  $g_{9/2}$ super-intruder approaches Fermi Level at high frequency
- Large-Scale Shell model calculations are in progress
- Cranked Relativistic Mean-Field Calculation by A.V.Afanasjev

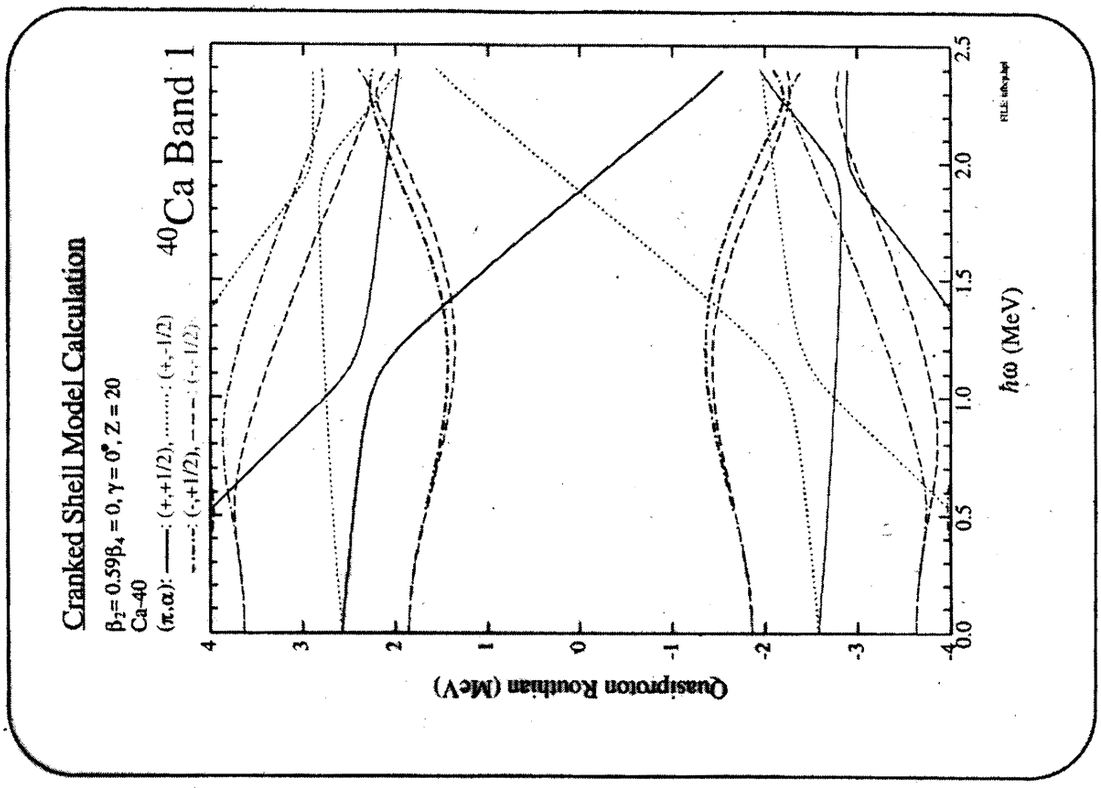
Cranked Shell Model Calculation
β2= 0.59β4 = 0, γ = 0°, Z = 20
Ca-40
(π,α): ——: (+,+1/2), ...: (+,-1/2)
-.-.-: (-,+1/2), - - - : (-,-1/2)
40Ca Band 1
Quasiproton Routhian (MeV)
ħω (MeV)

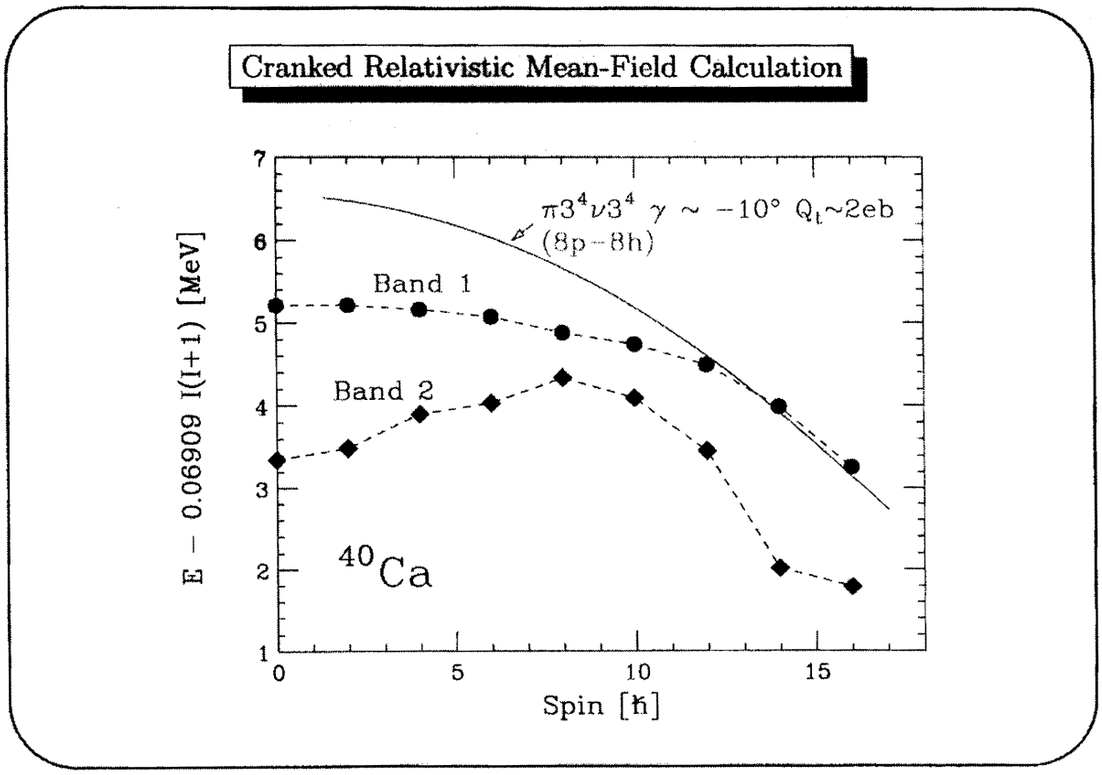
Cranked Relativistic Mean-Field Calculation
π3⁴ν3⁴ γ ~ −10° Qt~2eb
(8p−8h)
Band 1
Band 2
40Ca
E − 0.06909 I(I+1) [MeV]
Spin [ħ]

Summary

- A discrete-line superdeformed band has been found in ^{40}Ca
- A normal deformed band (band 2)
- Linking transitions to band 2 and ground state
- Large Q_t value, $1.80^{+0.39}_{-0.29}$ eb, $\beta_2 = 0.59^{+0.11}_{-0.07}$
- CRMF calculations (more coming)
- Shell Model Calculations (in progress)

Collaboration

E. Ideguchi[1], D.G. Sarantites[1], W. Reviol[1], M. Devlin[1], F. Lerma[1], J.N. Wilson[1], C. Baktash[2], A. Galindo-Uribarri[2] A.V. Afanasjev[3] D. Rudolph[4] D.R. LaFosse[5], M.P. Carpenter[6], R.V.F Janssens[6], T. Lauritsen[6], C.J. Lister[6], P. Reiter[6], D. Seweryniak[6], A. Axelsson[7], M. Weiszflog[7]

1. Washington University
2. Oak Ridge National Laboratory
3. University of Notre Dame
4. Lund University
5. SUNY-Stony Brook
6. Argonne National Laboratory
7. Uppsala University

Pulse-shape analysis of CNS segmented Ge detector

Meiko Kurokawa

CNS, University of Tokyo

Pulse Shape Analysis of CNS Segmented Ge Detector

M. Kurokawa, S. Shimoura, H. Iwasaki, H. Baba[a], H. Murakami[a] and H. Sakai

CNS, University of Tokyo
a) Rikkyo University

method to extract the interaction position and some experimental data will be introduced

a Ge Detector

cylindrical shape: r = 3.5 cm, z = 2.0 cm
effective radius: r = 3.0 cm
segment size: < 2.0^3 cm^3
tow detectors are encapsulated(high voltaed surfaces face each other)
-> total siganl = Σsegment
planar type -> pararell electric field in the effective volume
-> easier to simulate the movement of charge carriers (electron and hole)

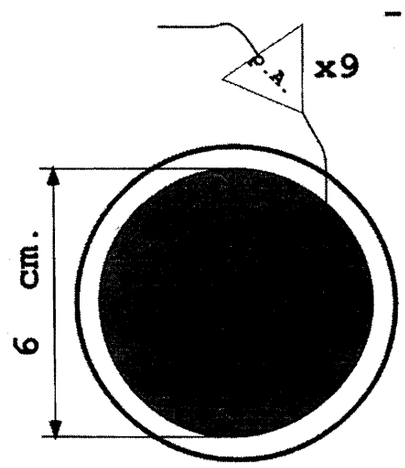

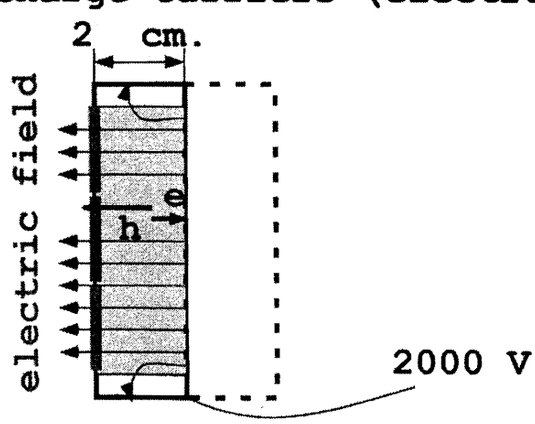

Pulse Shape Simulation

important to decide the method for the extraction of interact position

step for the simulation

1. evaluation of amount of induced charge on a segment, when a carrier is at position (r′, ϕ′, z′).

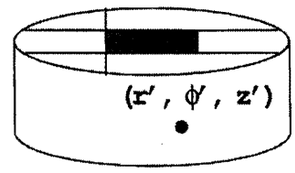

2. obtain the position of a carrier z′, as the function of the time

3. RC integration with time constant of preamplifier

Step 1

electro magnetic problem in cylindrical coordinate system
Ref.) Jackson

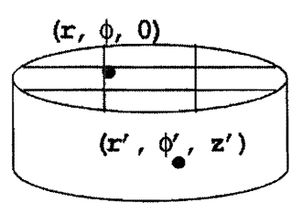

$$\sigma(\rho,\phi) = -\frac{1}{\pi a^2}\left(\sum_{n=1}^{\infty}\frac{J_0(\frac{x_{0n}}{a}\rho)J_0(\frac{x_{0n}}{a}\rho')\sinh(\frac{x_{0n}}{a}(L-z'))}{(J_1(x_{0n}))^2\quad\sinh(\frac{x_{0n}}{a}L)} + 2\sum_{m=1}^{\infty}\sum_{n=1}^{\infty}\cos(m(\phi-\phi')) \times \frac{J_m(\frac{x_{mn}}{a}\rho)J_m(\frac{x_{mn}}{a}\rho')\sinh(\frac{x_{mn}}{a}(L-z'))}{(J_{m+1}(x_{mn}))^2\quad\sinh(\frac{x_{mn}}{a}L)}\right). \qquad (1)$$

Then, integration over the area of a segment

Step 2

parameters must be fixed

$v_e = \mu_e E(z)$

$v_h = \mu_h E(z)$

μ_e (μ_h) :mobility of electron (hole)

E(Z): depend on the impurity density ρ

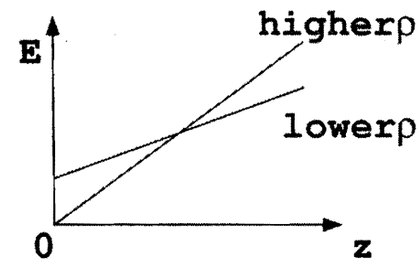

when v_e or v_h is near to their saturation velocity v_s, linearity will still be maintained ?

decided from observed signals obtained by collimated source

Experimental Set up

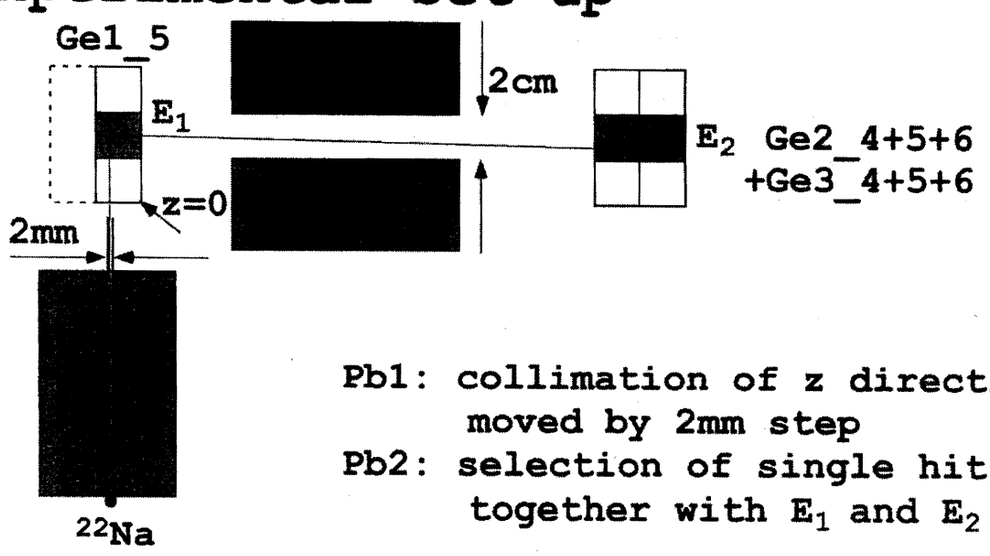

Pb1: collimation of z direction moved by 2mm step

Pb2: selection of single hit event together with E_1 and E_2 gate

x and y position is not selected

output signals from the Ge1 preamplifier are recorded

Output Signals from the Preamplifiers

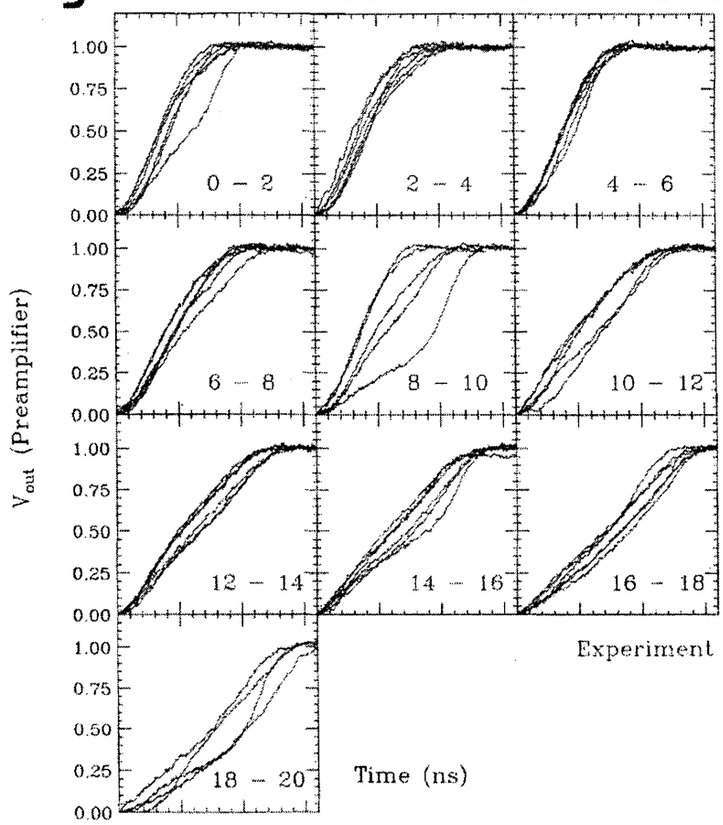

Decision of Parameters

Rise time is strongly correlated with interaction depth z, but not with x and y as expected.
z=0-2: only the movement of electron is reflected
z=18-20:only the movement of hole is reflected

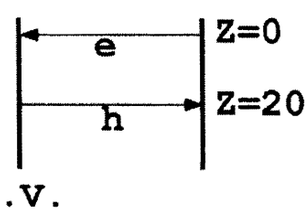

electron is faster than hole, though $\mu_e < \mu_h$.

$v_e = \mu_e E(z)$, until reaches the v_s

$v_h = \mu_h E(z)/(1 + \mu_h E(z)/v_s)$

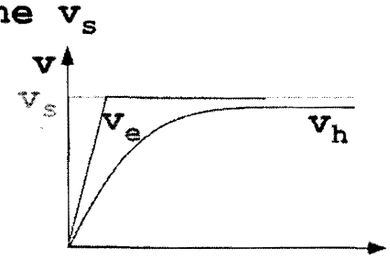

Comparison of Experimental Data and Simulation

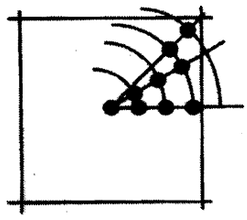

sampling point

impurity density
-> 0.9 X 10^10 (cm^{-3})

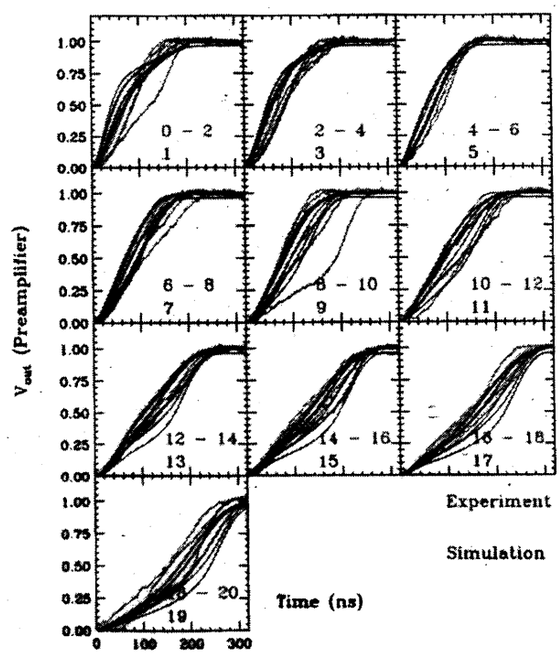

Method to Extract Interaction Depth

Some kinds of pulse shape analysis such as T_{total} - T_5 analysis are examined based on the simulated output signals from the preamplifier.

Requirement on the method:
distinguish pulses with the same rise time but with different shape

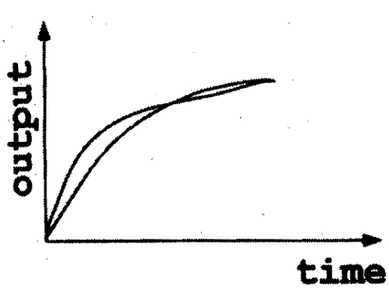

second delivertive is appropriate to extract the time where pulse changes most drastically

CR^2-RC^4 method with τ = 50ns

Example of CR²-RC⁴ Shaped Signals

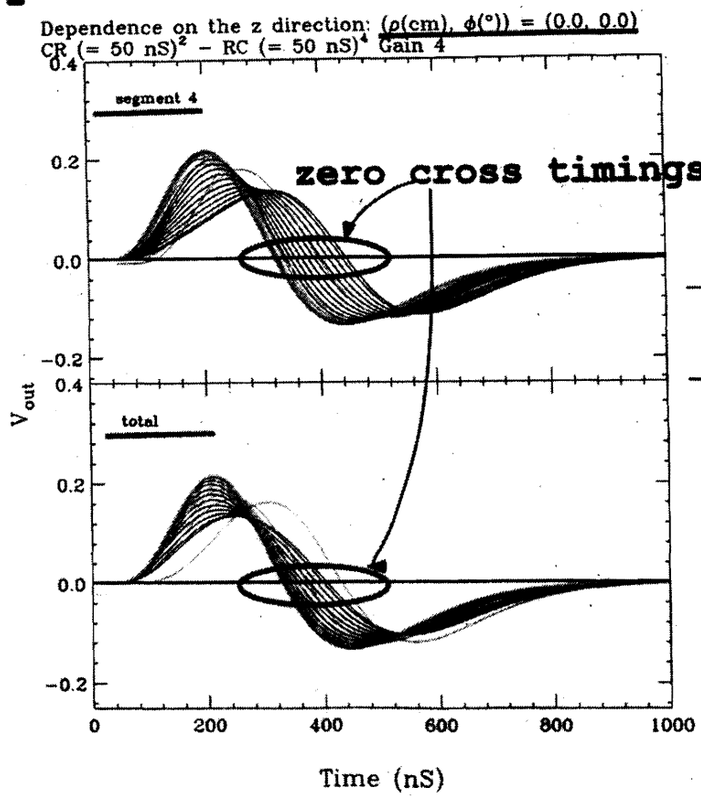

Zero Cross Timings

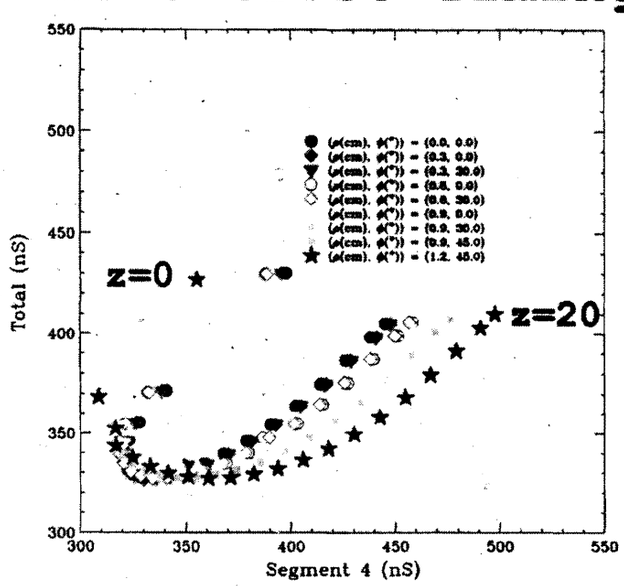

Δr_{min}= 4 ns

(ρ,ϕ) or (x,y) will be obtained from transient signals of neighbour segments

there is x = y region

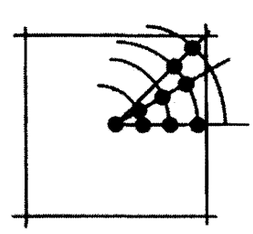

sampling point

Experimental Set up

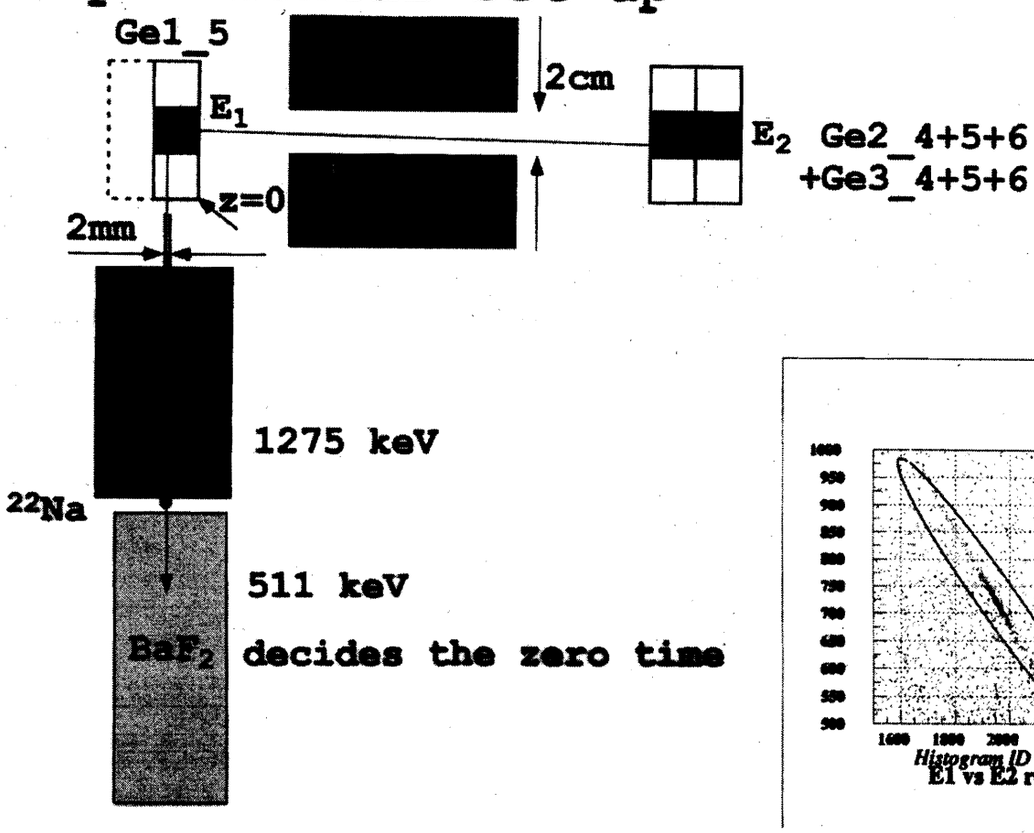

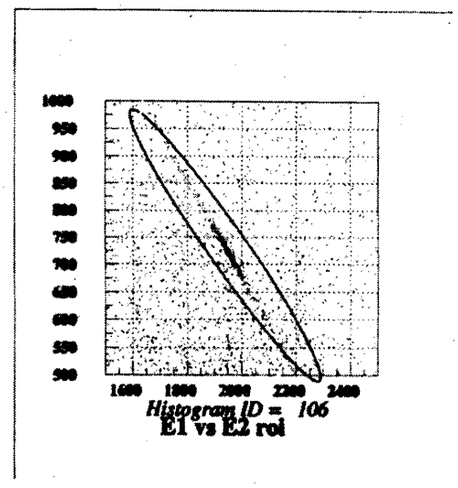

Experimental Results

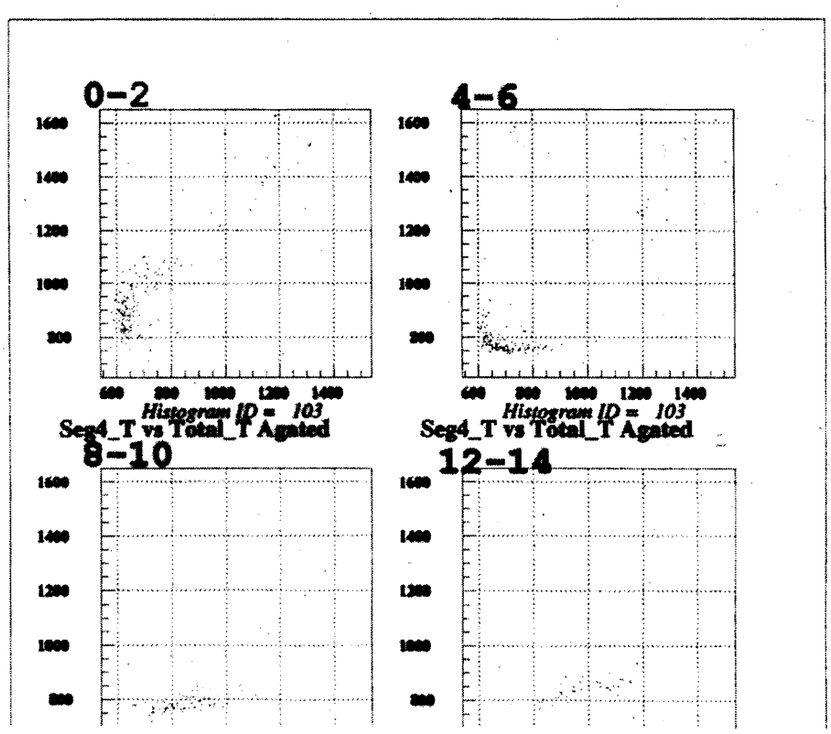

Conclusion

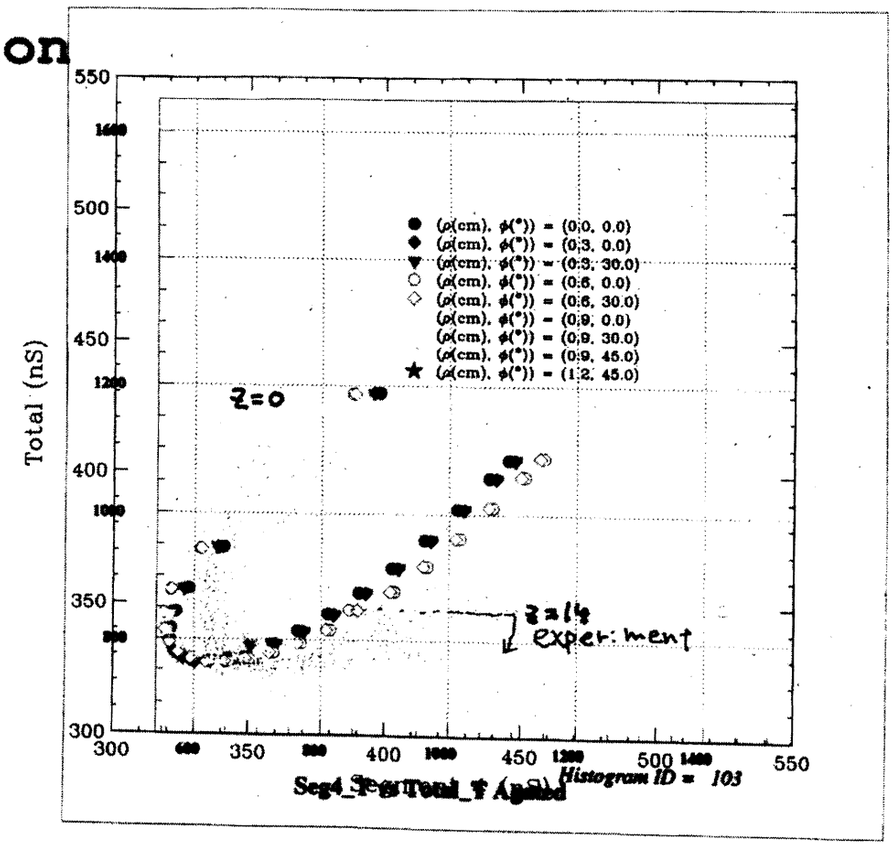

Summary and Future Plan

Method to simulate the output signal from preamplifiers was established . Based on the simulation, CR2-RC4 shaping was emplyed to extract the interaction position. The experimental confirmation is now going on. From very preliminaly results, position resolution of 1mm is expected to be achieved.

We have to take into acount the event with more than two interaction points.The effect will be studied experimentally and by using the GEANT4 simulation code.

Hyperball and a new frontier in hypernuclear physics

H. Tamura

Department of Physics, Tohoku University, Sendai 980-8578, Japan

Recently, we constructed "Hyperball", a large Ge detector array, dedicated to hypernuclear γ spectroscopy and started a series of experiments [1].

Ge detectors were not available before for hypernuclear experiments because of too high energy deposit rates caused by scattered and halo particles in high energy meson beams. We solved the problem by using special fast electronics, low-gain transistor-reset preamplifiers and gated-integrator-type amplifiers. Hyperball consists of 14 sets of Ge detectors (60% relative efficiency for each) and the total photo-peak efficiency is about 3% at 1 MeV. Each Ge detector is surrounded by BGO counters, which are used not only for Compton suppression but for rejection of serious background of high energy photons from π^0. Performance of the Ge detectors is always monitored during the beam time with a monitoring system using triggerable ^{60}Co sources.

By using Hyperball, structure of light hypernuclei has been investigated in detail. We revealed the level structure of $^7_\Lambda$Li by observing 4 transitions [2]. The $B(E2)$ of $^7_\Lambda$Li ($5/2^+ \rightarrow 1/2^+$) was measured with Doppler shift attenuation method. It is found to be 1/3 of the corresponding $B(E2)$ of the core nucleus ^{6}Li ($3^+ \rightarrow 1^+$), which is an evidence of the "hypernuclear shrinking effect" [3]. From the energy spacing of the ground state doublet of $^7_\Lambda$Li, the strength of the spin-spin interaction between a Λ and a nucleon was determined [2].

In $^9_\Lambda$Be, we succeeded in observing a typical "hypernuclear fine structure"; we resolved doublet states ($5/2^+$,$3/2^+$) split by only $31.4^{+2.5}_{-3.6}$ keV, by observing two $E2$ transitions going to the ground state ($5/2^+ \rightarrow 1/2^+$, $3/2^+ \rightarrow 1/2^+$) separately [4]. The small spacing of the doublet indicates a very small spin-orbit force of Λ, which cannot be explained by present meson-exchange models of baryon-baryon interactions.

We are currently studying $^{16}_\Lambda$O and ^{10}B at BNL. From a fine structure in $^{16}_\Lambda$O we will be able to extract the strength of the ΛN tensor force.

References

[1] H. Tamura, Nucl. Phys. A639 (1998) 83c.
[2] H. Tamura *et al.*, Phys. Rev. Lett. 84 (2000) 5963.
[3] K. Tanida *et al.*, Phys. Rev. Lett. 86 (2001) 1982.
[4] H. Akikawa *et al*, Nucl. Phys. A 691 (2001) 134c; submitted to Phys. Rev. Lett.

Dec. 13, 2001
Ge detector ws

Hyperball and a new frontier in hypernuclear physics

H.Tamura
Tohoku Univ.

1. Introduction
2. Hyperball -- technical issues
   - Requirements
   - Ge detectors and electronics
   - BGO counters
   - Monitoring system
3. Physics results
   - "Hypernuclear fine structure" and ΛN interactions
   - B(E2) and shrinking effect
4. Future plans
   - Near future -- Upgraded Hyperball
   - Far future -- JHF
5. Summary

Spectroscopy of Λ Hypernuclei

With magnetic spectrometers 1970-	γ with Ge detectors extremely difficult before
Energy Resolution	
(K^-,π^-), (π^+,K^+) SKS $\gtrsim$ 1.5 MeV FWHM $(e,e'K^+)$ 0.6 MeV	2 keV for bound states Hyperball 1998-
Physics Interests	
Major shell structure s_Λ, p_Λ, d_Λ, f_Λ,.. -> V_0^Λ Core excited states $^{11}C^* \times s_\Lambda$ LS splitting?	Hypernuclear Fine Structure -> ΛN spin-dependent (spin-spin, LS, tensor) interactions B(E2), B(M1) shrinking effect, g_Λ in nucleus

●*Why difficult?*

- High energy-deposit-rate problem

  High energy meson beams (~1 GeV/c K/π)

  beam halo due to meson decays

  ($K^- \rightarrow \mu^-\nu / \pi^-\pi^0$, $\pi^\pm \rightarrow \mu^\pm\nu$)

  thick target (~10 g/cm^2) -> scattered particles

  => Typical energy rate of one Ge detector

  (15cm from target, $4\times10^6 \pi^+$/sec)

  ~ 50 MeV (penetration) x 20 kHz = 1 TeV /sec

  >> Operation limit of normal Ge detectors

  ~ several 10 GeV / sec (several 10 kHz x 1 MeV)

- Very small γ-ray yields

  $d\sigma/d\Omega * \Delta\Omega * N_{beam} * N_{target} * \varepsilon_{Ge}$

  $< 10\mu b/sr * 50msr * 0.5\times10^6/s * 6\times10^{23} * 10^{-3}$

  ~ 1 event / day / detector

=> Introduce special fast electronics

Need a large Ge array (and install Ge's as close as possible to the target)

●*Past experiments* (1960's-1995)

Only 5 transitions, All by NaI counters, Low statistics

A textbook example of single-particle states of Λ

$^{89}Y\ (\pi^+,K^+)\ ^{89}{}_{\Lambda}Y$

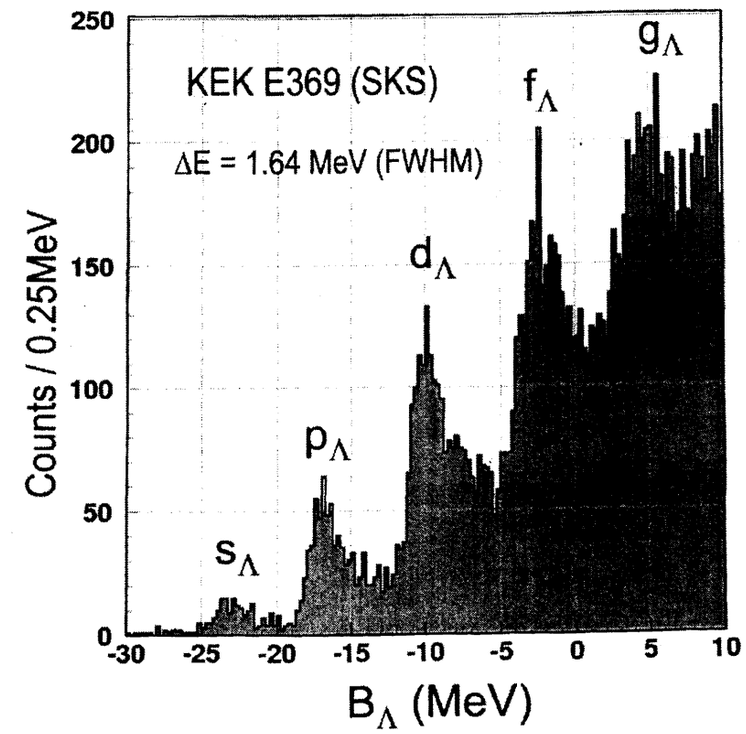

原子核内部でも単一粒子描像(→殻模型)が成立している証拠

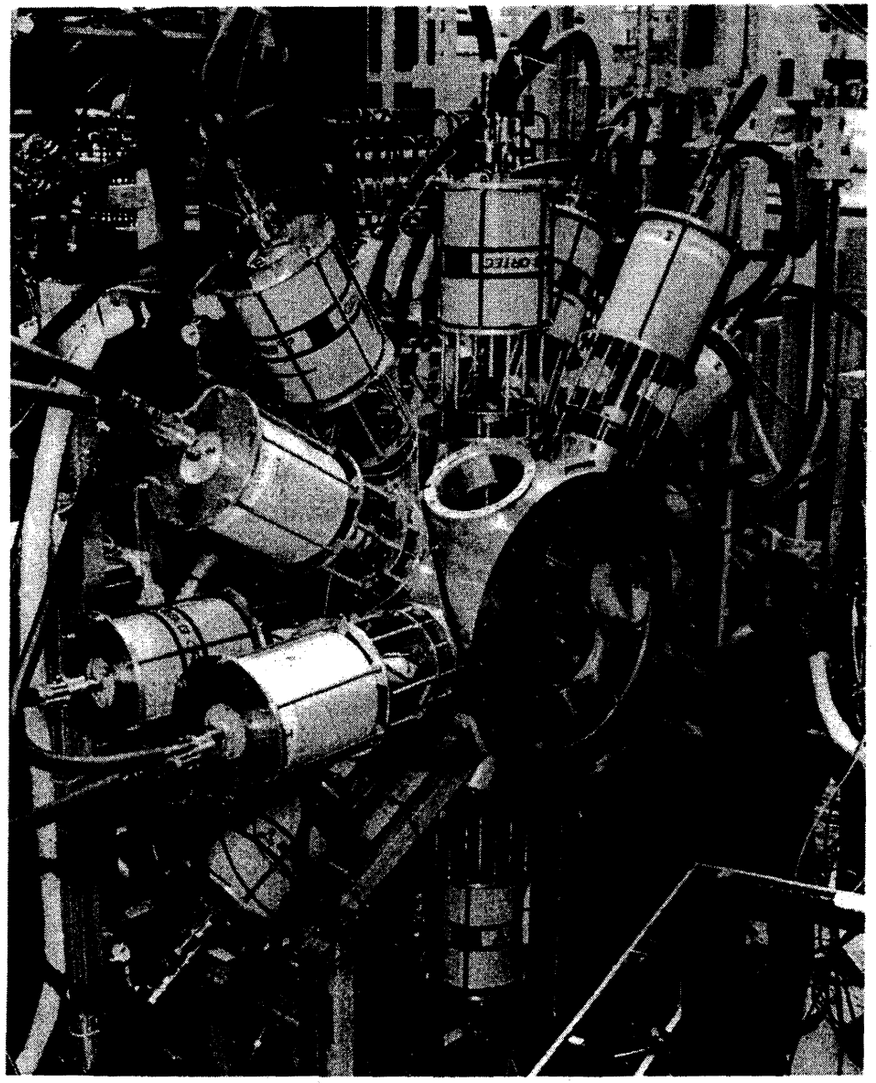

Hyperball

[60% N-type Ge + BGO counters] x 14

Ω ~15% x 4πsr, ε ~ 2.5% at 1 MeV

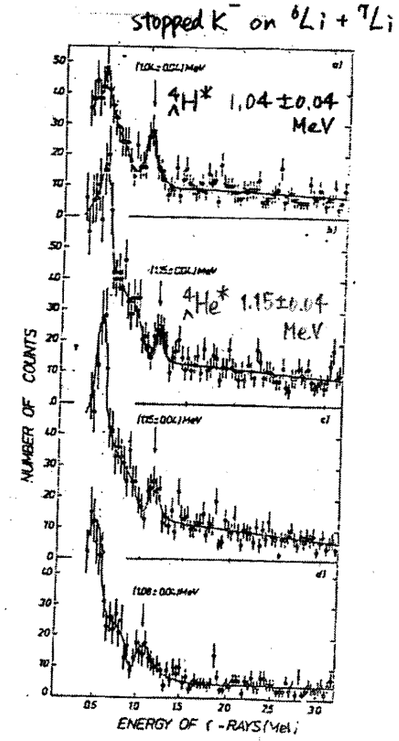

Fig. 2. The γ-spectra obtained with K^- stopped in ^{6}Li and ^{7}Li targets and taken in coincidence with charged pions and π^0 mesons. (a) Added γ-spectrum for ^{6}Li and ^{7}Li targets, $N_{K^-} = 6.5 \times 10^8$, $E_{\pi ch} = (48-58)$ MeV. (b) Same as A, but $E_{\pi^0} = (45-85)$ MeV. (c) The γ-spectrum for a ^{6}Li target, $N_{K^-} = 4.2 \times 10^8$, $E_{\pi^0} = (200-400)$ MeV. (d) The γ-spectrum for ^{7}Li target, $N_{K^-} = 2.3 \times 10^8$, $E_{\pi^0} = (100-180)$ MeV.

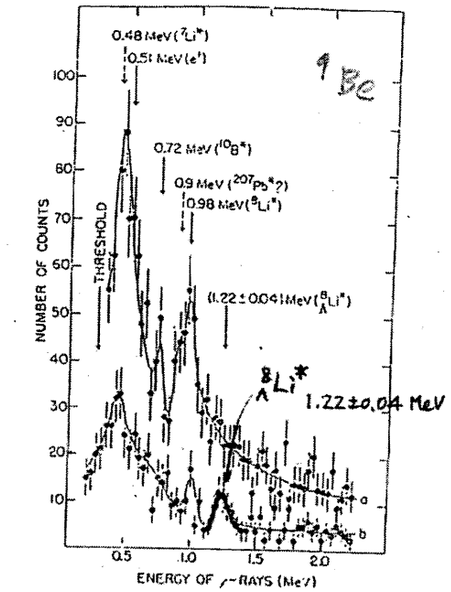

Fig. 3. Same spectrum as in fig. 2, but the additional coincidence of charged pions has been required. (a) $E_{\pi\,charged} \gtrsim 40$ MeV. (b) 40 MeV $< E_{\pi\,charged} < 48$ MeV.

図4: Bedjdian et al. のγ線スペクトル。静止 K^- 吸収でのγ線スペクトルを，同時に発生した π^- がハイパー核の崩壊にあたるエネルギーを持っているという条件で tag したもの。(1)-(a) ^{6}Li および ^{7}Li 標的，1.04 MeV の $^4_\Lambda$H のγ線が見える。[7] (2) ^{9}Be 標的，$^4_\Lambda$H のγ線はみえない。1.2 MeV のピークは $^8_\Lambda$Li のγ線とされている。[11]

● *Requirements in Hyperball Design*

- Should works (dead time < 50%)
  under energy rate up to 1 TeV/s
  counting rate up to 100 kHz
- Wide energy range of interest: 0.07 -- 6 MeV (11MeV)
- Both of Doppler shifted lines (E(M1)>0.3MeV, $|\beta\cos\theta| < 0.05$)
  and unshifted lines (E(M1)<0.3MeV; E(E2)<3MeV)
  -> good energy resolution and granuality
- High accidental rate -> good time resolution, pileup rejection
- High radiation damage by $\pi^{\pm}$and n -> easily annealed
- Serious background (π^0, h.e.charged particles, compton)
  -> suppression by counters (BGO)
- Critical operating condition for deadtime, resolution, damage, etc.
  during a long beam time (>1 month)
  -> Goog monitoring system

And covers maximum solid angle within a limited budget

On the other hand,
- Multiplicity low -- a few γ's + a few particles
- Easy trigger -- by (K^-,π^-) or (π^{-+},K^+) reactions

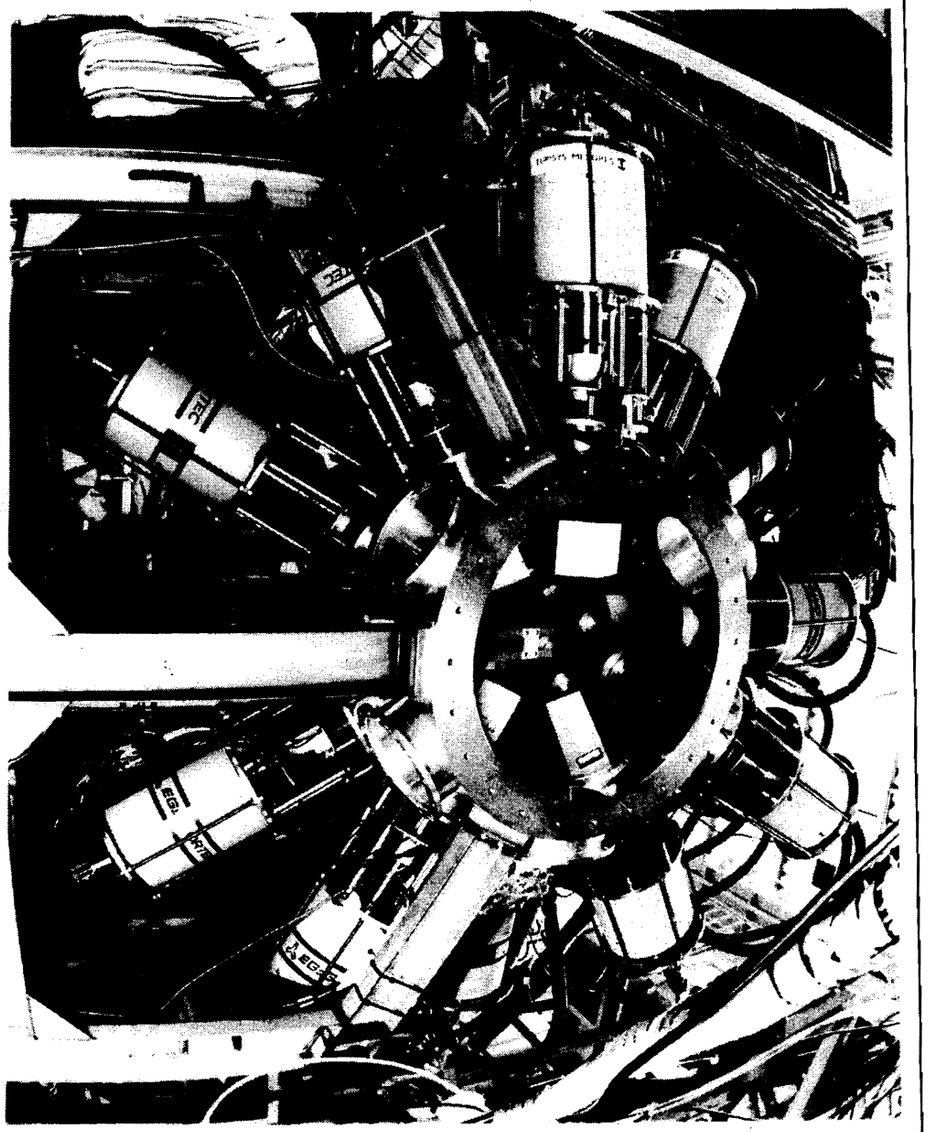

Hyperball

N-type Ge detector (rel.eff.60%) w/ fast electronics
+ BGO counters for Compton/ π^0 suppression
x 14 Ω_{Ge} ~ 15 - 25 %

Photo-peak Efficiency of Hyperball

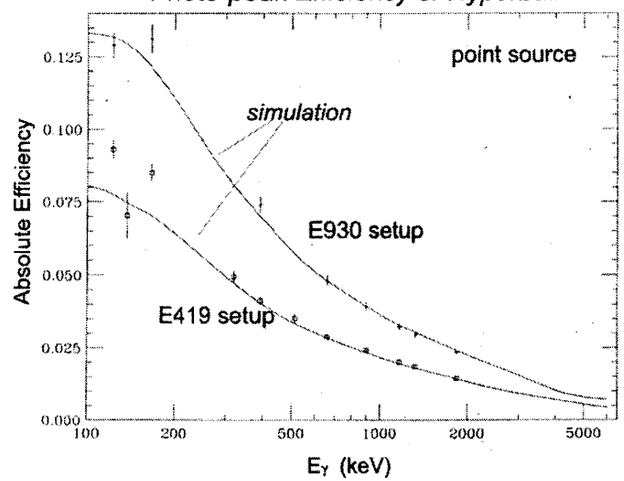

In-beam performance in KEK E419
[Count rate ~ 20-60 kHz, Energy rate ~0.4TeV/sec]
*Resolution ~3 keV at 1.33 MeV
*Deadtime ~ 30-50%
*Peak shift < 1 keV
*Slight radiation damage in one month run

●*Ge detectors*

- Coaxial HP Ge, N-type, unsegmented
  rel.eff. 60% (~70 mm x 70 mmϕ)
  4 Eurisys + 10 ORTEC
- ΔE < 2.2 keV at 1.33MeV
- Barrel form (not a "ball")
  10 -- 15 cm from beamline (changeable)
  ε_{peak} = **2.2 - 3.6** % at 1 MeV
  Ω ~ 15 - 25%
- Annealing kit (heater and thermometer)
- LN2 filled by an automatic supplyer (1-2 times /day)

● BGO counters

--- Background in Ge spectrum ---

- Compton
- π^0 ($\Lambda \rightarrow n\pi^0$)
- high-energy charged particles (π, μ, p)

can be rejected with BGO counters

- n, n-induced γ

--- Structure ---

- rather thin BGO (19 mm *t* x 150 mm *l*) (made in China)
- wide opening

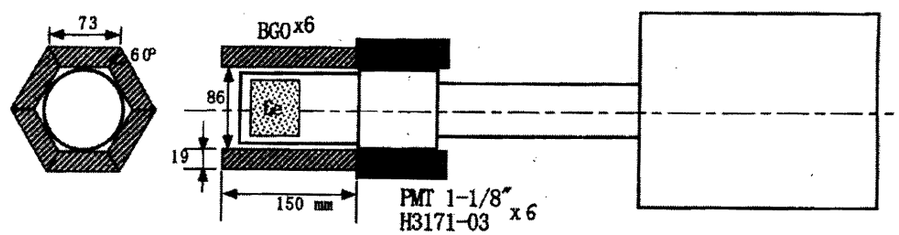

--- Performances ---

- $\Delta E \sim$ 20-25% FWHM at 662 keV
- $\Delta t \sim$ 6ns FWHM at 1MeV (discri.thres. < 1 photon p.h.)
- Suppression Factor > 3 for ~1 MeV γ Compon
  >10 for high-energy γ from π^0

● Readout electronics

- **Low-gain Transistor Reset Preamp.**
  Possible lowest C_F : reset level ~150 MeV [output ~30mV/MeV]
  Reset time <5 μs (normally ~30 MeV)
- **Fast shaping amp. + Gated integrator**
  ORTEC973U (Ultra-High-Rate Amp.)
  Pile-up time = Integration time(3μs) x 2,
  Resolution 2.2 -> 2.6 keV

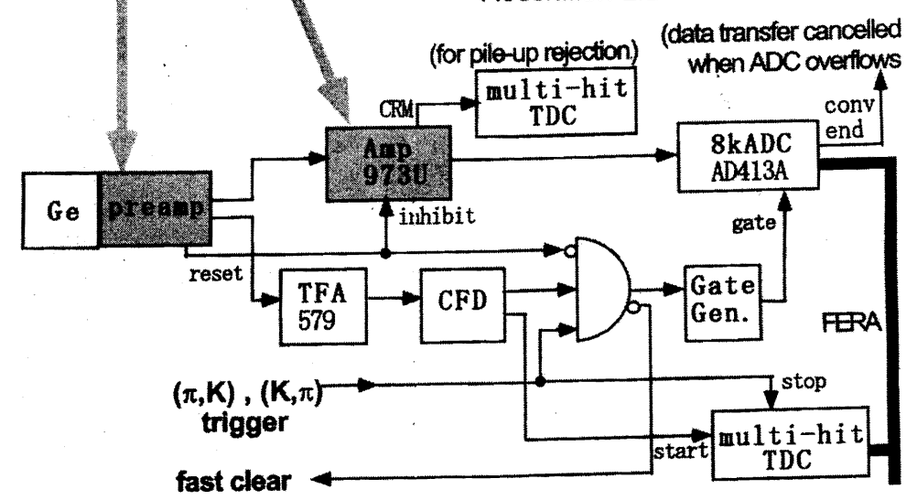

Dead time = 6 μs x 50 kHz + 20 μs x 10 kHz
(Pile-up: 6 μs x 50 kHz; Reset + s-amp overload recovery: 20 μs x 10 kHz)
= 30% + 20% = 50%

Trigger rate ~ 200 /spill(1 sec) X 1-2 k words in total
...no problem in DAQ

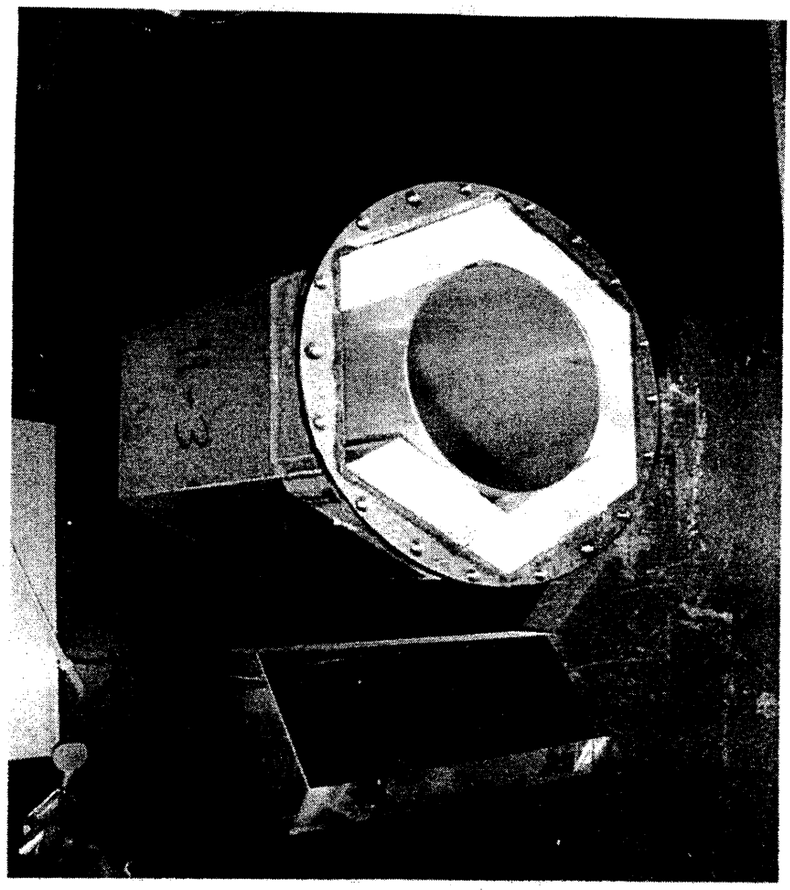

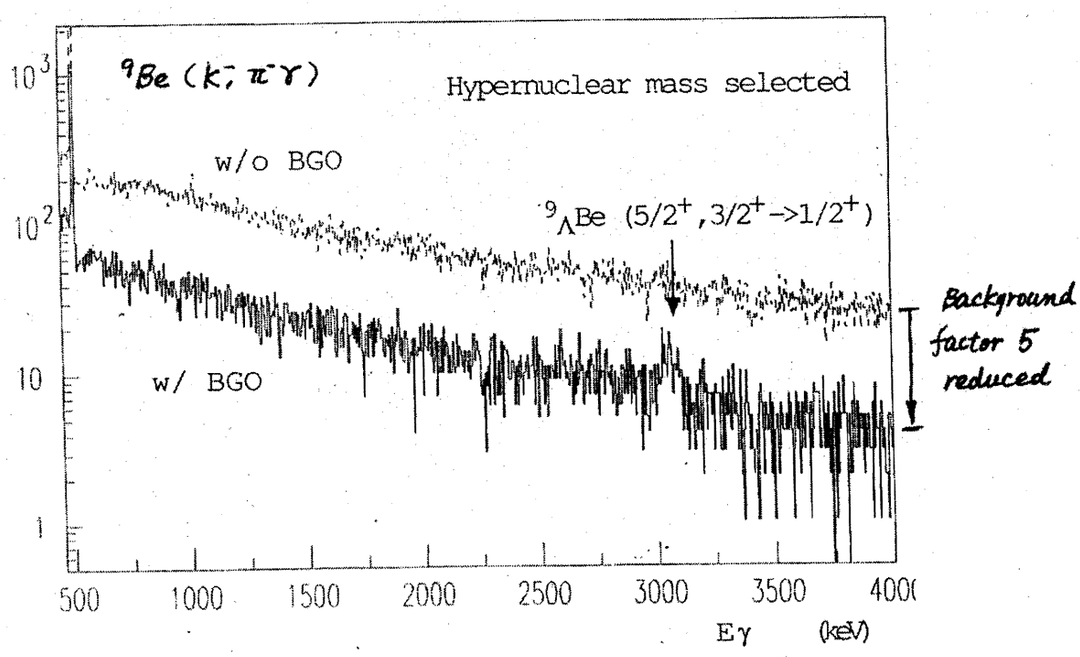
^{9}Be (K$^-$, $\pi^-\gamma$)
Hypernuclear mass selected
w/o BGO
$^9_\Lambda$Be (5/2$^+$, 3/2$^+$ ->1/2$^+$)
w/ BGO
Background factor 5 reduced
10^3
10^2
10
1
500
1000
1500
2000
2500
3000
3500
4000
Eγ (keV)

●*Ge monitoring system*

--- What to be monitored ---

- Live time ratio (in-beam /off-beam)
- Resolution in-beam
- Peak shift
- Radiation damage (<- off-beam peak shape)
- Crystal temperature (<- reset rate)

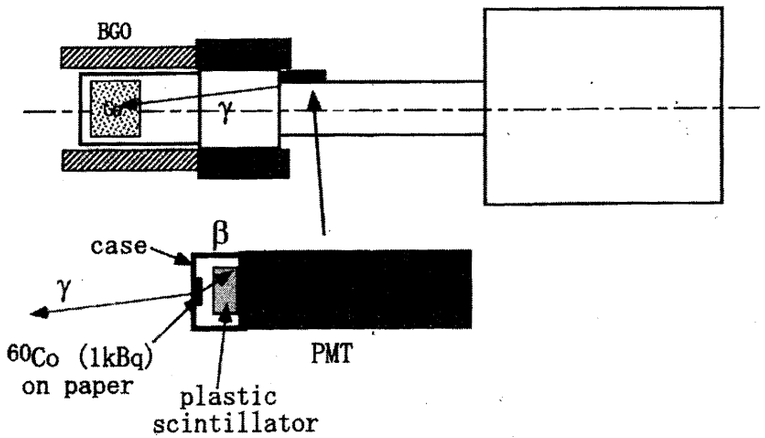

--- Method ---

- ^{60}Co+plastic β–γ pulser
  installed behind ***each*** Ge detector
- Take ADC, TDC, scalers for single rate and reset rate using ***independent DAQ*** with "pulser x Ge" trigger

---> Successfully monitored performance of each Ge all through the beam time

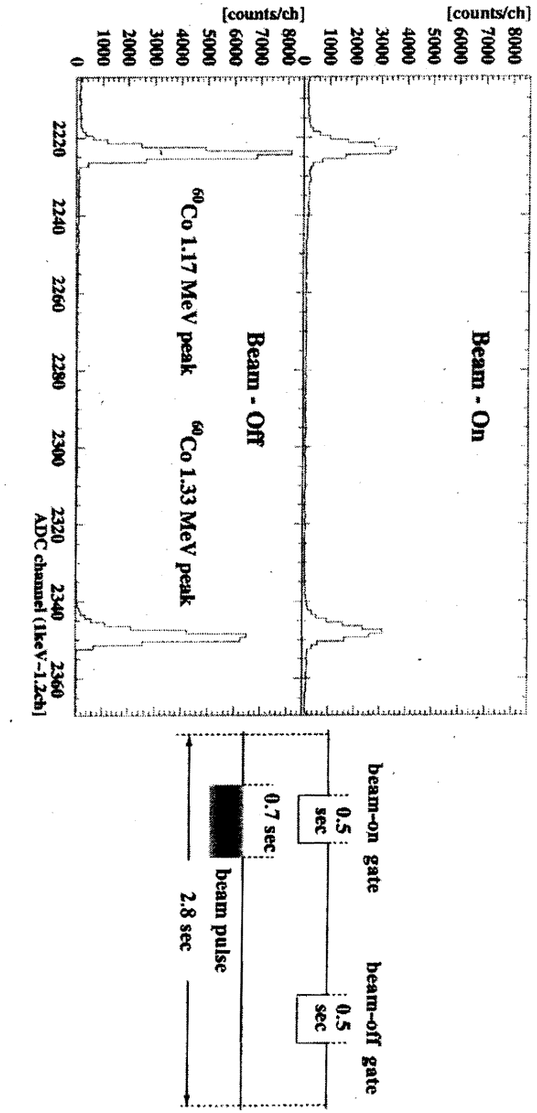

モニターシステムで測定された
ビームオン/オフ時の ^{60}Co ピーク

KEK-PS E419 collaboration

Tohoku Univ.
H. Tamura, O. Hashimoto, T. Takahashi, Y. Fujii, Y. Sato, T. Endo, S. Satoh, T. Miyoshi, A. Nishida, J. Sasao, K. Ozawa, D. Abe, T. Saito

Univ. Tokyo
K. Tanida, H. Hotchi

Kyoto Univ.
K. Imai, H. Akikawa, T. Murakami

KEK
T. Fukuda, T. Nagae, H. Noumi, H. Outa, Y. Kakiguchi, M. Sekimoto

CIAE
S. Zhou, X. Haihong, L. Zhu

Seoul Univ.
Y. Kim, J. Kim, H. Bhang

Hampton Univ.
L. Tang

North Carolina A&T Univ.
R. Sawafta

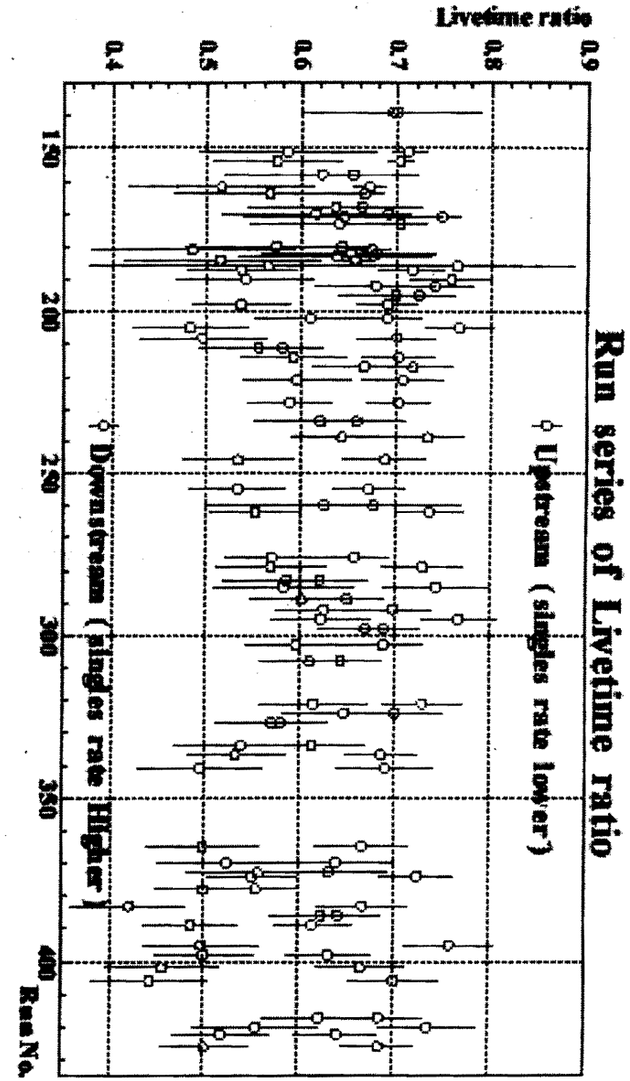

Ge検出器のビームオン/オフの相対検出効率の実験期間中の推移

BNL-AGS E930 collaboration (1998 run)

Tohoku Univ.
H. Tamura, J. Sasao

Kyoto Univ.
H. Akikawa, K. Imai

Univ. Tokyo
K. Tanida, J. Nakano, T. Tamagawa

BNL
M. May, A. Rusek, P.H. Pile, R.E. Chrien

Carnegie Mellon Univ.
G.B. Franklin, P.B. Quinn, R.A. Schumacher, P. Eugenio

Hampton Univ.
L. Tang, L. Gan, L. Yuan

CIAE
X.F. Zhu

Osaka Univ.
S. Ajimura

KEK
T. Fukuda

North Carolina A&T Univ.
R.I. Sawafta

Univ. of Feiburg
J.Franz, H.Schmitt

KEK-PS E419 setup

$\pi^+ n \rightarrow \Lambda K^+$

^{7}Li (π^+, $K^+\gamma$)

'98 May-June
~600 hours

Ge performances
- resolution ~3 keV FWHM at 1.3MeV
- deadtime 30~50%
- peak shift (on/off beam) < 1 keV

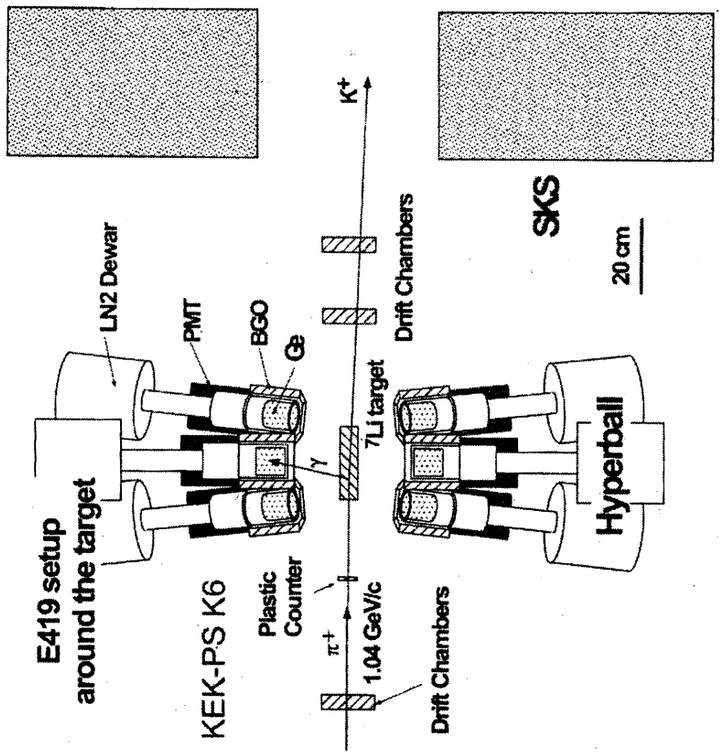

Summary of Hypernuclear γ-Ray Spectroscopy

November, 2001

		Hypernuclear Fine Structure	B(E2)
$^{7}_{\Lambda}$Li KEK,1998	$3/2^+$-$1/2^+$	$691.7 \pm 0.6 \pm 1.0$ keV -> spin-spin force *PRL 84 (2000) 5963*	$3.6 \pm 0.5 \pm^{0.5}_{0.4}$ e^2fm^4 ->19 ± 4% shrinkage *PRL 86 (2001) 1982*
$^{9}_{\Lambda}$Be BNL,1998	$3/2^+$-$5/2^+$	$31 \pm^{2.5}_{3.6}$ keV -> Λ-LS force *submitted to PRL*	$5.7 \pm^{2.1}_{2.0}$ e^2fm^4
$^{15}_{\Lambda}$N	$3/2^+$-$1/2^+$	-> tensor force	under analysis
$^{16}_{\Lambda}$O	0^--1^-	-> tensor force	
$^{10}_{\Lambda}$B BNL,2001	2^--1^-	-> spin-spin, Λ-LS force	

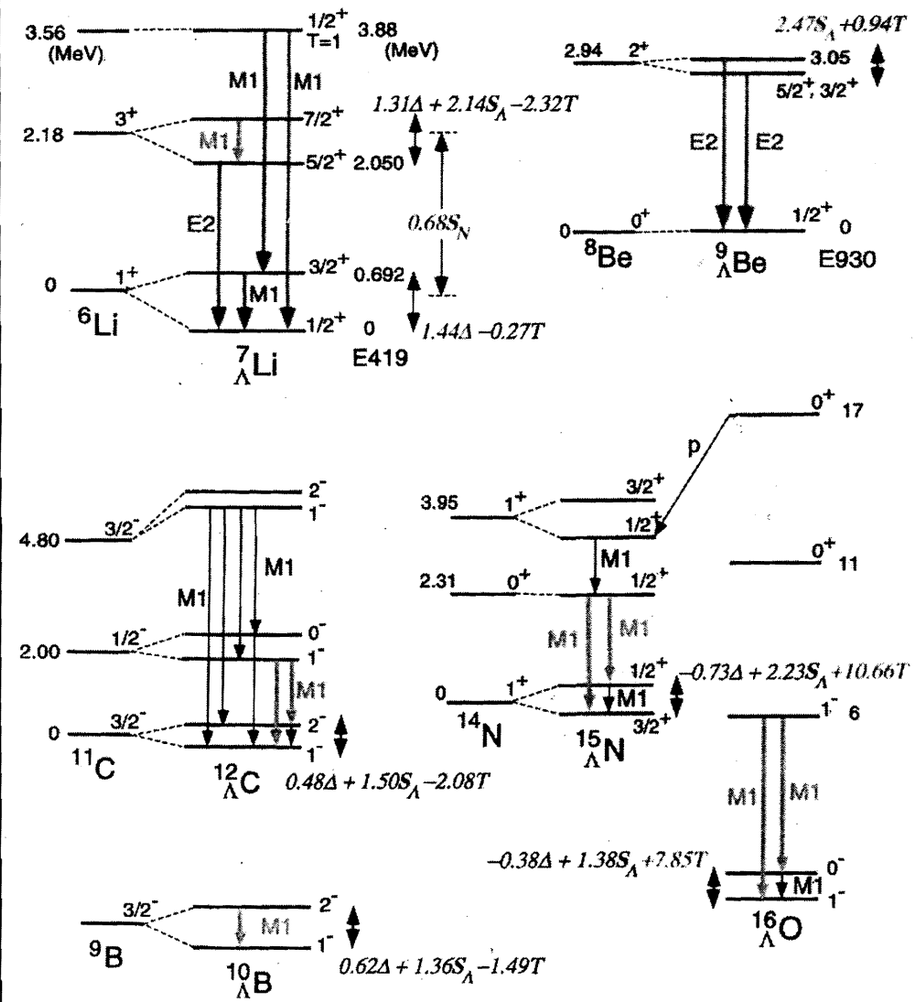

Hypernuclear γ Transitions to Study ΛN Interactions

Already observed (E419,E930) — To be observed (Important transitions) — Hopefully observed

"Hypernuclear Fine Structure"

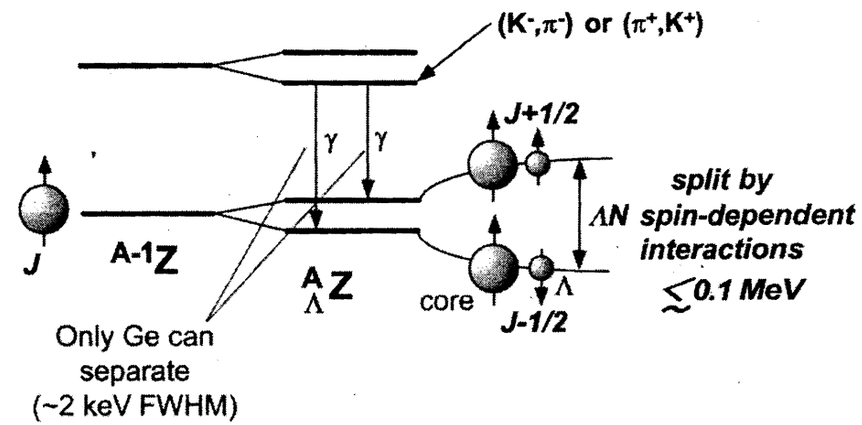

ΛN spin-dependent interactions

--- almost unknown -- No scattering data

$$V^{eff}_{\Lambda N} = V_0(r) + \boxed{\overset{\Delta}{V_\sigma(r)}\,\vec{s}_\Lambda \vec{s}_N + \overset{S_\Lambda}{V_\Lambda(r)}\,\vec{l}_{\Lambda N}\vec{s}_\Lambda + \underset{S_N}{V_N(r)}\,\vec{l}_{\Lambda N}\vec{s}_N + \underset{T}{V_\Lambda(r)}\,S_{12}}$$

p-shell :
4 radial integrals for $p_N\, s_\Lambda$ w.f.

Dalitz and Gal, Ann. Phys. 116 (1978) 167
Millener et al., Phys. Rev. C31 (1985) 499

KEK E419

Results of $^{7}_{\Lambda}$Li γ Spectroscopy

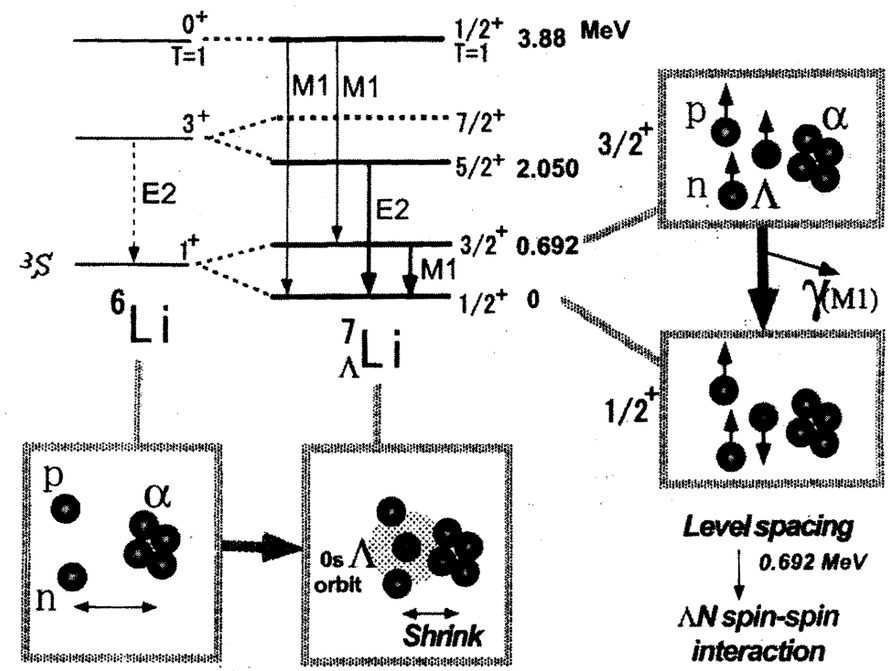

Level spacing

↓ *0.692 MeV*

ΛN spin-spin interaction

Δ ~ 0.50 MeV

PRL 84 (2000) 5963

B(E2) : 10.9± 0.9 ⟶ 3.6± 0.5± $^{0.5}_{0.4}$ [e²fm⁴]

19± 4% Shrinkage by Λ ~~Submitted to~~ Accepted PRL 86 (2001) 1982

— "glue-like role of Λ"

Bando, Motoba, Ikeda; Hiyama et al.

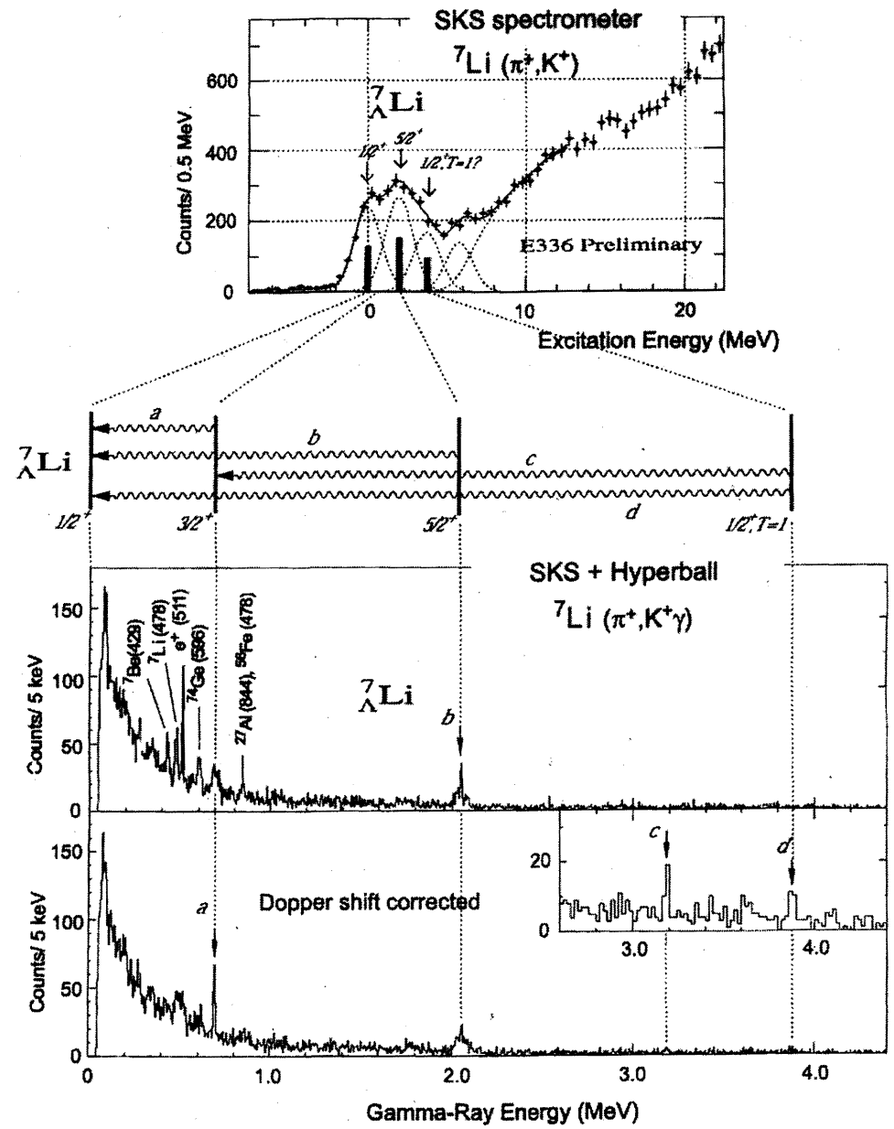

Lifetime Measurement using Dopper Shift Attenuation Method

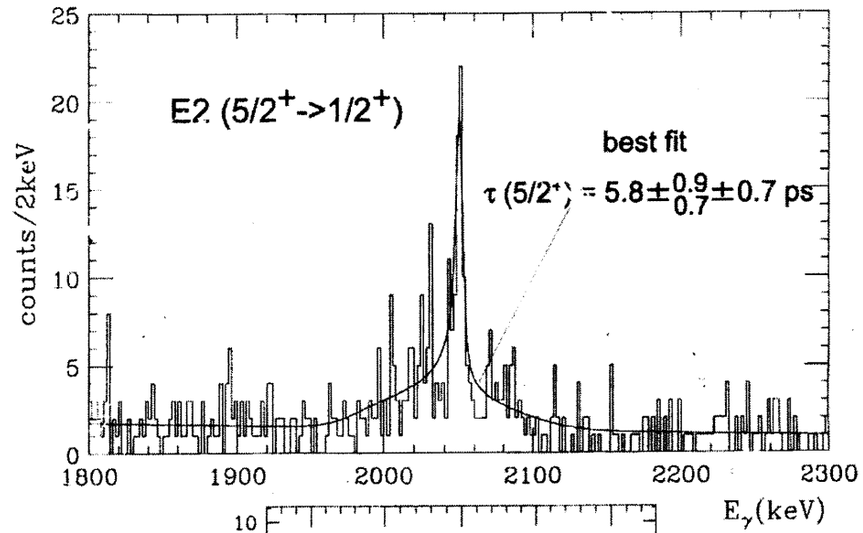

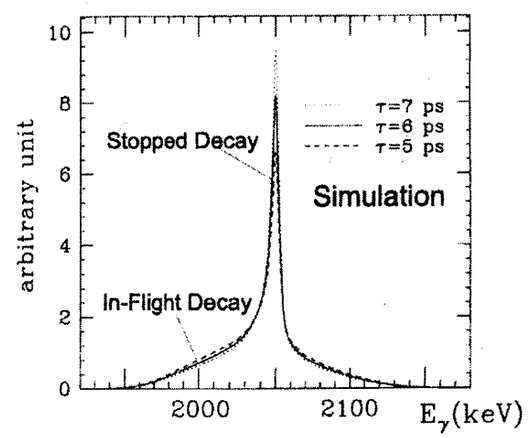

$\Gamma(E2;\ 5/2^+ \to 1/2^+) = BR / \tau(5/2^+) = 1.22 \times 10^9\ E^5\ B(E2)$

$BR = 93.6 \pm^{3.8}_{0.6}\ \%$

[weak decay $(230 \pm 40\ ps)^{-1}$, $BR(5/2^+ \to 3/2^+) = 3.8 \pm^{0.5}_{3.8}\%$]

$\Rightarrow\ B(E2) = 3.6 \pm 0.5 \pm^{0.5}_{0.4}\ e^2 fm^4$

Interpretation of the measured B(E2)

$B(E2;\ j_i \to j_f) \propto |\langle j_f | r^2 Y_2 | j_i \rangle|^2$

$\propto R^4$ — cluster model

or

$\propto (\beta \langle r^2 \rangle)^2$ — deformation

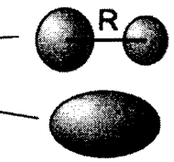

Size Factor

$$\sqrt[4]{\frac{9}{7}\,\frac{B(E2;\ {}^7_\Lambda Li:\ 5/2^+ \to 1/2^+)}{B(E2;\ {}^6Li:\ 3^+ \to 1^+)}}$$

$$= \frac{R_{\alpha\text{-}d}({}^7_\Lambda Li)}{R_{\alpha\text{-}d}({}^6Li)}\quad [1]$$

in cluster model

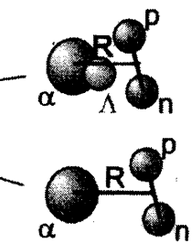

	$B(E2;\ {}^7_\Lambda Li)$	$B(E2;\ {}^6Li)$	Size Factor
Exp.	$3.6 \pm 0.5 \pm^{0.5}_{0.4}$	10.9 ± 0.9	0.81 ± 0.04
			significant shrinkage observed
Motoba, Bando, Ikeda ('83)	"glue-like role of Λ"		
α-d-Λ cluster model	2.5	6.6	0.84
Hiyama et al. ('99)			
${}^5_\Lambda$He-p-n cluster model	2.42	9.62	0.75
α-p-n-Λ cluster model	2.9	10.0	0.78

Showed that shrinkage takes place between α and p-n center, and [1] is still valid when d -> p n.

Our result : $19 \pm 4\%$ shrinkage of the α - (pn) distance

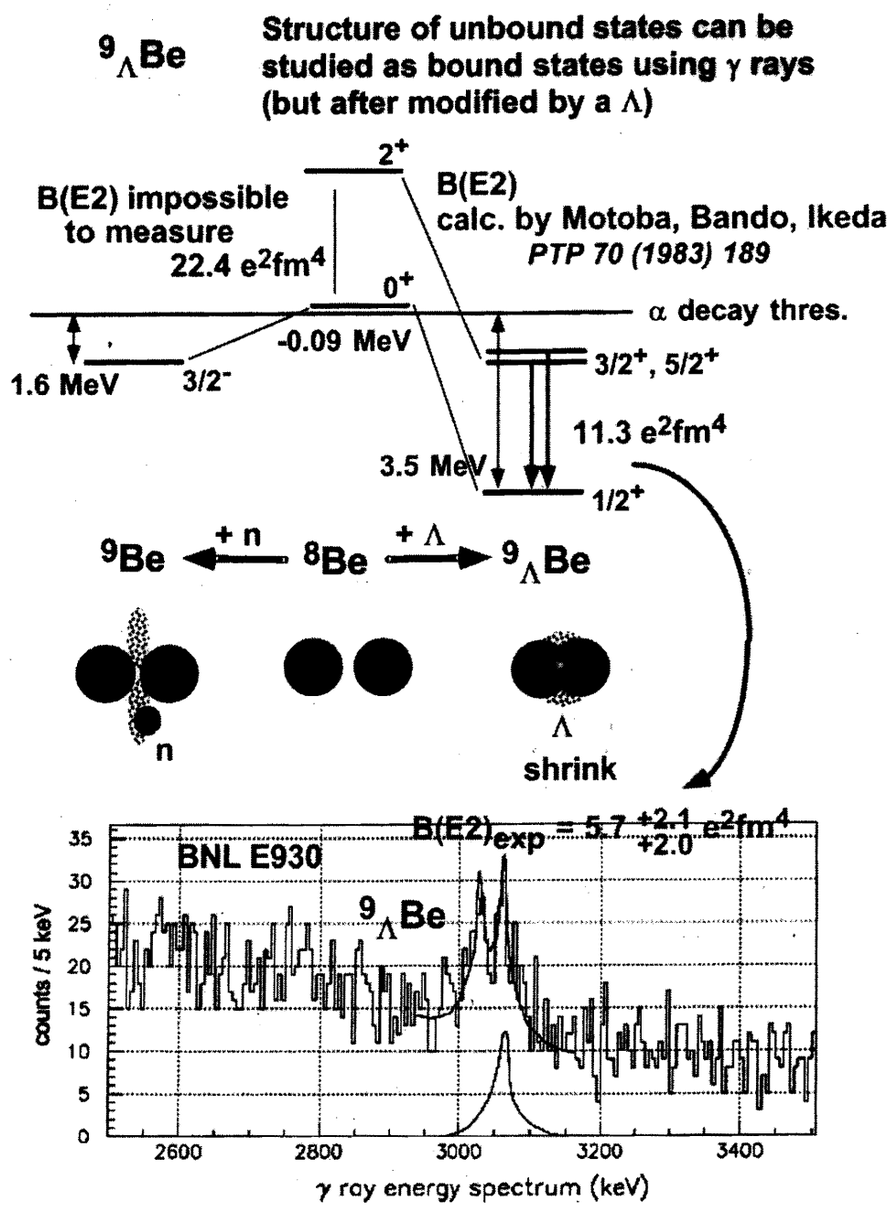

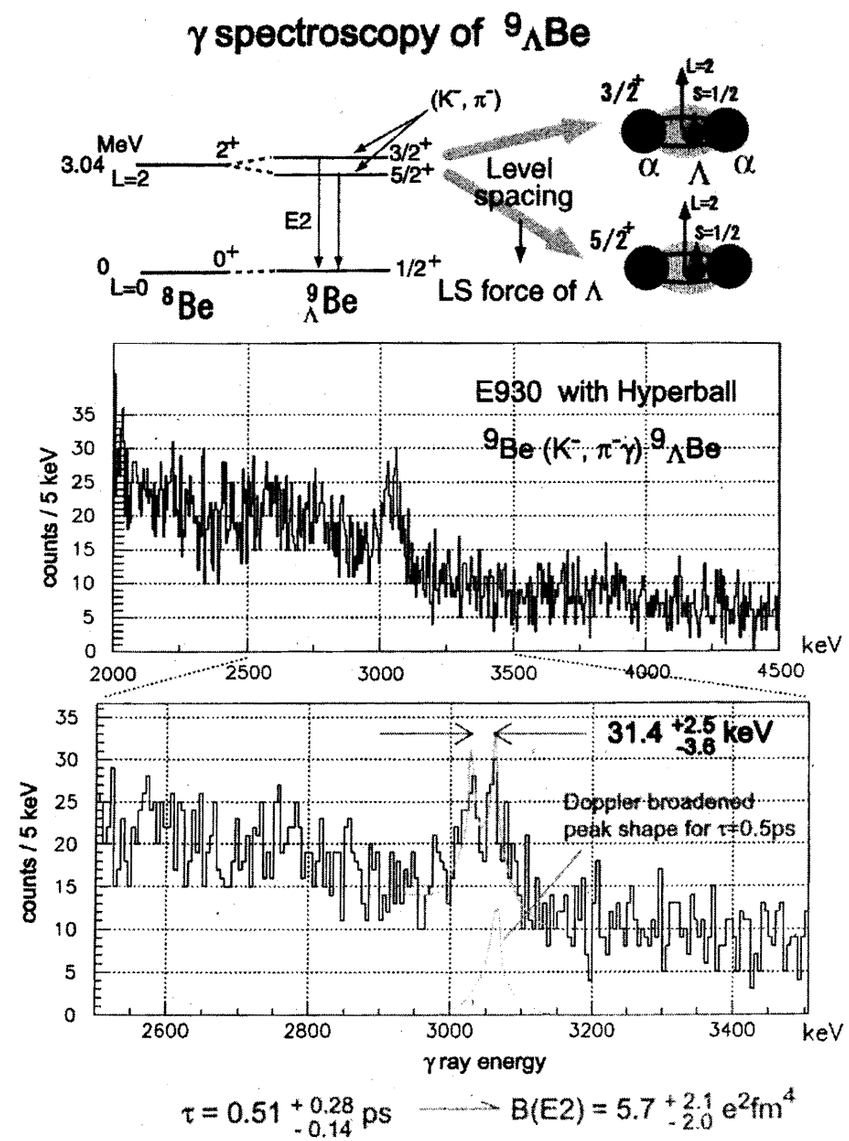

Submitted to PRL

Near Future Plan (2002–)

Double the Ge efficiency
by combining with 6 clover Ge detectors (TRP)
in Tohoku Cyclotron

Upgraded Hyperball

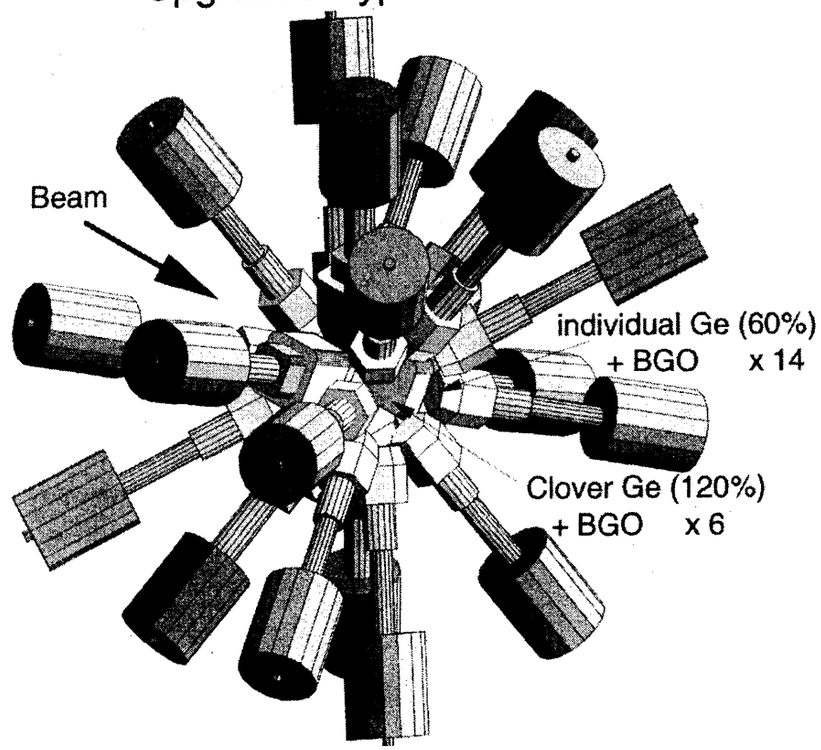

The observed splitting

$|E(3/2)-E(5/2)| = 31.4\ ^{+2.5}_{-3.6}$ keV

- Millener *[NPA 691 (2001) 93c]*

  $E(3/2)-E(5/2) = -0.035\,\Delta - 2.465\,S_\Lambda + 0.936\,T$

  => $-0.02 < S_\Lambda < 0.03$ MeV

  if $0 < T < 0.06$ MeV (OBE predistions)

  ($\Delta = 0.62$ scaled from $^7{}_\Lambda$Li)

  OBE predections: $S_\Lambda = 0.4$ --1.0 MeV

- Hiyama et al. *[PRL 85 (2000) 270]*

  ααΛ cluster model

  ΛN interactions from

  - OBE models (NSC971-f, ND, NF) :

    E(3/2)-E(5/2) = 80 -- 200 keV

  - Small LS force eqv. to quark model prediction :

    ~ 40 keV

Consistent with $^{13}{}_\Lambda$C result *[PRL 85 (2001) 4255]*

($p^\Lambda_{1/2}-p^\Lambda_{3/2}$ = 152±54±36 keV)

Conclusions

- Λ LS force: Much smaller than expected from OBE models

- $|S_N| >> |S_\Lambda|$ [$\boldsymbol{l}_{\Lambda N}\boldsymbol{s}_N$ term >> $\boldsymbol{l}_{\Lambda N}\boldsymbol{s}_\Lambda$ term]

  $S_N \sim -0.4$ MeV from $^7{}_\Lambda$Li, $^{12}{}_\Lambda$C, etc: Millener

  => ALS [$\boldsymbol{l}_{\Lambda N}(\boldsymbol{s}_\Lambda - \boldsymbol{s}_N)$] cancels with SLS [$\boldsymbol{l}_{\Lambda N}(\boldsymbol{s}_\Lambda + \boldsymbol{s}_N)$]

Far Future Plan (2006–)

JHF: High intensity 50 GeV proton synchrotron (Tokai)

K^- intensity $\sim$ 5–10× BNL-AGS, > 100× KEK-PS.

Hyperball for JHF

- Highest efficiency Ge array (> 10% at 1 MeV)
- Faster electronics
  - Read waveform data to decompose pileup events (waveform digitizer under development)
- Faster suppression counters : BGO → GSO

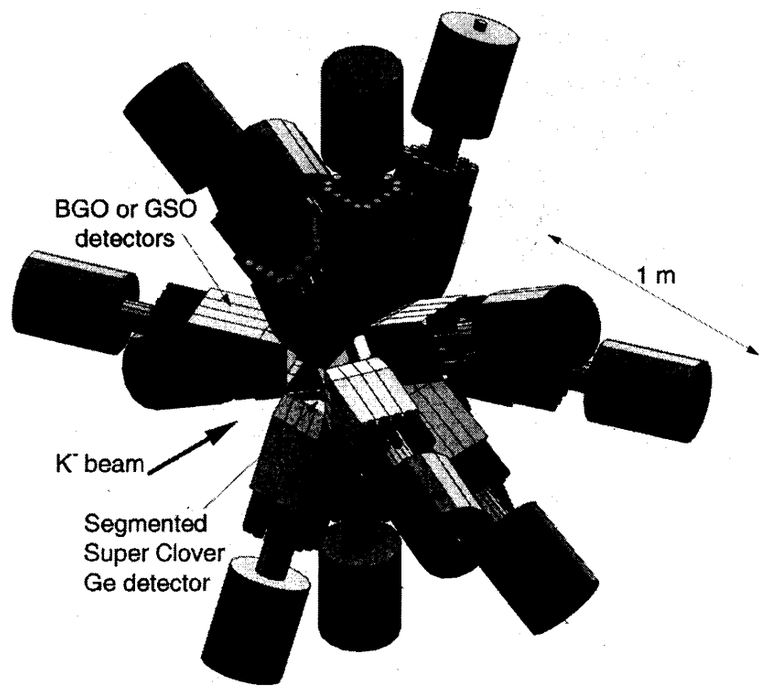

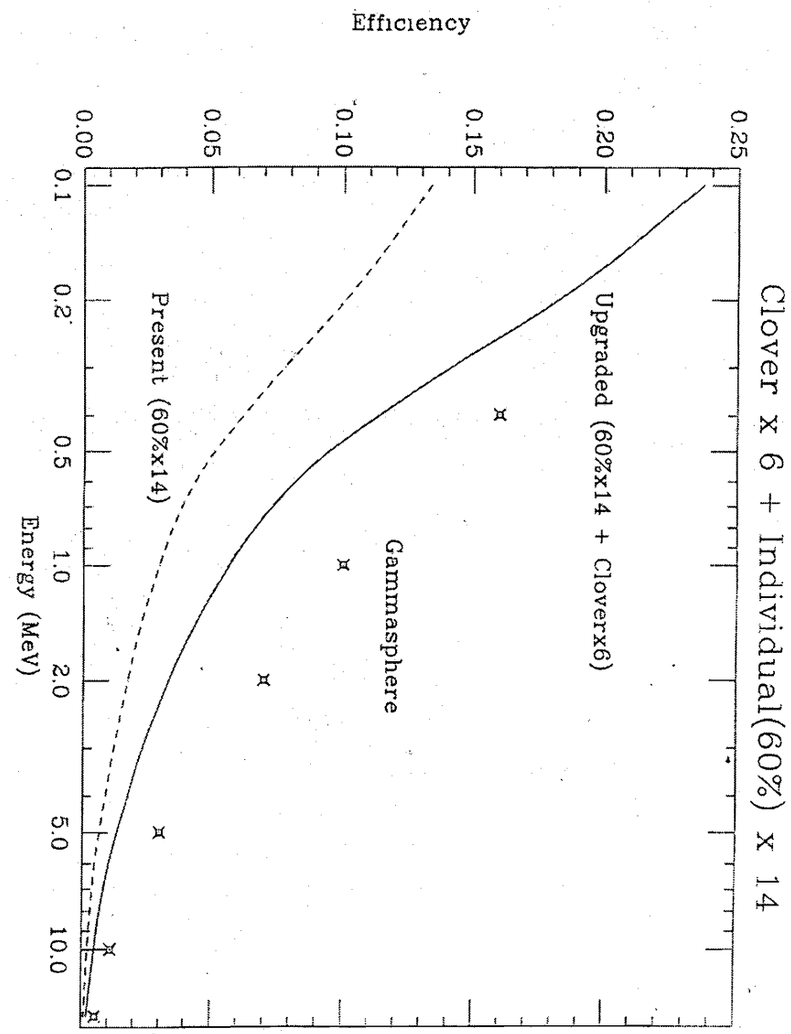

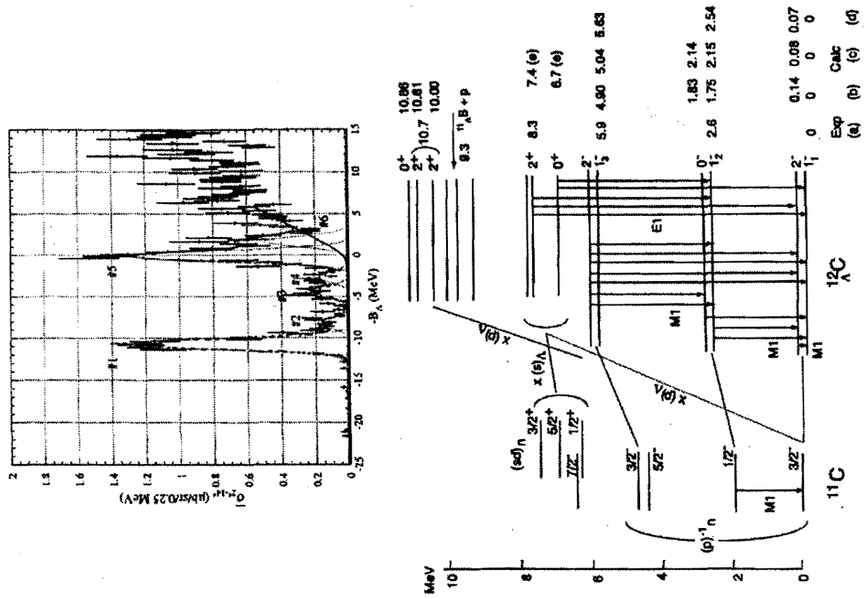

Figure 26: Top: $^{12}_{\Lambda}$C spectrum measured by the (π^+, K^+) reaction (KEK E369) [15]. The peaks #1, #2, #3, #4 are interpreted as 1^-_1, 1^-_2, 1^-_3, and 2^+_1 states. Bottom: Level scheme and expected γ transitions of $^{12}_{\Lambda}$C hypernucleus. (a) shows experimental level energies (E369), and (b), (c), (d) are calculated energies by Itonaga *et al.* [18], Fetisov *et al.* [21], and Millener *et al.* [19], respectively.

58

direct reactions

- ☐ (K^-, π^-), (π^+, K^+) n -> Λ
- ☐ (K^-, π^0), (π^-, K^0), (e, e'K^+) p -> Λ
- ☐ (K^-, π^+) pp -> Λn
- ☐ (π^+, K^0) nn -> Λp

Experimentally known bound hypernuclei (B_Λ known)

Should be bound

Critically bound or unbound ?

		— $^{8}_{\Lambda}$B	— $^{9}_{\Lambda}$B	^{9}B $^{10}_{\Lambda}$B	^{10}B $^{11}_{\Lambda}$B	^{11}B $^{12}_{\Lambda}$B	^{12}B $^{13}_{\Lambda}$B	^{13}B $^{14}_{\Lambda}$B	^{14}B $^{15}_{\Lambda}$B	^{15}B $^{16}_{\Lambda}$B	^{16}B $^{17}_{\Lambda}$B	^{17}B $^{18}_{\Lambda}$B
	— $^{6}_{\Lambda}$Be	— $^{7}_{\Lambda}$Be	^{7}Be $^{8}_{\Lambda}$Be	— $^{9}_{\Lambda}$Be	^{9}Be $^{10}_{\Lambda}$Be	^{10}Be $^{11}_{\Lambda}$Be	^{11}Be $^{12}_{\Lambda}$Be	^{12}Be $^{13}_{\Lambda}$Be	— $^{14}_{\Lambda}$Be	^{14}Be $^{15}_{\Lambda}$Be	— $^{16}_{\Lambda}$Be	
		— —	^{6}Li $^{7}_{\Lambda}$Li	^{7}Li $^{8}_{\Lambda}$Li	^{8}Li $^{9}_{\Lambda}$Li	^{9}Li $^{10}_{\Lambda}$Li	— $^{11}_{\Lambda}$Li	^{11}Li $^{12}_{\Lambda}$Li	— $^{13}_{\Lambda}$Li			
— —	^{3}He $^{4}_{\Lambda}$He	^{4}He $^{5}_{\Lambda}$He	— $^{6}_{\Lambda}$He	^{6}He $^{7}_{\Lambda}$He	— $^{8}_{\Lambda}$He	^{8}He $^{9}_{\Lambda}$He	— $^{10}_{\Lambda}$He	— $^{11}_{\Lambda}$He				
^{1}H —	^{2}H $^{3}_{\Lambda}$H	^{3}H $^{4}_{\Lambda}$H	— $^{5}_{\Lambda}$H	— $^{6}_{\Lambda}$H								
Λ												

Z ↑ N →

Λ Hypernuclear Chart

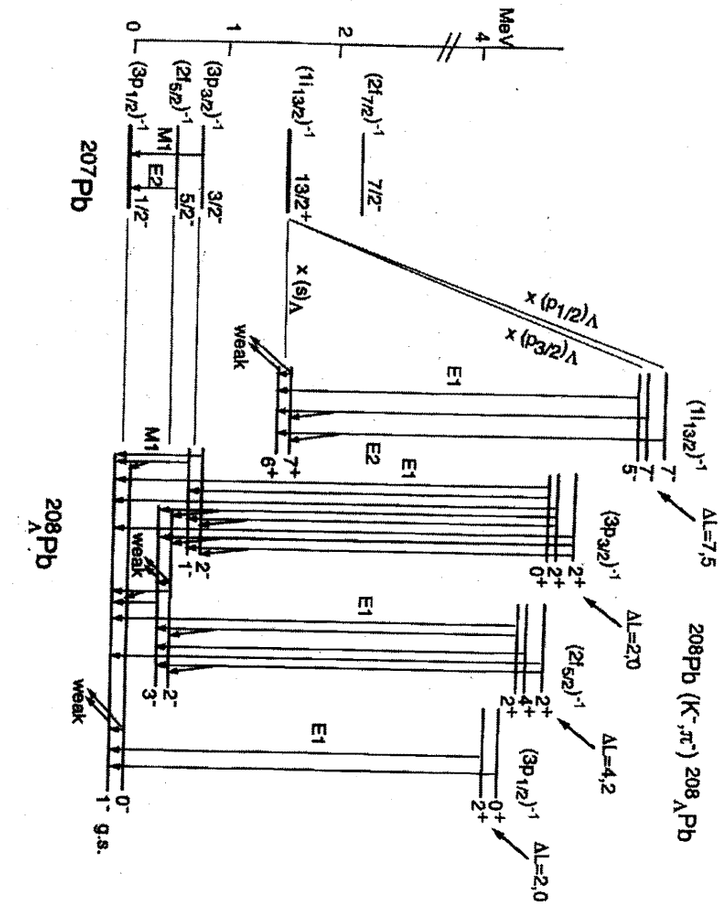

Figure 27: Expected level scheme and γ transitions of $^{208}_{\Lambda}$Pb. Only the non-spin-flip states are shown for the p_Λ states.

Summary

- We opened a new field
  "Hypernuclear γ spectroscopy"

- Hyperball
  - Fast electronics, BGO for π^0 background
  - Monitoring system

- "Hypernuclear fine structure" gave
  ΛN spin-dependent interactions.
  - Spin-spin force: established from $^{7}_{\Lambda}$Li .
  - Λ-LS force: very small from $^{9}_{\Lambda}$Be.
    suggesting quark mechanism?
  - Tensor force: to be obtained from $^{15}_{\Lambda}$N / $^{16}_{\Lambda}$O.
- B(E2) measured for $^{7}_{\Lambda}$Li, $^{9}_{\Lambda}$Be
  Shrinking effect by Λ

- Upgrade soon by x2
- Need to develop a new, faster, larger Ge array for JHF

Ge-Telescope and Compton camera

Y.Gono[1], S.Motomura[1], Q.Y.Pan[1,2,3], Y.F.Yang[2], S.Enomoto[3], Y.Yano[3] and K.Asahi[3]

1. Department of Physics, Kyushu University, Hakozaki 6-10-1, Higashi-ku, Fukuoka 812-8581, Japan
2. Institute of Modern Physics, Chinese Academy of Science, Lanzhou 730000, China
3. RIKEN, Hirosawa 2-1, Wako-shi, Saitama 351-0198, Japan

In order to correct a sever Doppler shift of a γ-ray energy, a Ge-telescope system was developed. This system was prepared for a high-spin isomer beam experiment [1] where a secondary fusion reaction was made in inverse kinematics. Resulted reaction products were recoiled out of a target with a velocity of 0.1c. The telescope consisted of a segmented Ge and a clover detector placed in this sequence facing to a target. A planar Ge of 20 mm thick was segmented to 25 pixels of 10 x 10 mm^2. Two such segmented Ge's could be used as a Compton camera. This idea was adopted to a multitracer project. A multitracer has been developed in RIKEN for many purposes such as chemistry and biology. A test experiment to identify three source positions simultaneously was successfully made by using these two segmented Ge's.

To improve a position resolution, an optimization was carried out by a computer simulation [2]. A new system was proposed and made by using two strip Ge's placed in one cryostat.

Further improvement is expected in data analysis, namely a γ-ray linear polarization information may be used to reduce back-ground for a γ-ray imaging. Presently a system can be used only to identify source positions, however our goal would be an imaging in a medical use.

References

1. Y. Gono et al., Nucl. Phys. A588 (1995) 241c.
2. Y.F. Yang et al., IEEE trans. Nucl. Sci. 48 (2001) 656.

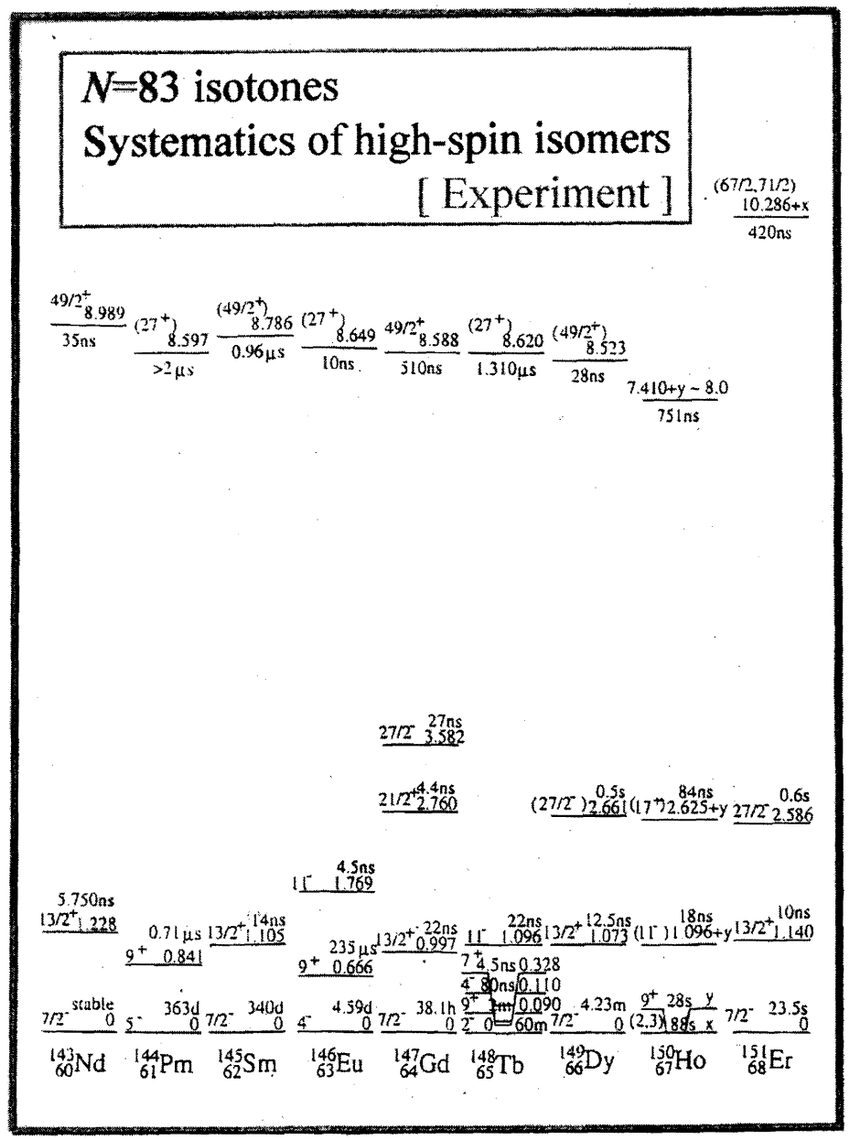

Ge-Telescope and Compton Camera

CNS: Ge-Workshop

December 11-13, 2001

Y. Gono

Kyushu University

Collaborators (Compton camera*)

Kyushu U.: Y.Gono, S.Motomura*, T.Fukuchi, S.Tanaka, M.Inoue, T.Sasaki, Y.Wakabayashi

RIKEN: T.Kishida, H.Watanabe, E.Ideguchi, T.Kubo, M.Ishihara, S.Enomoto*, Y.Yano*, K.Asahi*

Nishinippon Inst. Tech.: A.Odahara

Inst.Modern Phys.: Y.F.Yang*, Q.Y.Pan* (China)

Reactions used to study isomers in N=83 isotones

$^{143}_{60}$Nd: ^{130}Te(^{18}O, 5n)^{143}Nd (Kyushu U. KEK-T, CNS-U.Tokyo)

X.H.Zhou et al., Phys.Rev. C61, 014303 (2000)

$^{144}_{61}$Pm: ^{14}N (^{136}Xe, 6n)^{144}Pm (RIKEN)

^{138}Ba(^{10}B, 4n)^{144}Pm (Tsukuba)

Y.H.Zhang et al., High Ene. Phys. and Nucl.Phys. 21, 110 (1997)

$^{145}_{62}$Sm: ^{16}O (^{136}Xe, 7n)^{145}Sm (RIKEN)

^{138}Ba(^{13}C, 6n)^{145}Sm (JAERI)

^{139}La(^{10}B, 4n)^{145}Sm (Kyushu U.)

A.Odahara et al., Z.Phys. A350, 185 (1994)

Nucl.Phys. A620, 363 (1997)

$^{146}_{63}$Eu: ^{139}La(^{13}C, 6n)^{146}Eu (JAERI)

E.Ideguchi et al., European Phys.J. A6, 387 (1999)

$^{147}_{64}$Gd: ^{20}Ne(^{136}Xe, 9n)^{147}Gd (RIKEN)

$^{148}_{65}$Tb: ^{141}Pr(^{13}C, 6n)^{148}Tb (JAERI)

E.Ideguchi et al. Z.Phys. A352, 363 (1995)

$^{149}_{66}$Dy: ^{141}Pr(^{16}O, p7n)^{149}Dy (CNS U.Tokyo)

T.Fukuchi, Master Thesis of Kyushu U. (2000)

↓

Cyric (Tohoku-U.)

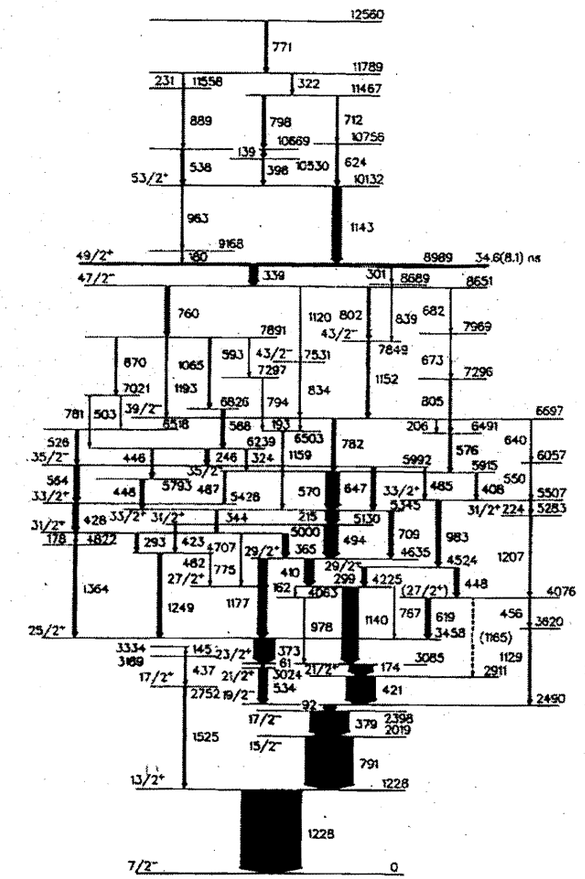

143Nd

X.H.Zhou et al., Phys.Rev.C61, 014303 (2000)

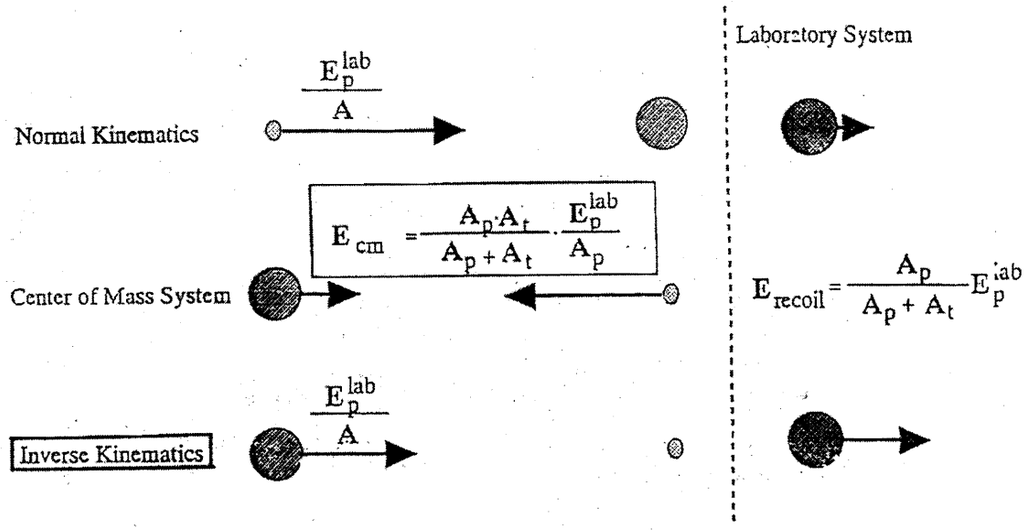

Example

			E_{recoil} (MeV)	(MeV/u)	v/c
$^{136}Xe(^{16}O, 7n)^{145}Sm^*$	$\frac{E_p^{lab}}{A} = 8.0$ MeV/u	$E_O^{lab} = 128$ MeV	13.5	0.8	0.04
$^{16}O(^{136}Xe, 7n)^{145}Sm^*$		$E_{Xe}^{lab} = 1088$ MeV	973.5	7.2	0.12

$E_{cm} = 115$ MeV

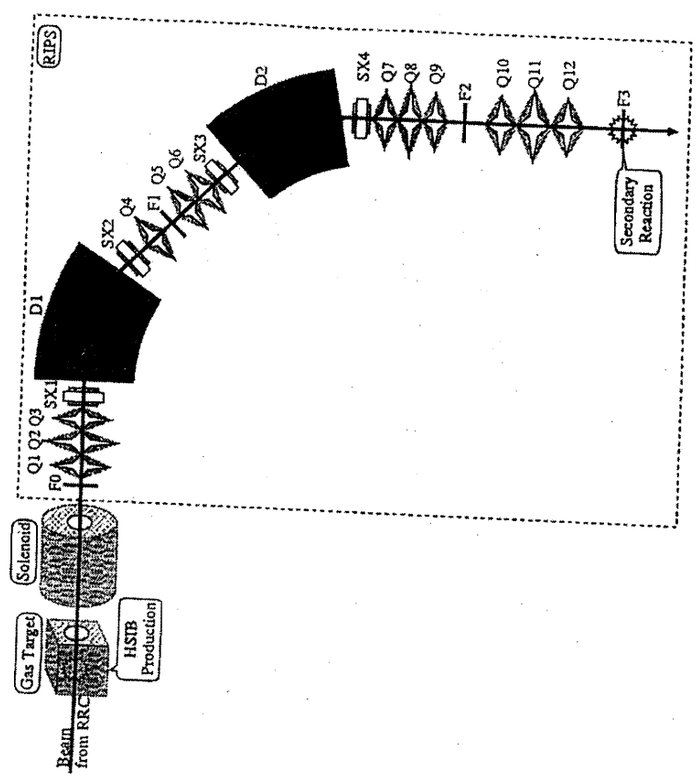

Figure 2.1: Schematic layout of the HSIB beam line mainly consisted of three parts; a windowless gas target, a superconducting solenoid, and the RIPS.

Sagara Gas Target Top View

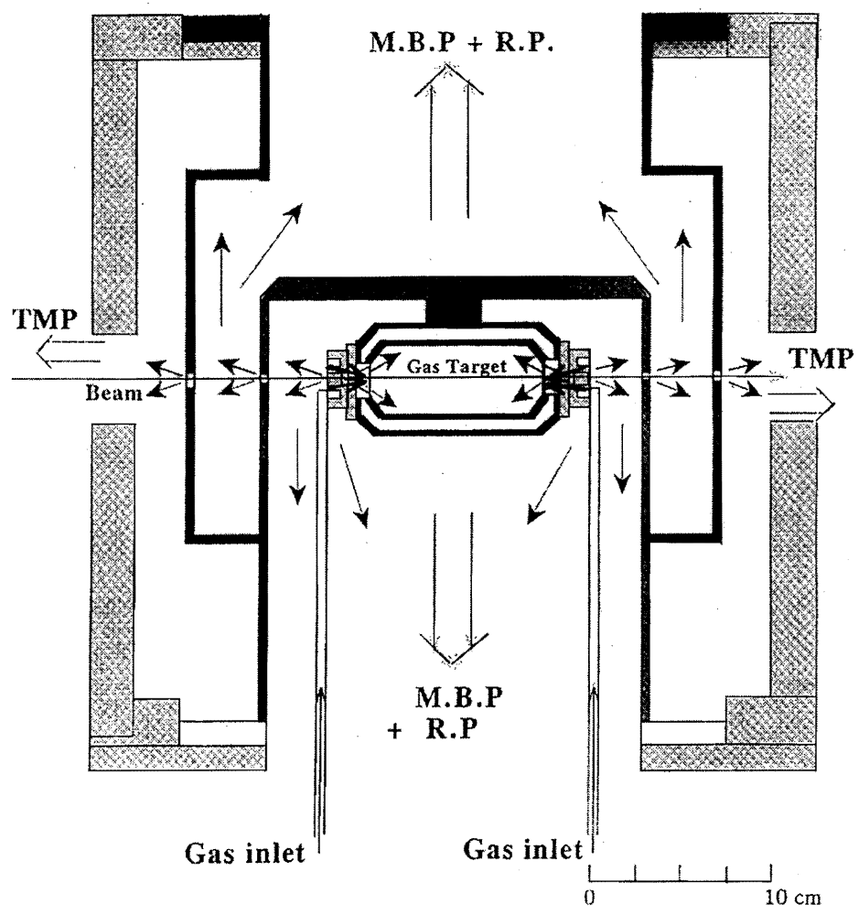

Experimental conditions for 2ndary fusion

Primary reaction: $^{16}O\ (^{136}Xe,\ 7n)^{145m}Sm$

$E_{^{136}Xe} = 7.6$ MeV/u, 70pnA

Primary target: ^{16}O (CO_2 Gas) 0.7 mg/cm^2

Cross section: ~ 500 mb

Yield of ^{145m}Sm : ~ 2×10^6 sec^{-1}

Transport efficiency: ~5 %
(spatial acceptance(50%),
charge state distribution(20%),
Decay in flight(50%)

Secondary beam on target: 1×10^5 sec^{-1}

Experiment performed: $^{13}C + {}^{145m}Sm \longrightarrow$ ~~$^{158}Er + xn$~~ $^{158-x}Er$

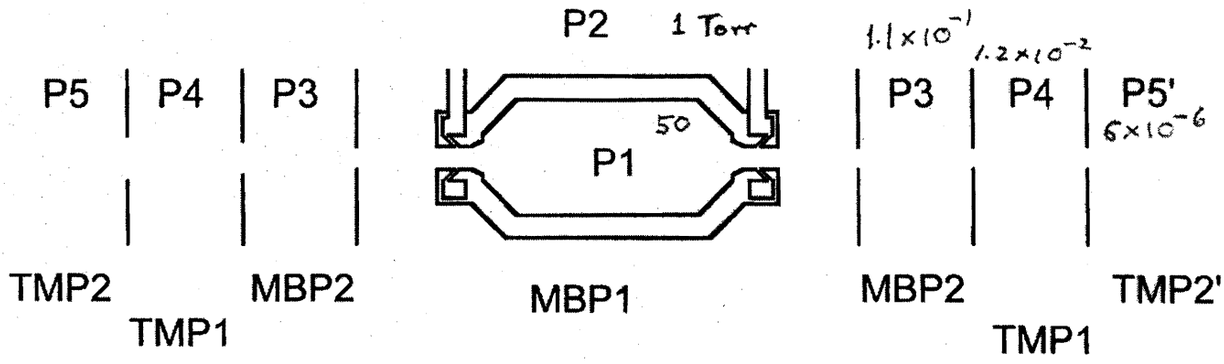

MBP1 :	MB-1400VM	1020 m^3/h
MBP2 :	MB-600FVM	600 m^3/h
TMP1 :	TMP-1500	1450 l/s
TMP2 :	TMP-550	550 l/s

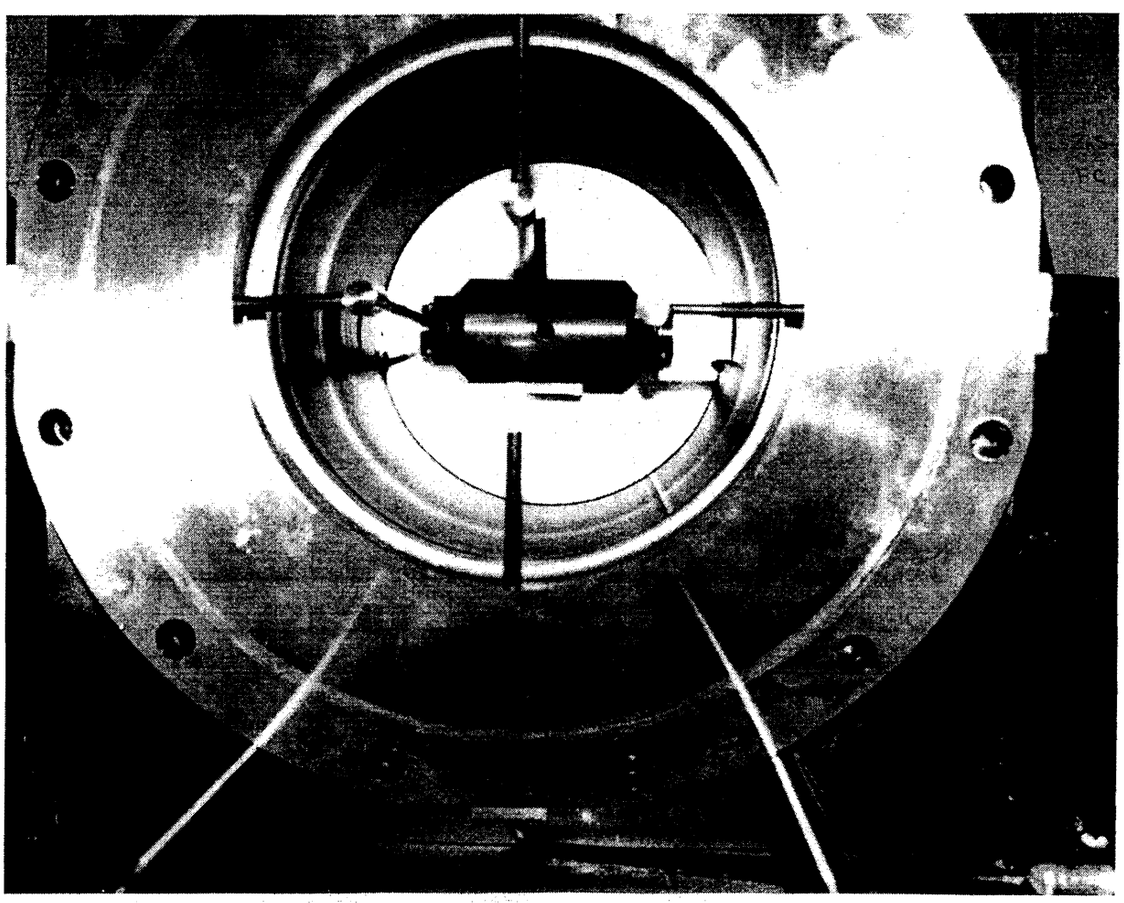

Ge - Telescope

for Position Sensitive γ-Ray Detection

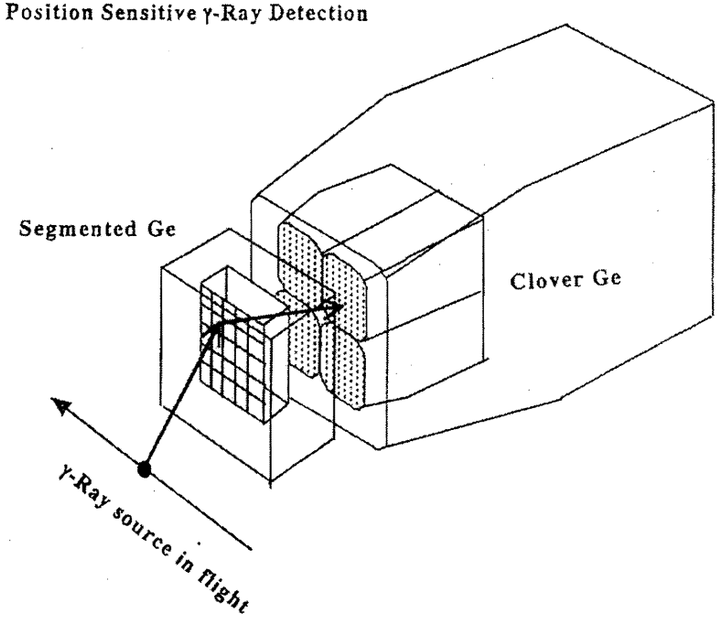

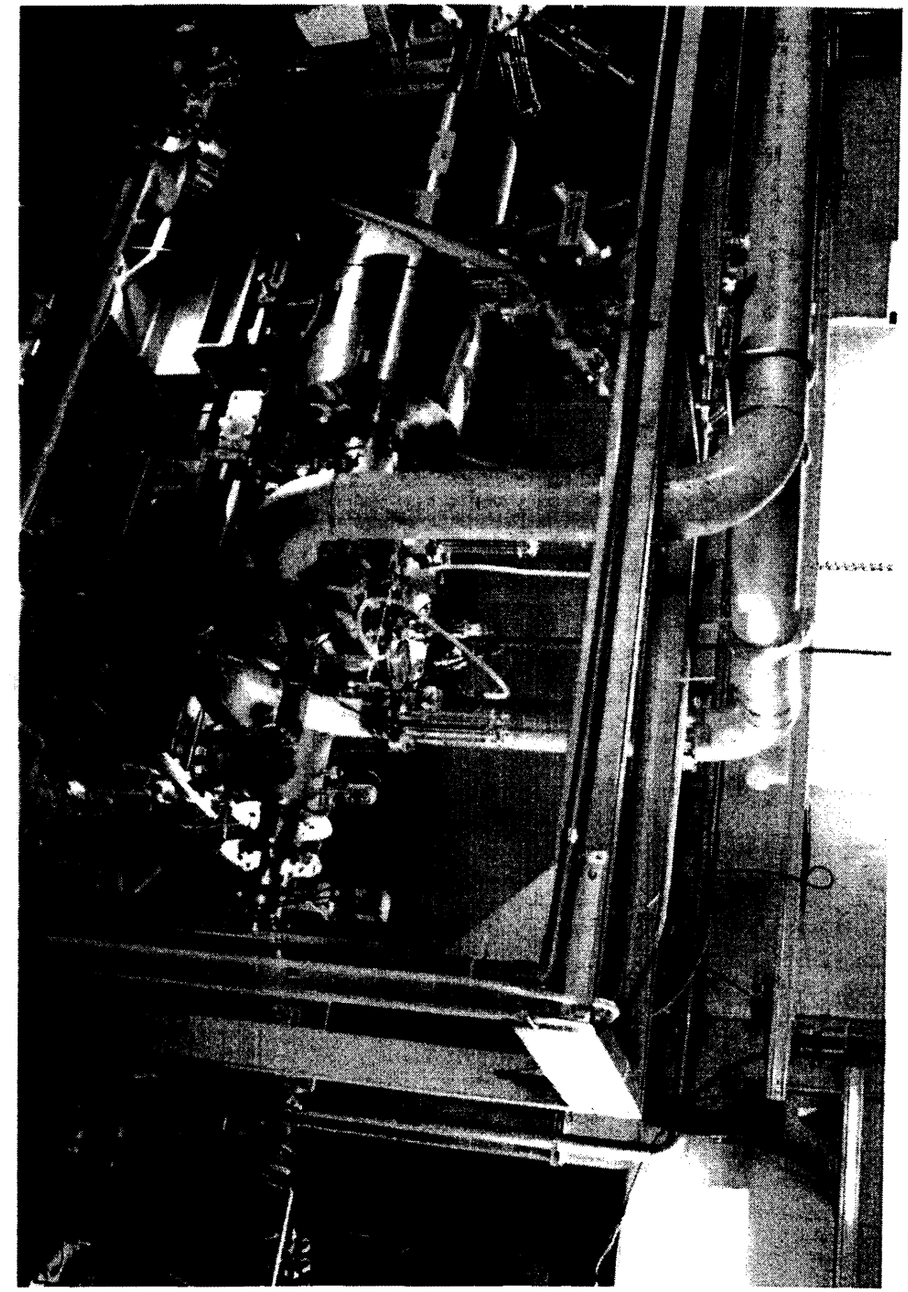

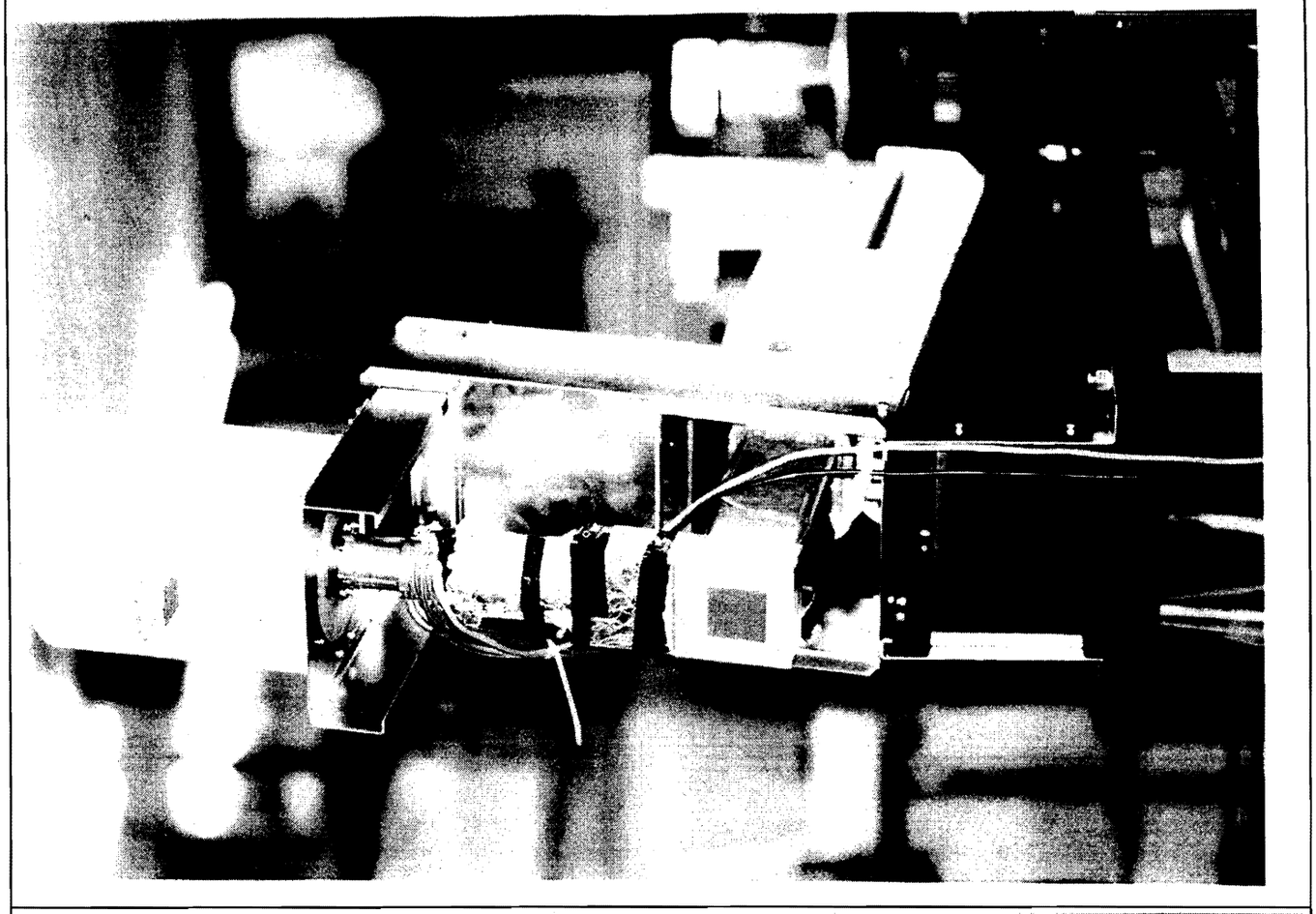

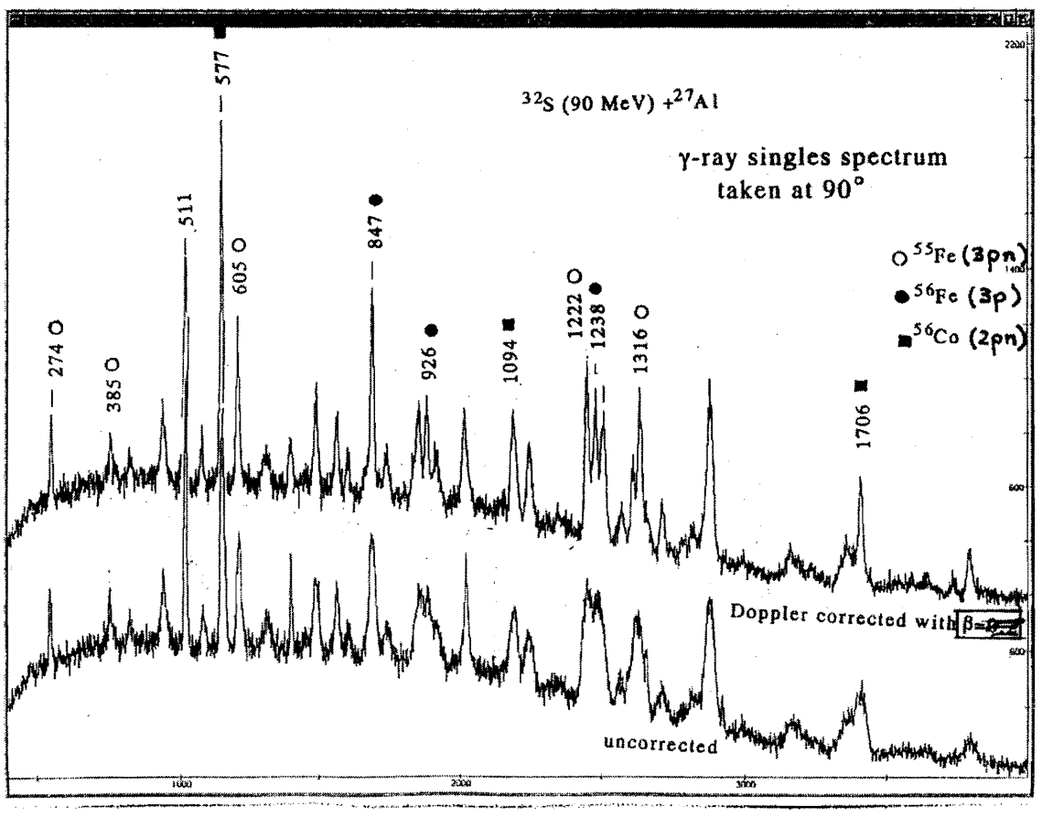
^{32}S (90 MeV) +^{27}Al
γ-ray singles spectrum
taken at 90°
○ ^{55}Fe (3pn)
● ^{56}Fe (3p)
■ ^{56}Co (2pn)
274 ○
385 ○
511
577 ■
605 ○
847 ●
926 ●
1094 ■
1222 ○
1238 ●
1316 ○
1706 ■
Doppler corrected with β=0.02
uncorrected
1000
2000
3000

MT-GEI 装置の原理

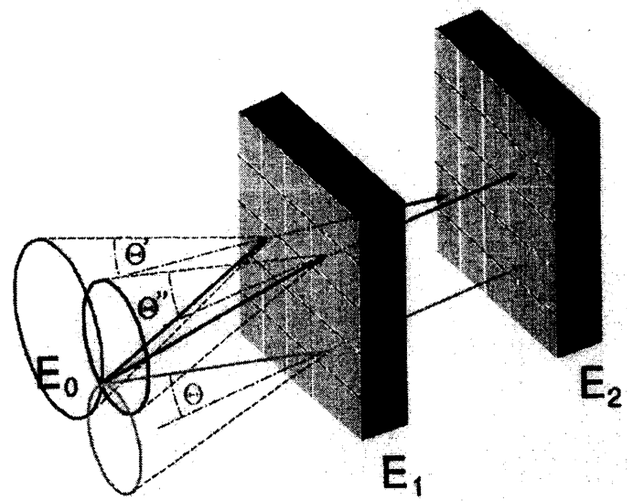

コンプトン散乱

$$E_0 = E_1 + E_2 , \qquad \alpha = E_0 / m_e c^2$$

$$E_2 / E_0 = 1 - \alpha (1 - \cos \Theta)$$

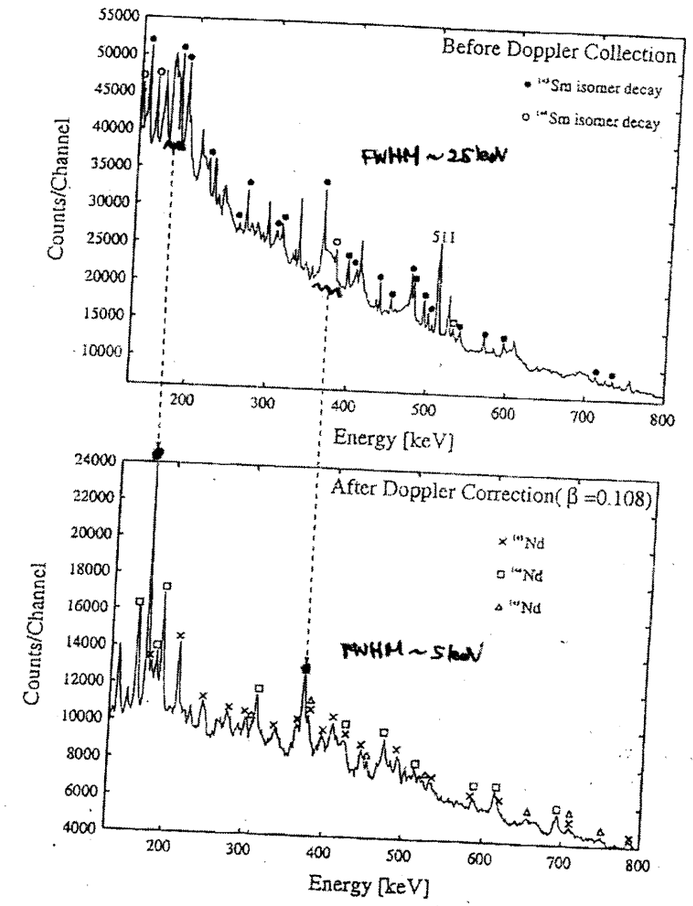

Figure 4.4: γ-ray spectra measured by the telescope Ge counter. The upper figure is a spectrum before the Doppler correction, and the lower is after the Doppler correction with $\beta_R = 0.108$. Meaning of marks in this figure is same as those in Fig.4.3.

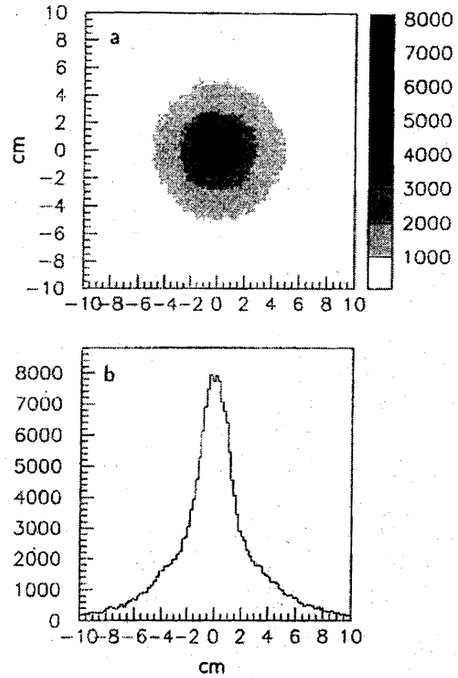

Fig. 5. (a) Two dimensional-image of a point source in an imaging plane from a practical Compton camera. (b) Horizontal slice. The Compton camera consists of two planar type Ge detectors of $50mm \times 50mm \times 20mm$ that are segmented to 25 segments of $10mm \times 10mm \times 20mm$. The two detectors are placed in parallel and the distance between their centers is 6cm. The source is situated in the center axis of the detector system with a distance of 6cm from the center of the first detector and the energy of the source is 1332keV.

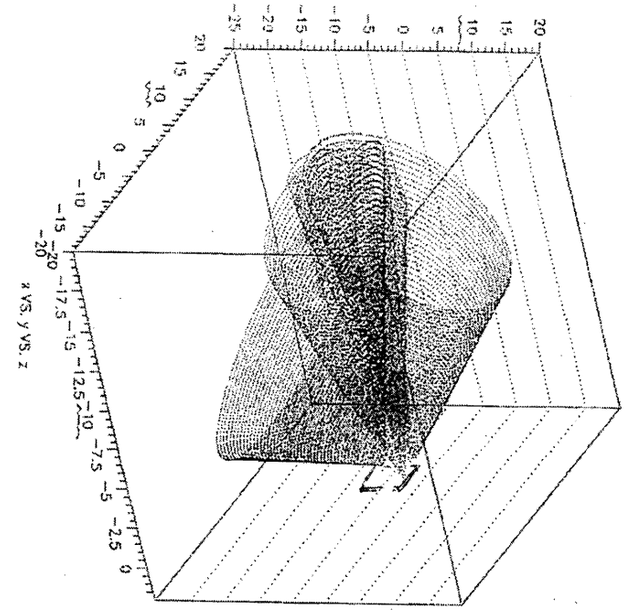

シミュレーションの結果

円錐が重なって、濃くなった部分がガンマー線源の位置に対応する。

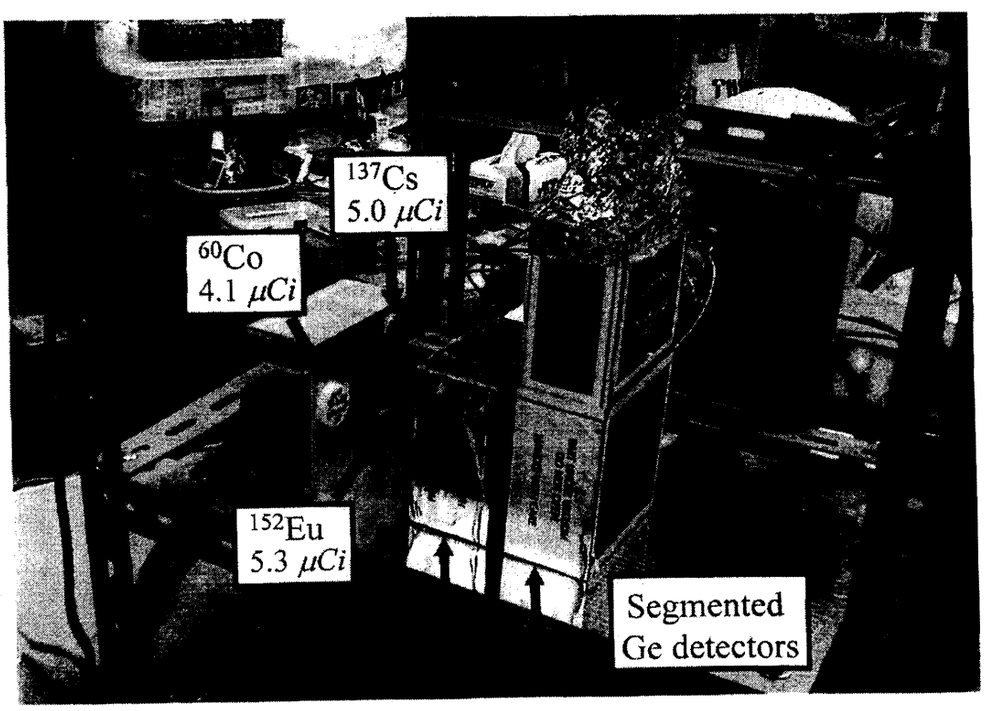
^{137}Cs
5.0 μCi
^{60}Co
4.1 μCi
^{152}Eu
5.3 μCi
Segmented
Ge detectors

核種の同定

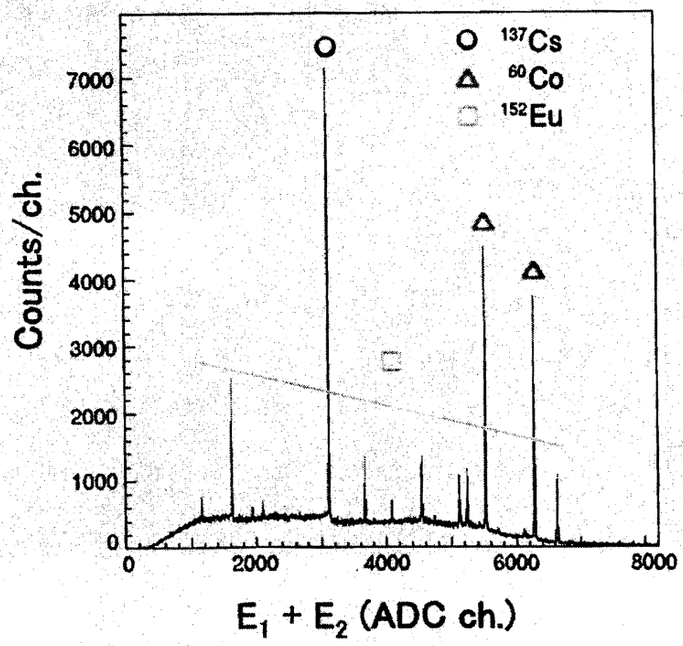
137Cs
60Co
152Eu
Counts/ch.
0
1000
2000
3000
4000
5000
6000
7000
0
2000
4000
6000
8000
E1 + E2 (ADC ch.)

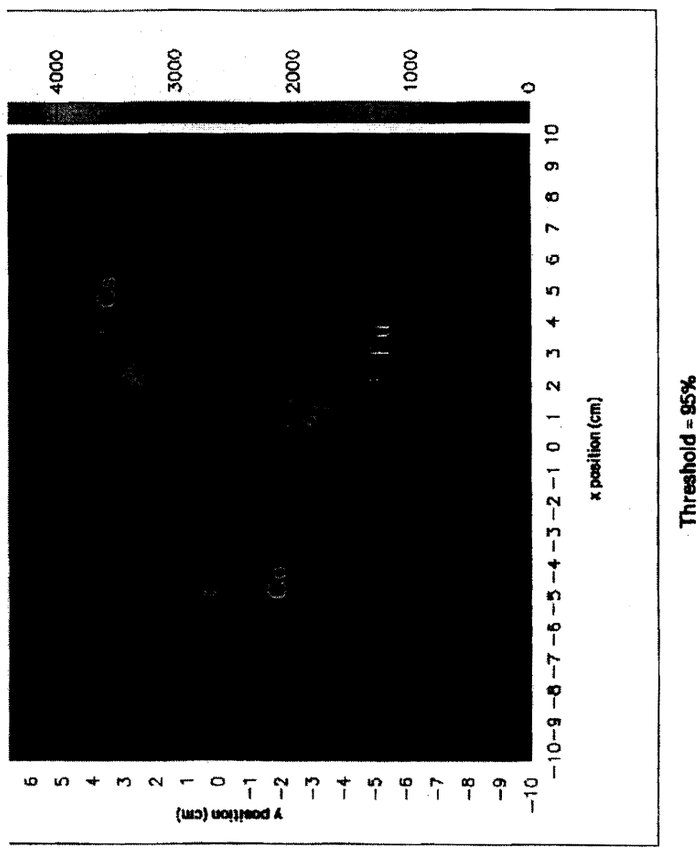
4000
3000
2000
1000
0
y position (cm)
x position (cm)
Threshold = 95%

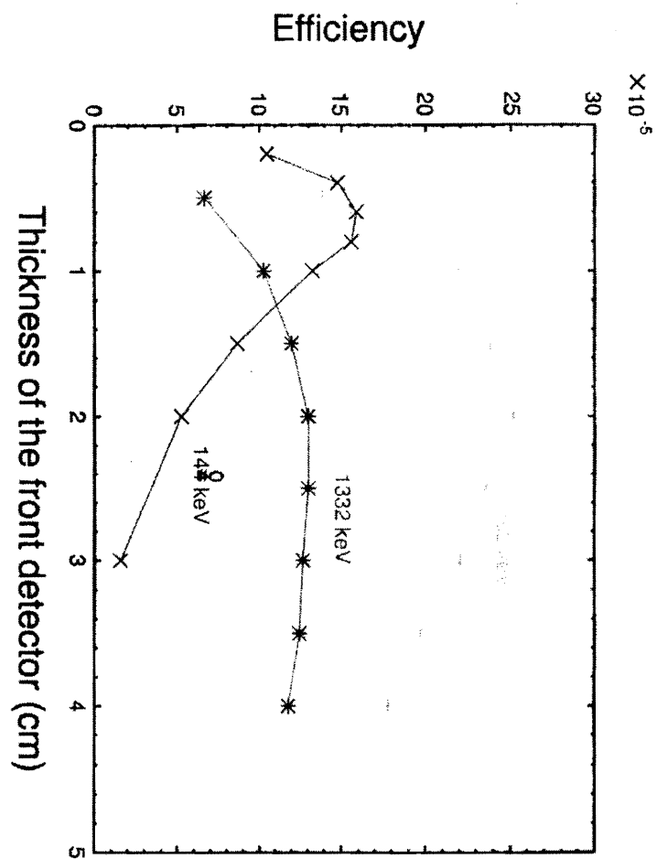

測定 1

ガンマ線源 : ^{137}Cs
線源の強度 : 5.0 μCi
線源の位置 : (3.0 cm, 3.0 cm, -6.0 cm)
測定時間 : 7.7 hours

測定 2

ガンマ線源 : ^{152}Eu, ^{137}Cs, ^{60}Co
線源の強度
^{152}Eu : 5.3 μCi
^{137}Cs : 5.0 μCi
^{60}Co : 4.1 μCi
線源の位置
^{152}Eu : (2.0 cm, -3.0 cm, -8.0 cm)
^{137}Cs : (3.0 cm, 3.0 cm, -8.0 cm)
^{60}Co : (-4.0 cm, 1.0 cm, -8.0 cm)
測定時間 : 4.1 hours

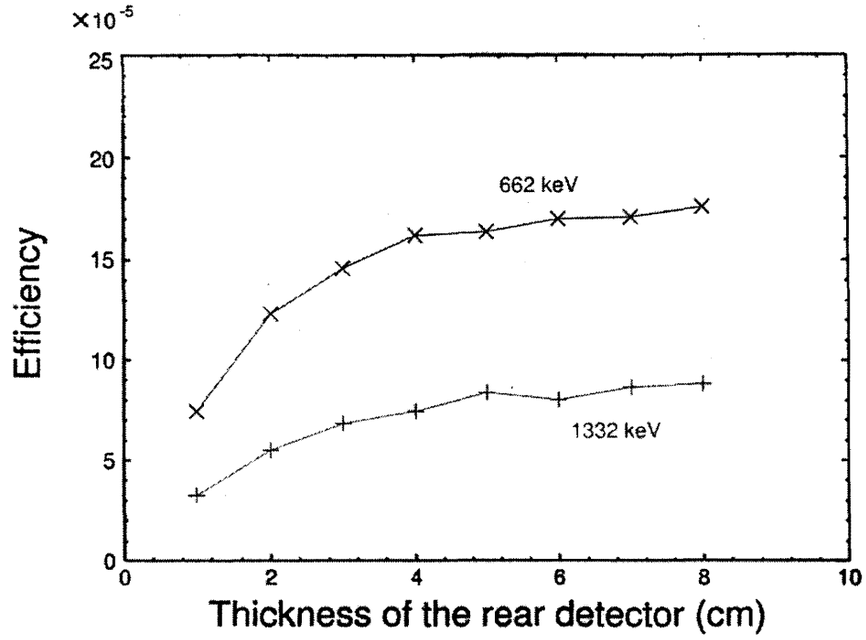
×10⁻⁵
Efficiency
662 keV
1332 keV
Thickness of the rear detector (cm)

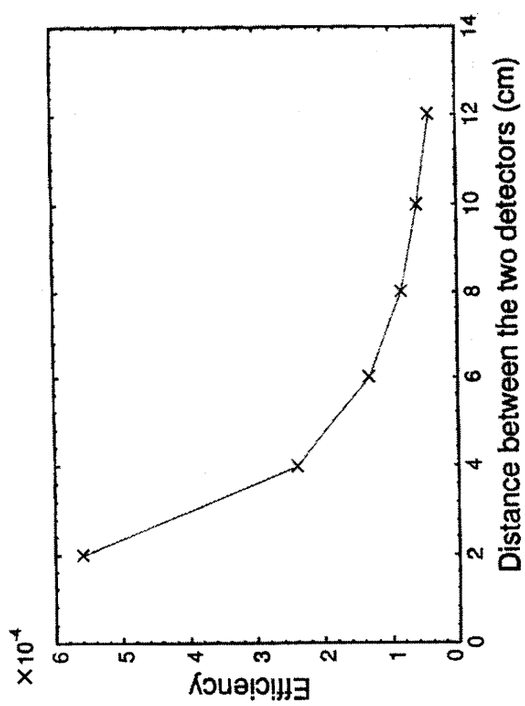
×10⁻⁴
Efficiency
Distance between the two detectors (cm)

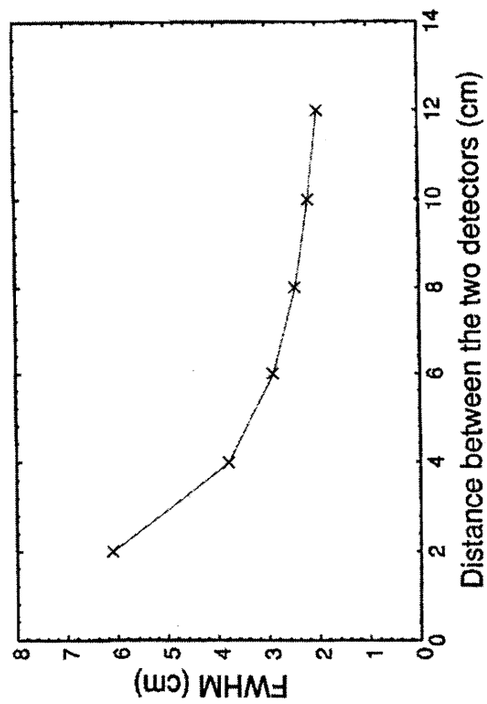
FWHM (cm)
Distance between the two detectors (cm)

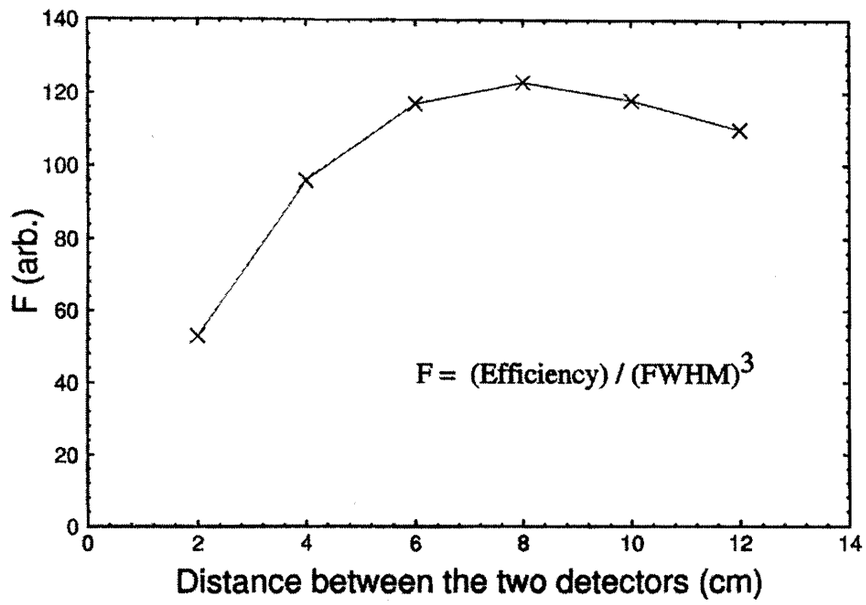

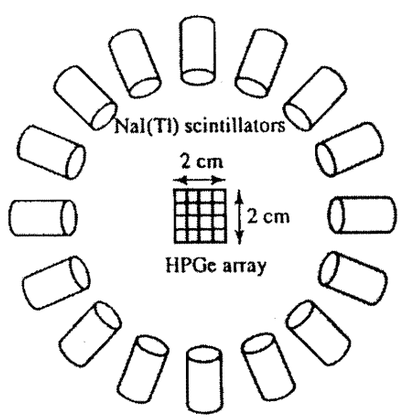

Fig. 4 Schematic illustration of the Ring Compton Camera.

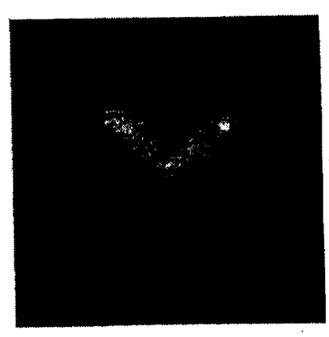

Fig. 5 Image of 511keV Gamma rays from M-shaped ^{64}Cu source. (Copyright 1994 IEEE)

J.B. Martin et al, IEEE NS-41 (1994) 1019
(Univ. Michigan)

3. 今後の展望

CdTe, CdZnTe
$10^4 \sim 10^5$ channel

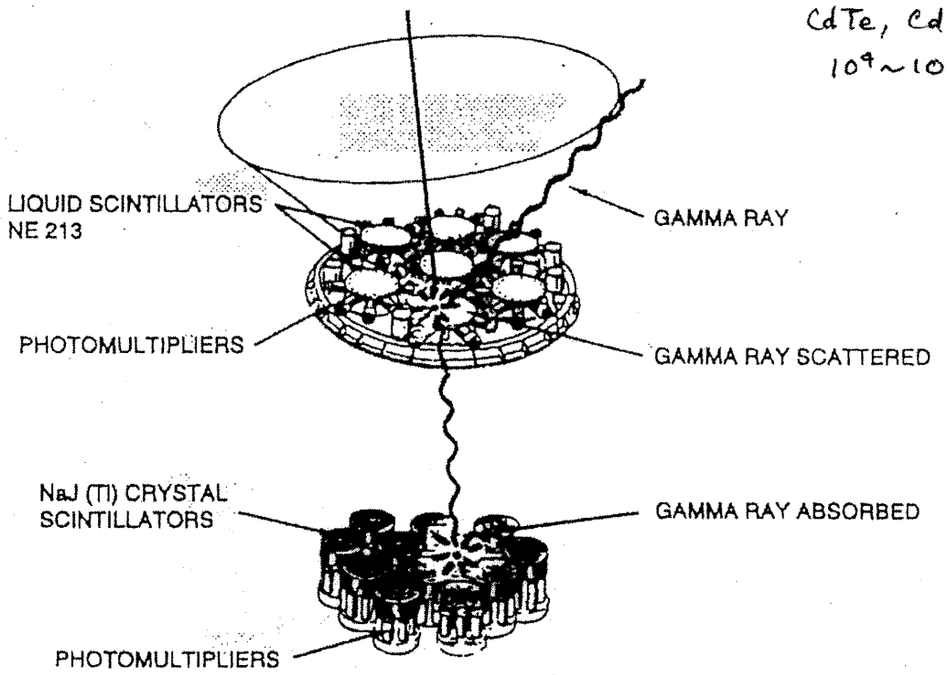

Figure 1. COMPTEL instrument on NASA's *COMPTON* Gamma Ray Observatory. (Courtesy of V. Schönfelder)

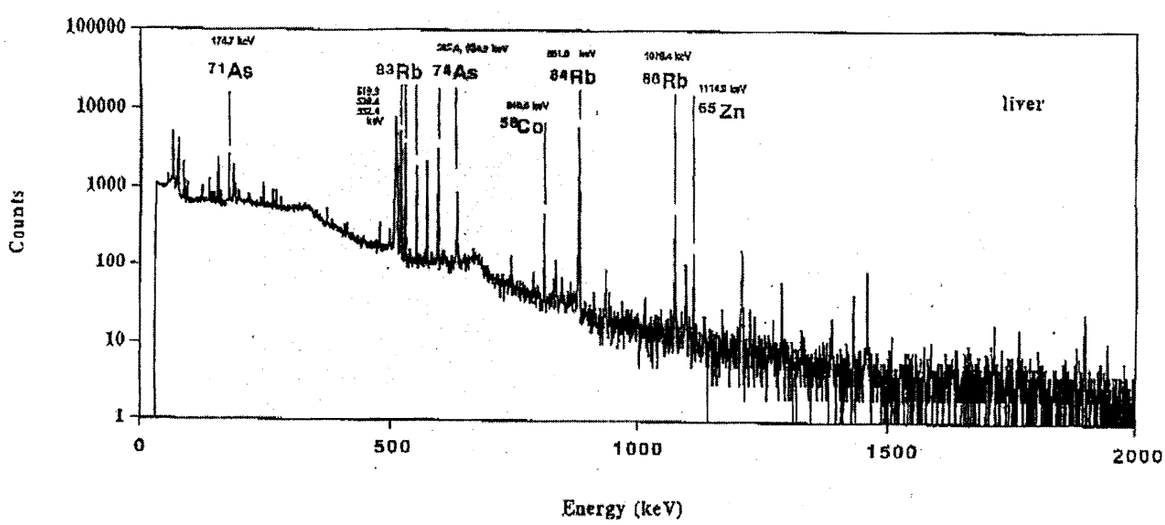

EURISYS MESURES

RESEAU EURISYS

GERMANIUM X-Y STRIP DETECTOR

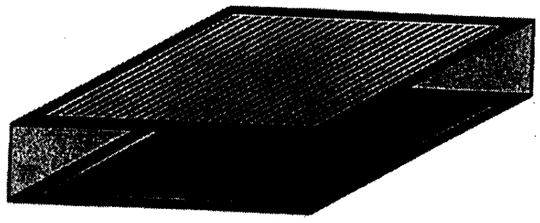

Lenght = 50 mm Width = 50 mm Thickness = 10 mm

2 x 25 strips : ***FWHM = 1,8 Kev at 662 Kev***
Pitch = 2 mm

Fabricated by **EURISYS MESURES** - Phone : 33 3 88 77 43 50 - Fax 33 3 88 78 68 22

Gamma-camera
consisted of two 2mm Strip Ge-detectors

50 x 50 x 10 mm^3- (45 mm apart) - 50 x50 x 20 mm^3

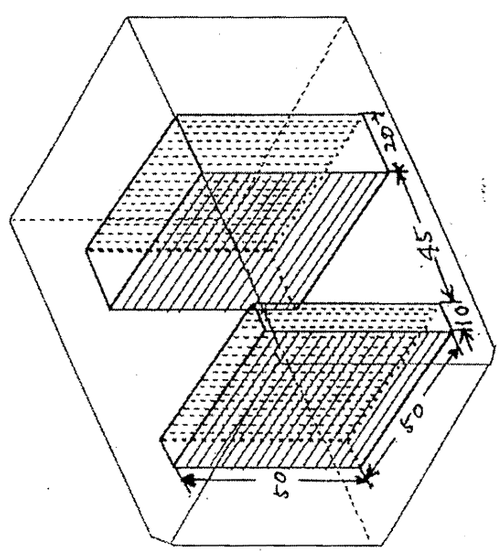

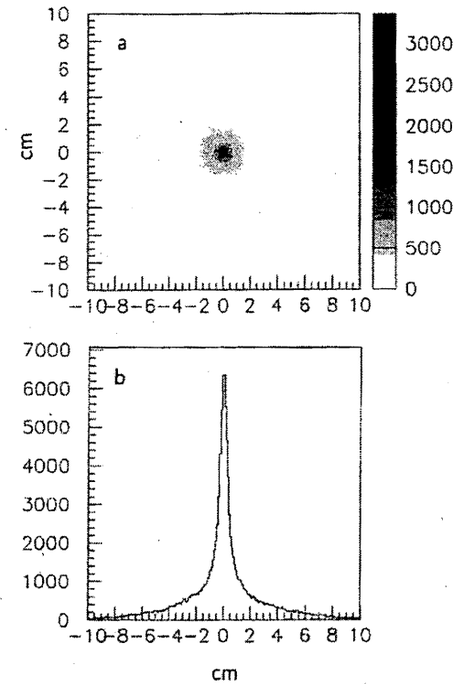

Fig. 12. (a) Two dimensional image of a point source from a Compton camera consisting of detectors with a 2mm position resolution in three dimensions. (b)Horizontal slice.

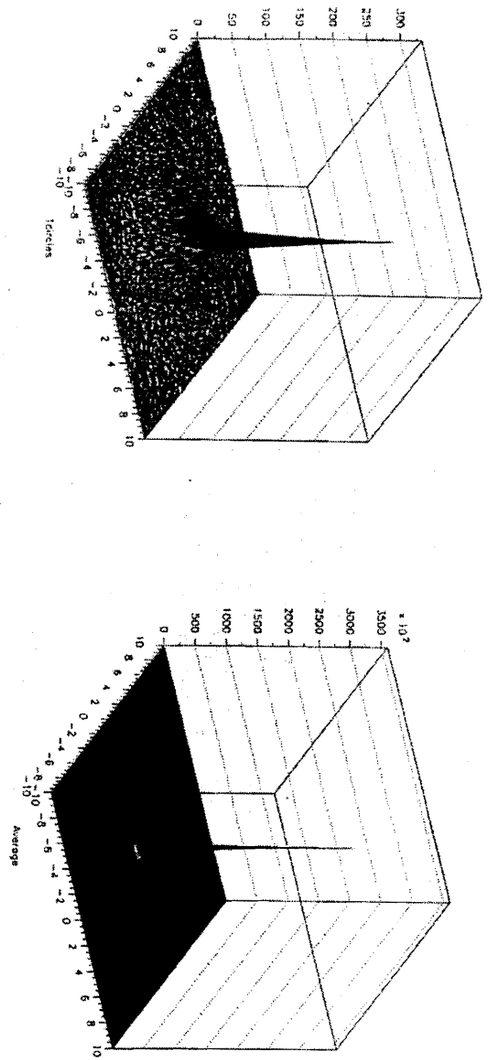

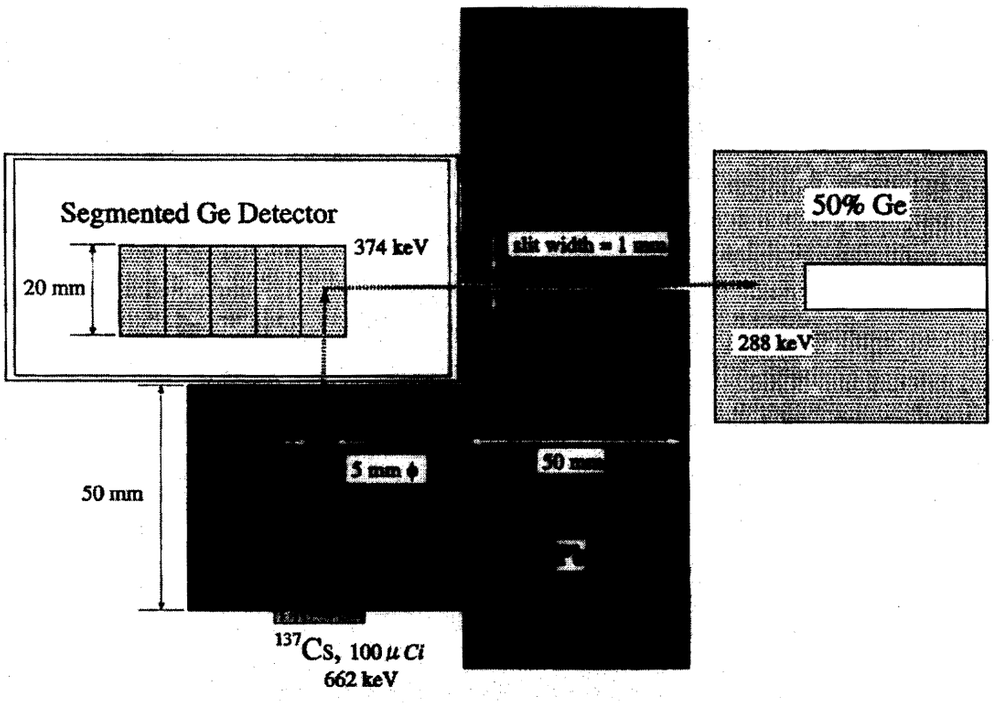
Segmented Ge Detector
374 keV
20 mm
slit width = 1 mm
50% Ge
288 keV
5 mm φ
50 mm
50 mm
^{137}Cs, 100 μCi
662 keV

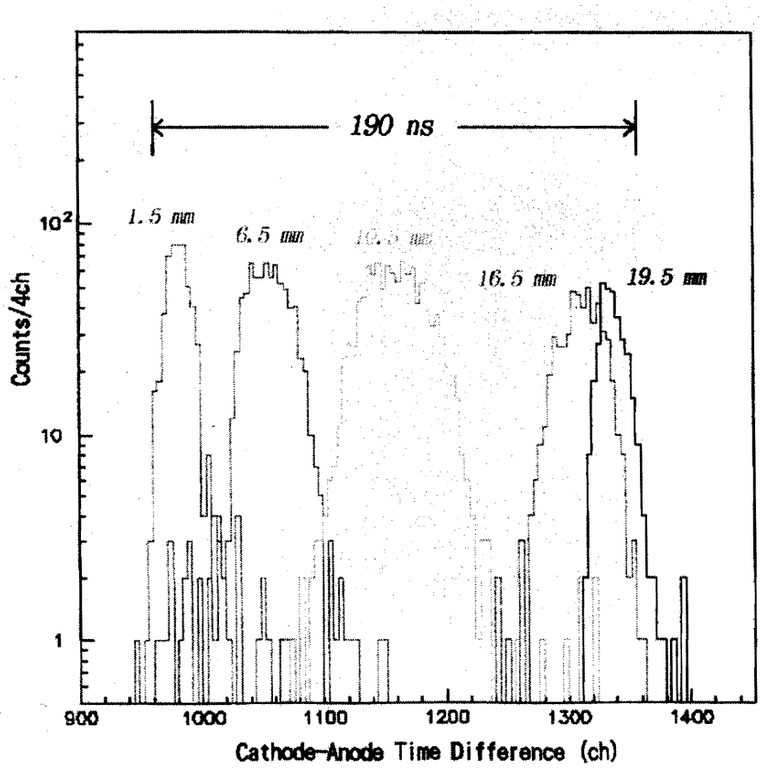
190 ns
1.5 mm
6.5 mm
16.5 mm
19.5 mm
Counts/4ch
10^2
10
1
900
1000
1100
1200
1300
1400
Cathode-Anode Time Difference (ch)

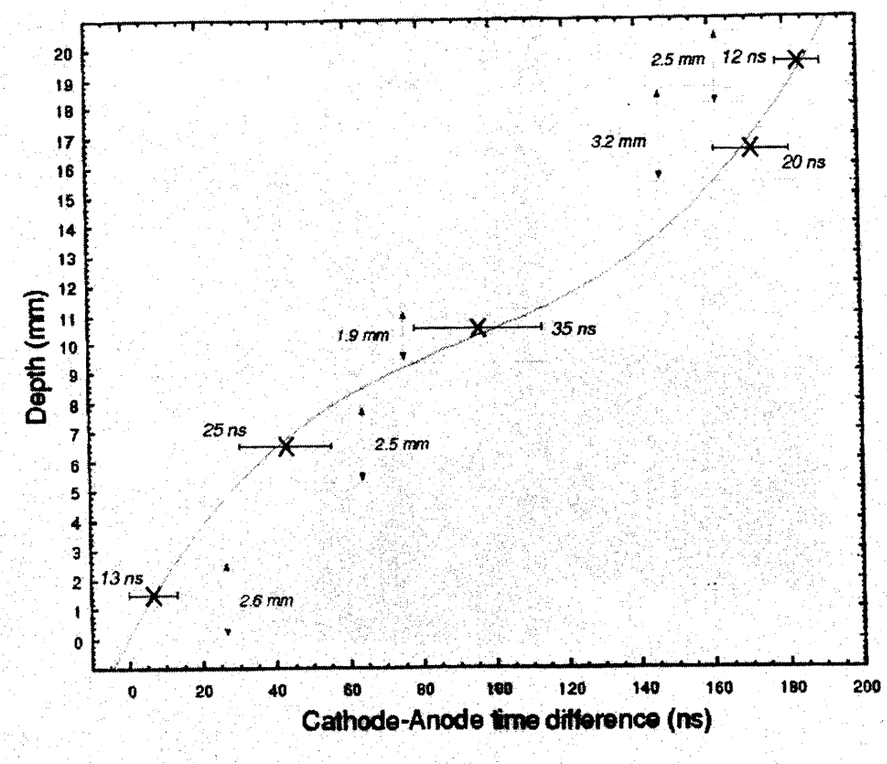
Depth (mm)
Cathode-Anode time difference (ns)
2.5 mm
12 ns
3.2 mm
20 ns
1.9 mm
35 ns
25 ns
2.5 mm
13 ns
2.6 mm

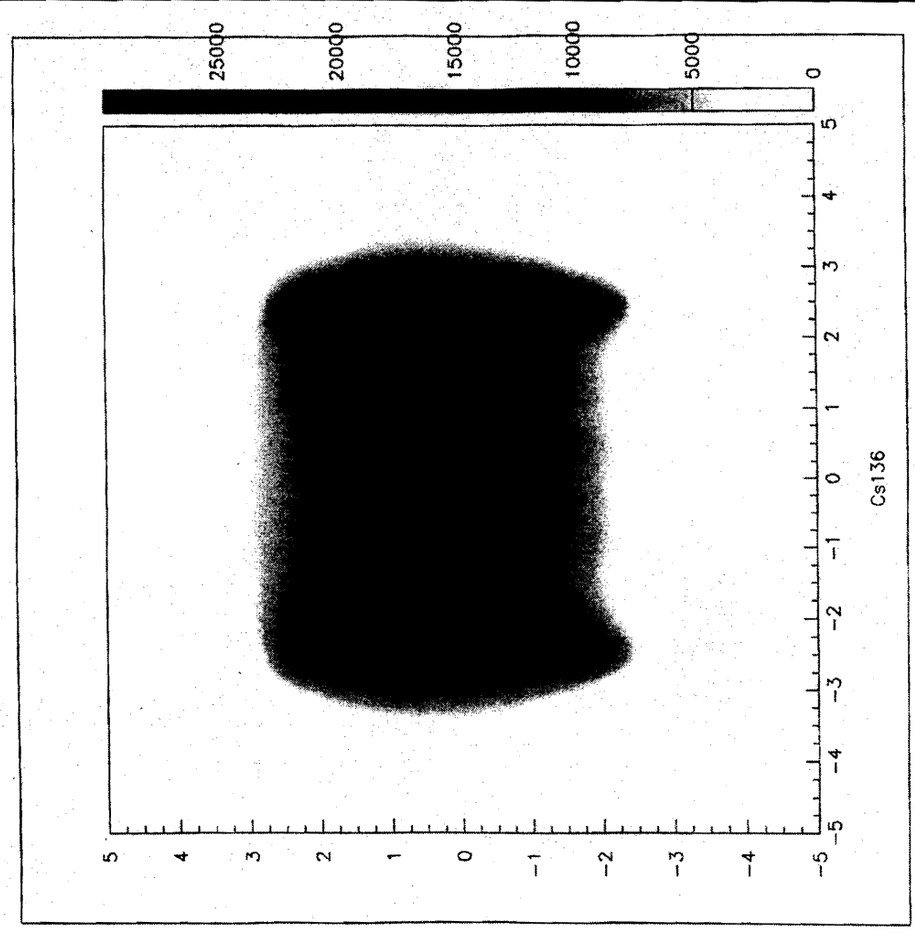
25000
20000
15000
10000
5000
0
Cs136

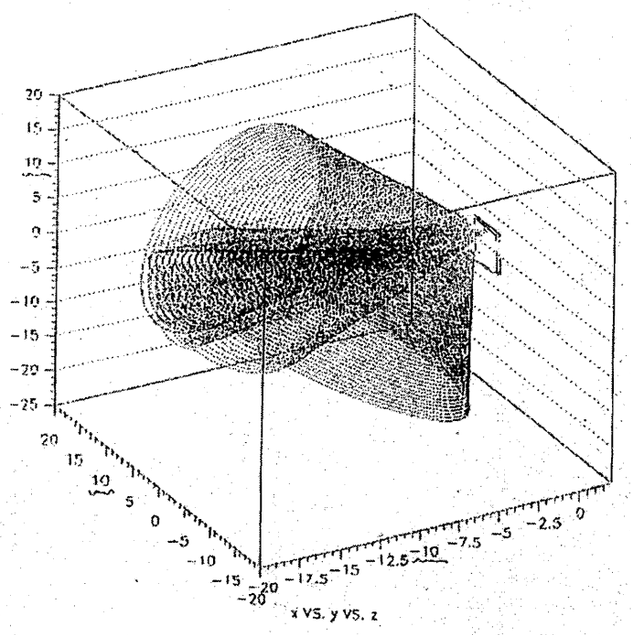

シミュレーションの結果

円錐が重なって、濃くなった部分がガンマー線源の位置に対応する。

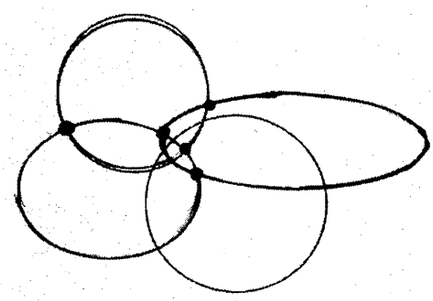

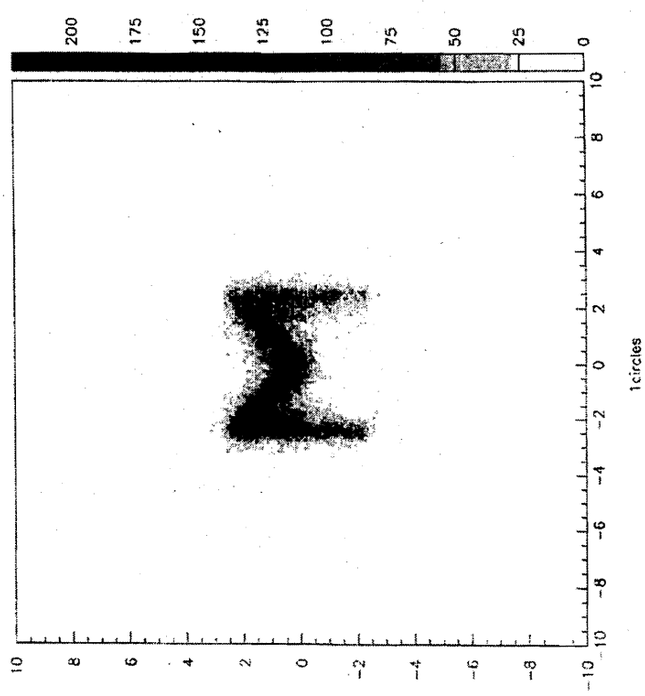

Summary

1. Ge-telescope consisted a segmented Ge and a clover Ge was developed for Doppler correction of γ-rays.
   For a HSIB experiment, a blow-in type gas-target was developed as well.

2. Compton camera is under development for a multitracer use. A camera consisted of two segmented Ge's was successfully tested to identify the position of three γ-ray sources simultaneously.

3. A gamma-ray imaging of a distributed source is now under development.

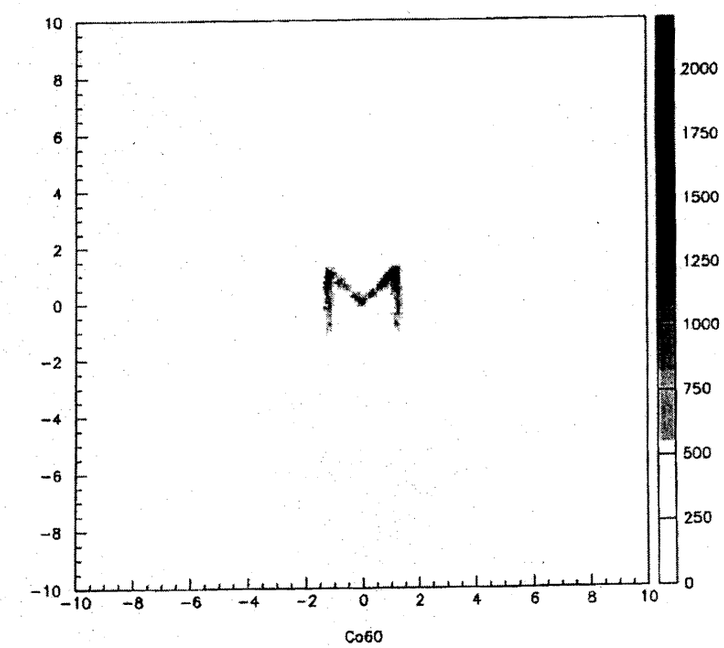

From EUROBALL to AGATA : Physics highlights and new frontiers for 4π gamma-ray spectroscopy

F.A. Beck - IReS Strasbourg

Abstract :

During the 20 last years continous developments in 4π gamma spectrometers have allowed to reach completly new fields in nuclear structure studies. The photopic efficiency was regularly improved first by the increase of the volume of the Ge detectors and when it was no more possible to gain in crystal diameter by the developments of composite detectors like clovers and clusters. A major improvement in resolving power was obtained by the use of anti-Compton shields , composed first by NaI scintillators and than by BGO scintillators, the latter allowing a much more compact Compton suppressor geometry.

Presently it is quite impossible to hope to achieve a large gain in photopeak efficiency and resolving power compared to the existing 4π arrays, EUROBALL in Europe and GAMMASPHERE in USA, by using these now conventionnal detectors arrangement. A major gain is forseen if the 30-40 % of the 4π solid angle devoted to the anti-Compton shields could also been covered by Ge detectors. However this "ball" should have a very high number of detectors (N > 1000) to reach good performances at high multiplicity (multiple hits) and at large recoil velocity (Doppler broadening). The recent developments of segmented Ge detectors has allowed to think to reduce the total number of detectors by using Ge detectors segmented both radialy and longitudinaly. The idea is to follow the track of the γ-ray in the Ge crystals by measuring with a high accuracy the interaction points in the Ge detector. This determination requires a complex on-line pulse shape analysis of the signals of the hitted segments and of the mirror charges generated in the neighbouring segments. Based on the Compton scattering equation different codes have been developped in an european collaboration supported by an EU TMR program to check the feasibility of such a gamma tracking method and to evaluate the possible performances. Generaly these codes were supposing the use of Ge coaxial detectors.

At Strasbourg we have developped an other tracking method based on the Compton cross section probability. This code do not need an accurate determination of the interaction points since only the probability to scatter to one or an other segment versus energy is used. Howewer these calculations were based on a detector geometry which enables a crystal segmentation in nearly identical cubic pixels. The geometry of planar detectors is particularly well sited for such geometries and consequently calculations have been performed for a 4π geometry composed with 72 planar stacks including each 4 planar detectors of large size 7.5 x 10 x 2 cm. The results show photopeak efficiency values quite identical to those obtained with the usual tracking method based on coaxial detectors. Concerning the reduction of the Doppler broadening of gamma lines an energy resolution of 8 keV is obtained for v/c =10 % at an energy of 1.33 MeV. This value can be reduced to less than 3 keV by the use of a method developped at CNS-Japan which proposes to determine the interaction depth in the planar detector by measuring the time difference between anode and cathode with an adequate hardware circuit. This would not affect the general idea of this gamma tracking method based on Compton scattering probability which has the major merit to be independent on the accuracy of the determination of the interaction radius in contrary of the method based on the use of coaxial detectors.

A first prototype of a planar segmented stack detector is currently under test at IReS Strasbourg. It comprises two planar detectors 5.3 x 5.3 cm and 2 cm thick which are segmented in 4x4 = 16 segments and in 3x3 = 9 segments respectively. This leads to 25 cathode outputs and one common anode output. First results show very good energy resolution for the cathode outputs with very clean pulse shape information. Further developments on planar detectors are forseen with EURISYS Mesures company to improve some important features like the passivation technique , the replacement of the Li contact and the reduction of the guard ring size. The achievement of this goal is also of general interest for the performances of gamma detection with planar detectors like in medical imagery.

The improvement of the the detector sensitivity of 4π gamma spectrometers over the last 20 years has led to a lowering of the fraction of the reaction channel which is possible to measure in regular gamma cascades from around 10^{-1} to 10^{-4}. This enabled to discover numerous properties of the nuclei at high angular momentum up to the discovery of the superdeformed bands bands and their many intriguing properties. With AGATA the limit of detection is expected to go from 10^{-4} to a few 10^{-7} which gain is a not far away from that one obtained during the prevoius 20 years period. It would allow completely new physics as well in high spin physics (hyperdeformation, triaxial octupole deformations, super-heavy nuclei approach, study of N=Z nuclei, ...) as well as in medium and low spin physics with radioactive beams (very neutron rich nuclei, coulomb excitation, secondary fragmentation reactions, etc.) where the high reduction in Doppler broadening associated to the total photopeak efficiency will be essential.

Characteristics requested for a new generation 4 πγ array

- **Photopic efficiency :** probability to detect the total energy of a γ-ray
  - large increase necessary to :
    - @ counterbalance the weak intensity of the radioactive beams
    - @ achieve much lower detection limits for the measurements of more exlusive phenomena
- **Good Pic/total ratio :** necessary for the resolving power especialy at high fold
- **High angular resolving power :** Large Doppler broadening reduction for high recoil velocities ranging up to 50 %
- **High counting rate capability :** in radioactive beam measurements the background can be very important as compared to the researched effects
- **Large inner diameter of the arrays :** very important to allow the possibilty to insert other type of detectors like charged particule detectors, heavy ions detectors, ...

From the present multidetectors to the gamma tracking arrays

EUROBALL

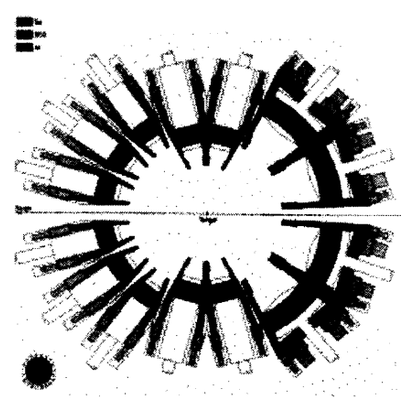

4π space coverage :

40 % Ge

40 % BGO anti Compton

20 % containers

BGO purpose : Compton rejection (P/T) and shielding between Ge detectors (scattering)

239 Ge in 71 cryostats ; ~ **1000 BGO**

How to increase photopic efficiency without deteriorating the Pic/total ratio ?

- by covering 80 % of the space with Ge detectors (increase of ω and intrinsic of efficiency by « add-back »)
- by «following » the gamma-ray path in the segments of several Ge : increase of the add-back efficiency and increase of the P/T to a value better than these obtained with anti-Compton shields

→ **tracking gamma**

Gamma « tracking » basic elements (1)

➢ **EUROBALL / GAMMASPHERE**

Ge crystals surrounded with BGO anti-Comptonshields

(P/T increased to ≈ 0,5)

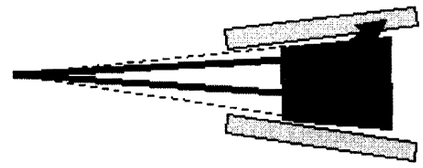

➢ **Multidetectors of the future :**

- **increase of the photopic efficiency by :**
  - **increase of the angular coverage by a factor 2**
  - **add-back of the energies deposit in several detectors by the same gamma-ray**
- **P/T ratio equal or better than the present ~ 0.5 value**

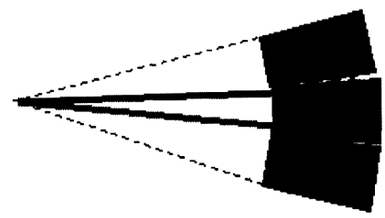

→ **will need a high segmentation of the Ge crystals to be able to measure with accuracy the main characteristics of the interaction points (energy relaxed and scatering angle)**

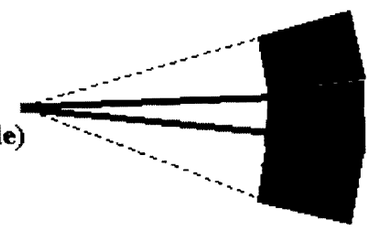

Gamma « tracking » basic elements (2)

➢ **Compton scattering equation**

$$E_{\gamma_{i+1}} = \frac{E_{\gamma_i}}{1 + \frac{E_{\gamma_i}}{m_0 c^2}(1 - \cos(\theta))}$$

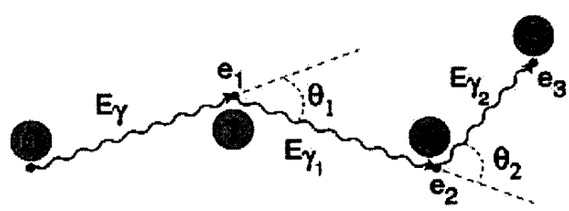

gamma path reconstruction with the help of the scattering équation

➢ **Clusterisation**

$$E_\gamma = E_\Sigma = \Sigma_i e_i$$

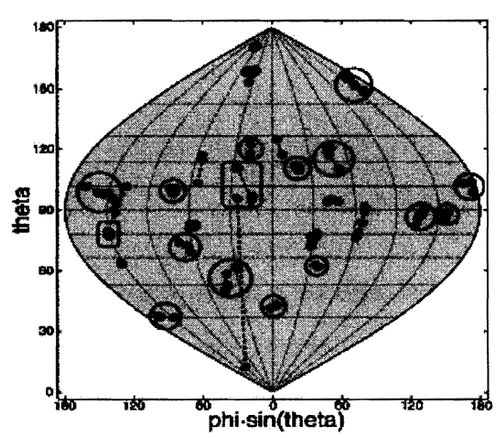

Gamma « tracking » basic elements (3)

- **Variation, for M= 30, of the total photopic efficiency and of the ration P/T as a function of :**
  - the half angle of the cluster
  - the resolution in the space (x,y,z)

→ reconstruction accuracy highly dépendent on the accuracy of the (x,y,z) determination

→ the present tracking method requests :
- high (x,y) segmentation
- measurement of the interaction radius (pulse shape analysis)

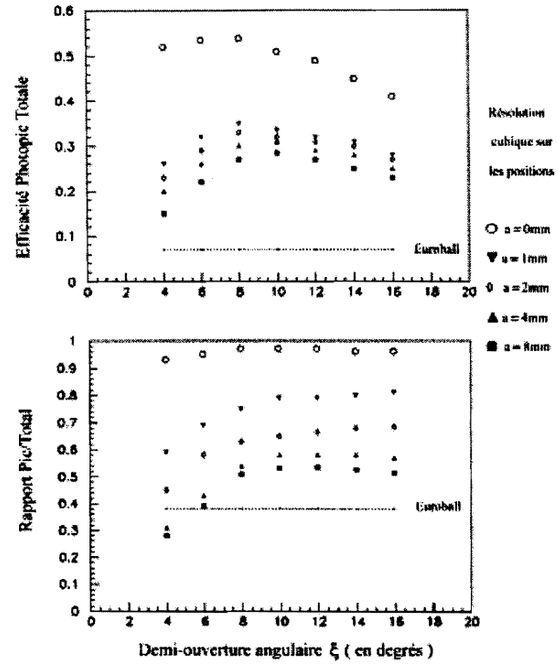

(from E.Pachoud thesis, ULP-Strasbourg, july 2000)

Coaxial segmented detector and difference in collecting time

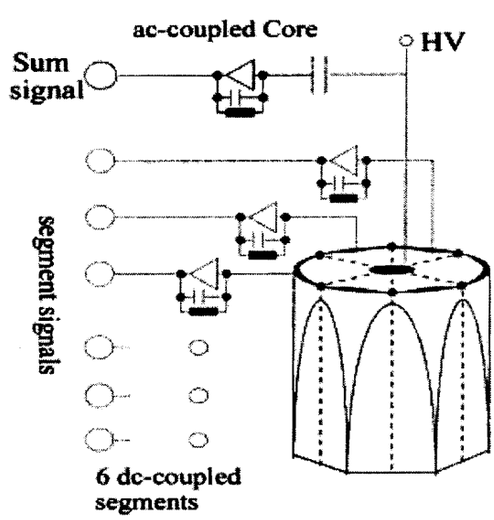

Amplitude of the induced currents as a function of the interaction radius value

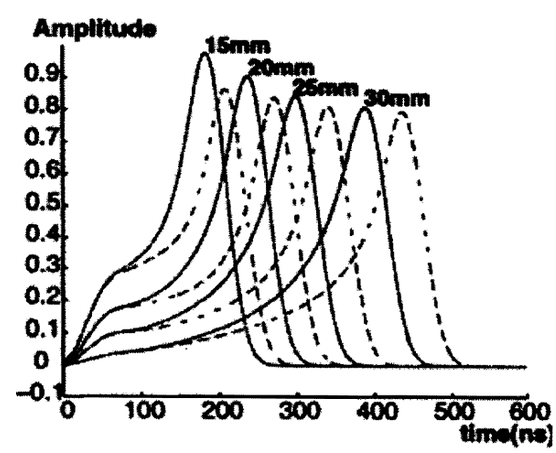

→ **possible to measure an accurate « mean value » of the interaction radius**

→ **very difficult to have a high accuracy in an on line event by event calculation especialy in the case of 3 to 4 interactions like it is the probability for a gamma energy of 1.3 Mev**

Proposition for an other tracking method

➢ **Based on the Klein-Nishina scattering coss section as a function of energy :**

$$\sigma = f\,(E\gamma_{i+1}, E\gamma_i, \theta)$$

- **clusterisation method similar to the tracking method based on the scattering equation**
- **Compton scattering probability as a function of the gamma energy, the scattering angle and the mean mean path of the γ-ray**
- **present simulation calculations were done with the hypothesis of identical elementary volumes with a nearly cubic symetry (facilitates calculations) :**

  → planar detectors are quite ideal for such geometries

- **in these basic version the method based on the «reconstruction of the gamma energy » do not request any pulse shape analysis to obtain photopic and P/T values similar to those calculated with the usual tracking method**

  Moreover : a pulse shape analysis would even enhance this performances (due to the electric field geometry the analysis would be easier with planar detectors than with coaxial detectors)

However : planar detector technology needs R&D for reduction of dead layers (Li contact, passivation, linearisation of the electric field)
(currently under development between IReS-Strasbourg and EURISYS Mesures company)

Segmented planar detector and difference in collecting time

Segmented planar detector

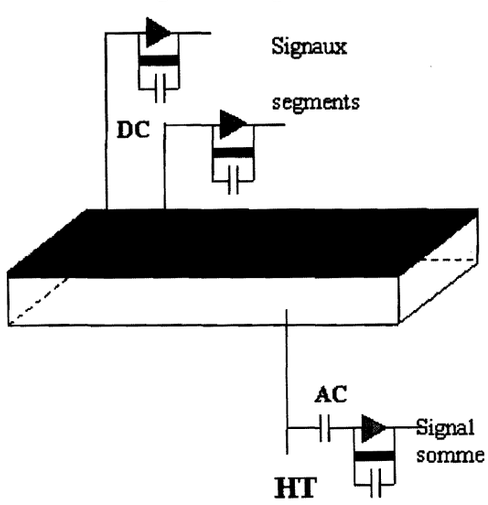

Difference in collection time

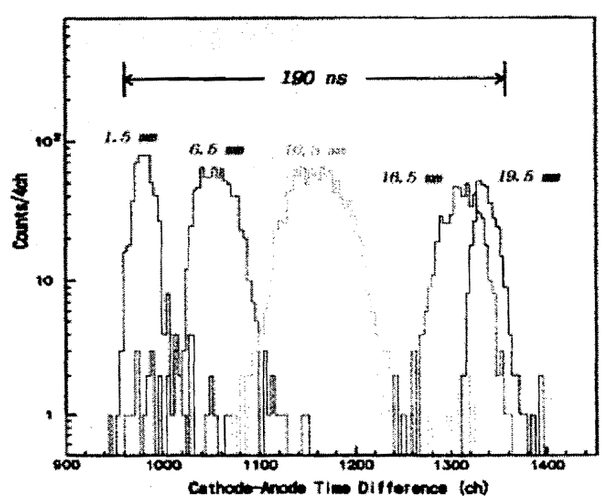

→ much easier to do an on-line collection time-interaction point correlation with planar detectors than with coaxial detectors

Test of a stack of two planar detectors

Stack prototype of 2 planar detectors 5.4 x 5.4 cm, 2 cm thick at IReS Strasbourg
- left one segmented in 3 x 3 (9 elements)
- right one segmented in 4 x 4 (16 elements)

Segment	FWHM (122 keV)	FWHM (1332 keV)
B10	0.86	1.71
C10	0.82	1.71
D10	0.82	1.69
B20	0.84	1.74
C20	0.83	1.71
D20	0.89	1.75
B30	0.86	1.86
C30	0.82	1.65
D30	0.82	1.70

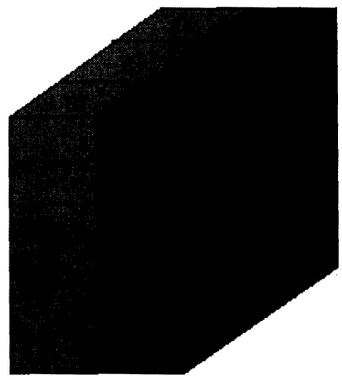

Segment	FWHM (122 keV)	FWHM (1332 keV)
A1	0.82	1.84
B1	0.78	1.92
C1	0.80	1.93
D1	1.01	1.88
A2	0.77	1.87
B2	0.83	1.80
C2	0.73	1.84
D2	1.06	1.86
A3	0.84	1.93
B3	0.82	1.85
C3	0.86	1.81
D3	0.83	1.89
A4	0.88	1.73
B4	0.78	1.82
C4	0.76	2.04
D4	0.94	1.90

- very clean cathodes and anode signals
- good signal to noise ratio for mirror charge signals

Geometry for a 4π spectrometer with planar stacks

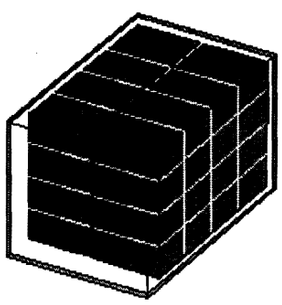

Basic planar stack : four planar detectors segmented 4 x 4 with a common anode by pair of crystals
64 + 2 = 66 electronic channels

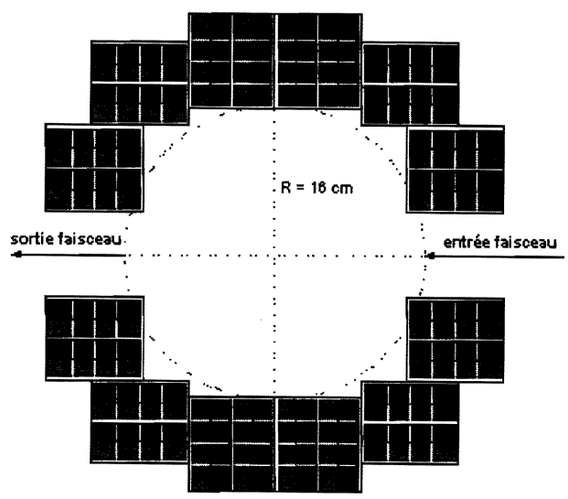

4 π array : Château of 72 planar stacks
288 single planars 4 x 4 = 4608 segments
4608 + 144 = 4752 electronic channels

Comparison for E_γ = 1332 keV of the photopic efficiency and the P/T ratio values between AGATA geometries and existing spectrometers

		$M_\gamma = 1$		$M_\gamma = 30$	
		$\varepsilon_p \omega$	P/T	$\varepsilon_p \omega$	P/T
EUROBALL		0.094	0.50	0.065	0.37
EXOGAM		0.20	0.47	-	-
AGATA	coaxial	0.40	0.55	0.21	0.45
	planar*	0.42	0.54	0.22	0.40
Ideal sphere		*0.65*	*0.85*	*0.36*	*0.60*

* without pulse shape analysis

Doppler broadening

- **Doppler broadening :** $(\Delta E)^2 = (\Delta E_{intrinsic})^2 + (\Delta E_{Doppler})^2$

  $(\Delta E_{Doppler})^2 = (\Delta E_{(target+ recoil cone)})^2 + (\Delta E_{angule opening of the detectors})^2$

- **Coaxial detectors :**
  - **position of the first interaction obtained by tracking and pulse shape analysis**

- **Planar detectors : two possibilities**

  1. **First interaction deduced just by the «gamma energy reconstruction» tracking method**

  2. **Addition of an on line hardware pulse shape analysis :** estimated space resolution : ~ 0.2 cm

  (possible because of the linearity of the electric field in case of planars : see previous transparents)

Doppler broadening reduction (at E_γ = 1332 keV) as a function of recoil velocity

Recoil velocity	ΔE (keV) without pulse shape analysis			ΔE (keV) with pulse shape analysis		
v/c	EUROBALL	EXOGAM	AGATA	EUROBALL	EXOGAM	AGATA*
2 %	3.1	3.3	2.7 keV	-	2.6	2.2 keV
10 %	15.3	17.2	7.5 keV	-	8.8	2.7 keV
50 %	69	85	35 keV	-	43	7.5 keV

- Similar values are obtained with either coaxial or planar detectors, but for planar detectors it is possible to do a hardware on line meaurement of the pulse shape of the signals

Limit of observation at high angular momentum

Is function of (see the figure) :

- **the photopic efficiency $\varepsilon_p\omega$**
- **the resolving power**
  PR = P/T x δE / ΔE

for M=30 :

	EUROBALL	→	AGATA
fold	**4**	→	**6**
$(\varepsilon_p\omega)^f$	**1.8 10^{-5}**		**8.6 10^{-5}**
$(PR)^f$	**5.7 10^4**		**6.1 10^6**
limite d'obs.	**10^{-4}**	→	**a few 10^{-7}**

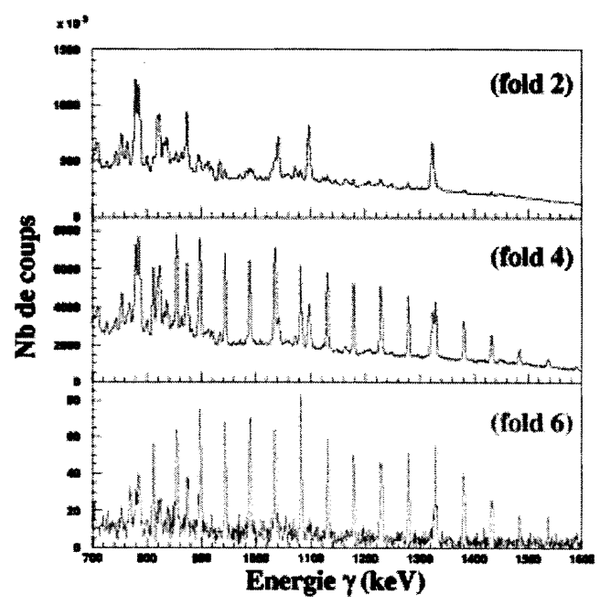

Intensity and peak to background ratio for the gamma spectrum of the ^{151}Tb yrast yrast superdeformed band as a function of the coincidence fold

Limit of Observation at high angular momentum

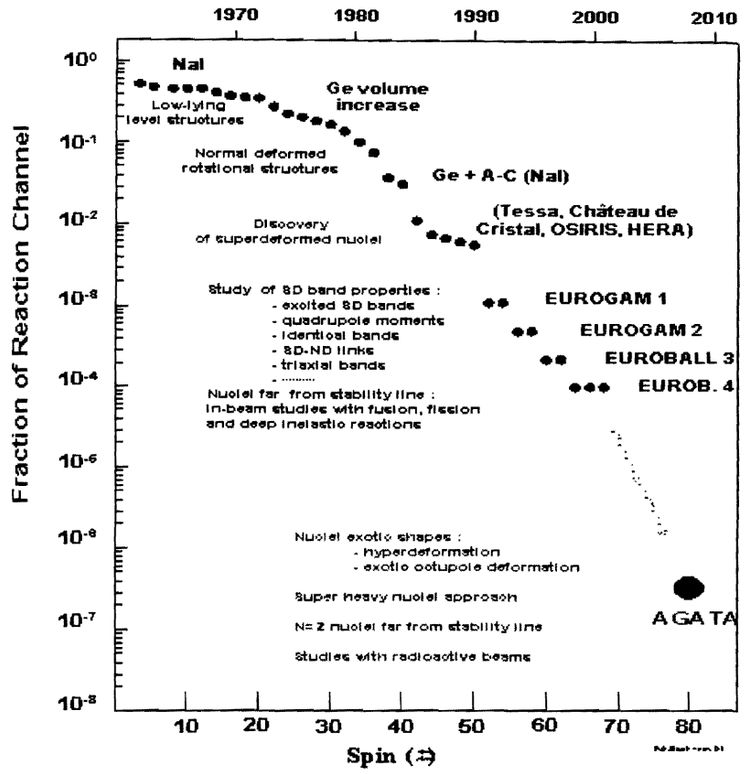

Pulse shape analysis with the MARS gamma-ray tracking detector

Th. Kröll[A], D. Bazzacco[B], R. Venturelli[B], B. Quintana Arnes[B,C], C. A. Ur[B], M. Bellato[B], R. Isocrate[B], Ch. Manea[B], P. Pavan[B], C. Rossi Alvarez[B], E. Farnea[A], A. Gadea[A], D. Rosso[A], P. Spolaore[A], F. Camera[D], B. Million[D], A. Pullia[D], O. Wieland[D], G. Casati[E], A. Geraci[E], G. Ripamonti[E], M. Descovich[F]

[A] *INFN - Laboratori Nazionali di Legnaro, Italy;* [B] *INFN and Università di Padova, Italy;* [C] *Universidad de Salamanca, Spain;* [D] *INFN and Università di Milano, Italy;* [E] *INFN and Politecnico di Milano, Italy;* [F] *University of Liverpool, United Kingdom*

Email: thorsten.kroell@lnl.infn.it

MARS - Mini ARray of Segmented detectors - is the Italian effort to explore the feasibility of building a 4π array for γ-ray spectroscopy of the next generation based on γ-ray tracking [1].

The concept of γ-ray tracking is to identify the individual γ-rays by reconstructing their scattering paths through the array. Therefore, the determination of the three-dimensional position and the energy deposit for every interaction point is a crucial step. This aim will be achieved by utilising highly segmented detectors. Since a spacial resolution in the order of the segment size is insufficient for γ-ray tracking, an improved characterisation of the interaction points of the γ-rays will be obtained by analysing the shapes of the signals from the segments [2].

The prototype for MARS is a cylindrical closed-end crystal of n-type HPGe and has a 25-fold segmentation of the outer contact: 6 angular "sectors", 4 "slices" in depth, and an additional segment on the front face. The detector is completely operational since November 2000 [3].

Most of the development of algorithms for pulse shape analysis has to be based on simulations. For the calculation of signals from highly segmented detectors with different geometries, computer programs applying the FEM have been developed [4]. The accuracy of the simulations has been proven by comparison with experimental signals obtained with collimated sources.

Usually, there is more than one interaction point in the detector or even in one segment and the measurable signals are the sum of the signals originating from the individual interactions. Goal of the pulse shape analysis is the decomposition of these multiple interactions and the characterisation of each of them. For this task we are using methods of artificial intelligence, artificial neural networks (ANN) and genetic algorithms (GA). Our approaches have been tested with both simulated and measured signals.

In order to verify the entire concept experimentally, i.e. digital signal processing, pulse shape analysis, and reconstruction of the scattering path, we performed an in-beam experiment.

The status of the project and preliminary results will be presented and discussed.

This project is part of the TMR Research Network "Development of Gamma-Ray Tracking Detectors for 4π Gamma-Ray Arrays" which involves Denmark, France, Germany, Italy, Sweden, and UK. The network is supported by the EC under contract ERBFMRX-CT97-0123.

References

[1] Th. Kröll *et al.*, Proceedings of Bologna2000, World Scientific (2001)
[2] I. Y. Lee, Nucl. Instr. and Meth. A 422, 195 (1999)
[3] D. Bazzacco *et al.*, LNL Annual Report 2000, 166 (2001)
[4] Th. Kröll and D. Bazzacco, Nucl. Instr. and Meth. A 463, 227 (2001)

Ge array / spectroscopy

T. Motobayashi (Rikkyo U.)

high-spin states, isomers,
low-lying states in EXOTIC nuclei

requirements

efficiency, resolution, ...
<= high spin studies
multiplicity
<= RI-beam-based studies

moving sources
<= hyper nuclear spectroscopy
counting rate
large b.g. pulses

GRETA-Lee, AGATA-Gerl
EXOGAM-de France,
CNS-array-Shimoura, Kurokawa
Hyperball-Tamura
telescope / camera-Gono

wide rage of application

general (versatile) desig

⇓ ⇑

specialized versions

- fast and cheap ?

tracking

3-D tracking-Lee, Gerl

Compton camera-Gono

- 3 -

position determination

pulse shape analysis-Kurokawa, ...

experimental methods

1) @ 5 MeV/nucleon

ORNL, JAERI, (SPIRAL), ...

coulex, transfer-Baktash,

deep-inelastic-Ishii,

fusion-Ideguchi, Gono, ...

2) @ 50 MeV/nucleon or higher

- 4 -

RIKEN, GANIL, MSU, ..
GSI, RIBF, RIA, ...
fragmentation, coulex,
charge exchange, ...

-Gerl, Shimoura, de France, ...

importance of channel selection

plastic hodoscope
recoil mass separator
spectrograph VAMOS
ΔE-E telescope

- 5 -

SKS (π, K, ..)

electronics developments

digital pulse processing
analogue technique
low-nose preamplifier
data acquisition
fast amps. (reset, shaping)

targets

liquid-Shimoura, de France
gas-Gono

- 6 -

workshop of a good size !

good to continue !

good to start collaboration !

Publicity of Rikkyo

Research Center

- scientific measurements